DISSERTATION

MEMBRANE BEHAVIOR AND DIFFUSION IN UNSATURATED SODIUM BENTONITE

Submitted by

Kristin M. Sample-Lord

Department of Civil and Environmental Engineering

In partial fulfillment of the requirements

For the Degree of Doctor of Philosophy

Colorado State University

Fort Collins, Colorado

Spring 2015

Doctoral Committee:

Advisor: Charles D. Shackelford

Christopher A. Bareither
Gregory L. Butters
Ning Lu
Thomas C. Sale

ABSTRACT

MEMBRANE BEHAVIOR AND DIFFUSION IN UNSATURATED SODIUM BENTONITE

Sodium-bentonite (Na-bentonite) is a highly active clay commonly used as a barrier or a component of a barrier for chemical containment applications (e.g., landfills, waste impoundments, vertical cutoff walls) due to the ability of Na-bentonite to limit solute (contaminant) transport resulting from high swell and low hydraulic conductivity. However, Na-bentonite also may exhibit semipermeable membrane behavior or solute restriction, which can result in enhanced performance of the barrier by reducing liquid and contaminant flux. Experimental studies to date have focused on the correlation between membrane behavior and diffusion of solutes almost exclusively under fully saturated conditions (i.e., degree of water saturation, S, of 1.0). However, clay barriers can exist at various degrees of water saturation (S < 1.0), and, based on our current, conceptual understanding of the mechanisms causing membrane behavior in saturated clays, the influence of membrane behavior on solute transport is likely to be even more significant in clays under unsaturated conditions.

Based on these considerations, an innovative testing apparatus was developed to allow for the simultaneous measurement of membrane behavior and diffusion in unsaturated Na-bentonite. The test specimens were prepared using a dialysis method that allowed for control of the cation species on the exchange complex of the bentonite, removal of excess soluble salts, and estimation of diffusion properties. Membrane efficiencies (ω) and effective diffusion coefficients (D^*) of bentonite specimens with S ranging from 0.79 to 1.0 were measured by

performing multistage tests using solutions of potassium chloride (KCl). The source concentrations (C_{ot}) of the KCl solutions were 20 mM, 30 mM, and 50 mM, which resulted in average concentrations in the specimen at steady-state diffusion (C_{ave}) of approximately 10 mM, 15 mM, and 25 mM. For all values of *S*, a decrease in *S* correlated with an increase in ω and a decrease in D^*. For example, for C_{ot} of 50 mM, ω increased from 0.31 to 0.41 and D^* for chloride decreased from 4.1 x 10^{-10} m^2/s to 3.1 x 10^{-10} m^2/s as *S* decreased from 1.0 to 0.84. The results of this study advance our fundamental understanding of solute transport mechanisms in Na-bentonite and contribute to the base of knowledge that must be established prior to incorporating membrane behavior effects in the design of barriers for chemical containment facilities.

ACKNOWLEDGEMENTS

I would like to extend my sincere gratitude to Dr. Charles Shackelford for serving as my advisor, mentor and advocate throughout my graduate education. I also would like to thank Dr. Ning Lu, Dr. Christopher Bareither, Dr. Thomas Sale, and Dr. Gregory Butters for serving on my PhD committee.

I would like to thank my fellow graduate students for their assistance and support throughout this research endeavor, including Gretchen Bohnhoff, Catherine Soo Jung Hong, David Castelbaum, Amara Meier, Shan Tong, and Stephanie Moore. Thanks to Joe Wilmetti for his assistance in the laboratory and providing his mechanical magic that kept my research on track.

Most importantly, I would like to thank my mother, Linda Sample, mother- and father-in-law, Tom Lord and Rebecca Thatcher-Lord, sister-in-law, Sarah Lord, husband, Chad Lord, and daughter, Ava, for their love and unending support. There are no words to sufficiently express my gratitude to my husband for his patience, encouragement, and comedic relief throughout my pursuit of this degree. To my daughter Ava – thank you for keeping me grounded and providing me with true purpose and motivation.

Financial support for this project was provided by the U.S. National Science Foundation (NSF), Arlington, VA under Grant No. CMMI-0926205. The author thanks Colloid Environmental Technologies Co. (CETCO) for providing the bentonites used in this study. This support is gratefully acknowledged. The opinions expressed in this document are solely those of the author and are not necessarily consistent with the policies or opinions of the sponsors.

TABLE OF CONTENTS

LIST OF TABLES

LIST OF FIGURES

CHAPTER 1. INTRODUCTION

1.1 Background

Sodium bentonite (Na-bentonite) is a clay soil that exhibits high swell and low hydraulic conductivity in the presence of water and dilute solutions of salts (Eisenhour and Brown 2009; Gates et al. 2009). As a result, Na-bentonite often is considered for use as a barrier or barrier component in chemical containment applications, e.g., landfill clay liners, vertical cutoff walls, waste lagoons, radioactive waste disposal sites (Shackelford and Sample-Lord 2014). Such barriers/barrier components include Na-bentonite sandwiched between two geotextiles in the form of manufactured geosynthetic clay liners (GCLs), mixtures of Na-bentonite and sand placed as compacted clay liners (CCLs), mixtures of Na-bentonite, trenched spoils, and Na-bentonite slurry placed as soil-bentonite backfills (SBBs) for vertical cutoff walls, and highly-compacted Na-bentonite used as buffers for disposal of high-level radioactive waste (HLRW).

In addition to high swell and low hydraulic conductivity, Na-bentonite also may exhibit semipermeable membrane behavior, or the ability to selectively restrict the migration of dissolved chemical species (solutes) through the pores of the clay (e.g., Kemper and Maasland 1964; Kemper and Rollins 1966; Malusis et al. 2001; Malusis and Shackelford 2002; Kang and Shackelford 2009, 2010, 2011; Dominijanni et al. 2013). Membrane behavior (also referred to as anion repulsion) occurs in clays due to electrostatic repulsion of charged solutes by the electric fields surrounding the clay particles (Fritz 1986). Membrane behavior typically is quantified in terms of a membrane efficiency coefficient, ω, where values of ω range from 0 for no membrane behavior to 1.0 representing 100 % solute restriction corresponding to a perfect membrane (Shackelford et al. 2003). The existence of membrane behavior may enhance chemical

containment performance of Na-bentonite used in chemical containment applications by reducing diffusive transport of contaminants and promoting hyperfiltration and chemico-osmotic flow across the barrier (Shackelford 2013). However, current design and evaluation of such barriers typically neglect membrane behavior, largely due to a lack of fundamental knowledge of the phenomenon.

Previous measurement of membrane behavior of clays has been performed in the laboratory with both open and closed testing systems (Shackelford 2013). In both types of test systems, a concentration difference, ΔC, is applied across the specimen. If the clay behaves as a semipermeable membrane ($\omega > 0$), there will be a tendency for chemico-osmotic flow (q_π) to occur from the boundary with lower solute concentration (high water activity) to the boundary with higher solute concentration (low water activity). In an open system, q_π is allowed to occur and the measured value of q_π is used to calculate ω. In a closed system, q_π is prevented, resulting in the development of a chemico-osmotic pressure difference ($-\Delta P$) across the specimen to counteract the tendency for q_π. The measured values of $-\Delta P$ in the closed-system are used to determine ω. The use of a closed system allows for several testing advantages relative to open systems (Malusis et al. 2012; Shackelford 2013), including more accurate measurement of membrane behavior, easier control of boundary conditions, and achievement of linear concentration profiles across the specimen at steady-state diffusion allowing for simpler diffusion analyses (see Chapter 4). Thus, the use of a closed-system testing apparatus was preferred in this study.

Experimental studies to date have focused on membrane behavior and diffusion of solutes almost exclusively under saturated conditions (i.e., degree of water saturation, S, of the specimen of 1.0 or 100 %), even though clay barriers in field applications may exist under unsaturated

conditions. Based on our current, conceptual understanding of the mechanisms causing membrane behavior in clays, solute restriction under unsaturated conditions should be more significant than that under saturated conditions, all other factors being equal (Sample-Lord and Shackelford 2014). As a result of the aforementioned considerations, a study was undertaken to research the extent and magnitude of membrane behavior of Na-bentonite under unsaturated conditions and the effects of such membrane behavior on rates of diffusive transport.

1.2 Objectives of research

Given the limitations in our current understanding of the role of membrane behavior under unsaturated soil conditions, the goal of this study was to evaluate the existence and significance of membrane behavior in unsaturated Na-bentonite. This goal was accomplished by evaluating the following hypothesis:

> The significance of semipermeable membrane behavior in Na-bentonite exhibiting membrane behavior, as reflected by the membrane efficiency, increases as the degree of water saturation decreases, all other factors being equivalent.

This hypothesis was evaluated by completing the following objectives:

(1) develop and evaluate a new, closed-system testing apparatus for measuring membrane behavior and diffusive transport in unsaturated clays;
(2) develop and implement a procedure to prepare Na-bentonite specimens with properties that would result in measureable membrane behavior and diffusion under unsaturated

conditions;

(3) measure solute diffusion as a function of the degree of water saturation and solute concentration in the pore water of the bentonite and compare the results with available literature; and

(4) measure semipermeable membrane behavior as a function of the degree of water saturation and solute concentration in the pore water of the bentonite and compare the results with expectations based on our current, conceptual understanding of membrane behavior and data previously reported for saturated Na-bentonite.

Increased membrane behavior in Na-bentonite due to a reduction in degree of saturation was verified experimentally, achieving the goal of the study by confirming the proposed hypothesis. The results presented herein represent the first time membrane behavior has been measured for an unsaturated clay using a closed-system testing apparatus. In addition, the data represent the first experimental results for membrane behavior of Na-bentonite specimens maintained under unsaturated conditions. The results of this study advance our present understanding of membrane behavior in clays and contribute to the base of knowledge that must be established prior to incorporating membrane behavior effects in the design of barriers for chemical containment facilities.

1.3 Overview of dissertation

This dissertation includes six chapters. Chapters 1 and 6 provide the introduction and conclusions, respectively, for the overall study. The substantive results of the study are included in Chapters 2 through 5.

Chapter 2 is entitled, "Apparatus to Measure Membrane and Diffusion Behavior of Unsaturated Clays," and presents the design, fabrication and calibration of the new, closed-system testing apparatus to measure simultaneously both salt diffusion through and membrane behavior of unsaturated specimens of Na-bentonite. Details of the design and testing procedure are provided and the advantages and disadvantages of the new testing apparatus are discussed.

Chapter 3 is entitled, "A Dialysis Method for Homo-ionization of Bentonite," and describes a simple dialysis procedure that can be used to modify the exchange complex of bentonite specimens such that the bentonite becomes homo-ionized with respect to exchangeable sodium (Na^+). To enhance membrane behavior, the bentonite was treated to increase the percentage of Na^+ on the exchange complex of the clay, as well as remove excess soluble salts in the pore water. The dialysis method has been used extensively in the soil sciences to homo-ionize clays, but typically is not utilized in geotechnical and geoenvironmental research. In addition to specimen preparation, the dialysis procedure also was evaluated as a potential method to measure the apparent diffusion coefficient, D_a, of a clay slurry using available models that have been used to evaluate diffusion based leaching of contaminants from stabilized waste forms.

Chapter 4 is entitled, "A Through-Diffusion Method for Evaluating Solute Diffusion through Unsaturated Sodium Bentonite," and describes the use of the new testing apparatus for measurement of effective diffusion coefficients (D^*) of a salt (KCl) diffusing through unsaturated clays. The advantages and disadvantages of the closed-system test apparatus for diffusion testing of unsaturated soils are discussed and the analysis method to evaluate the test data is described in detail. The results of four multistage experiments for diffusion of KCl through unsaturated Na-bentonite specimens with S ranging from 0.79 to 1.0 are described. Measured values of D^* for

K^+ and Cl^- were reported and compared with the available literature. The results of the diffusion analyses were required for evaluation of the membrane behavior of the bentonite, as described in Chapter 5.

Chapter 5 is entitled, "Membrane Behavior of Unsaturated Sodium Bentonite," and presents the results of the experimental program to evaluate the measured membrane behavior of Na-bentonite as a function of S and solute concentration. The values of ω were determined via simultaneous measurement of the chemico-osmotic pressure difference induced by membrane behavior ($-\Delta P$) and D^* (as described in Chapter 4). The values of D^* were correlated with the membrane behavior to determine the values of the apparent and restrictive tortuosity factors of the bentonite specimens. The results are compared with membrane behavior literature for saturated Na-bentonite and conclusions are drawn regarding the significance of the effect of S on the solute restrictive behavior of Na-bentonite.

Chapter 6 summarizes the overall conclusions for the study. In addition, recommendations for future research are provided.

REFERENCES

Dominijanni, A., Manassero, M., and Puma, S. (2013) "Coupled chemical-hydraulic-mechanical behavior of bentonites." *Géotechnique*, 63(3), 191-205.

Eisenhour, D., and Brown, R. (2009). "Bentonite and its impact on modern life." *Elements*, 5(2), 83-88.

Fritz, S. (1986). "Ideality of clay membranes in osmotic processes: A review." *Clays and Clay Minerals*, 34(2), 214-223.

Gates, W., Bouazza, A., and Churchman, G. (2009). "Bentonite clay keeps pollutants at bay." *Elements*, 5(2), 105-110.

Kang, J., and Shackelford, D. (2009). "Clay membrane testing using a flexible-wall cell under closed-system boundary conditions." *Applied Clay Science*, 44(1-2), 43-58.

Kang, J. and Shackelford, C. (2010). "Membrane behavior of compacted clay liners." *Journal of Geotechnical and Geoenvironmental Engineering*, 136(10), 1368-1382.

Kang, J. and Shackelford, C. (2011). "Consolidation enhanced behavior of a geosynthetic clay liner." *Geotextiles and Geomembranes*, 29(6), 544-556.

Kemper, W., and Maasland, D. (1964). "Reduction in salt content of solution passing through thin films adjacent to charged surfaces." *Proceedings of the Soil Science Society of America*, 28(3), 318-323.

Kemper, W. and Rollins, J. (1966). "Osmotic efficiency coefficients across compacted clays." *Proceedings of the Soil Science Society of America*, 30(5), 529-534.

Malusis, M., and Shackelford, C. (2002). "Chemico-osmotic efficiency of a geosynthetic clay liner." *Journal of Geotechnical and Geoenvironmental Engineering*, 128(2), 97-106.

Malusis, M., Shackelford, C., and Maneval, J. (2012). "Critical review of coupled flux formations for clay membranes based on nonequilibrium thermodynamics." *Journal of Contaminant Hydrology*, Vol. 138-139, 40-59.

Malusis, M., Shackelford, C., and Olsen, H. (2001). "A laboratory apparatus to measure chemico-osmotic efficiency coefficients for clay soils." *Geotechnical Testing Journal*, 24(3), 229-242.

Shackelford, C. (2013). "Membrane behavior in engineered bentonite-based containment barriers: State of the art." *Proceedings of Coupled Phenomena in Environmental Geotechnics (CPEG)*, M. Manassero, A. Dominijanni, S. Foti, and G. Musso, eds., July 1-3, Torino, Italy, CRC Press/Balkema, Taylor & Francis Group, London, 45-60.

Shackelford, C., Malusis, M., and Olsen, H. (2003). "Clay membrane behavior for geoenvironmental containment." *Soil and Rock America Conference 2003*, P. J. Culligan, H. H. Einstein, and A. J. Whittle, Eds., Verlag Glückauf GMBH, Essen, Germany, 1: 767-774.

Shackelford, C., and Sample-Lord, K. (2014). "Hydraulic conductivity and compatibility of bentonite for hydraulic containment applications." *From Soil Behavior Fundamentals to Innovations in Geotechnical Engineering*, M. Iskander, J. Garlanger, and M. Hussein, Eds., Geotechnical Special Publication 233 Honoring Roy E. Olson, ASCE, Reston, VA, 370-387.

Sample-Lord, K., and Shackelford, C. (2014). "Membrane behavior of unsaturated bentonite barriers." *Proceedings of Geo-Congress 2014: Geo-Characterization and Modeling for Sustainability*, M. Abu-Farsakh, X. Yu, and L.R. Hoyos, Eds., Geotechnical Special Publication 234, ASCE, Reston, VA, 1900-1909.

CHAPTER 2. APPARATUS TO MEASURE MEMBRANE AND DIFFUSION BEHAVIOR OF UNSATURATED CLAYS

2.1 Introduction

High activity clays (e.g., bentonite) commonly used as barrier materials in chemical containment applications (e.g., landfills, radioactive waste disposal, animal waste lagoons, mine tailings containment) may behave as semipermeable membranes, whereby dissolved chemical species (solutes) in the pore water are selectively restricted from passage through the clay (e.g., Shackelford 2013). Because the primary objective of such chemical containment barriers is to reduce the rate and extent of migration of the chemicals into the surrounding environment, the existence of such solute restriction, referred to as membrane behavior, enhances the containment function of the clay barrier (Shackelford et al. 2003). Thus, a significant amount of effort has been extended towards the characterization of membrane behavior in a variety of clay barriers commonly used in chemical containment barrier systems (e.g., Malusis et al. 2001; Malusis and Shackelford 2002a,b; Manassero and Dominijanni 2003; Shackelford et al 2003; Lu et al. 2004; Dominijanni and Manassero 2005; Yeo et al. 2005; Henning et al. 2006; Evans et al. 2008; Kang and Shackelford 2010, 2011; Mazzieri et al. 2010; Dominijanni et al. 2013; Shackelford 2013; Bohnhoff et al. 2014; Meier et al. 2014; Tang et al. 2014, 2015).

Membrane behavior occurs in clays due to electrostatic repulsion of charged solutes by the electric fields associated with the clay particles (Fritz 1986). Under such conditions, chemico-osmotic flow (q_π) may occur, whereby water flows from higher water activity (lower solute concentration) to lower water activity (Shackelford et al. 2003). The extent to which the clay restricts the passage of solutes is quantified in terms of a reflection coefficient, σ, or

chemico-osmotic efficiency coefficient, ω, where σ or ω typically ranges from 0 for no membrane behavior to 1.0 representing 100 % solute restriction corresponding to a perfect membrane. The membrane efficiency for most natural clays that exhibit membrane behavior is in the range $0 < \sigma$ or $\omega < 100\%$ because of the variation in pore sizes. As a result, such clays are referred to as imperfect (or semipermeable) membranes. In the engineering literature, the symbol ω is preferred to represent the membrane efficiency, because the symbol σ commonly is used to represent applied or total stress (Shackelford 2013). Therefore, ω was used to represent membrane efficiency throughout this study.

Experimental research programs to measure membrane behavior of clays have utilized both open and closed hydraulic control systems (Shackelford 2013). In both types of test systems, reservoirs at each boundary of the specimen contain chemical solutions with different concentrations of the same solute to induce a concentration difference (ΔC) across the specimen. If the clay behaves as a semipermeable membrane ($\omega > 0$), then q_π will occur from the boundary with lower solute concentration (high water activity) to the boundary with higher solute concentration. In an open system, q_π is allowed to occur and may be measured to evaluate membrane behavior. In a closed system, q_π is prevented, resulting in the development of a chemico-osmotic pressure difference ($-\Delta P$) across the specimen to counteract the tendency for q_π. Since q_π is zero in a closed system, measured values of $-\Delta P$ are used to determine ω.

The use of a closed system allows for several testing advantages relative to open systems (Malusis et al. 2012; Shackelford 2013), including: (1) easier and more accurate measurement of parameters necessary to quantify membrane behavior (e.g., $-\Delta P$ typically can be measured more accurately that q_π); (2) easier control of boundary conditions than in open systems; and (3) linear concentration profiles across the specimen at steady-state diffusion, which allow for less

complex analyses than are required in open systems with nonlinear concentration profiles (see Chapter 4). Thus, development of a closed-system apparatus was preferred in this study for the measurement of coupled membrane behavior and diffusion in unsaturated clays.

Experimental research to date has focused on membrane behavior and diffusion in clays almost exclusively under water saturated conditions. The lack of experimental data that exists for membrane behavior of unsaturated clays is due, in part, to the increased complexity of the testing systems required to accommodate and control unsaturated conditions. However, there is a need for further experimental evaluation of unsaturated membrane behavior, as some clay containment barriers are likely to exist at various degrees of water saturation in some applications, such as disposal of high-level radioactive waste and in covers for landfills. Also, based on our current conceptual understanding of the phenomenon, membrane behavior under unsaturated conditions is expected to be more significant than under saturated conditions (Sample-Lord and Shackelford 2014).

The amount of experimental studies undertaken to evaluate membrane behavior in unsaturated soils has been limited (e.g., Letey et al. 1969; Bresler 1973; Bresler and Laufer 1974; James and Rubin 1986; Allred 2007). In addition, all of these previous studies have employed the use of open systems to quantify the membrane efficiency of the unsaturated soils, none of which were bentonite. Finally, conclusions regarding the relationship between observed membrane behavior and degree of saturation of the soils have been mixed. To the author's knowledge, there is little to no data available for membrane behavior in unsaturated, high activity clays such as sodium bentonite (Na-bentonite). Thus, the purpose of this study was to develop a closed-system testing apparatus that can measure coupled membrane behavior and diffusion in

unsaturated clays. The design and calibration of the new testing apparatus are described herein, and the results of a broader testing program are presented in Chapters 4 and 5.

2.2 Background

Several testing apparatuses to measure semipermeable membrane behavior of clayey soils have been reported (e.g., Letey et al. 1969; Olsen 1969; Whitworth and Fritz 1994; Keijzer et. al 1997,1999; Malusis et al. 2001; Shackelford and Lee 2003; Dominijanni et. al. 2013; Shackelford 2011, 2013). The most common, open-system method is the filtration (or hyperfiltration) method, whereby an electrolyte solution is forced through the soil specimen and the amount of filtered solute due to membrane behavior is quantified based on the difference between the known influent concentration and the collected effluent concentration (e.g., McKelvey et al. 1957; McKelvey and Milne 1962; Kemper 1961; Kharaka and Berry 1973; Hanshaw and Coplen 1973; Kharaka and Smalley 1976; Fritz and Marine 1983; Whitworth and Fritz 1994; Ishiguro et al. 1995; Hart and Whitworth 2005). An alternative, open-system method is to maintain a concentration gradient across the specimen (and no hydraulic gradient), and measure the amount of q_π that occurs (e.g., Kemper 1961; Kemper and Evans 1963; Kemper and Rollins 1966; Kemper and Quirk 1972; Keijzer et al. 1997, 1999). However, this latter open-system method is less common due, in part, to the difficulty of measuring the small flow quantities of chemico-osmotic flow and the difficulty in controlling the boundary concentrations (Shackelford and Lee 2003; Takeda et. al. 2014).

As previously described, prevention of chemico-osmotic flow in closed systems results in the development of a chemico-osmotic pressure difference, -ΔP, to counteract the tendency for chemico-osmosis (e.g., Elrick et al. 1976; Malusis et al. 2001; Malusis and Shackelford 2002a,b;

Shackelford and Lee 2003; Yeo et al. 2005; Kang and Shackelford 2009, 2010; Bohnhoff and et al. 2014). In these systems, differential pressure transducers and/or gauge pressure transducers at each boundary of the specimen are used to monitor the development of $-\Delta P$, which is used to determine ω. Such closed systems have been employed the use of both rigid-wall cells (e.g., Malusis et al. 2001; Bohnhoff et al. 2014) and flexible-wall cells (e.g., Kang and Shackelford 2009; Bohnhoff 2012) for testing clay specimens under a saturated condition. In the rigid-wall cell, the specimen is maintained at a constant volume throughout testing. In contrast, some volume change can occur in a flexible-wall cell during the refilling stage between circulation cycles, although the system is closed during the actual membrane measurement stages of the test such that no volume change is possible (Kang and Shackelford 2009). To limit the volume change of the unsaturated specimens during testing, a rigid-wall cell design was chosen for this research.

2.3 Testing apparatus

Several modifications to the aforementioned closed-system testing apparatuses commonly used for testing clay specimens under a saturated condition were required in this study to measure the membrane and diffusion behavior of unsaturated specimens. Most notably, high air-entry (HAE) disks were required at each boundary of the specimen to maintain the specimen at constant water content, an air pressure port in the cell walls was required to apply air pressure to the specimen and maintain positive pore-water pressures, and a flexible membrane between the specimen and the rigid sidewall was used to eliminate short-circuiting along the perimeter of the specimen.

In total, two independent apparatuses were developed to perform unsaturated membrane

and diffusion testing. Each apparatus was comprised of the following, dedicated components: (1) rigid-wall cell that contains the specimen; (2) hydraulic control system, including flow pumps, syringes, and stainless steel plumbing; (3) reservoirs for solution storage; (4) instrumentation for measurement and monitoring of pressures; and (5) a computer and data acquisition system. The testing system labeled Apparatus No. 1 is shown in Figure 2.1a, and was fabricated specifically for measuring membrane behavior and diffusion of unsaturated clays. In addition to evaluating membrane behavior, Apparatus No. 1 was designed with the capability to control and adjust the water content of a specimen during testing to allow for measurement of the soil-water-characteristic curve (SWCC) and data for the hydraulic conductivity function (HCF) between each stage of membrane testing. However, this feature of Apparatus No.1, which required the addition of a second flow pump and additional plumbing, was not utilized as part of this research due to time constraints.

The testing system labeled Apparatus No. 2, shown in Figure 2.1b, represents a version of the apparatus used by Bohnhoff (2012) that was modified to accommodate unsaturated conditions. For example, acrylic extensions were added to the top and base pedestals to accommodate the addition of the HAE disks. Also, the acrylic, outer cylinder was split vertically to allow for easier setup and disassembly and the use of a rubber membrane between the specimen and the outer cylinder. An air pressure port was added to the outer cylinder to allow for constant application of air pressure to unsaturated specimens. Additional details of each component in both testing systems (No.1 and No. 2) are discussed subsequently.

2.3.1 Rigid-wall cell

The rigid-wall cell developed in this study represented a modified version of the rigid-wall cell described by Malusis et al. (2001) for testing the membrane behavior of saturated specimens. In their cell (Figure 2.2a), the specimen was contained within a clear, hollow, acrylic (non-conductive) tube that serves as the rigid outer walls and between porous disks (GenPore porous sheet TO-6; General Polymer Corp., Reading, PA). The tube fits over the top piston and base pedestals machined from solid, acrylic cylinders, and o-rings placed around the circumference of the base pedestal and top piston to provide a seal with the outer cylinder. Inflow and outflow ports in the base pedestal and top piston allow for circulation of liquids through the porous plastic disks along the top and bottom boundaries of the specimen. Additional ports were located in the center of the top piston and base pedestal for measurement of the boundary water pressures at the top and bottom of the specimen, respectively.

For testing the unsaturated specimens in this study, the rigid-wall cell shown in Figure 2.2a was modified to accommodate custom machined, HAE disks (Soilmoisture Equipment Co., Santa Barbara, CA) located immediately above and below the specimen to control and maintain the gravimetric water content, *w*, during testing (Figures 2.2b and 2.3). For the rigid-wall cell in Apparatus No.1, the outer diameters of the top and base were increased to 83 mm, and a 65-mm-diameter step was machined to seat the HAE disk. For the rigid-wall cell used in Apparatus No.2, a hollow, acrylic tube with the same outer dimension as the top and base pedestals was sliced into 7.2-mm-thick pieces that were used to extend the top and base pedestal to accommodate the 7.14-mm-thick HAE disks (see Figure 2.4).

The HAE disks are ceramic disks that have small pores of relatively uniform size and act as a membrane between the air and water phases (Fredlund and Rahardjo 1993; Lu and Likos

2004). Once the disks are saturated, air does not pass through the pores unless the matric suction, ψ_m (air pressure adjacent to the disk minus the water pressure in the disk), exceeds the air-entry pressure of the disks. The value of the air-entry pressure of an HAE disk is controlled primarily by the radius of curvature of the largest pore in the disk (Fredlund and Rahardjo 1993). Therefore, disks with smaller pore sizes have higher values of air-entry pressure, and can accommodate higher matric suctions. Values for the air-entry pressure typically are provided by the manufacturer.

As shown in Figure 2.2, the HAE disks act as an interface between the unsaturated soil specimen and the pore-water pressure lines, allowing for measurement of the pore-water pressure at the specimen boundaries without changing the degree of water saturation, *S*, of the specimen. If the suction exceeds the air-entry pressure of the disks, air bubbles can pass from the specimen, through the disks, and into the pressure lines, resulting in errors in pressure measurements. Thus, a minimum difference of 50 kPa between the initial suctions and the rated entry pressures of the disks was used to allow for potential variability in the specimen suction or imperfections in the disks. For this study 3-bar (300-kPa) and 5-bar (500 kPa) HAE disks were used to accommodate specimens values of ψ_m up to 250 kPa and 450 kPa, respectively.

During testing, solutes within the chemical solutions being circulated at the boundaries of the HAE disks must diffuse through the disks prior to reaching the boundaries of the clay specimen (see Figure 2.2b). However, published information regarding effective diffusion coefficients of HAE disks for salts is limited (e.g., Barbour et al. 1996), and such information was unavailable for the disks required in this study (3-bar and 5-bar). Therefore, calibration tests (without a soil specimen) were performed to measure the diffusion properties of the HAE disks. The calibration tests also confirmed that the HAE disks did not exhibit any measurable

membrane behavior (i.e., $-\Delta P = 0$) and, therefore, did not affect the $-\Delta P$ measurements. Further details of the calibration testing are described subsequently (see Section 2.5).

Another design modification to the rigid-wall cell required for unsaturated testing was the ability to maintain positive pore-water pressures, *u*, and avoid potential cavitation during testing of specimens at low gravimetric water content, *w* (i.e., at high suctions). Therefore, a constant air pressure greater than the matric suction of the specimen was applied during testing via the air pressure port (see Figure 2.2c) to maintain positive *u*. The pressure line from the regulated air pressure source to the testing cell was routed through a vapor chamber partially filled with de-ionized water (DIW) to limit evaporation from the specimen. The air-pressure port was aligned with the midpoint of the specimen (vertically) during assembly. Filter paper and a geotextile were secured between the air-pressure port and the edge of the specimen to ensure there was no loss of solid material through the port during setup. A thin strip of filter paper was placed along the specimen perimeter and in contact with the air pressure port to distribute the applied air pressure (see Lu et al. 2006).

A concern for membrane testing when chemical solutions with high concentrations are used is the development of "short-circuiting" between the perimeter of the specimen and the rigid, sidewall due to shrinkage of the specimen (e.g., Bohnhoff 2012; Bohnhoff et al. 2014). Such shrinkage can result in the loss of contact between the clay and the rigid wall, thereby resulting in a short circuit or bypass between the pressure at the top and bottom of the specimen, such that the $-\Delta P$ induced by solute restriction can no longer be maintained in the test system (i.e., $-\Delta P \rightarrow 0$). Therefore, the cell for unsaturated membrane testing was modified to accommodate the addition of a flexible membrane between the specimen and the rigid, side wall that would maintain a tight seal with the specimen to prevent such short circuiting. In addition,

if the water content of the specimen was reduced (e.g., on purpose, via axis translation, as described subsequently) and shrinkage occurred under the higher suction, then the flexible membrane would continue to maintain good contact with the specimen perimeter to avoid short-circuiting.

Another important difference between the designs of the new and previous test cells was the acrylic, outer cylinder. The modified outer cylinders were split vertically to allow for easier setup and disassembly and, correspondingly, less disturbance to the specimen. The halves of the outer cylinder were secured via four metal bands around the perimeter, as shown in Figure 2.5.

2.3.2 Hydraulic control system

A hydraulic control system is required to establish and maintain a concentration gradient across the specimen in order to evaluate the membrane efficiency and diffusion properties of the clay specimen. Pictorial and schematic views of the hydraulic control system used in this study, which was based on that described by Malusis et al. (2001), are provided in Figures 2.1 and 2.6, respectively.

In order to establish and maintain a difference in concentration, ΔC, across the specimen during testing, chemical solutions and DIW were circulated continuously across the top and bottom boundaries of the specimen, respectively, using a dual-carriage flow-pump (Model 944, Harvard Apparatus, Holliston, MA) with two stainless-steel syringes on separate tracks. On the "infuse" setting, the pistons inside each syringe displace the liquids (i.e., either chemical solution or DIW) from the front of the syringes at a constant rate through the porous plastic disks adjacent to the HAE disks. The solutions are circulated through the porous plastic disks at each boundary of the specimen to establish a ΔC across the specimen to induce membrane behavior. After

circulating across the boundaries, the solutions emanate from the outflow ports and then into the back end of the syringes (i.e., behind the plungers). When the syringes are refilled with fresh solution (every two days in this study), the collected effluent is emptied into 50-mL vials for chemical analyses and measurement of electrical conductivity, *EC*, and pH. All of the plumbing between the flow pump and the cell consists of stainless-steel valves and tubing, typically with 3.2-mm (1/8-in) diameter, in an effort to minimize corrosion and potential volume change of the circulation system. Each circulation system (top and bottom) represents a closed loop, such that the amount of liquid contained in each circulation system remains constant during each circulation period (e.g., see Malusis et al. 2001). In addition, liquid flow through the specimen during the membrane measurement stage is prevented from occurring. Therefore, there is no volume change in the system during circulation of the solutions (i.e., the system is closed).

The testing is performed in stages. Generally, the first stage consists of circulating DIW across both top and bottom boundaries to establish the baseline value of $-\Delta P$. Once steady baseline pressures are established, the DIW at the top boundary is switched to KCl solution, resulting in an increase in the value of $-\Delta P$, i.e., if membrane behavior exists in the specimen. After both steady-state values of $-\Delta P$ and diffusion (discussed subsequently) have been established, the ΔC is increased via circulation of a higher concentration KCl solution to begin a new subsequent stage of the same test. The procedure is repeated using progressively higher salt concentrations across the top, such that progressively higher values of ΔC are established across the system.

Modifications were made to the unsaturated testing apparatus to allow for changing the *w* of the specimen during testing, if desired. Using axis translation, the *w* of the specimen may be changed by increasing the air pressure, withdrawing a controlled volume of water from the

specimen, and allowing the specimen to re-equilibrate at the new *w* and suction (Lu et al. 2006). The pressures (suctions) at the top and bottom boundaries of the specimens are monitored with differential pressure transducers (see subsequent section). A second syringe pump can be used for withdrawing a specified volume of water, as well as for performing a constant-flow hydraulic conductivity (*k*) test at each new *w* value as described by Olsen et al. (1991). Thus, the modified apparatus is capable of measuring not only unsaturated membrane behavior, but also the soil-water-characteristic curve and hydraulic conductivity function of the same specimen between stages of the multistage membrane test, although neither of these capabilities was utilized in the current study.

2.3.3 Instrumentation, data acquisition and chemical analyses

Differential and gauge pressure transducers were used in the membrane testing apparatuses to measure the water pressures at each boundary (u), water pressures relative to the applied air pressure (i.e., suctions, ψ), and pressure differences across the specimen induced by membrane behavior ($-\Delta P$). In Apparatus No. 1, two differential pressure transducers (DPT2 and DPT3) were used to measure water pressure at the top and bottom specimen boundaries (u_{top} and u_{bottom}) relative to the applied air pressure (P_{air}), representing the total suction (ψ_t) at each boundary (i.e., $P_{air} - u_{top} = \psi_{t,top}$, $P_{air} - u_{bottom} = \psi_{t,bottom}$). In addition, two separate differential pressure transducers were used to measure the $-\Delta P$ across the specimen (DPT1 and DPT4). The range of measurable pressure differences for DPT1, DPT2 and DPT3 were +/- 207 kPa (30 psi) (Omega Engineering Inc., Model PX26-030DV, Stamford, CT), whereas that for DPT4 was +/- 34 kPa (5 psi) (Omega Engineering Inc., Model PX26-05DV, Stamford, CT). The pressure lines

to DPT4 were opened only during low pressure conditions (e.g., < 34 kPa (5 psi)), when higher resolution of pressure data was desired.

In Apparatus No. 2, two gauge pressure transducers (Omega Engineering Inc., Model PX209-015G10V, Stamford, CT) were used to measure the boundary pressures, and one differential transducer (Validyne Engineering Corp., Model DP15, Northridge, CA) was used to directly measure the $-\Delta P$ across the specimen. The air pressure was measured separately via a gauge pressure transducer attached to the plumbing to the air pressure port (model No. PX181-100G5V, Omega Engineering Inc., Stamford, CT). The maximum values of the gauge and differential pressures for the transducers connected to the boundaries of the specimen were 103 kPa (15 psi) and 86 kPa (12.5 psi), respectively. The range of the gauge transducer for the air pressure line was 689 kPa (100 psi).

For each apparatus, all of the pressure data was recorded with data acquisition (DAQ) systems consisting of a circuit board (SCB-68, National Instruments, Austin, TX), a DAQ device (National Instruments, Austin, TX), and LabVIEW software (National Instruments, Austin, TX). A relative humidity and ambient temperature recorder (Extech Instruments, Model RH520A, Nashua, NH) was mounted near both apparatuses to monitor atmospheric changes that may affect pressure readings. The pH and *EC* of the circulation outflows collected during the refilling of the syringes every two days were measured with a conductivity meter (150 A+ Conductivity Meter; Thermo Orion, Beverly, MA). Anion concentrations (e.g., Cl^-) were analyzed using ion chromatography, or IC (Dionex® 4000i IC Module, Dionex Co., Sunnyvale, CA), whereas cation concentrations (e.g., K^+, Na^+, Ca^{2+}) were measured with inductively coupled plasma-atomic emission spectrometry, or ICP-AES (IRIS® Advantage/1000 ICAP Spectrometer, Thermo Jarrel Ash Co., Franklin, MA).

2.3.4 Solutions and reservoirs

The liquids circulated at the specimen boundaries during membrane testing consisted of DIW and electrolyte solutions of KCl (certified A.C.S., Fisher Scientific, Fair Lawn, NJ) dissolved in DIW. Membrane behavior research is still at a fundamental level of study and, therefore, chemical solutions used in laboratory testing typically have been comprised of simple salt solutions (e.g., KCl, NaCl, $CaCl_2$) versus, for example, the more complex chemical solutions commonly encountered in practice (e.g., leachates). The measured solution concentrations of KCl in the solutions used in this study ranged from 7.0 mM to 50 mM. The KCl solutions were prepared and stored in 20-L carboys (Nalgene®, Thermo Fisher Scientific, Rochester, NY), which were used to fill the acrylic reservoirs attached to the hydraulic plumbing of each testing apparatus. To confirm the desired concentrations of the prepared solutions, the *EC* of the solutions were measured with the conductivity probe, and collected samples were analyzed via IC and ICP, as previously described.

After the acrylic reservoirs were filled with fresh solution from the carboys, vacuum was applied to the reservoirs using a vacuum pump (Model LAV-3, Fischer Technical Co., Roselle, IL) to eliminate air bubbles in the solution. The vacuum was maintained on the reservoirs until the syringes were refilled. During refilling, the vacuum pressure was released, and solution was drawn from the reservoirs to the syringes. After refilling, vacuum was reapplied and the reservoirs were closed.

2.4 Testing procedure

2.4.1 System preparation

Prior to starting a new test to measure diffusion and membrane behavior of a bentonite

specimen, the following steps were required to prepare the testing system:

- to ensure the HAE disks were saturated, the disks were submerged in de-aired water for several days (> one week) and then placed inside a reservoir, to which a vacuum was applied using the aforementioned vacuum pump;
- all of the reservoirs were emptied, cleaned, and refilled with fresh, de-aired DIW;
- all plumbing, syringes and pressure lines were flushed with de-aired DIW to remove air bubbles and/or solution from previous tests;
- all pressure transducers were recalibrated and new calibration factors were entered into the LabVIEW software;
- the unsaturated specimen was assembled in the testing cell, a constant air pressure greater than the matric suction was applied immediately to maintain positive water pressures, and the system was allowed to equilibrate for at least 5 days; and
- several (> 7), two-day circulation cycles were completed with DIW circulating at each boundary to flush any remaining bubbles from the system and establish baseline pressures.

After completion of the system preparation procedure, and establishment of steady baseline pressures and *EC* during DIW circulation, the first stage for membrane behavior testing was initiated. A general representation of the baseline pressure during the DIW stage, as well as typical $-\Delta P$ data measured during a multi-stage test, is shown in Figure 2.7.

Since the applied concentration gradient was zero during the DIW stage, the $-\Delta P$ due to membrane behavior theoretically should be zero. However, slightly non-zero values may result,

for example, due to imperfections in the machining of the syringes (i.e., the volume capacities of each syringe are not exactly the same), resulting in slight differences in the volume flow rates from each syringe, and/or from slightly different hydraulic conductivity values for the porous disks, resulting in different head (pressure) losses between the entrance points for the circulation liquids and the locations in the middle of the disks where the pressures on top and bottom are monitored (Malusis et al. 2001).

2.4.2 Membrane behavior and diffusion testing stage

Continuous circulation of DIW or electrolyte solution at each boundary resulted in a constant ΔC across the HAE disk-specimen-HAE disk system. A constant ΔC across the specimen was achieved once steady-state diffusion was reached. If the specimen acted as a semipermeable membrane, then a $-\Delta P$ developed across the specimen in response to the ΔC. Each concentration stage (e.g., 20 mM, 30 mM) was continued until steady-state diffusion (quantified by the chemical flux from the measured outflow concentrations) and steady values of $-\Delta P$ were observed. After both steady-state diffusion and $-\Delta P$ were established, the concentration of the KCl solution was increased to begin a new, subsequent stage of the test.

The circulation rate of the liquid was dependent on the displacement rate and cross-sectional area of the syringes. During the circulation phase of the membrane tests, the rate was maintained at 2.3×10^{-10} m^3/s (approximately 40 mL every two days). This rate, which was chosen based on previous studies (e.g., Malusis et al. 2001; Shackelford and Lee 2003; Bohnhoff 2012), allowed for maintaining approximately "perfectly flushing" boundary conditions and achieving a steady value of $-\Delta P$ during each circulation period. At this circulation rate, each

circulation cycle lasted approximately two days until the liquid capacity of the syringes was exhausted such that the syringes had to be refilled.

2.4.3 Hydraulic conductivity testing

If desired, at the end of the circulation stage with DIW, and prior to circulation with electrolyte solutions, a constant-flow *k* test may be performed utilizing the flow pump. The benefits of including this additional step are two-fold: (1) to flush remaining soluble salts from the specimen if desired for the purpose of enhancing the likelihood of significant membrane behavior (e.g., Malusis and Shackelford 2002a); and (2) to obtain data to construct a hydraulic conductivity function (HCF) curve for the clay. However, due to time constraints, the *k* testing stage was conducted only for the test with the saturated specimen ($S = 1$). The time that would be required for matric suction and water content conditions to return to equilibrium throughout the unsaturated specimens after a constant-flow *k* test was unknown, such that this optional step was not undertaken to minimize the durations of the tests with unsaturated specimens.

During the *k* testing stage for the saturated specimen, one syringe on the flow pump was used to force freshly de-aired, DIW through the specimen and HAE disks. A constant-flow rate, *q*, of DIW from the bottom, upward and through the specimen was maintained. The pressure difference across the specimen, Δu ($= u_{top} - u_{bottom}$), induced by *q* was measured with the same pressure transducers used to measure $-\Delta P$ during the membrane test stages. Once a steady value of Δu was achieved, *k* could be calculated based on Darcy's law written as follows:

$$k = -\frac{qL}{A\frac{\Delta u}{\rho_w g}} \tag{2.1}$$

where A and L are the specimen cross-sectional area and thickness, respectively, ρ_w is the density of water (1 kg/m^3), and g is acceleration due to gravity (9.81m/s^2). The maximum q that could be applied was limited by the range of the pressure transducers, i.e., the Δu that could be accommodated by the testing system. The values of k and, thus, Δu that will be induced by the applied q during the k testing stage may be unknown prior to testing, particularly for the unsaturated specimens. Therefore, initial attempts in performing a constant-flow k test required carefully monitoring the pressure buildup to make sure this does not approach the limit of the pressure transducer. If the pressure buildup does approach a limiting value, the applied flow should be stopped to allow the buildup in pressure to fully dissipate, and then the procedure can be restarted using a slower applied flow rate. Thus, careful, real-time monitoring is required during the k testing stage.

2.5 System calibration tests

2.5.1 System baseline pressures

If a constant-flow k testing stage is performed, then the pressure difference across the system, Δu, induced by the applied q should be measured and used to calculate the k of the specimen in accordance with Darcy's law. However, because of the existence of the porous HAE disks on both sides of the specimen, a constant-flow k test was performed only using the HAE disks (no specimen) in order to determine the magnitude of the pressure difference across the system that is attributable to the HAE disks. This test, referred to as a "blank-sleeve" test (Lu et al. 2006), was performed as part of the calibration process for each testing apparatus.

A schematic of the setup for the blank-sleeve test is provided in Figure 2.8. Example results are shown in Figures 2.9 for the 3-bar and 5-bar HAE disks. An estimate of the value of

the saturated k, k_{sat}, of the HAE disks (+/- 10 %) was provided by the manufacturer (Soilmoisture Equipment Co., Santa Barbara, CA), such that the portion of Δu that occurs across the disks during a k test also could be estimated. However, completion of blank-sleeve tests was required to determine the actual value of k_{sat} for each set of disks and to calculate an accurate value of k for the specimens.

The measured values of k_{sat} for the HAE disks, as well as the values provided by the manufacturer, are summarized in Table 2.1. The measured value of k_{sat} for the 3-bar disk was 1.6 x 10^{-9} m/s, which was slightly lower than the range of k_{sat} values reported by the manufacturer of 2.2 x 10^{-9} m/s to 2.8 x 10^{-9} m/s. The measured value of k_{sat} for the 5-bar disk was 9.0 x 10^{-10} m/s, which also was slightly lower than the range of k_{sat} values reported by the manufacturer of 1.1 x 10^{-9} m/s to 1.3 x 10^{-9} m/s. Multiple k tests were performed on each HAE disk and similar values of k were obtained in each test, which suggested the disks were fully saturated and that the measured results were accurate. For example, for the 3-bar disks, eight k tests were performed for constant flow rates ranging from 1 x 10^{-10} m^3/s to 5 x 10^{-9} m^3/s and the measured values of k all fell within the range of 1.3 x 10^{-9} m/s to 1.7 x 10^{-9} m/s. The differences between the measured values of k_{sat} and the average values reported by the manufacturer are likely due, in part, to slight differences in the pore structure of each disk (i.e., ceramic disks with the same air-entry may not by completely identical) and differences in the methods used to determine k_{sat}.

2.5.2 Diffusion across high air-entry disks

To accurately analyze the diffusion behavior of the clay specimens, the diffusion properties of the HAE disks also must be known. However, limited information pertaining to the chemical diffusion properties of ceramic HAE disks is available in the literature or from

manufacturers. Barbour et al. (1996) measured diffusion and adsorption of ions in unsaturated, sandy soils, utilizing the axis-translation technique and HAE disks (0.5 bar) to control ψ_m. Potassium (K^+) and chloride (Cl^-) ions were used as the primary tracers. To calculate the diffusion and adsorption coefficients of the soils, Barbour et al. (1996) performed additional tests to quantify the properties of just the HAE disks. The effective diffusion coefficient, D^*, and distribution coefficient for adsorption, K_d, of the 0.5-bar HAE disks reported in Barbour et al. (1996) are shown in Table 2.1.

Similar calibrations tests were performed for the HAE disks associated with the two testing apparatuses described herein. For these calibration tests, KCl and DIW solutions were circulated across the top and bottom boundaries of the disks, respectively, mimicking the conditions to be applied during normal membrane testing (same setup, but without the clay specimen). A schematic of the setup for the calibration tests is shown in Figure 2.10. Since the HAE disks must remain fully saturated, there was no matric suction in the cell, such that the application of a constant air pressure (to maintain positive water pressures) was not necessary. The HAE disks did not exhibit membrane behavior, as expected, so the value of $-\Delta P$ was approximately zero throughout the calibration test.

Although the diffusion properties of the ceramic disks were expected to remain approximately constant, the calibration tests were performed as multi-stage tests to confirm that the diffusion properties did not change significantly upon exposure to increasing KCl concentrations (C_{ot}) ranging from 7.0 mM to 50 mM KCl. Salt diffusion occurred through both of the HAE disks, from the top boundary of the upper disk to the bottom boundary of the lower disk. The through-diffusion method was used to determine the steady-state diffusion parameters of the disks based on measured effluent concentrations (Shackelford 1991, 1995; Malusis et al.

2001; Malusis and Shackelford 2002b). A brief description of the procedure for analysis of diffusion test data using the through-diffusion method is provided subsequently.

The circulation outflow from the bottom boundary of the HAE disks was accumulated in the back of the syringe during the circulation stage. The time increment, Δt, for effluent collection (i.e., the duration of one circulation period) was two days. During the refilling stage, the effluent was collected in a 50-mL vial and the volume (ΔV) and *EC* of the sample were measured (Figure 2.11a). The cation and anion concentrations in the sample were determined via IC and ICP analysis (Figure 2.11b). The solute concentrations, C_b, of the species of interest were used to calculate the incremental mass of solute (Δm) that had diffused across the disks over the time increment, Δt (i.e., $\Delta m = \Delta V C_b$). The values of Δm for each time increment were summed to determine the cumulative solute mass m (= $\Sigma \Delta m$) versus the cumulative elapsed time, t. The value of m was divided by the cross-sectional area of the HAE disks to determine the cumulative mass per unit area, Q_t. As shown in Figure 2.12, Q_t was plotted versus t, and the steady-state portion of the curve (e.g., the linear portion) was used to calculate the steady-state D^* based on Equation 2.2:

$$D^* = -\left(\frac{L}{n\Delta C}\right)\left(\frac{\Delta Q_t}{\Delta t}\right)\Bigg|_{steady-state} \tag{2.2}$$

where L is the total length of the system (= 2 x L_{HAE} for the calibration tests, where L_{HAE} is the thickness of one HAE disk), n is the porosity of the HAE disks as reported by the manufacturer (0.34 for 3-bar disks, 0.31 for 5-bar disks), and ΔC is the total concentration difference across the disks. Example data for the HAE-disk diffusion tests are shown in Figures 2.11 and 2.12, and

the results are summarized in Table 2.1.

The measured values of D^* (Table 2.1) from the calibration tests performed in this study were in general agreement with those reported by Barbour et al. (1996). Similar to the saturated hydraulic conductivity, as the air-entry pressure of the disk increased (and the maximum pore size decreased), the value of D^* decreased. For example, as the air-entry pressure of the HAE disks increased from 3-bar to 5-bar (corresponding to a decrease in maximum pore size from 0.7 μm to 0.5 μm), the D^* decreased slightly from 1.64 x 10^{-10} m^2/s to 1.39 x 10^{-10} m^2/s. As shown in Figure 2.13, the measured value of D^* of the HAE disks increased with increasing values of k_{sat}.

Based on the results of the calibration tests, using HAE disks with a higher air-entry pressure likely would result in longer test durations to reach steady-state diffusion (due to lower D^* of the disks) during the multi-stage membrane tests for the unsaturated bentonite specimens. As a result, only disks with lower air-entry pressures (e.g., 3-bar and 5-bar) were considered in the development of the two testing apparatuses, which limited the range of ψ_m (i.e., range of S) the test apparatuses were able to accommodate.

2.6 Summary and conclusions

Previous experimental research programs focused on the measurement of membrane behavior and diffusion in clays have utilized both open and closed test systems. The use of a closed system allows for several testing advantages relative to open systems, including more accurate measurement of membrane behavior, easier control of boundary conditions, and the development of linear concentration profiles across the specimen at steady-state diffusion. Experimental research to date has focused on membrane behavior of clays almost exclusively

under water saturated conditions, even though membrane behavior under unsaturated conditions is expected to be more significant than under saturated conditions. The limited number of experimental studies that have been performed to evaluate membrane behavior in unsaturated soils only have employed the use of open systems to quantify membrane efficiency. Thus, the purpose of this study was to develop a closed-system testing apparatus that could measure coupled membrane behavior and diffusion in unsaturated clays.

A new testing apparatus to measure membrane behavior and diffusion in unsaturated clays was designed, fabricated, calibrated, and used as part of a broader testing program (see Chapters 4 and 5). The major components of the testing apparatus included the following: (1) rigid-wall cell that contained the specimen; (2) closed hydraulic control system, which included flow pumps, syringes, and stainless steel plumbing; (3) reservoirs for solution storage; (4) instrumentation for measurement and monitoring of water pressures, air pressures, and total suctions; and (5) a computer and data acquisition system. Unique aspects of the new apparatus relative to closed-system apparatuses that previously have been used to evaluate membrane behavior of saturated clays included: (1) the addition of HAE disks located immediately above and below the specimen to control and maintain water content and matric suction during testing; (2) application of constant air pressure to the unsaturated specimen to maintain positive water pressures and avoid cavitation in the pressure lines; (3) the addition of a flexible membrane between the specimen and the rigid, side wall to prevent short circuiting; and (4) the use of a split outer cylinder to allow for easier test setup and disassembly, minimizing disturbance to the prepared specimen.

In order to evaluate the membrane behavior and diffusion of unsaturated clay specimens tested in the new apparatus, calibration tests must be performed to determine the diffusion

properties of the HAE disks. The through-diffusion method was used to determine the steady-state diffusion properties of the disks based on measured effluent concentrations over time. The effective diffusion coefficients for KCl for the 3-bar and 5-bar HAE disks were 1.64×10^{-10} m^2/s and 1.39×10^{-10} m^2/s, respectively. The results of the calibration tests were used to analyze the results obtained from membrane behavior and diffusion testing of unsaturated bentonite specimens, as described in Chapters 4 and 5. The development of a closed-system testing apparatus capable of accommodating unsaturated soils advances the state-of-the-art for laboratory measurement of membrane behavior and diffusion in clays used as barrier materials for chemical containment applications.

Table 2.1. Properties of high air-entry disks.

Air-Entry Value of Disk (bars)	Saturated Hydraulic Conductivity, k_{sat} (m/s)		Porosity, n [a]	Measured Effective Diffusion Coefficients using KCl Solutions, D^* (m^2/s)	Measured Adsorption Coefficients using KCl Solutions, K_d (m^3/kg)
	Reported by Manufacturer [a]	Measured			
0.5	3.1×10^{-7} ± 10 %	NR	0.51	7.5×10^{-10} [b]	7×10^{-5} (Cl^-) 1×10^{-4} (K^+) [b]
3	2.5×10^{-9} ± 10 %	1.6×10^{-9}	0.34	1.64×10^{-10} [c]	3×10^{-4} (Cl^-) 1×10^{-3} (K^+) [c]
5	1.2×10^{-9} ± 10 %	9.0×10^{-10}	0.31	1.39×10^{-10} [c]	2×10^{-4} (Cl^-) 6×10^{-4} (K^+) [c]

NR = Not reported.

a. As reported by Soilmoisture Equipment Corp (Santa Barbara, CA).
b. Barbour et al. (1996); dry density (ρ_d) of 0.5-bar disks reported as 1,550 kg/m^3.
c. Results from first concentration stage of calibration tests performed as part of this research; dry density (ρ_d) of 3-bar and 5-bar disks are 1,731 kg/m^3 and 1,733 kg/m^3, respectively.

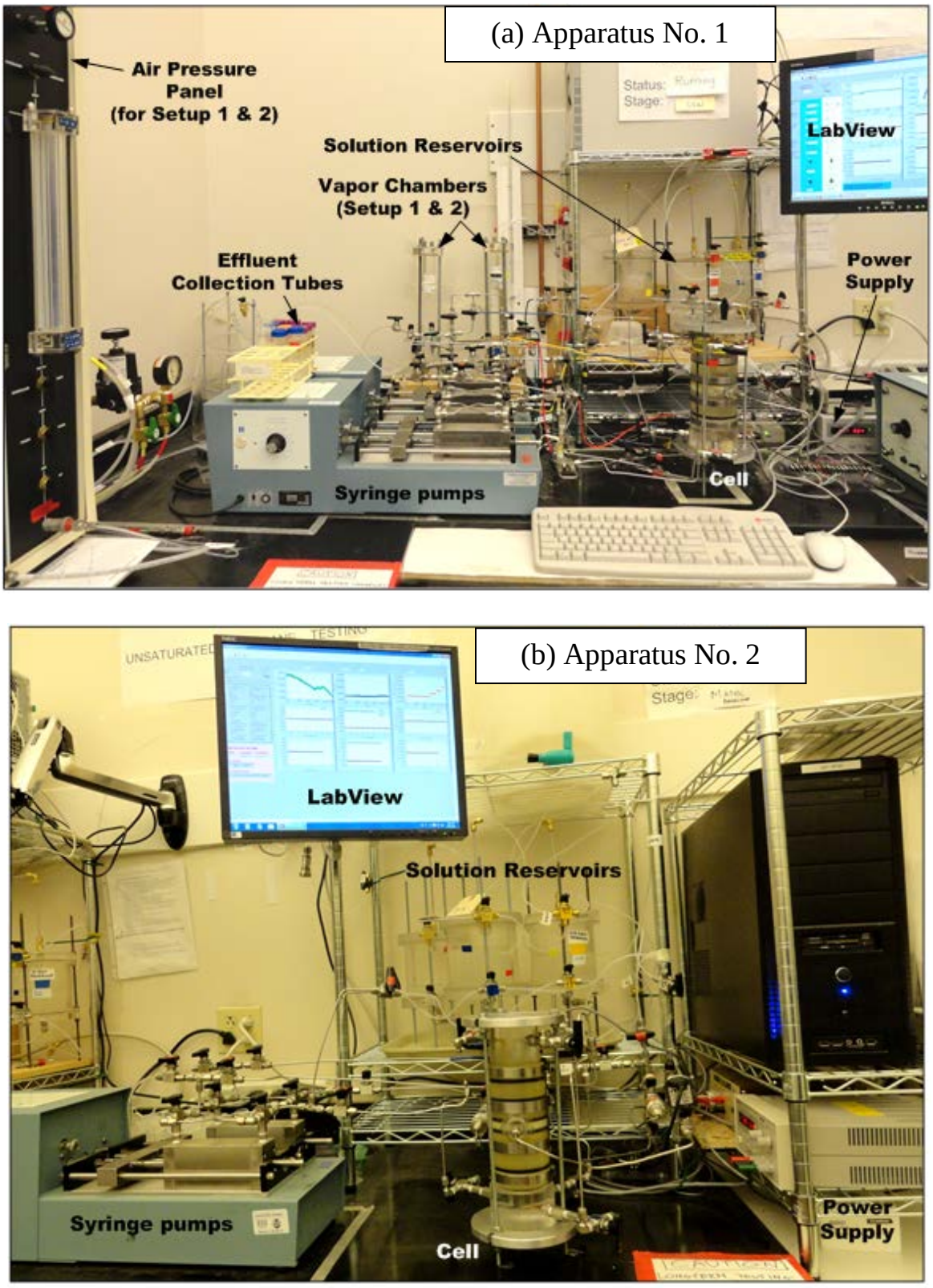

Figure 2.1. Pictorial views of (a) Apparatus No. 1 and (b) Apparatus No. 2.

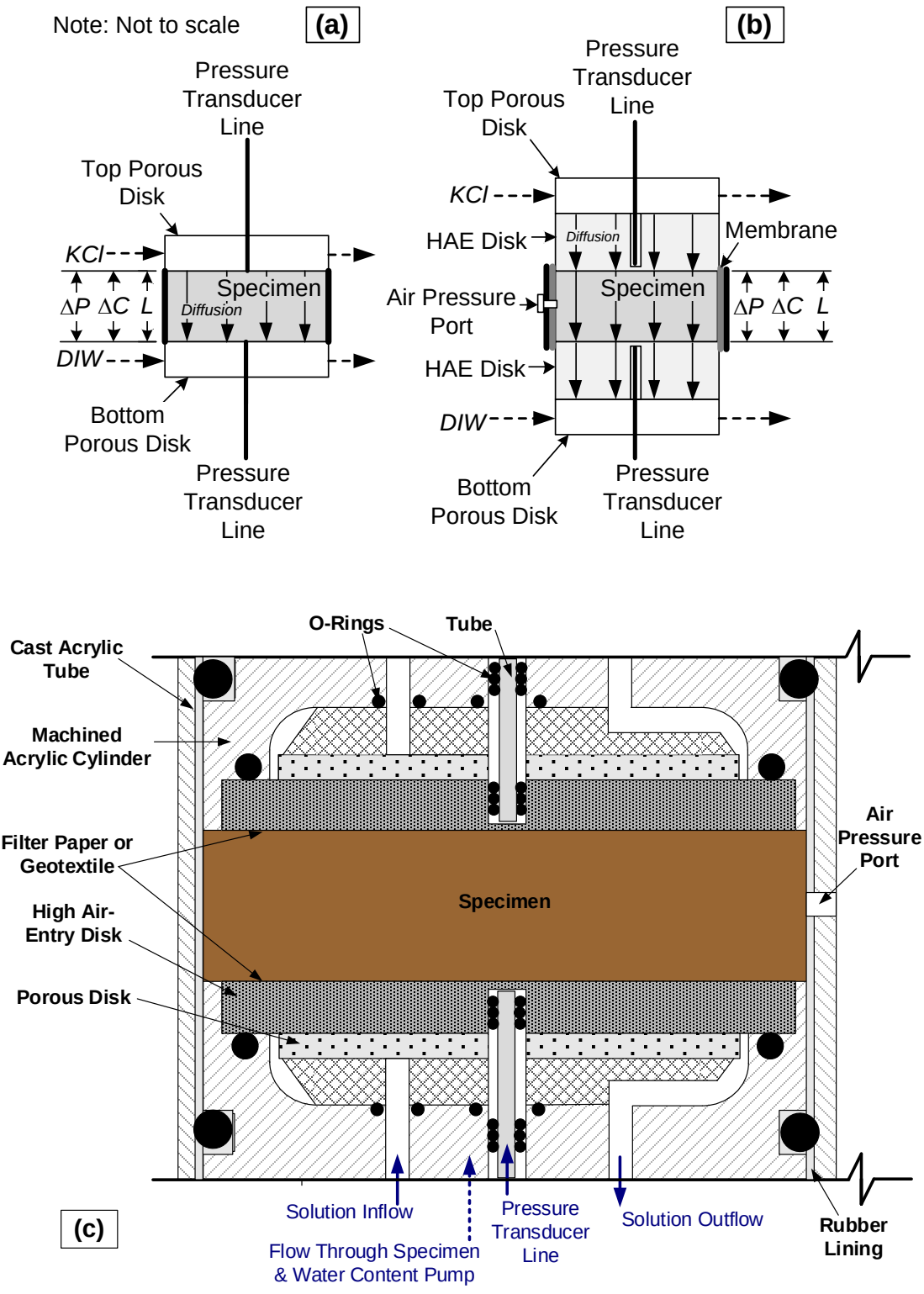

Figure 2.2. Schematics of rigid-wall cell designs used in membrane behavior studies: (a) saturated specimens (Shackelford 2013); (b,c) unsaturated specimens.

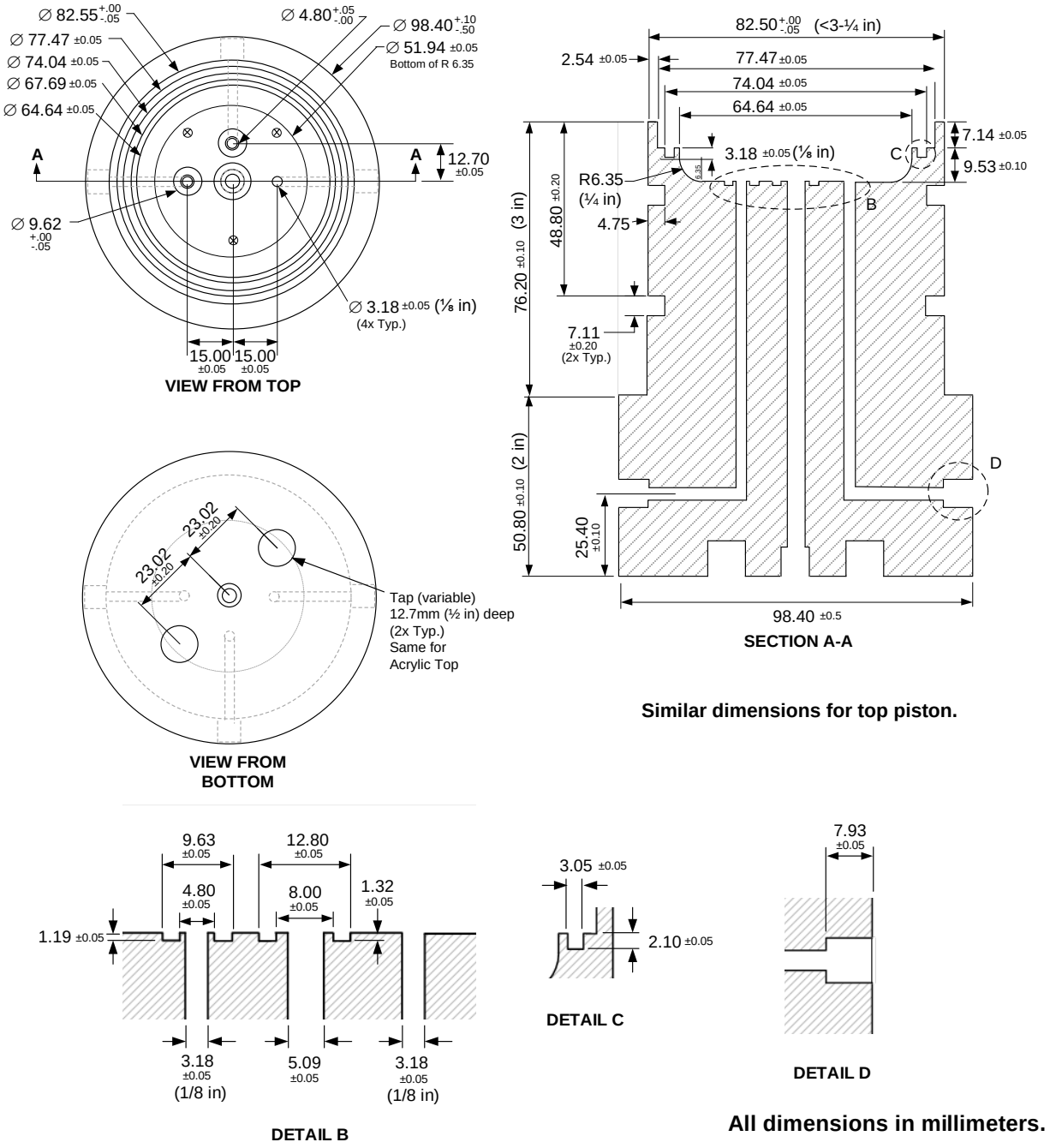

Figure 2.3. Detailed design of acrylic base for Apparatus No. 1.

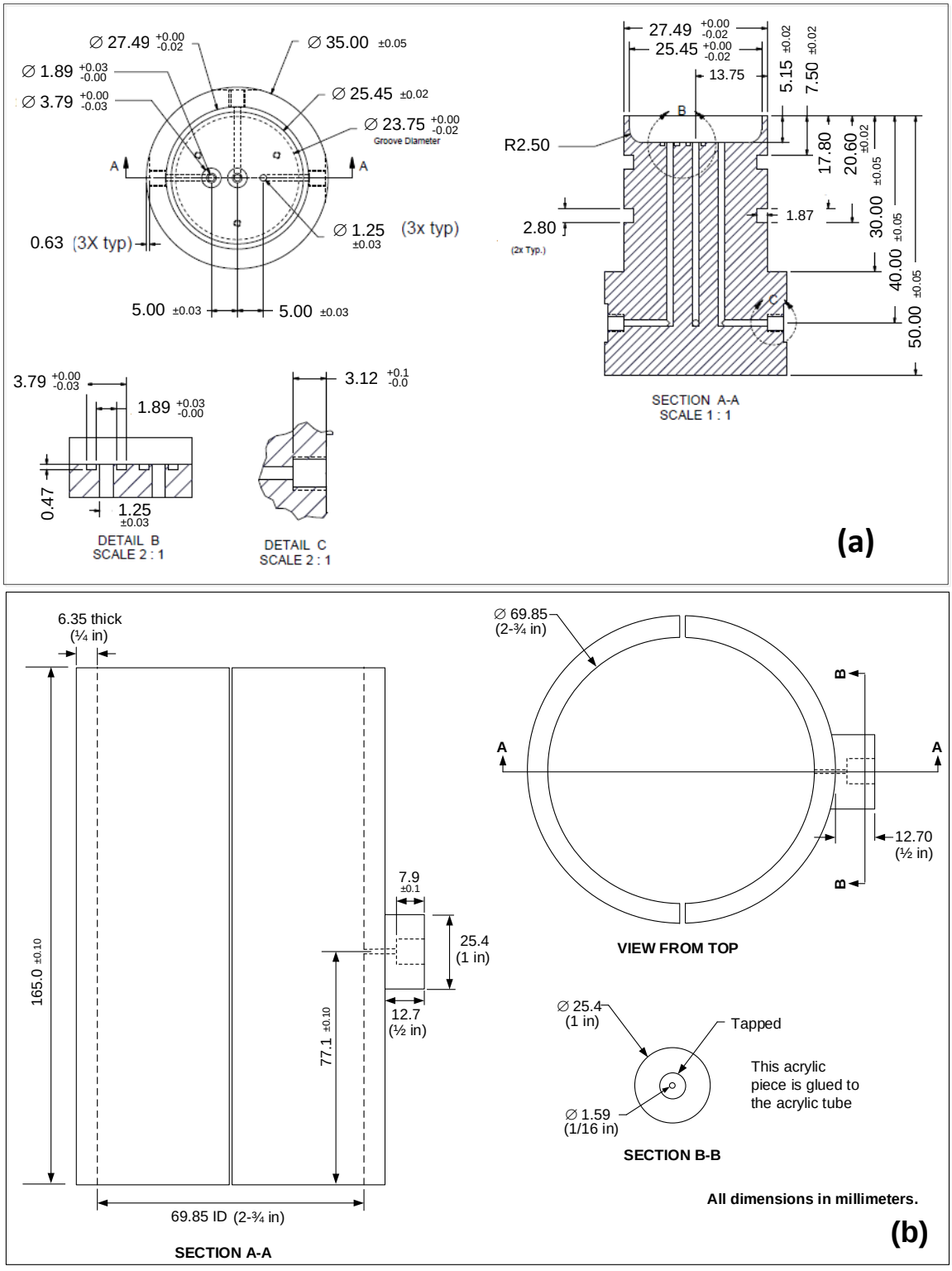

Figure 2.4. Detailed design of Apparatus No. 2: (a) original acrylic base (similar dimensions for top piston) for saturated specimens (Malusis et. al. 2001), and (b) split outer cylinder with port for air pressure for unsaturated testing.

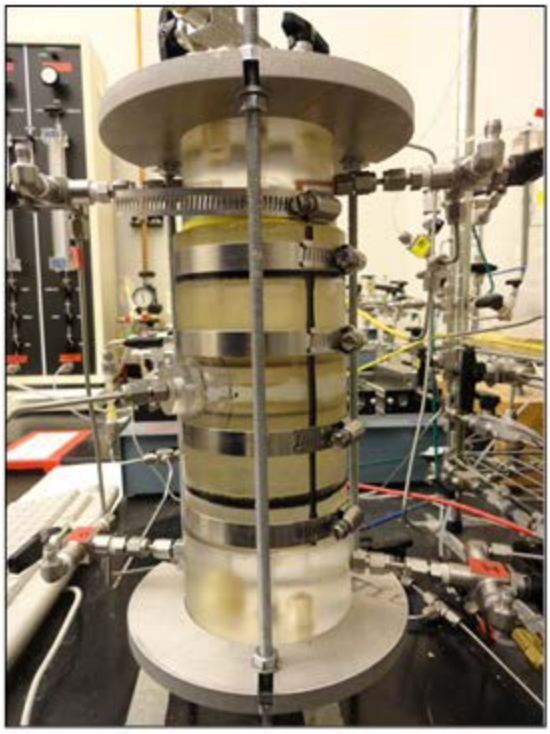

(a)

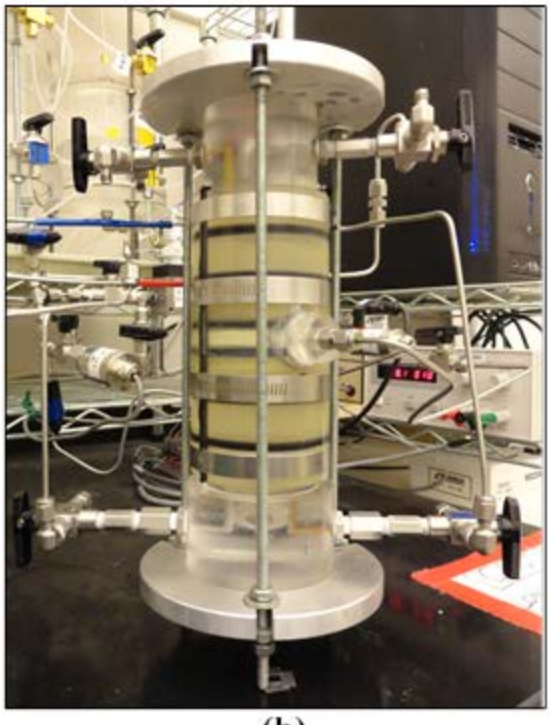

(b)

Figure 2.5. Pictures of rigid-wall cells in (a) Apparatus No. 1 and (b) Apparatus No. 2.

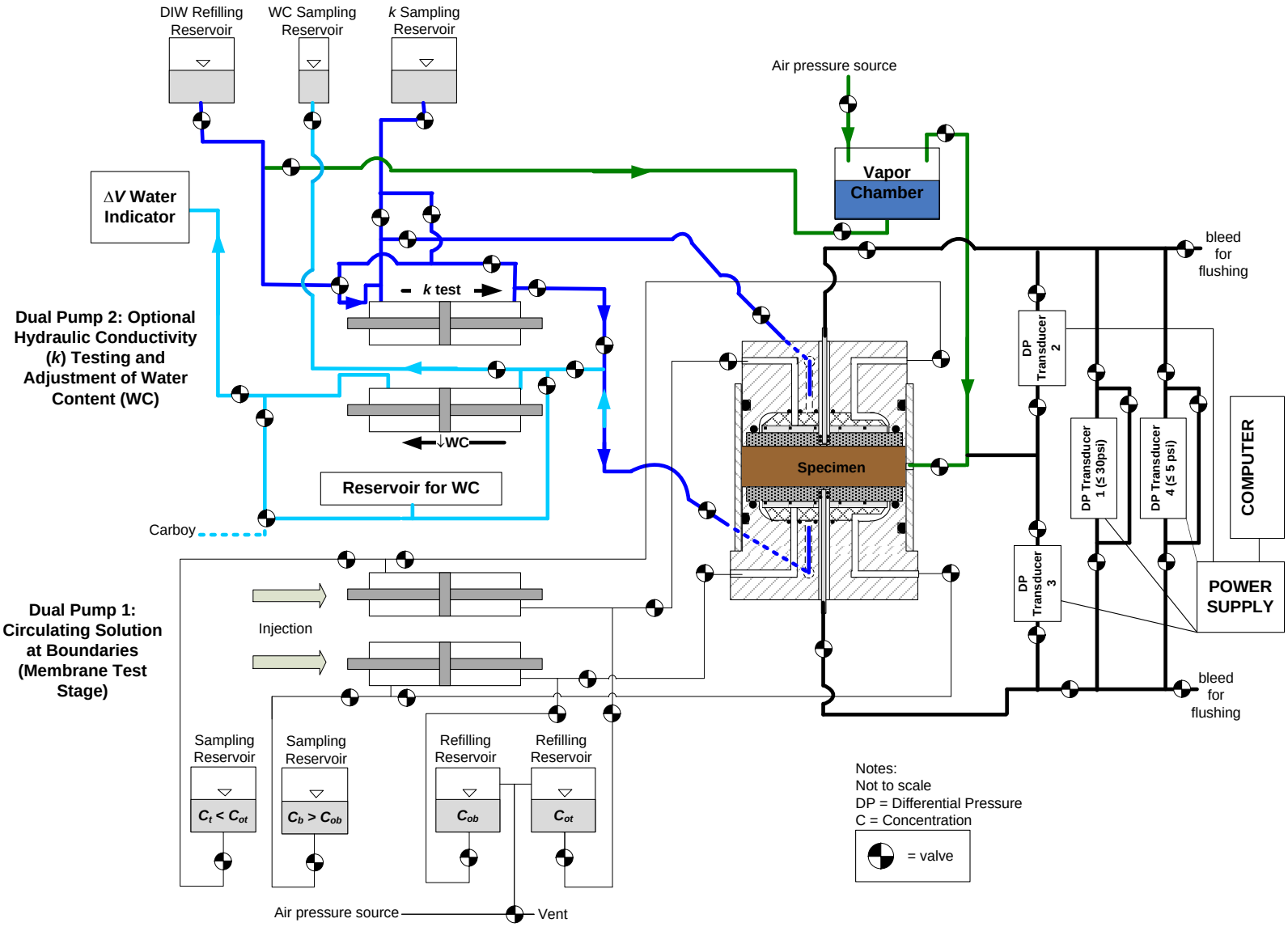

Figure 2.6. Schematic of testing Apparatus No. 1 for measurement of membrane behavior, soil-water characteristic curve, and hydraulic conductivity function of unsaturated clays.

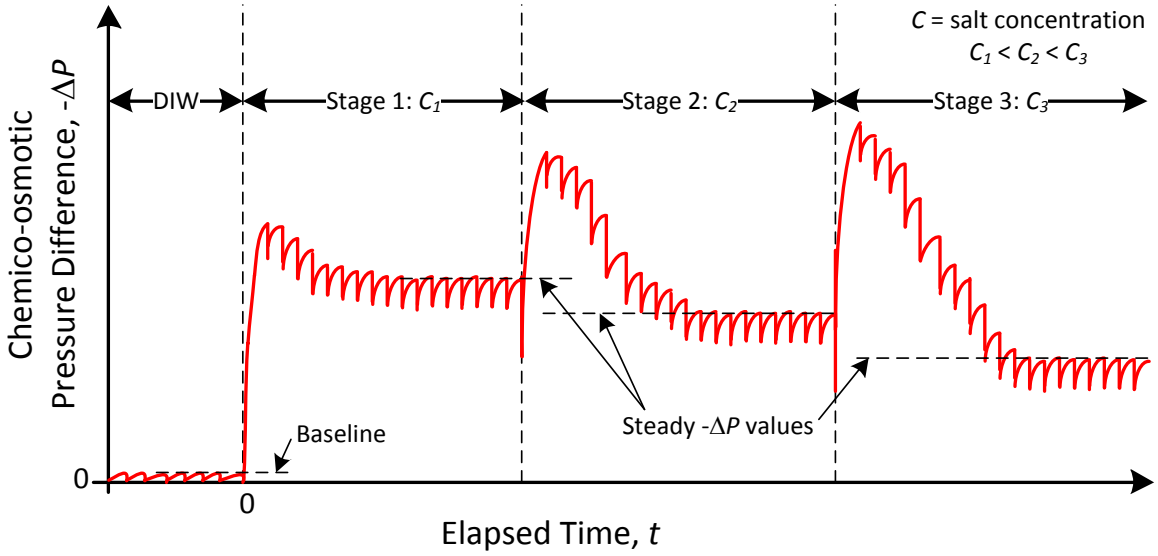

Figure 2.7. Schematic illustration of typical trends in chemico-osmotic pressure difference, -Δ*P*, measured during multistage membrane tests for bentonite specimens.

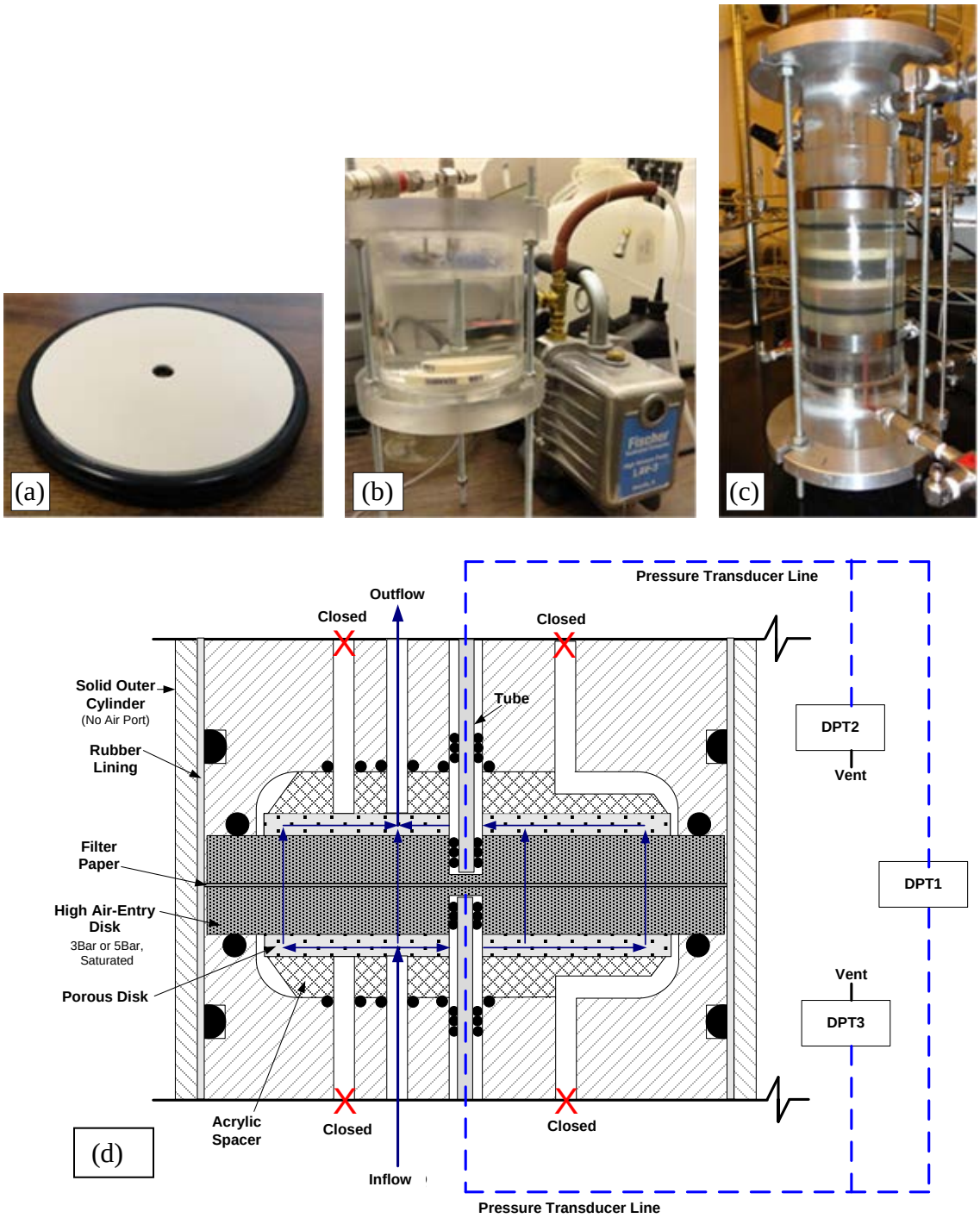

Figure 2.8. Pictures of (a) high air-entry (HAE) disk with perimeter and pressure-line o-rings (Apparatus No. 2), (b) saturation process for HAE disks using a reservoir with de-aired water and vacuum pump, (c) test cell with HAE disks (5-bar) during blank-sleeve calibration testing, and (d) schematic of blank-sleeve test (shown for Apparatus No. 1).

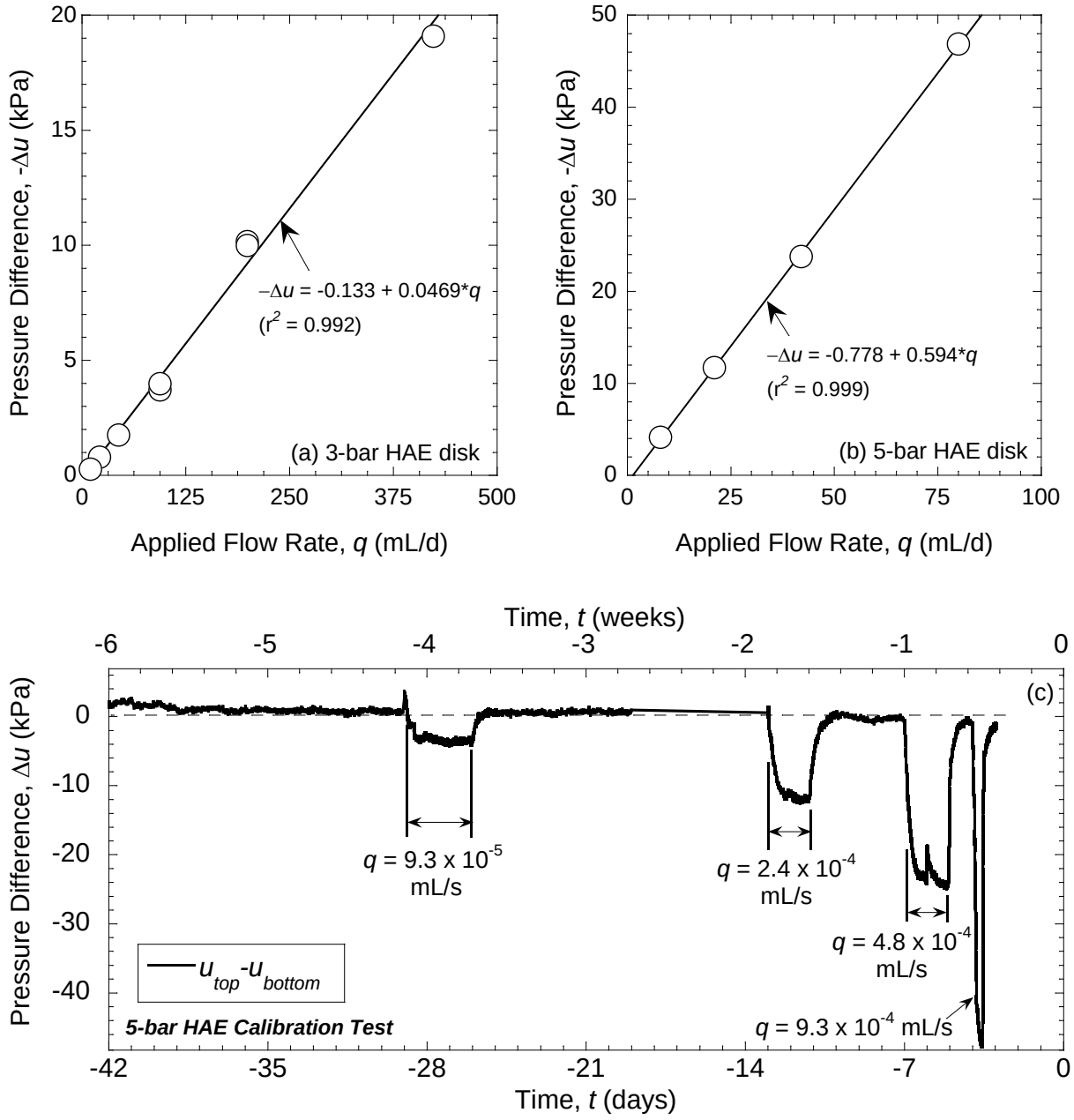

Figure 2.9. Example results of the blank-sleeve calibration tests to measure hydraulic conductivity, *k*, of the high air-entry disks: (a) pressure difference versus flow rate for 3-bar air-entry disk; (b) pressure difference versus flow rate for 5-bar air-entry disk; (c) pressure difference versus time for 5-bar air-entry disk, showing four *k* tests. [Note: Test days in plot (c) are negative because day 0 corresponds to the start of KCl circulation.]

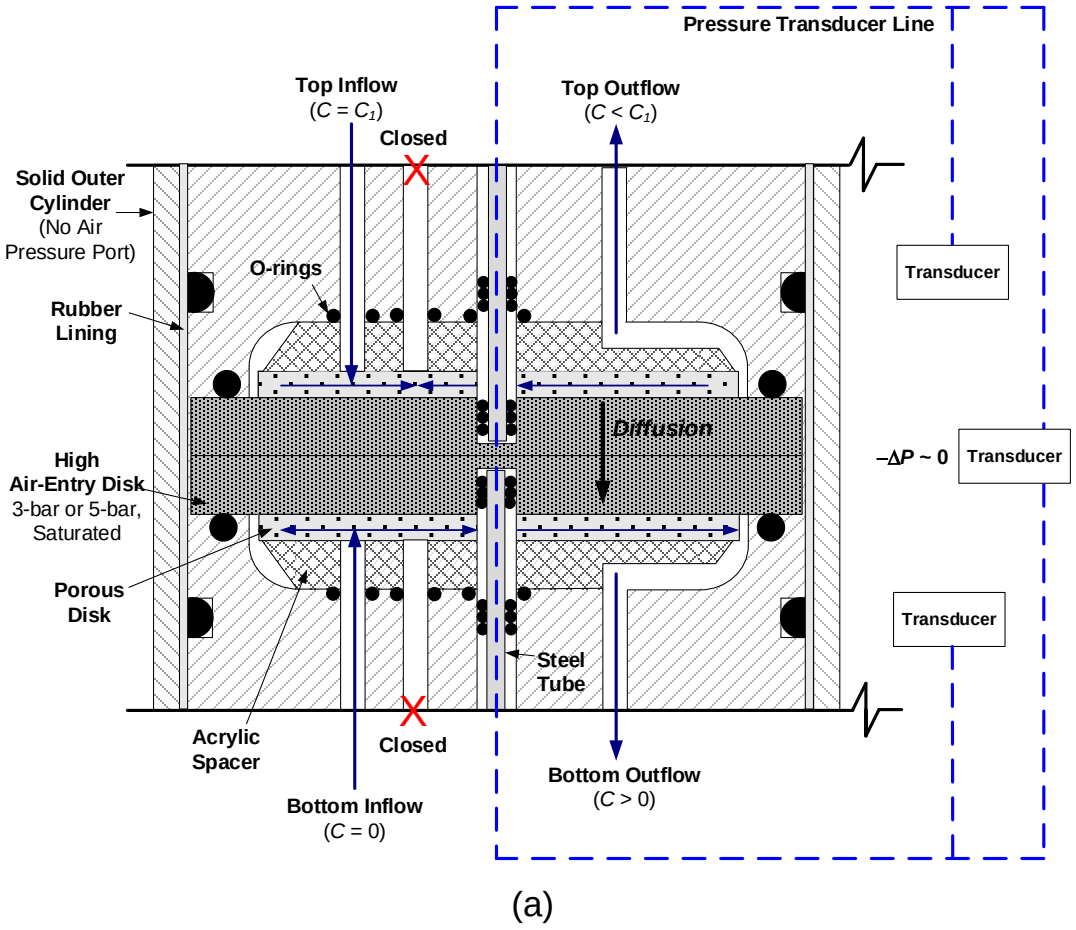

(a)

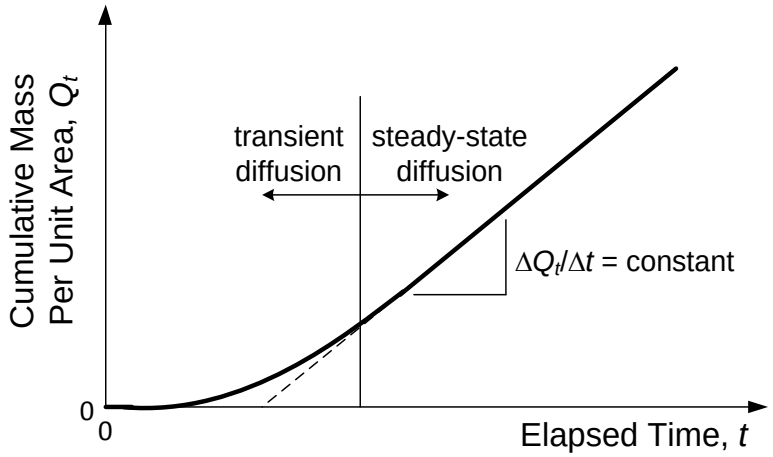

(b)

Figure 2.10. Schematic illustrations for diffusion calibration tests for high air-entry disks: (a) example setup (Apparatus No. 1 shown); (b) typical plot used in through-diffusion analysis to analyze diffusion of solutes through the air-entry disks.

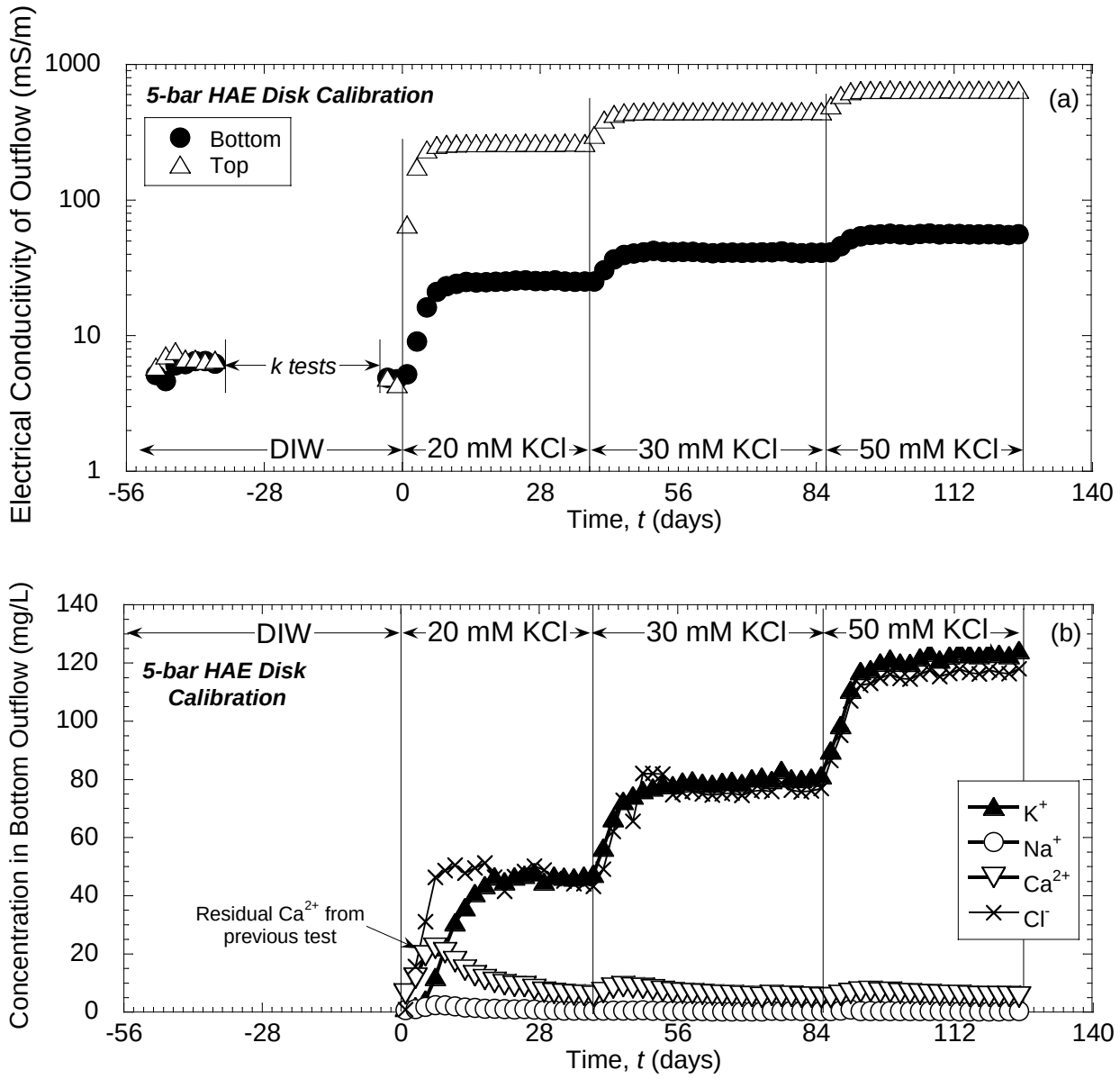

Figure 2.11. Example results of diffusion calibration test for 5-bar high air-entry disk: (a) electrical conductivity of the bottom and top outflows; (b) measured cation and anion concentrations in the outflow from the bottom boundary.

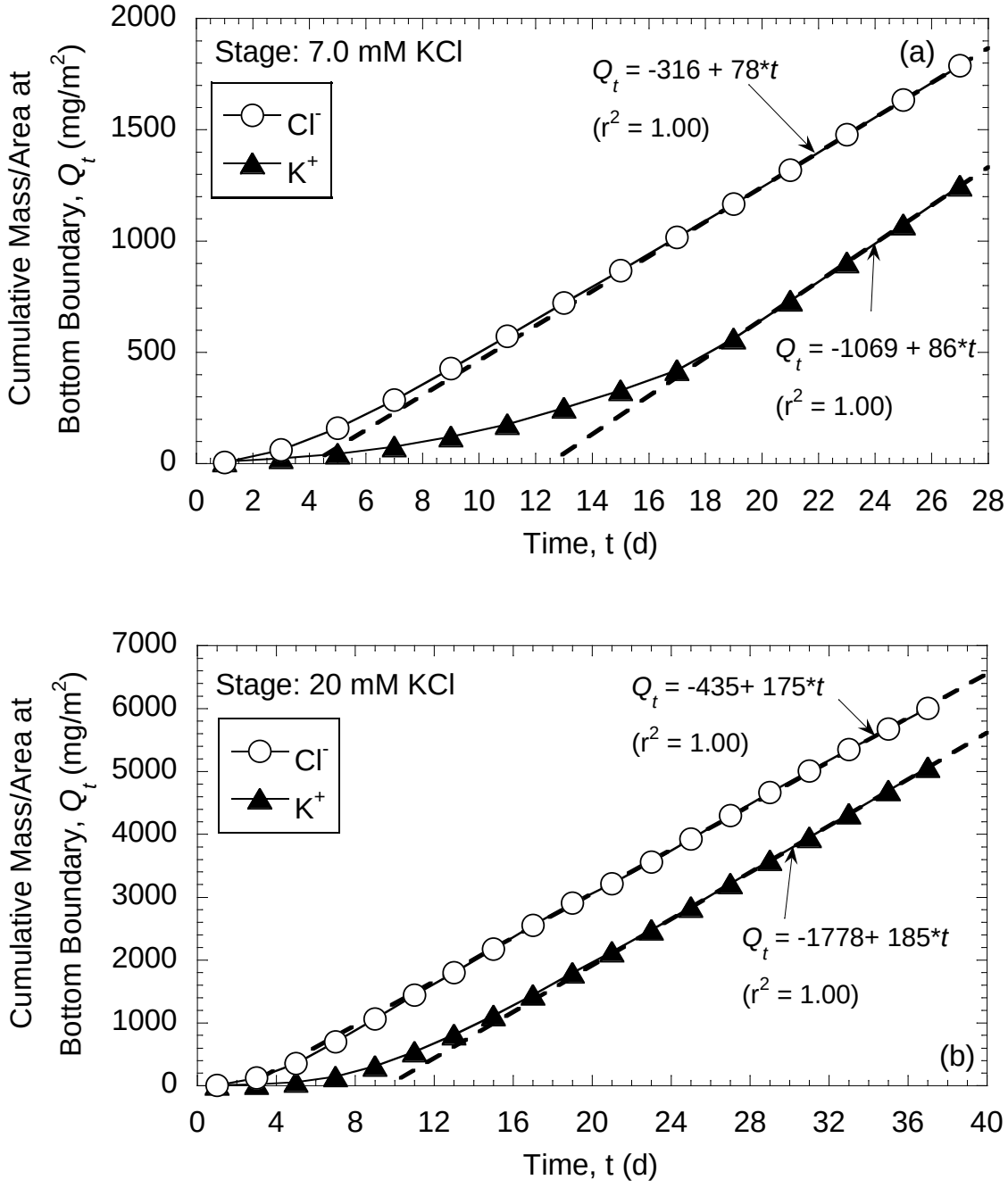

Figure 2.12. Example curves of cumulative mass per area (Q_t) versus elapsed time for individual concentration stages to determine diffusion properties: (a) 3-bar high air-entry disk; (b) 5-bar high air-entry disk.

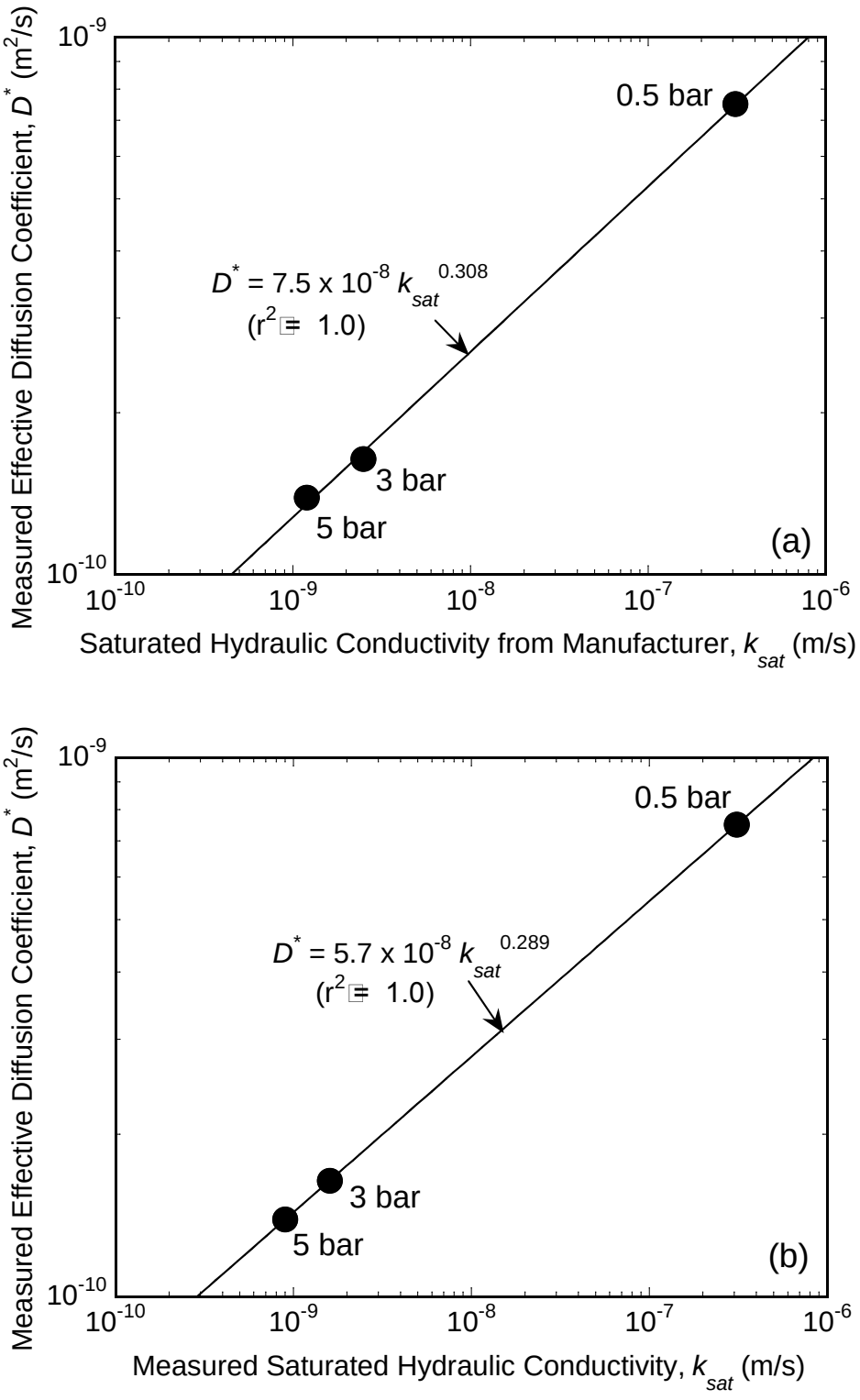

Figure 2.13. Measured effective diffusion coefficients for KCl diffusing through high air-entry disks versus the values of saturated hydraulic conductivity (a) reported by manufacturer, and (b) measured during calibration testing.

REFERENCES

Barbour, S., Lim, P., and Fredlund, D. (1996). "A new technique for diffusion testing of unsaturated soil." *Geotechnical Testing Journal*, 19(3), 247-258.

Bohnhoff, G. (2012). *Membrane Behavior, Diffusion, and Compatibility of a Polymerized Bentonite for Containment Barrier Applications*. PhD Dissertation, Colorado State University, Fort Collins, CO.

Bohnhoff, G., Shackelford, C., and Sample-Lord, K. (2014) "Calcium-resistant membrane behavior of polymerized bentonite." *Journal of Geotechnical and Geoenvironmental Engineering*, 140(3), 040113029-1 – 04013029-12.

Bresler, E. (1973). "Anion exclusion and coupling effects in non-steady transport through unsaturated soils: II. Theory." *Proceedings of the Soil Science Society of America*, 37(5), 663-669.

Bresler, E., and Laufer, A. (1974). "Anion exclusion and coupling effects in non-steady transport through unsaturated soils: II. Laboratory and numerical experiments." *Proceedings of the Soil Science Society of America*, 38(2), 213-218.

Dominijanni, A., and Manassero, M. (2005). "Modelling osmosis and solute transport through clay membrane barriers." *Proceedings of Geo-Frontiers 2005: Waste Containment and Remediation*, A. Alshawabkeh, C. Benson, P. Culligan, J. Evans, B. Gross, D. Narejo, K. Reddy, C. Shackelford, and J. Zornberg, Eds., Geotechnical Special Publication 142, ASCE, Reston, VA (CD version only).

Dominijanni, A., Manassero, M, and Puma, S. (2013). "Coupled chemical-hydraulic-mechanical behavior of bentonites." *Gèotechnique*, 63(3), 191-205.

Elrick, D., Smiles, D., Baumgartner, N., and Groenevelt, P. (1976). "Coupling phenomena in saturated homo-ionic montmorillonite: I. Experimental." *Proceedings of the Soil Science Society of America*, 40(4), 490-491.

Evans, J., Shackelford, C., Yeo, S., and Henning, J. (2008). "Membrane behavior of soil–bentonite slurry-trench cutoff walls." *Soil and Sediment Contamination*, 17(4), 316–322.

Fredlund, D., and Rahardjo, H. (1993). *Soil Mechanics for Unsaturated Soils*, John Wiley & Sons, Inc., New York.

Fritz, S. (1986). "Ideality of clay membranes in osmotic processes: A review." *Clays and Clay Minerals*, 34(2), 214-223.

Fritz, S., and Marine, W. (1983). "Experimental support for a predictive osmotic model of clay membranes." *Geochimica et Cosmochimica Acta*, 47(8), 1515-1522.

Hanshaw, B., and Coplen, T. (1973). "Ultrafiltration by a compacted clay membrane; II. Sodium ion exclusion at various ionic strengths." *Geochimica et Cosmochimica Acta*, 37(10), 2311-2327.

Hart, M., and Whitworth, T. (2005). "Hyperfiltration of potassium nitrate through clay membranes under relatively low-head conditions." *Geochimica et Cosmochimica Acta*, 69(2), 4817–4823.

Henning, J., Evans, J., and Shackelford, C. (2006). "Membrane behavior of two backfills from field-constructed soil-bentonite cutoff walls." *Journal of Geotechnical and Geoenvironmental Engineering*, 132(10), 1243–1249.

Ishiguro, M., Matsuura, T., and Detellier, C. (1995). "Reverse osmosis separation for a montmorillonite membrane." *Journal of Membrane Science*, 107(1-2), 87-92.

James, R. and Rubin, J. (1986). "Transport of chloride ion in a water-saturated soil exhibiting anion exclusion." *Soil Science Society of America Journal*, 50(5), 1142-1149.

Kang, J., and Shackelford, D. (2009). "Clay membrane testing using a flexible-wall cell under closed-system boundary conditions." *Applied Clay Science*, 44(1-2), 43-58.

Kang, J. and Shackelford, C. (2010). "Membrane behavior of compacted clay liners." *Journal of Geotechnical and Geoenvironmental Engineering*, 136(10), 1368-1382.

Kang, J. and Shackelford, C. (2011). "Consolidation enhanced behavior of a geosynthetic clay liner." *Geotextiles and Geomembranes*, 29(6), 544-556.

Keijzer, T., Kleingeld, P., and Loch, J. (1997). "Chemical osmosis in compacted clayey material and the prediction of water transport." *Geoenvironmental Engineering, Contaminated Ground: Fate of Pollutants and Remediation*, R. Yong and H. Thomas, Eds., *Thomas Telford Publ.*, London, 199-204.

Keijzer, T., Kleingeld, P., and Loch, J. (1999). "Chemical osmosis in compacted clayey material and the prediction of water transport." *Engineering Geology*, 53(2), 151-159.

Kemper, W. (1961). "Movement of water as affected by free energy and pressure gradients: II. Experimental analysis of porous systems in which free energy and pressure gradients act in opposite directions." *Proceedings of the Soil Science Society of America*, 25(4), 260-265.

Kemper, W., and Evans, N. (1963). "Movement of water as effected by free energy and pressure gradients: III. Restriction of solutes by membranes." *Proceedings of the Soil Science Society of America*, 27(5), 485-490.

Kemper, W., and Quirk, J. (1972). "Ion mobilities and electric charge of external clay surfaces inferred from potential differences and osmotic flow." *Soil Science Society of America*, 36(3), 426-433.

Kemper, W., and Rollins, J. (1966). "Osmotic efficiency coefficients across compacted clays." *Proc. Soil Science Society of America*, 30(5), 529-534.

Kharaka, Y. and Berry, F. (1973). "Simultaneous flow of water and solutes through geologic membranes, I. Experimental investigation." *Geochimica et Cosmochimica Acta*, 37(12), 2577-2603.

Kharaka, Y., and Smalley, W. (1976). "Flow of water and solutes through compacted clays." *Bulletin of the American Association of Petroleum Geologists*, 60(6), 973-980.

Letey, J., Kemper, W., and Noonan, L. (1969). "The effect of osmotic pressure gradients on water movement in unsaturated soil." *Proceedings of the Soil Science Society of America*, 33(1), 16-18.

Lu, N., Olsen, H., and Likos, W. (2004). "Appropriate material properties for advective-diffusive solute flux in membrane soil." *Journal of Geotechnical and Geoenvironmental Engineering*, 130(12), 1341- 1346.

Lu, N., Wayllace, A., Carrera, J., and Likos, W. (2006). "Constant flow method for concurrently measuring soil-water characteristic curve and hydraulic conductivity function." *Geotechnical Testing Journal*, 29(3), 230-241.

Malusis, M., and Shackelford, C. (2002a). "Chemico-osmotic efficiency of a geosynthetic clay liner." *Journal of Geotechnical and Geoenvironmental Engineering*, 128(2), 97-106.

Malusis, M., and Shackelford, C. (2002b). "Coupling effects during steady-state solute diffusion through a semipermeable clay membrane." *Environmental Science & Technology*, 36(6), 1312-1319.

Malusis, M., Shackelford, C., and Maneval, J. (2012). "Critical review of coupled flux formations for clay membranes based on nonequilibrium thermodynamics." *Journal of Contaminant Hydrology*, Vol. 138-139, 40-59.

Malusis, M., Shackelford, C., and Olsen, H. (2001). "A laboratory apparatus to measure chemico-osmotic efficiency coefficients for clay soils." *Geotechnical Testing Journal*, 24(3), 229-242.

Manassero, M. and Dominijanni, A. (2003). "Modelling the osmosis effect on solute migration through porous media." *Géotechnique*, 53(5), 481-492.

Mazzieri, F., Di Emidio, G., and Van Impe, P. (2010). "Diffusion of calcium chloride in a modified bentonite: impact on osmotic efficiency and hydraulic conductivity." *Clays and Clay Minerals*; 58(3), 351-363.

McKelvey, J., and Milne, I. (1962). "The flow of salt solutions through compacted clay." *Proceedings of the 9th National Conference on Clays and Clay Minerals*, Pergamon Press, NY, 248-259.

McKelvey, J., Spiegler, K., and Wyliie, M. (1957). "Salt filtering by ion-exchange grains and membranes." *Journal of Physical Chemistry*, 61(2), 174-178.

Meier, A., Sample-Lord, K., Castelbaum, D., Kallase, S., Moran, B., Ray, T., and Shackelford, C. (2014) "Persistence of semipermeable membrane behavior for a geosynthetic clay liner." *Proceedings, 7th International Conference on Environmental Geotechnics*, A. Bouazza, S. Yuen, and B. Brown, Eds., Nov. 10-14, 2014, Melbourne, Australia (ISBN 978-1-922107-23-7), 496-503.

Olsen, H. (1969). "Simultaneous fluxes of liquid and charge in saturated kaolinite." *Proceedings of the Soil Science Society of America*, 33(3), 338-344.

Olsen, H., Gill, J., Willden, A., and Nelson, K. (1991). "Innovations in hydraulic conductivity measurements." *Transportation Research Record*, 1309, 9-17.

Sample-Lord, K., and Shackelford, C. (2014). "Membrane behavior of unsaturated bentonite barriers." *Proceedings of Geo-Congress 2014: Geo-Characterization and Modeling for Sustainability*, M. Abu-Farsakh, X. Yu, and L.R. Hoyos, Eds., Geotechnical Special Publication 234, ASCE, Reston, VA, 1900-1909.

Shackelford, C. (1991). "Laboratory diffusion testing for waste disposal – A review." *Journal of Contaminant Hydrology*, 7(3), 177-217.

Shackelford, C. (1995). "Cumulative mass approach for column testing." *Journal of Geotechnical Engineering*, 121(10), 696-703

Shackelford, C. (2011). "Membrane behavior in geosynthetic clay liners." *Geo-Frontiers 2011: Advances in Geotechnical Engineering*, J. Han and D. Alzamora, Eds., Geotechnical Special Publication 211, ASCE, Reston, VA, 1961-1970.

Shackelford, C. (2013). "Membrane behavior in engineered bentonite-based containment barriers: State of the art." *Proceedings of Coupled Phenomena in Environmental Geotechnics (CPEG)*, M. Manassero, A. Dominijanni, S. Foti, and G. Musso, eds., July 1-3, Torino, Italy, CRC Press/Balkema, Taylor & Francis Group, London, 45-60.

Shackelford, C., and Lee, J. (2003). "The destructive role of diffusion on clay membrane behavior." *Clays and Clay Minerals*, 51(2), 187-197.

Shackelford, C., Malusis, M., and Olsen, H. (2003). "Clay membrane behavior for geoenvironmental containment." *Soil and Rock America Conference 2003*, P. J. Culligan, H. H. Einstein, and A. J. Whittle, Eds., Verlag Glückauf GMBH, Essen, Germany, Vol. 1, 767-774.

Takeda, M., Hiratsuka, T., Manaka, M., and Ito, K. (2014). "Experimental examination of the relationships among chemico-osmotic, hydraulic, and diffusion parameters of Wakkanai mustones." *Journal of Geophysical Research: Solid Earth*, 119(5), 4178-4201.

Tang, Q., Katsumi, T., Inui, T., and Li, Zhenze (2014). "Membrane behavior of bentonite-amended compacted clay." *Soils and Foundations*, Japanese Geotechnical Society, 54(3), 329-344.

Tang, Q., Katsumi, T., Inui, T., and Li, Zhenze (2015). "Influence of pH on the membrane behavior of bentonite-amended Fukakusa clay." *Separation and Purification Technology*, Vol. 141, 132-142.

Whitworth, T., and Fritz, S. (1994). "Electrolyte-induced solute permeability effects in compacted smectite membranes." *Applied Geochemistry*, 9(5), 533-546.

Yeo, S., Shackelford, C., and Evans, J. (2005). "Membrane behavior of model soil-bentonite backfills." *Journal of Geotechnical and Geoenvironmental Engineering*, 131(4), 418-429.

CHAPTER 3. A DIALYSIS METHOD FOR HOMO-IONIZATION OF BENTONITE

3.1 Introduction

Clays with significant percentages of smectite minerals (e.g., montmorillonite), such as sodium bentonite (Na-bentonite), are commonly used as barriers or barrier components for chemical containment applications (e.g., liners for waste containment systems, slurried vertical cutoff walls), due to the high swell and low hydraulic conductivity properties of such clays (Shackelford and Sample-Lord 2014). Examples of such barriers include geosynthetic clay liners (GCLs), mixtures of sand and bentonite as compacted clay liners (CCLs), and soil-bentonite backfills (SBBs) as vertical cutoff walls. In addition to low hydraulic conductivity, Na-bentonite also may exhibit semipermeable membrane behavior, or the ability to restrict the migration of solutes through the clay, thereby further enhancing the containment function of the barrier (Shackelford 2013).

In general, the behavior and properties of bentonites typically are enhanced when monovalent cations (e.g., Na^{+}) dominate the exchange complex (e.g., Na-bentonite) relative to when multivalent cations (e.g., Ca^{2+}) occupy the majority of the exchange sites (e.g., Ca-bentonite) (e.g., Gleason et al. 1997). For this reason, treatment of natural bentonites to increase the percentage of monovalent cations in the exchange complex, commonly referred to as homo-ionization or clay purification, may be beneficial in terms of the use of these bentonites in barriers for chemical containment applications. In addition, such homo-ionization has been undertaken extensively in previous studies focused on understanding the fundamental mechanisms governing the behavior and properties of bentonites, such as the index properties (e.g., Sridharan et al. 1986), consolidation and compressibility (e.g., Olson and Mesri 1970),

hydraulic conductivity (e.g., Mesri and Olson 1971), soil suction (e.g., Likos and Lu 2002), and salt filtration (e.g., Kemper 1961; Hanshaw 1962; McKelvey and Milne 1962; Kemper and Rollins 1966; Mokady and Low 1966; Olsen 1969; Kemper and Quirk 1972; Whitworth and Fritz 1994; Ishiguro et al. 1995; Di Maio 1996). In these studies, the goal typically has been to homo-ionize the bentonites to the extent that a single, monovalent cation (e.g., Na^+) occupies the majority (e.g., > 95 %) of the exchange sites. However, this extent of homo-ionization often has been assumed, without verification via measurement of the composition of the exchange complex after treatment (e.g., ASTM D 7503).

Based on the aforementioned considerations, a dialysis procedure was developed to allow for preparation of bentonite specimens with a high percentage (≥ 70 %) of Na^+ on the exchange complex. The effectiveness of the dialysis procedure was evaluated for the purpose of verifying that homo-ionization can be achieved using salt solution concentrations similar to those described in the literature for clay purification methods, and providing recommendations for dialysis methods associated with the fundamental study of bentonite behavior. Finally, the proposed dialysis procedure also was evaluated as a basis for measuring the diffusion behavior of bentonite pastes.

3.2 Background

3.2.1 Bentonite mineralogy

Most bentonites are a product of volcanic ash, with deposits existing on almost every continent (Grim 1968; Grim and Güven 1978; Odom 1984). The principle mineralogical constituents of bentonite are montmorillonite and beidellite, both of which are dioctahedral smectites (Deer et al. 1992). Both of these clay minerals belong to a group of minerals known as

the layered alumino-silicates. In the layered alumino-silicate minerals, oxygen and hydroxyl anions combine with various cations to form sheets of silicon tetrahedrons and aluminum octahedrons. These sheets combine via ionic and covalent bonding to form stacks of sheets. The smectite structure consists of an octahedral sheet sandwiched between two silica sheets, referred to as a 2:1 layered alumino-silicate (see Figure 3.1a,b). The space between adjacent stacks is referred to as the interlayer region, which may be occupied by water (H_2O) and various cations (e.g., K^+, Na^+, Ca^{2+}, Mg^{2+}, etc.), depending on the type of clay mineral. The stacks of sheets combine to form individual clay particles. A schematic representation of the process for formation of clay minerals is provided in Figure 3.1c.

The theoretical composition of an electrically neutral smectite mineral is $(OH)_4Si_8Al_4O_{20}\bullet n(\text{interlayer})H_2O$ (Mitchell and Soga 2005). However, smectite minerals typically undergo isomorphic substitution, whereby the aluminum cation (Al^{3+}) in the octahedral sheet is replaced by a cation of lower valence (e.g., Mg^{2+}, Fe^{2+}, Zn^{2+}, Ni^{2+}, etc.) during formation of the clay mineral, resulting in a permanent net negative charge. Isomorphic substitution also may occur within the tetrahedral sheet, where silicon (Si^{4+}) is replaced by aluminum (Al^{3+}) or phosphorous (P^{3+}) (Mitchell and Soga 2005).

The dioctahedral structure of montmorillonite is a result of isomorphic substitution of every sixth Al^{3+} with Mg^{2+}, resulting in a new, unit cell formula of $(OH)_4Si_8(Al_{3.34}Mg_{0.66})O_{20}$. The charge deficiency of montmorillonite, which on average is 0.66 negative equivalents per unit cell (ranges from 0.5 to 1.2 negative equivalents per unit cell), is balanced by exchangeable cations on the particle surfaces and within the interlayer regions, the latter of which are referred to as interlayer cations (Mitchell and Soga 2005). For example, in the case where sodium cations balance the charge deficiency, the cell formula may be written as:

$(OH)_4Si_8(Al_{3.34}Mg_{0.66})O_{20} \rightarrow Na_{0.66}$. This charge imbalance of the montmorillonite leads to the relatively high cation exchange capacity, *CEC*. The large surface area (typically 50 to 120 m^2/g of primary surface area and up to 800 m^2/g when including the crystalline interlayer area), high cation exchange capacity (typically 80 to 150 $cmol_c/kg$), and net negative charge of the clay particles result in a soil that is highly sensitive to water content and pore-fluid chemistry (McBride 1994).

The interlayer cations may form inner-sphere complexes (i.e., direct binding of the cation to the mineral surface) or outer-sphere complexes (i.e., hydrogen bonding between the mineral and the water molecules surrounding the cation). Also, the interlayer spacing (designated as d_{001} in Figure 3.1a) can vary based on hydration and the types of exchangeable cations that are present. The d_{001} may vary from 9.6 Å (when fully collapsed) to more than 19 Å when hydrated (Deer et al. 1992), resulting in the high swell potential of montmorillonite-rich soils such as bentonites.

The exchange sites of natural bentonites are occupied by a mixture of cations, most notably the alkali earth metals sodium (Na^+) and potassium (K^+) and the alkaline earth metals calcium (Ca^{2+}) and magnesium (Mg^{2+}). Bentonites generally are labelled in terms of the cation that predominates the exchange sites of the individual clay particles. For example, when Na^+ is the predominant exchangeable cation, the bentonite is referred to as a sodium bentonite (Na-bentonite), whereas when Ca^{2+} is the predominant cation, the bentonite is referred to as a calcium bentonite (Ca-bentonite). The percentage of exchange sites that are occupied by Na^+ can be related to the exchangeable sodium percentage, *ESP* (e.g., Sparks 2003):

$$ESP = \frac{\text{Exchangeable } Na^+}{CEC} \cdot 100\% \tag{3.1}$$

where exchangeable Na^+ ($cmol_c/kg$) and *CEC* ($cmol_c/kg$) are determined via laboratory testing (e.g., ASTM D 7503).

Cation exchange typically is diffusion-controlled, reversible, and stoichiometric (Sparks 2003; Brigatti et al. 2006). Selectivity for one cation relative to another for the exchange sites of the montmorillonite surface generally is based on both hydrated radius and primary valence. For cations with the same valence, the bonding energy (the energy with which an adsorbed cation is held to the clay particle) varies inversely with the effective radius of the hydrated ion (Baver 1956). The ion with the larger hydrated radius is displaced by the ion with the smaller hydrated radius (e.g., Li^+ is displaced by Na^+). Thus, preference for cations (of the same valence) increases as hydrated radius decreases, such that the general order of selectivity is $Cs^+ > Rb^+ > K^+ > Na^+ > Li^+ > H^+$ for monovalent cations and $Ba^{2+} > Pb^{2+} > Sr^{2+} > Ca^{2+} > Mg^{2+}$ for divalent cations (Sayre et al. 1963; van Olphen 1963; Sparks 2003). Bonding energy also generally increases with increasing valence, leading to a general preference for multivalent cations over monovalent cations. Therefore, the typical order of preference or selectivity for the common cations is $Ba^{2+} > Pb^{2+} > Sr^{2+} > Ca^{2+} > Ni^{2+} > Cd^{2+} > Cu^{2+} > Co^{2+} > Zn^{2+} > Mg^{2+} > Ag^+ > Cs^+ > Rb^+ > K^+ > NH_4^+ > Na^+ > Li^+$ (Helfferich 1962).

3.2.2 Clay purification methods

Natural clays typically have a mixture of cations occupying the exchange complex and some non-zero concentration of soluble salts. For laboratory studies, the ability to control the type and percentage of cations on the exchange complex, as well as remove excess soluble salts, provides greater control over testing conditions, amplification or suppression of clay behaviors (e.g., swell, osmotic suction, membrane behavior), and the ability to evaluate the role of

exchangeable cations on clay properties. Laboratory methods for salt removal and modification of ion form have been used extensively by soil scientists, and generally are referred to as clay purification (e.g., see references in Table 3.1). The most common clay purification methods include washing and centrifuging, dialysis, and electrodialysis (van Olphen 1963). An extensive list of studies where bentonite has been purified as part of the specimen preparation procedure for a variety of testing purposes is summarized in Table 3.1. While clay purification methods have been used by soil scientists for several decades to prepare homo-ionic soil specimens with low soluble salt contents, the procedures for such purification methods are not commonly used in geotechnical and geoenvironmental testing research.

For most of the studies listed in Table 3.1, the primary purpose of the purification procedure was to prepare homo-ionized bentonite. Homo-ionized bentonites theoretically are bentonites that have a single cation species occupying all of the exchange sites. However, preparation of clay with 100 % of the exchange positions occupied by a single cation species typically is difficult (van Olphen 1963). Thus, for practical purposes, bentonites may be considered to be homo-ionized when the exchange sites are occupied by a significant majority of a single cation, such as > 95 %. For example, a bentonite may be considered to be homo-ionized with respect to sodium when > 95 % of the exchange sites are occupied by Na^+ (i.e., *ESP* > 95 %).

3.2.2.1 Washing and centrifuging

As described previously in Section 3.2.1, cations with higher valence and/or smaller hydrated radius are preferred for cation exchange, replacing cations with lower valence and/or larger hydrated radius. Thus, exchange preference or affinity (selectivity) for Ca^{2+} and K^+ is

higher than that for Na^+. However, ion exchange reactions also depend upon ion concentration, such that the use of a high concentration (e.g., 1 M) NaCl solution can lead to replacement of Ca^{2+} and K^+ on the exchange complex with Na^+ (Di Maio 1996). This concentration effect is often referred to as a mass action effect. Thus, one method to modify the exchange complex of a clay is to wash the clay several times with a strong salt solution of the desired cation form (e.g., 1 M NaCl for a Na-bentonite). Upon mixing the clay with a strong salt solution to form a suspension, the clay may flocculate and settle out of suspension. A centrifuge may be used to expedite separation of the solid clay particles from the supernatant. The supernatant is removed, replaced with fresh solution, and the process is repeated. Typically, the clay then is washed with de-ionized water (DIW) to remove excess soluble salts (i.e., salts that are not held electrostatically to the clay particle surfaces and, therefore, are soluble within the pore water).

For example, Likos and Lu (2002) converted Wyoming bentonite to Na^+-saturated bentonite to evaluate the water sorption behavior of smectitie-kaolinite mixtures. The bentonite was soaked in 1.0 M NaCl for 24 h and then centrifuged. This process was repeated with fresh NaCl solution a total of three times. Afterward, the clay was rinsed with distilled water until excess chloride was no longer detected.

To convert a Ca^{2+}-saturated clay to a Na^+-saturated clay, Carrado et al. (2006) recommended the following procedure: (1) disperse the clay in 1 M NaCl using 400 mL of NaCl per 30 g of clay; (2) shake the mixture in a rotary shaker overnight; and (3) centrifuge at 3000 rpm for 2 h to separate the supernatant. Carrado et al. (2006) reports that this procedure, if repeated six times, will achieve close to 99 % Na^+ on the exchange complex (no data was provided). Similar versions of the washing/centrifuging procedure described by Carrado et al. (2006) have been used in numerous other studies (see Table 3.1).

The removed supernatant contains cations that have been replaced and removed from the exchange complex. To check if the exchange process is complete, samples of the supernatant can be analyzed to confirm that cations other than the species in the salt solution are no longer detectable (i.e., no longer being released from the exchange complex). An alternate method of confirming that exchange is complete is to analyze the salt solution before and after exposure to the clay (van Olphen 1963). If the desired cation is no longer being removed from solution, then the clay exchange complex is assumed to be saturated (i.e., homo-ionized).

After treatment with the salt solution is complete, the clay must be rinsed of excess soluble salts. The clay is mixed with DIW and, if necessary, centrifuged to separate the supernatant. Then, the supernatant is decanted and replaced with fresh water, and the process is repeated several times. To confirm that the rinsing process is complete, the electrical conductivity (*EC*) of the supernatant liquid after each centrifugation can be measured (van Olphen 1963). Once the *EC* readings are approximately constant, the clay is considered rinsed or flushed of excess soluble salts. For example, Kemper (1961) prepared sodium homo-ionized clays by washing Wyoming bentonite and Pierre shale four times with 1 M NaCl. Then, the samples were shaken with DIW and centrifuged repeatedly, until the NaCl concentration in the supernatant was less than 0.02 M (based on *EC* readings).

3.2.2.2 Dialysis

Another common method of clay purification described in the soil science literature is dialysis, which is based on diffusion of dissolved solutes across a selectively permeable membrane due to a concentration gradient (e.g., Kemper and Rollins 1966; Kemper and van Schaik 1966; Elrick et al. 1976; Mercier and Detellier 1994; Whitworth and Fritz 1994;

Churchman and Weismann 1995; Ishiguro et al. 1995; Sherwood and Craster 2000; Oduor and Whitworth 2005). Smaller solutes (e.g., dissolved Na^+ and Cl^-) can pass through the membrane, while larger particles (e.g., soil particles) are restricted to one side of the membrane (i.e., permeable to chemical species but not to soil particles). A schematic of this process is shown in Figure 3.2. The soil sample is placed inside a tube of dialysis membrane, sealed via clamps at each end of the tube, and immersed in the salt solution or DIW (i.e., the dialysis bath water). In the 1960s, sausage casing was used as the membrane material (e.g., Kemper and Rollins 1966; Kemper and van Schaik 1966). Current dialysis procedures use commercially available membrane material, such as regenerated cellulose (e.g., Oduor and Whitworth 2005; Segad et al. 2010).

The dialysis process is similar to the washing and centrifuging procedure, as the soil is immersed in strong salt solutions to modify the exchange complex, followed by rinsing with DIW to remove excess salts. The solution or DIW is replaced at regular intervals until each stage is considered complete. As described previously, chemical analysis and *EC* measurements of the bath water may be used to determine the extent of homo-ionization and rinsing of excess salts. The dialysis process may take a couple days to a couple weeks, depending on the strength of the salt solution, the mass of solution relative to the mass of soil, and how frequently the solution is replenished. An advantage of the dialysis procedure is that the process is simple and utilizes relatively inexpensive materials and equipment.

Previous studies have combined the washing and dialysis techniques to purify clays (e.g., Kemper and Rollins 1966; Kemper and van Schaik 1966; Hawthorne and Solomon 1972; Elrick et al. 1976; Mercier and Detellier 1994; Whitworth and Fritz 1994; Ishiguro et al. 1995). For rinsing excess salts, Carrado et al. (2006) recommended a combination of washing and dialysis.

The procedure involves mixing the clay with water and then shaking the mixture in a rotary shaker overnight. The suspension then is centrifuged at 7000 rpm for 3 h. The agitating and centrifuging process is repeated three to four times, until the stability of the colloidal dispersion has increased sufficiently such that separation of the supernatant becomes difficult. To remove the remaining salts, dialysis in water is performed for seven days.

3.2.2.3 Electrodialysis

Electrodialysis is a modified version of dialysis, where soil is placed in a compartment with semipermeable membranes on each side. Electrodes are located on the opposite sides of the membranes and are used to apply an electric field across the soil. The dissolved electrolytes (charged solutes) move through the membranes similar to the dialysis method, but at an accelerated rate due to the electric field. However, electrodialysis is not recommended for clay soils due to an increase in hydrolysis (van Olphen 1963). The hydrogen cation (proton) resulting from hydrolysis can interfere with the cations on the exchange complex and reduce the effectiveness of the homo-ionization procedure.

3.2.3 Confirmation of homo-ionization

The achievement of homo-ionization upon treatment of a clay often is assumed, without actual verification via measurement of the makeup of the exchange complex after treatment (e.g., ASTM D 7503). Although limited, some studies have performed x-ray diffraction or measured cations on the exchange complex after the homo-ionization procedure. However, the results from these studies regarding the effectiveness of the procedures and achievement of homo-ionization have been mixed. For example, Leonard and Low (1963) washed and centrifuged

Belle Fourche, Utah, Aberdeen, and Cheto clays with NaCl solutions. The concentration of the NaCl solution was not reported, but was described as "sufficient to far exceed the exchange capacity of the suspended clay." The Cheto clay was washed three times with NaCl solution, while the other clays were only washed once with NaCl. To remove excess salts, the clays were washed with water and centrifuged until the supernatant tested negative for chloride, based on the $AgNO_3$ testing method (Page et al. 1982). Then, Leonard and Low (1963) measured the exchangeable cations of the clays after treatment and found that the percentage of exchangeable sodium was highly variable. For example, the *ESP* values were 86 %, 82 %, 51 %, and 40 % for the Cheto, Belle Fourche, Aberdeen, and Utah clays, respectively. The higher percentage of sodium saturation for the Cheto clay was expected, as that material underwent three NaCl washes (versus only one for the other clays), but was still well below a value that would be considered homo-ionized (e.g., *ESP* > 95 %).

Olson and Mesri (1970) treated Wyoming bentonite with multiple washes of NaCl or $CaCl_2$ to achieve Na- or Ca-saturated clays. The strength of the solutions and the number of washes were not reported. However, based on measurement of the exchangeable cations, all of the material was reported to be homo-ionized with greater than 96 % of the desired cation on the exchange complex.

Di Maio (1996) reported successful homo-ionization of Ponza bentonite, based on X-ray diffraction. However, the initial soil was Na-bentonite, which was converted to K- or Ca-bentonite. In addition, the bentonite was allowed to soak in KCl or $CaCl_2$ solutions for three weeks (i.e., versus the shorter durations of $\leq$ 24 h typically used for washing).

3.2.4 Clay purification and engineering properties

Although diffuse double-layer (DDL) theory is strictly applicable only to colloidal suspensions, DDL theory historically has been used to provide at least a qualitative indication of clay behavior (e.g., Mitchell and Soga 2005). Based on DDL theory, the physico-chemical behavior of clays is affected by surface charge density, charge of the adsorbed cations, dielectric constant of the pore fluid, and electrolyte concentration in the free pore fluid (e.g., Olson and Mesri 1970). In addition to these chemical variables, physical properties such as particle shape and size, geometric arrangement of particles, and surface area can play a role in physico-chemical effects. When particles have a smooth, plate-like shape and are in a parallel arrangement, there is increased interaction between diffuse double layers of adjacent particles. Also, the smaller the particle size, the greater the surface area per unit mass, and the greater the susceptibility of the soil to the influence of physico-chemical interactions. Finally, the smaller the particle size, the more important the role of the adsorbed layer of cations in affecting the clay behavior (Santamarina et al. 2002).

Diffuse double layers are thicker and, therefore, may affect the behavior of the clay more when monovalent cations are on the exchange complex, versus divalent or multivalent cations (van Olpen 1963; Olson and Mesri 1970). Homo-ionization of clays allows for control of the cations on the exchange complex and, thereby, some control over behavior related to hydraulic conductivity (*k)*, consolidation, diffusion, membrane behavior, soil suction, plasticity, and shear strength. For example, the values of *k* for bentonite used in GCLs for chemical containment typically range from 1×10^{-11} m/s to 3×10^{-11} m/s when permeated with DIW, but can increase to greater than 10^{-7} m/s when permeated with salt solutions due to cation exchange (Daniel et al. 1997; Shackelford et al. 2000). Lower ranges of *k* have been measured for homo-ionized

bentonites with monovalent cations on the exchange complex. For example, Fritz and Marine (1983) performed hyperfiltration tests through thin (7.0-mm-thick) specimens of compacted Na-bentonite, and measured average k values of 1.5 x 10^{-13} m/s and 7.3 x 10^{-14} m/s for specimens with void ratios, e, of 1.4 and 0.69 (porosities, n, of 0.59 and 0.41), respectively. Olson and Mesri (1970) measured the k of sodium homo-ionized kaolinite, illite and smectite, and reported k values for the Na-smectite ranged from 8.1 x 10^{-11} m/s to 9 x 10^{-13} m/s for specimens with e ranging from 19 to 4.6, respectively.

The cation species on the exchange complex also can affect the consolidation behavior of the clay. For example, Salas and Serratose (1953) performed one-dimensional consolidation tests on homo-ionized bentonite in water, and concluded that the compression indices, swelling indices, and e values of the bentonite were inverse functions of the valence of the absorbed cation. These results were in accordance with expectations based on DDL theory.

Olson and Mesri (1970) published data for one-dimensional consolidation and swelling of homo-ionized smectite in various chemical solutions (i.e., water, ethyl alcohol, carbon tetrachloride). Similar to Salas and Serratose (1953), Olson and Mesri (1970) found that the positions of the swelling and compression curves of smectite specimens were strongly influenced by the valence of the adsorbed cation. The swell index (C_s), measured during unloading of the specimens, decreased as the valence of the adsorbed cation increased. For example, the C_s ranged from 1.53 to 3.60 and 0.26 to 0.34 when the adsorbed cations were Na^+ and Ca^{2+}, respectively. When the smectite specimens were allowed to swell in carbon tetrachloride, the observed swelling was negligible (C_s of 0.03) relative to swelling observed when the liquid was water. During one-dimensional consolidation testing with water, under the same consolidation pressure, the Na-smectite maintained higher void ratios than the Ca-smectite. For example, for a

consolidation pressure of 4.8 kPa (100 psf), the void ratios of the Na- and Ca-smectite specimens ranged from approximately 21 to 33 and 6.2 to 6.7, respectively. Olson and Mesri (1970) concluded that physico-chemical, rather than mechanical, effects dominated the consolidation behavior of the smectite, and they attributed the ability of the sodium smectite to maintain high void ratios under loading to long-range double-layer forces.

Di Maio (1996) performed experiments to evaluate the effects of exposure to salt solutions on the mechanical behavior of bentonites. The results supported the hypothesis that diffusion of ions into or out of the clay caused changes in the thickness of the DDL. As salt concentration in the bulk solution increases, the thickness of the DDL decreases. In addition, the DDL increases with increasing hydrated radius of the ion as indicated by the Stern (1924) model, such that the DDL for Na-montmorillonite will be thicker than that for K-montmorillonite (Sridharan 1991). The DDL thickness also will be greater for Na-montmorillonite than Ca-montmorillonite, as DDL thickness and cation charge are inversely related (van Olphen 1963). As expected, when monovalent cations dominate the exchange sites, higher membrane efficiencies or salt-sieving ability is typically observed, relative to clays with significant multivalent cations, partly due to the increased DDL thickness (e.g., Kemper and Maasland 1964).

3.3 Materials and methods

3.3.1 Original bentonites

The clay specimens were prepared from GCL-grade, granular bentonite (CETCO, Hoffman Estates, IL). A photograph of the granular bentonite, prior to preparation for testing, is provided in Figure 3.3a, and some relevant properties of the granular bentonite are summarized

in Table 3.2. The bentonite contained 90 % clay-size particles (in accordance with ASTM D 422), and the specific gravity was measured (ASTM D 854) as 2.71. The bentonite classified as high plasticity clay (CH) according to the Unified Soil Classification System (ASTM D 2487). From the mineralogical analysis performed by Mineralogy, Inc. (Tulsa, OK), the relative abundance of montmorillonite was 91 %.

The properties in Table 3.2 for the bentonite used in this study can be compared with those for other bentonites reported in the literature as summarized in Table 3.3. Based on information provided in Tables 3.2 and 3.3, the granular bentonite used in this study may be considered representative of conventional bentonites used in barrier applications, such as geosynthetic clay liners, compacted sand-bentonite, soil-bentonite backfills, and bentonite buffers for high-level radioactive waste. For example, the plasticity index (*PI*) of the bentonite was 428 %. Typical values of *PI* reported in the literature for bentonite, as summarized in Table 3.3, range from 320 % to more than 700 %.

3.3.2 Chemical solutions

The liquids used in this study included DIW (pH = 7.35, *EC* at 25 ^{o}C = 0.06 mS/m) and chemical solutions of sodium chloride (NaCl) (certified A.C.S.; Fisher Scientific, Fair Lawn, NJ) dissolved in DIW with NaCl concentrations ranging from 0.1 M to 1 M. Concentrations of Na^{+} were measured using inductively coupled plasma-atomic emission spectrometry or ICP-AES (IRIS® Advantage/1000 ICAP Spectrometer, Thermo Jarrel Ash Co., Franklin, MA). Concentrations of chloride (Cl^{-}) were measured using ion chromatography or IC (Dionex® 4000i 131 IC Module, Dionex Co., Sunnyvale, CA). The measured *EC* of the NaCl solutions at 25 ^{o}C ranged from 1,080 mS/m to 8,770 mS/m.

3.3.3 Modification of the exchange complex

To control the cations on the exchange complex of the clay specimens, the granular bentonite was treated via dialysis using 0.1 M, 0.5 M, and 1.0 M NaCl solutions. Specimens were prepared by placing 25 g (dry mass) of granular bentonite in a dialysis bag comprised of standard grade, regenerated cellulose (RC) membrane tubing with a flat width of 100 mm (Spectra/Por 1, MWCO:6,000–8,000 Daltons, Spectrum Laboratories, Inc., Rancho Dominguez, CA). Standard RC material is appropriate for solutions with pH ranging from 2 to 12 and temperatures ranging from 4 ºC to 121 ºC (Spectrum Laboratories, Inc. 2011). The molecular weight cut off (MWCO) of the standard RC material, which is a rating of retention performance for dialysis membranes defined as the molecular weight solute that is 90 % retained by the membrane during a 17-h period, is 6,000 to 8,000 Daltons, such that NaCl and H_2O may pass through the membrane, whereas bentonite particles are restricted (Spectrum Laboratories, Inc. 2011). Dialysis also was performed using only 10 g of bentonite to evaluate the effect of the amount of bentonite on the effectiveness of the procedure. However, the default bentonite content for all other dialysis treatments was 25 g.

To prepare the dialysis bag, a section of standard RC membrane (which was received as a 30-m-long roll) was cut to a length of 260 mm. As recommended by the manufacturer, the section of membrane material was soaked in DIW for at least 30 min prior to use to remove impurities. After soaking, one end of the membrane tubing was sealed with a 110-mm-wide nylon closure (universal closures, Product No. 142113, Spectrum Laboratories, Inc., Rancho Dominguez, CA). Granular bentonite then was poured through the open end into the dialysis membrane bag, followed by approximately 300 mL of NaCl solution, and the open end was sealed with another nylon closure. The specimen contained in the dialysis membrane bag then

was placed in a 7.6-L glass jar containing 7 L of NaCl solution (the dialysate), which was stirred continuously with a magnetic stirrer (Isotemp Basic Magnetic Stirrer, Fischer Scientific, Atlanta, GA), as shown in Figure 3.2a. The jar was covered with plastic wrap (Glad Products Company, Oakland, CA, USA) to minimize evaporation. Conceptually, the high concentration of Na^+ in the solution bath results in replacement of the cations on the exchange sites of the bentonite (e.g., Na^+ for Ca^+), and subsequent diffusion of the replaced cations from the clay into the surrounding dialysate. To expedite this process, the NaCl solution was replaced daily. Prior to replacing the solution, samples of the dialysate (the NaCl solution in the jar) were collected to confirm cation exchange via chemical analysis by ICP (see Section 3.4). The *EC* of the dialysate was measured daily and recorded with an *EC* probe (150 A+ Conductivity Meter; Thermo Orion, Beverly, MA) to confirm consistency in preparation of NaCl solutions and the dialysis procedure.

To evaluate the increase in Na^+ on the exchange complex and whether homo-ionization of the bentonite actually was obtained, tests were performed to measure the CEC, soluble cations, and bound (exchangeable) cations of the dialyzed bentonite material. To prepare material for testing, the bentonite was air-dried and gently ground with a pestle and mortar. The dried material was transported to the Soil, Water and Plant Testing Laboratory (SWPTL) at Colorado State University to measure CEC, and soluble and exchangeable cations, in general accordance with ASTM D 7503-10.

3.3.4 Removal of soluble salts via reverse dialysis

After dialysis of the bentonite to induce sodium homo-ionization with the NaCl solution, the procedure was reversed to remove excess soluble salts in the bentonite via dialysis using DIW as the dialysate rather than the NaCl solution (Fig. 3.2c,d). The objective in removing

soluble salts was to enhance the potential for semipermeable membrane behavior of the bentonite in the subsequent membrane tests. For example, in previous membrane behavior studies involving bentonites, excess soluble salts in the specimens typically have been reduced by flushing or leaching via permeation of the specimens with DIW under an applied hydraulic gradient (e.g., Malusis et al. 2001; Malusis and Shackelford 2002a; Shackelford and Lee 2003; Yeo et al. 2005; Kang and Shackelford 2009; Di Emidio 2010; Bohnhoff et al. 2014). The effluent was collected at regular intervals and the *EC* of the solution was measured as an indicator of the remaining salt concentration in the specimen. However, despite the use of relatively high hydraulic gradients (e.g., > 100), the durations of permeation required to reduce soluble salts contents in the pore waters of the specimens to acceptably low levels (e.g., $EC < 10$ mS/m) generally have been exceedingly long, on the order of 6 months to a year, due to the low k (e.g., $k < 2 \times 10^{-11}$ m/s) of the specimen (Shackelford 2013).

In an effort to reduce the time required for soluble salt removal, Dominijanni et al. (2013) used an alternative "squeezing" method to prepare specimens for membrane behavior testing. The squeezing method consisted of a series of consecutive phases of bentonite hydration with DIW, followed by drained consolidation (maximum load of 500 kPa). The *EC* of the drained solution was measured to evaluate the soluble salt concentration. The *EC* of the collected solution decreased from an initial value of 175 mS/m (at the start of the first consolidation phase) to approximately 45 mS/m (at the end of the fifth consolidation phase). Using this technique, Dominijanni et al. (2013) were able to prepare 500 g (dry mass) of flushed bentonite over a duration of 40 to 50 days.

As described previously, dialysis with DIW has been used extensively in the soil sciences to remove excess soluble salts from clay soils within short timeframes, but less so in

geotechnical and geoenvironmental research. Thus, this reverse dialysis procedure using DIW was evaluated as a procedure that may result in similar results (*EC* of pore fluid < 10 mS/m), but within a much shorter time frame (e.g., a couple of weeks versus months). During dialysis with DIW as the dialysate, excess dissolved salts diffused out of the slurried specimen, with a consistency more like a paste at this stage, through the dialysis bag, increasing the *EC* of the DIW bath over time from an initial value ranging from about 0.02 to 0.04 mS/m. The DIW was replaced daily to maintain a high concentration gradient, and the incremental change in *EC* in the dialysate was recorded. Several trial tests were performed at the beginning of the study to identify acceptable termination criteria for this stage. Based on this preliminary assessment, the reverse dialysis process to remove soluble salts was considered complete when changes in *EC* became negligible (i.e., $\Delta EC \leq 0.01$ to 0.03 mS/m over a 24-h period). Although the time required to achieve this criteria ranged from 7 to 10 d, the stage was performed for 13 to 14 d to be conservative. Upon completion of the soluble salt removal stage, the dialyzed bentonite paste was removed from the dialysis bag and stored in a sealed container. If the material was to be analyzed for CEC and exchangeable cations, a sample of the paste was removed and air-dried. A photograph of the resulting fully dialyzed material, prior to storage, is shown in Fig. 3.3b.

3.3.5 Atterberg limits

Atterberg limits testing was performed in general accordance with ASTM D 4318-10. The liquid limit (*LL*) and plastic limit (*PL*) were measured for both the untreated bentonite and the bentonite after treatment with 0.1 M NaCl and dialysis with DIW. After completion of dialysis, the treated bentonite paste was air dried and gently ground with a mortar and pestle to prepare the material for testing.

3.3.6 Mass leaching model to determine diffusion properties

After the NaCl treatment stage, the fluid in the pore space of the bentonite paste contained inside the dialysis bag is theoretically at equilibrium with the concentration of the NaCl solution used for treatment (i.e., 0.1 M, 0.5 M, or 1.0 M NaCl). To confirm this assumption, the pore water was extracted from some of the bentonite paste specimens after treatment with NaCl solution. The paste was diluted with DIW to allow for separation of the pore water via vacuum extraction through filter paper into a Buchner funnel. The measured NaCl concentrations of the pore waters (after corrections for dilution) were approximately the same as the concentrations of the NaCl treatment solutions (e.g., 0.097 M NaCl for the slurry treated with 0.1 M NaCl). Thus, the assumption of equilibrium between the pore water and the treatment solution at the end of the NaCl treatment stage was considered reasonable.

During the DIW dialysis stage after the NaCl treatment, the NaCl in the pore space diffuses out of the bentonite paste, through the dialysis membrane and into the bulk solution of the dialysis jar. Thus, the 14-day period of the DIW dialysis stage represents a mass leaching problem, whereby the paste in the dialysis bag represents a mass with initial concentration, C_o, and the DIW in the jar (which is replaced with fresh DIW every 24 h) represents an approximately flushing boundary condition. The procedure whereby the dialysate is replaced on a daily basis is analogous to the dynamic leaching test that has been used extensively to evaluate the leaching of contaminants from stabilized waste forms (e.g., Godbee et al. 1980; Côté et al. 1987; Sharma and Lewis 1994; ASTM 2008; Patra et al. 2011; EPA 2013; Shackelford 2014). This process is represented schematically in Figure 3.2c,d. Bulk diffusion models (BDM) for a mass leaching condition were used in conjunction with the *EC* data to calculate diffusion

coefficients of the bentonite paste at the end of the DIW dialysis stage (e.g., Kim et al. 2002; Shackelford 2014).

The initial time, t_o ($t = 0$), corresponds to the end of the NaCl treatment, prior to the start of DIW dialysis. At $t = t_o$, the paste was assumed to be monolithic with a uniform initial concentration, C_o, of NaCl in the pore space. The paste was assumed to be a diffusion-controlled matrix, where the release of the solutes follows first-order diffusion, and is the result of a concentration gradient between the paste in the dialysis bag and the DIW in the jar. For a porous material, Fick's second law for diffusion is as follows (e.g., Shackelford 1991):

$$\frac{\partial C}{\partial t} = D_a \frac{\partial^2 C}{\partial x^2} \tag{3.2}$$

where C is concentration, t is time, D_a is the apparent diffusion coefficient, and x is the spatial coordinate. The apparent diffusion coefficient is related to the free-solution (aqueous) diffusion coefficient, D_o, as follows (Shackelford 1991):

$$D_a = \frac{D_o \tau_a}{R_d} = \frac{D^*}{R_d} \tag{3.3}$$

where τ_a is the dimensionless apparent tortuosity factor, R_d is the retardation factor, and D^* is the effective diffusion coefficient. If the exchange complex of the bentonite is assumed to be sufficiently saturated with Na^+ such that retardation of diffusion of NaCl is negligible (i.e., $R_d \approx 1$), Equation 3.3 reduces to the following:

$$D_a \approx D_o \tau_a \approx D^* \tag{3.4}$$

Mass leaching analyses to determine values of D_a for the bentonite paste were performed assuming the slurry was either a semi-infinite or finite-cylindrical medium, as described in detail in the following sections.

3.3.6.1 Leaching from a semi-infinite medium

If the bentonite paste is assumed to be a semi-infinite medium, the initial condition and two boundary conditions are as follows (e.g., Kim et al. 2002):

$$\begin{aligned} &C(x>0, t=0) = C_o \\ &C(x=0, t>0) = 0 \\ &C(x=\infty, t>0) = C_o \end{aligned} \tag{3.5}$$

The solution to Equation 3.2 using the relationship for D_a in Equation 3.3 (i.e., without any assumptions regarding the value of R_d) and the conditions in Equation 3.5 is as follows (e.g., Nathwani and Phillips 1980):

$$C(x,t) = C_o erf\left(\frac{x}{2\sqrt{D_a t}}\right) \tag{3.6}$$

where *erf* is the error function. The cumulative mass of NaCl leached from the bentonite paste at time t, M_t, can be estimated using the *EC* measurements of the dialysis water (taken prior to replacing the DIW every 24 h) and the linear correlation between *EC* and NaCl concentration provided in Figure 3.4, as follows:

$$M_t(\text{mg NaCl}) = \Sigma\Delta m = \Sigma\left[\frac{8.45\times10^{-5}\ \text{mol/L}}{\text{mS/m}}\times\Delta EC(\text{mS/m})\times 7\,\text{L}\times\frac{58,440\text{mg/L}}{\text{mol/L}}\right] \quad (3.7)$$

Example data for ΔEC and the corresponding Δm and M_t values are shown in Figures 3.5a-c. The ratio of M_t to the total, initial mass of NaCl in the bentonite, M_∞, is the cumulative fraction leached, *CFL* (Nathwani and Phillips 1978, 1980; Godbee et al. 1980; Kim et al. 2002), or:

$$CFL = \frac{M_t}{M_\infty} = 2\left(\frac{S}{V}\right)\left(\frac{D_a t}{\pi}\right)^{1/2} \quad (3.8)$$

where S is the surface area of the dialysis bag, and V is the volume of the dialysis bag. The value of M_∞ is calculated based on the volume of the paste in the dialysis bag and the assumption that, at the end of the NaCl treatment stage (immediately prior to the start of the DIW dialysis and the onset of mass leaching), the pore water in the bentonite paste is in equilibrium with the NaCl solution used for treatment (i.e., after 7 days of exposure to 0.1 M, 0.5 M, or 1.0 M NaCl). Example results for *CFL* are shown in Figure 3.5d. By rearranging Equation 3.8, the D_a value of the bentonite at the end of DIW dialysis (t = 13-14 d) can be calculated as follows:

$$D_a = \frac{\pi}{t}\left(\frac{CFL}{2}\frac{V}{S}\right)^2 \quad (3.9)$$

The model used for leaching from a semi-infinite medium is summarized in Table 3.4, and the calculated D_a values for the bentonite paste are presented in Section 3.4 and Table 3.5.

3.3.6.2 Leaching from a finite cylindrical medium

If the *CFL* values are high (e.g., *CFL* > 0.2), the simplifying assumption of a semi-infinite medium may not be appropriate (Godbee et al. 1980; ASTM 2008). Leaching models have been developed for finite waste mediums of cylindrical and spherical shape, which take into account the depletion of the solid due to leaching (e.g., Pescatore 1990; Kim et al. 2002; ASTM 2008). For example, the solution for a cylindrical solid of height *H* and radius *R* is as follows:

$$CFL = \frac{M_t}{M_\infty} = 1 - \frac{32}{\pi^2} \sum_{n=1}^{\infty} \frac{\exp\left[-((2n-1)\pi / H)^2 D_a t\right]}{(2n-1)^2} \sum_{m=1}^{\infty} \frac{\exp\left[-(\beta_m / R)^2 D_a t\right]}{{\beta_m}^2} \qquad (3.10)$$

where β_m represents the m^{th} zero of the zeroth order cylindrical Bessel function. Numerical convergence of the open series in Equation 3.10 is extremely slow, such that closed-form solutions have been developed where the open series is truncated. Upper bound values for *n* and *m* (represented by *N* and *M*, respectively) may be chosen, and the error due to truncating the series can be evaluated as described in Pescatore (1990). Applying upper bound limits, Equation 3.10 becomes:

$$CFL = \frac{M_t}{M_\infty} = 1 - \frac{32}{\pi^2} \sum_{n=1}^{N} \frac{\exp\left[-((2n-1)\pi / H)^2 D_a t\right]}{(2n-1)^2} \sum_{m=1}^{M} \frac{\exp\left[-(\beta_m / R)^2 D_a t\right]}{{\beta_m}^2} \qquad (3.11)$$

Based on suggested values in the literature (Pescatore 1990; ASTM 2008), both *M* and *N* were set to values of 20 for this study. Several calculation iterations were performed, varying the values of *M* and *N*, to confirm that the error due to truncating the series in Equation 3.10 did not

affect the calculated values of the *CFL*. Once the values of *M* and *N* exceeded 5, the calculated value of the *CFL*, which was evaluated to 15 decimal points, did not change with increasing values of *M* and *N*. Thus, upper bound values of 20 for *M* and *N* were considered more than sufficient for the calculations performed in this study.

3.4 Results

Preparation of Na-bentonite consisted of two dialysis stages: (1) NaCl treatment to increase the percentage of Na^+ on the exchange complex; and (2) removal of excess soluble salts via dialysis with DIW. Example results for each stage are discussed in the following sections.

The dialysis process is controlled by the rate of diffusion across the cellulose membrane and within the bentonite paste. Factors that affect the rate of salt diffusion across the membrane include the pH, concentration and temperature of the dialysate, duration between dialysate replacement, sample and dialysate volumes, the previous number of dialysate changes, membrane surface area, membrane thickness, molecular charges and dialysate agitation (stirring) (Spectrum Laboratories, Inc. 2011). To maximize the efficiency of the specimen preparation methods used in this study, the effects of dialysate volume, duration between dialysate changes, and dialysate agitation were initially evaluated with several trial tests. As expected, stirring, daily replacement of dialysate, and the use of larger dialysate volumes (i.e., 7 L vs. 1 L) resulted in faster completion of each dialysis stage. These conditions decrease completion time by maintaining greater concentration gradients between the dialysate and the bentonite in the dialysis bags. Thus, only these conditions (7 L of dialysate, daily replacement, magnetic stirring) were used for the remaining testing program, and all the results presented were obtained under such conditions.

3.4.1 NaCl treatment stage

As described previously, strong NaCl solutions (e.g., ≥ 0.1 M) were used to increase the *ESP* of the bentonite via dialysis. Prior to replacing the NaCl with fresh solution after each 24-h period, samples of the NaCl solution (in the jar, outside of the dialysis bag) were collected to confirm cation exchange by measuring the concentrations of cations other than Na^+ (i.e., K^+, Ca^{2+}, Mg^{2+}). The concentrations were measured via ICP-AES (same model as described previously).

Example results for the cumulative masses of K^+, Ca^{2+}, and Mg^{2+} removed from the specimen during the first four days of NaCl treatment are shown in Figures 3.6a and 3.6b for bentonite exposed to 0.5 M and 1.0 M NaCl, respectively. The initial (source) NaCl solution had non-measurable (below detection level) concentrations of cation species other than Na^+. After four days of treatment with the 0.5 M NaCl solution (i.e., after four, 24-h cycles where NaCl solution was replaced every 24 h), the cumulative masses of K^+, Ca^{2+}, and Mg^{2+} removed from the bentonite were 106 mg, 99 mg, and 26 mg, respectively. As expected, more cation exchange occurred with the 1.0 M NaCl than the 0.5 M NaCl treatment, as indicated by the higher cumulative masses of removed K^+, Ca^{2+}, and Mg^{2+}. For the bentonite exposed to 1.0 M NaCl, the cumulative masses of K^+, Ca^{2+}, and Mg^{2+} removed from the specimen after four, 24-h cycles were 195 mg, 141 mg, and 64 mg. Based on the example data shown in Figure 3.6, as the concentration of the NaCl solution used for dialysis increased, the rate of cation exchange of Na^+ for other existing cations on the exchange complex increased. The trend of increasing Na^+ on the exchange complex with increasing NaCl concentration was confirmed via measurement of exchangeable cations of the treated bentonite, i.e., after the NaCl and DIW dialysis stages (see Section 3.4.1.3).

To evaluate whether homo-ionization of the bentonite was obtained using the dialysis procedure for 7 days (7 daily salt-bath cycles of 0.1 M, 0.5 M, or 1.0 M NaCl), the bound (exchangeable) cations of the original (untreated) and dialyzed material were measured as previously described. As indicated by the results shown in Table 3.6 and Figure 3.7, the mole fraction of Na^+ on the exchange complex of the bentonite increased as the concentration of the NaCl solution used to treat the bentonite increased, as expected. For example, as the concentration of the NaCl solution used in the dialysis was increased from 0.1 M to 1.0 M, the mole fraction of Na^+ on the bentonite increased from 0.69 to 0.89 (i.e., *ESP* increased from 69 % to 89 %). Although the dialysis treatment resulted in a significant increase in the *ESP* relative to the *ESP* of the untreated bentonite of 47 %, the *ESP* was not increased sufficiently to consider the bentonite homo-ionized (e.g., *ESP* > 95 %).

3.4.2 De-ionized water treatment stage

After treatment with NaCl solution, the dialysis bag was placed in a bath of DIW, which was replaced every 24 h. Diffusion of NaCl occurred out of the bentonite, through the dialysis membrane and into the DIW bath. Over each 24-h period, the *EC* of the bath water increased with time, due to the increase in NaCl concentration. The initial *EC* of the DIW bath water was always less than 0.1 mS/m. As shown in Figure 3.8, the *EC* measured after each 24-h cycle decreased with each subsequent cycle, as NaCl was removed from the bentonite and the concentration gradient between the bentonite and the bath water decreased.

As expected, the *EC* of the bath water after the first 24-h cycle increased as the concentration of the NaCl solution that was used to treat the bentonite increased (Figure 3.8a). The higher the concentration used to treat the bentonite prior to DIW dialysis, the higher the

initial concentration inside the dialysis bag and the resulting concentrating gradient. For example, the values of *EC* for the bath water at the end of the first 24-h cycle in DIW were 229 mS/m and 36.8 mS/m for bentonite specimens treated with 1.0 M and 0.1 M NaCl, respectively.

As shown in Figure 3.8b, for bentonite specimens treated with the same NaCl concentration (1.0 M), the *EC* of the bath water after the first 24-h period increased as the mass of bentonite in the slurry specimen decreased. The values of *EC* were 273 mS/m and 229 mS/m for the specimens comprised of 10 g and 25 g (dry mass) of bentonite, respectively. The higher *EC* of the bath water surrounding the dialysis bag with 10 g of bentonite indicates that the diffusion coefficient initially was higher than that of the 25-g specimen. This relative difference is expected, as the paste in the dialysis bag with less bentonite mass would have a higher porosity and, therefore, higher rate of diffusion.

A comparison of the measured concentrations of soluble salts before and after the dialysis procedure is shown in Figure 3.7b. Measurement of the soluble cations (ASTM D 7503) indicated that the dialysis procedure was a very effective method for reducing the concentration of soluble salts in the bentonite. Prior to any dialysis treatment (i.e., the original bentonite), the concentrations of soluble Na^+, K^+, Mg^{2+}, and Ca^{2+}were 19, 1.0, 0.57 and 0.25 meq/100 g. With the dialysis procedure, the concentrations of soluble Na^+ and K^+ were reduced to 2.2 and 0.3 meq/100g, respectively, and the concentrations of Ca^{2+} and Mg^{2+} were below the ICP-AES detection limits.

3.4.3 Diffusion coefficients

As shown in Figure 3.9 and Table 3.5, the values of D_a for the bentonite specimens calculated assuming bulk diffusion from semi-infinite and finite cylindrical mediums ($D_{a,SI}$ and

$D_{a,FC}$, respectively) ranged from 5.5 x 10^{-11} m^2/s to 1.5 x 10^{-10} m^2/s and from 1.5 x 10^{-10} m^2/s to 3.8 x 10^{-10} m^2/s, respectively. These values fall within the typical ranges reported in the literature for Na-bentonites at high water contents and porosities. For example, for saturated GCL specimens comprised of Na-bentonite with porosities (n) between 0.78 and 0.80, Malusis and Shackelford (2002b) reported effective diffusion coefficients (D^*) for Cl^- ranging from 7.1 x 10^{-11} m^2/s to 2.3 x 10^{-10} m^2/s. Kozaki et al. (2005) measured D_a values for Na^+ ranging from 7.4 x 10^{-11} m^2/s to 8.2 x 10^{-11} m^2/s for Na-montmorillonite specimens prepared at a dry density of 0.7 Mg/m^3 (n = 0.74, if G_s is assumed to be 2.7). Malusis et al. (2014) reported D^* values for Cl^- ranging from 4.3 x 10^{-11} m^2/s to 2.8 x 10^{-10} m^2/s for GCL specimens with n ranging from 0.66 to 0.81, respectively.

As expected, for the same treatment concentration and dialysis bag volume, D_a increased as the dry mass of bentonite in the dialysis bag decreased. For a NaCl concentration of 1.0 M and dialysis bag volume of 352 mL, $D_{a,SI}$ and $D_{a,FC}$ increased from 5.5 x 10^{-11} m^2/s to 6.0 x 10^{-11} m^2/s and from 1.5 x 10^{-10} m^2/s to 1.6 x 10^{-10} m^2/s, respectively, as the dry mass of bentonite decreased from 25 g to 10 g. A decrease in dry mass of bentonite for a constant volume results in increased void volume and porosity and, thus, an increase in D_a.

3.5 Discussion

3.5.1 Effectiveness of NaCl treatment

The effectiveness of the dialysis procedure was compared with similar clay purification methods described in the soil science, geotechnical and geoenvironmental literature. Several studies where NaCl solutions were used to increase the *ESP* of bentonite such that the clay could be considered sodium homo-ionized (e.g., *ESP* > 95 %) are summarized in Table 3.1. Generally,

the concentration of the NaCl solutions used in washing, centrifuging, and/or dialysis procedures to prepare homo-ionized clays ranged from 0.001 M to 1.0 M, with 1.0 M being the most commonly used concentration (see Table 3.1). While several studies confirmed reduction of excess salt concentrations by measuring the *EC* or Cl^- concentration of the supernatant or pore water after the salt removal procedures (e.g., Kemper 1961; Leonard and Low 1963; Kemper and van Schaik 1966; Shainberg and Kemper 1972; Churchman and Weismann 1995; Likos and Lu 2002; Tarchitzky and Chen 2002; Kozaki et al. 2008), very few studies performed measurements to confirm homo-ionizaton or the final *ESP* of the clay (e.g., Leonard and Low 1963; Mesri and Olson 1971).

The maximum values of *ESP* reported by Leonard and Low (1963) were 85 % and 86 % for Wyoming bentonite passed through exchange resins and for Cheto bentonite mixed three times with NaCl solution (concentration not reported), respectively. Olson and Mesri (1970) reported an *ESP* greater than or equal to 96 % for Wyoming bentonite that had been washed multiple times with NaCl (concentration and number of washes not reported). For the remainder of the literature summarized in Table 3.1, the clay was assumed, rather than confirmed, to be homo-ionized after NaCl treatment.

The concentration of NaCl solution used in this study was 0.1 M to 1.0 M, which was consistent with concentration ranges reported in the literature. However, the duration of the NaCl stage of the dialysis treatment (7 d) was longer than that reported in most of the literature (e.g., < 2 to 4 d), in an effort to ensure that the bentonite became homo-ionized. While the dialysis treatment did result in a significant increase in the *ESP* relative to the *ESP* of the untreated bentonite, the highest *ESP* value of 89 % was still not high enough to consider the bentonite homo-ionized. The *ESP* value of 89 % was obtained after dialysis with 7.0 L of 1.0 M

NaCl solution (for 25 g (dry mass) of clay), which was replaced daily for seven days. The *ESP* obtained under such conditions was expected to be closer to 95 %, based on comparison with the literature. The lower measured values of *ESP* indicate that the bentonite and dialysis method used in this study required longer durations of dialysis or the use of higher concentrations of NaCl to homo-ionize the clay, or, that sodium homo-ionization (quantified as *ESP* > 95 %) of bentonite was not actually achieved in some of the literature. Regardless, the results shown in Figure 3.10 indicate that simple modifications to the dialysis procedure, such as use of slightly stronger NaCl solution (e.g., 2.0 M), would likely result in bentonite with an *ESP* greater than 95 %, such that the clay would be considered homo-ionized for all practical purposes.

3.5.2 Effect of dialysis treatment on plasticity

The liquid limit (*LL*) and plastic limit (*PL*) were measured for both the untreated bentonite and the bentonite after treatment with 0.1 M NaCl and dialysis with DIW. Based on the results of the Atterberg limits tests (see Table 3.3), the dialysis treatment did not significantly affect the *PL* of the bentonite. The values of *PL* for the original bentonite and the bentonite after dialysis treatment were 34 % and 35 %, respectively. However, the *LL* of the treated bentonite was more than double that of the untreated bentonite, with the *LL* increasing from a value of 428 % to 871 %. Consequently, the plastic index (*PI*) also more than doubled, with the value increasing from 394 % to 836 % with the treatment. All of the *PL* and *LL* results fell within the typical ranges reported in literature for smectitic clays. For example, Olson and Mesri (1970) reported *LL* and *PL* ranges of 190 % to 1160 % and 31 % to 47 %, respectively, for Wyoming bentonite exposed to a variety of pore fluids. Cornell (1951) reported *LL* and *PL* values of

710 % and 54 %, respectively, for sodium montmorillonite. Additional examples for the Atterberg limits of bentonite from the literature are provided in Table 3.2.

The significantly higher values of *LL* for the Na-treated bentonite (relative to the untreated bentonite) are consistent with observations reported in the literature for bentonites with increased percentages of Na^+ occupying the exchange complex. For example, Sridharan et al. (1986) measured the Atterberg limits of bentonites that were homo-ionized (via washing) using chloride salt solutions containing either monovalent (Na^+, K^+, Li^+, NH_4^+), divalent (Mg^{2+}, Ca^{2+}) or trivalent cations (Fe^{3+}, Al^{3+}). An increase in the valency of the cation on the exchange complex resulted in a decrease in *LL*. The highest *LL* values corresponded to the Li- and Na-bentonites, with values of 675 % and 495 %, respectively. The lowest *LL* values of 108 % and 120 % resulted for the Al- and Fe-bentonites, respectively. The *PL* ranged from 49 % to 64 % for all of the bentonites, with inconsistent trends between *PL* and cation valence.

Mishra et al. (2009) measured the *LL* of various basalt soil-bentonite mixtures and observed that as the *ESP* of the bentonite increased, the *LL* increased. The mixtures were prepared at a basalt soil-to-bentonite ratio of four to one (by dry mass). The mixture containing the bentonite with the highest *ESP* value of 66 % exhibited the highest *LL* of 140 % for testing with DIW. In contrast, the mixture containing the bentonite with the lowest *ESP* value of 35 % only had a *LL* of 78 %.

As previously described (Section 3.4.2), in addition to increasing the *ESP*, the dialysis procedure significantly reduced the concentration of soluble salts. The *LL* of high plasticity clays also has been shown to increase as the concentration of soluble salts decreases, whereas the *PL* remains relatively constant (e.g., Rao et al. 1993; Di Maio 1996; Gleason et al. 1997; Di Maio et al. 2004; Arason and Yetimoglu 2008; Yukselen-Aksoy et al. 2008). For example, for

Na-bentonite comprised of 90 % montmorillonite (*CEC* = 127.9 meq/100 g), Yukselen-Aksoy et al. (2008) measured values of *LL* of 124 % and 396 % when the clay was mixed with natural seawater (Cl^- concentration = 21,321 ppm) and distilled water, respectively. The *PL* remained relatively constant with values of 50 % and 52 % measured for the seawater and distilled water, respectively.

Based on the trends reported in literature, the significant increase in *LL* (by 443 percentage points) and, consequently, *PI* in this study due to the dialysis treatment provides additional evidence that the procedure was successful in both increasing the percentage of Na^+ on the exchange complex and removing excess soluble salts. Thus, the dialysis procedure that has been used extensively by soil scientists provides a simple and quick (i.e., < 14 d) method to to control the exchange complex and soluble salt concentration of clays used in geoenvironmental research.

3.5.3 Effect of Exchangeable Sodium Percentage (ESP) on diffusion coefficient

As shown previously in Figure 3.9, the calculated values of D_a for the bentonite specimens based on bulk diffusion from semi-infinite and finite-cylindrical mediums generally decreased as the *ESP* of the bentonite increased (i.e., as the concentration of NaCl used to treat the bentonite increased). For example, the $D_{a,SI}$ values for bentonite with *ESP* values of 69 %, 80 %, and 89 % were 1.3 x 10^{-10} m^2/s (average of 10 tests), 6.9 x 10^{-11} m^2/s and 5.5 x 10^{-11} m^2/s, respectively. Decreasing rates of diffusion with increasing *ESP* due to increasing swell in clays has been documented in the soil science literature (e.g., Dufey et al. 1976, 1983). For example, Dufey et al. (1976) evaluated diffusion of Na^+ through suspensions of montmorillonite clays (27 g dry mass/L) with variable ratios of Na^+ and Ca^{2+} on the exchange complex. For tests

performed at 16 °C, D_a values for Na^+ decreased from 7.6 x 10^{-10} m^2/s to 3.1 x 10^{-10} m^2/s as the *ESP* increased from 15 % to 100 %. Thus, the diffusion results obtained with the dialysis procedure are in general agreement with expected trends and published data for smectitic clays.

3.5.4 Effect of method used to analyze diffusion

The mass-leaching model based on the assumption of a semi-infinite medium is the simplest analysis to perform, but typically is not appropriate for porous materials that result in high values of the *CFL* (e.g., > 0.2) (Godbee et al. 1980; ASTM 2008). The semi-infinite model may be used to analyze a finite specimen as long as the concentration profile in the specimen is similar to the profile that would exist in a semi-infinite medium. However, as mass continues to diffuse out of the specimen with time, the concentration profile in the finite specimen will diverge from the profile predicted based on a semi-infinite medium. Thus, a solution accounting for the finite mass and depletion of the solute due to leaching is required to accurately determine D_a at high *CFL* (Godbee et al. 1980). The errors associated with the assumption of a semi-infinite medium increase as specimen size decreases, leaching duration increases, and diffusion coefficient increases (i.e., *CFL* increases) (Pescatore 1990). For *CFL* values > 0.2, models based on finite mediums are recommended as per ASTM (2008).

For a given *CFL* value measured for a finite-cylindrical medium, the semi-infinite model will result in lower D_a values than the finite-cylindrical model. For example, Godbee et al. (1980) analyzed leaching of cesium from a cement product with a cylindrical geometry (radius = 12.5 mm, height = 51.0 mm). Example values of D_a determined with the semi-infinite and finite-cylindrical models for the same specimen were approximately 2.0 x 10^{-14} m^2/s and 2.5 x 10^{-13} m^2/s, respectively. Thus, the finite-cylindrical model predicted diffusion rates approximately one

order of magnitude higher than the semi-infinite model based on the measured *CFL*.

For the dialyzed, bentonite paste, the $D_{a,FC}$ values were consistently higher than the $D_{a,SI}$ values, as expected (Figure 3.9). The ratio of the D_a values determined from the finite-cylindrical and semi-infinite models ($D_{a,FC}$ / $D_{a,SI}$) ranged from 2.36 to 2.80. As shown in Figure 3.11, the ratio increased (i.e., the agreement between the two models decreased) as the *CFL* at the end of the leaching period increased. This observation is consistent with the expectation that the error due to assuming a semi-infinite medium becomes more significant as the *CFL* increases, and the concentration profile in the finite medium can no longer be approximated with the semi-infinite model. Therefore, the finite-cylindrical model is recommended for determination of D_a values of clay slurries and pastes when using the dialysis procedure.

3.6 Conclusions and recommendations

A dialysis procedure was developed to allow for preparation of bentonite specimens with a high percentage of Na^+ on the exchange complex (e.g., *ESP* > 70 %) and low concentration of soluble salts. Control of the cation species present on the exchange complex and reduction in initial soluble salt concentrations of bentonites may be desirable for understanding fundamental mechanisms governing soil behavior as well as for improving the containment properties of the bentonites (e.g., swell, hydraulic conductivity, diffusion, membrane efficiency). While clay purification methods have been used by soil scientists for several decades to prepare homo-ionic soil specimens with low soluble salt contents, these procedures are not commonly used in geotechnical engineering testing research. Based on measurement of the bound cations before and after treatment, the *ESP* of the bentonite increased from 47 % for the untreated bentonite to 89 % for bentonite after dialysis with 1.0 M NaCl solution. Measurement of soluble cations

indicated that the dialysis procedure also reduced the concentration of soluble salts (see Figure 3.7). The significant increase in *LL* (by 443 percentage points) and, consequently, *PI*, of the bentonite after dialysis treatment provided further support that the procedure was successful in both increasing the *ESP* and removing excess soluble salts.

The dialysis procedure was compared with similar clay purification methods described in the literature. The procedures used in this study resulted in a significant increase in the *ESP* of the bentonite, but the maximum *ESP* value of 89 % obtained via dialysis with 1.0 M NaCl solution was not high enough to consider the bentonite homo-ionized (e.g., *ESP* > 95 %), despite the use of NaCl concentrations similar to those reported in the literature. However, simple modifications to the dialysis procedure, such as use of stronger NaCl solution (e.g., 2.0 M), are expected to result in homo-ionized Na-bentonite.

Finally, the dialysis procedure was evaluated as a potential method to measure the apparent diffusion coefficient, D_a, of a clay slurry using available mass leaching models. The values of D_a measured with the dialysis procedure fell within the typical ranges reported in the literature for Na-bentonites evaluated using traditional diffusion test methods. Due to the errors associated with the assumption of a semi-infinite medium, the finite-cylindrical model is recommended for calculation of D_a values of clay pastes and slurries when using the dialysis procedure described herein.

In summary, the dialysis procedure provides a simple and quick (e.g., < 14 d) method to control the exchange complex and soluble salt concentration of bentonite. In addition, measurement of the *EC* of the dialysis water during the DIW stage allows for estimation of diffusion properties of bentonite slurries or pastes (or other highly-compressible materials), that otherwise may be difficult to evaluate using traditional laboratory equipment.

Table 3.1. Examples of clay purification methods reported in the literature.

Reference	Base Clay Type(s)	Desired Form(s)	Treatment to Homo-ionize	Soluble Salt Removal[1]	Additional Comments or Details Relevant to this Study
A) Studies Related to Membrane, Chemical Osmosis and/or Salt Filtration Behavior of Clays					
Kemper (1961)	Wyoming bentonite, Pierre shale	Na^+	Washed 4x with 1M NaCl solution	Shaken and centrifuged with DIW	Repeated procedure until supernatant was < 0.02 M (based on *EC*).
Hanshaw (1962)	Montmorillonite (85% MMT)	Na^+	Soaked, stirred and washed with 1M NaCl solution	Washed with DIW	Clay was soaked in HCl solution and washed prior to NaCl treatment. The NaCl solution was maintained at pH 8.
McKelvey and Milne (1962)	Shale	Na^+	Washed with NaCl solution	None	Focus was salt-filtering ability of semi-dry, powdered bentonite and shale.
Kemper et al. (1964), Kemper and van Schaik (1966)	Wyoming bentonite	Na^+ or Ca^{2+}	Repeatedly treated clay suspensions with NaCl or $CaCl_2$	Dialysis with sausage casing in distilled water	Kemper and van Schaik (1966) continued dialysis until no chloride was detected.
Abd-el-aziz and Taylor (1965)	Kaolinite	K^+	No details provided	---	Focus was flow of water and salt through unsaturated soils.
Kemper and Rollins (1966)	Wyoming bentonite	Na^+	Repeatedly washed with 1 M NaCl solutions	Dialysis with sausage casing in distilled water	Evaluated osmotic efficiency coefficients for NaCl and Na_2SO_4 solutions.
van Schaik and Kemper (1966), van Schaik et al. (1966)	Wyoming bentonite	Na^+ or Ca^{2+}	Repeatedly treated clay suspensions with NaCl or $CaCl_2$	Dialysis with sausage casing in distilled water	After dialysis, clays were repeatedly mixed with distilled water, centrifuged, and clear supernatant removed.
Mokady and Low (1968)	Aberdeen bentonite	Na^+	Mixed once with NaCl solution	Centrifuged and decanted	Aberdeen bentonite was prepared by Leonard and Low (1963).
	Wyoming bentonite	Na^+	Centrifuged with NaCl solution 4x	Centrifuged 4x with water	Wyoming bentonite was prepared by Mokady and Low (1966).
Olsen (1969), Olsen (1972)	Kaolinite	Na^+	Equilibrated with 0.001 M NaCl solution	None	---
Kemper and Quirk (1972)	Wyoming bentonite, Kaolinite, Willalooka Illite, Fithian Illite	Na^+	Saturated with Na^+ ions during <2 μm separation process	---	Focus was measurement of osmotic flow and electric and streaming potentials.

Reference	Base Clay Type(s)	Desired Form(s)	Treatment to Homo-ionize	Soluble Salt Removal[1]	Additional Comments or Details Relevant to this Study
Shainberg and Kemper (1972)	Wyoming bentonite	Na^+	Washed with 1 M NaCl solution 3x	Centrifuged repeatedly	Repeated centrifuge with distilled water until $AgNO_3$ test for salt was negative.
Coplen and Hanshaw (1973), Hanshaw and Coplen (1973)	Texas montmorillonite	---	None	Stirred 3d in distilled water	After stirring, the distilled water was used to make the test salt solutions.
Kharaka and Berry (1973)	Wyoming bentonite Illite (API No. 36) Shale	Na^+	Washed 5x with NaCl solution (at 2x concentration of NaCl solution used in experiment)	---	Performed filtration experiments with various solutions. Shale was from Kettleman North Dome Oil Field, CA.
Elrick et. al (1976)	Wyoming bentonite	Na^+	Shaken with sequence of 1 M NaCl solutions	Dialysis	Measured differential pressure due to NaCl concentration differences
Kharaka and Smalley (1976)	Wyoming bentonite Kaolinite (API No. 17)	Na^+	Same as Kharaka and Berry (1973)		Focus was filtration behavior of clays.
Fritz and Marine (1983)	Na-bentonite	---	None	None	Performed hyperfiltration tests with NaCl solutions.
Benzel and Graf (1984)	Cheto clay (smectite)	Na^+ Ca^{2+}	Suspended in brine for ≥ 30 days, at (by volume) 1 part brine to 3 parts clay	None	Prior to homo-ionization, washed with 4 L DIW ten times.
Demir (1988)	Cheto clay (smectite)	Na^+	Soaked in 1 M NaCl	Settled in DIW	Evaluated osmostic and electro-osmotic effects.
Whitworth and Fritz (1994)	Wyoming bentonite	Na^+	Slurried with 1 M NaCl	Dialysis	Performed hydraulic conductivity tests with DIW before starting hyperfiltration tests with salt solutions.
Ishiguro et al. (1995)	Wyoming bentonite	Na^+	Soaked in NaCl solution	Dialysis	Same method as Mercier and Detellier (1994).
Di Maio (1996)	Ponza bentonite	K^+ Ca^{2+}	Soaked in KCl or $CaCl_2$ for 3 weeks	Washed repeatedly with DIW	X-ray diffraction indicated had converted Na-montmorillonite to K- or Ca-montmorillonite.
Sherwood and Craster (2000)	Wyoming bentonite	---	None	Dialysis	---
Malusis et al. (2001), Malusis and Shackelford (2002a)	Na-bentonite (GCL)	---	None	Permeated under back-pressure with PTW	PTW = processed tap water. Focus was measurement of membrane behavior.

Reference	Base Clay Type(s)	Desired Form(s)	Treatment to Homo-ionize	Soluble Salt Removal[1]	Additional Comments or Details Relevant to this Study
Shackelford and Lee (2003)	Na-bentonite (GCL)	---	None	Permeated under back-pressure with PTW	Permeated until *EC* of effluent < 50 % of *EC* of weakest solution for membrane testing.
Oduor and Whitworth (2005)	Na-montmorillonite	---	---	Dialysis	---
Kang and Shackelford (2009)	Na-bentonite (GCL)	---	None	Permeated with DIW for 6+ months	Permeated in flex-wall permeameter until *EC* of effluent < 50 % of *EC* of weakest solution for membrane testing.
Bohnhoff (2012)	Na-bentonite (granular and powdered)	---	None	Permeated with DIW for 6+ months	Focus was measurement of membrane behavior.
B) Other Studies					
Leonard and Low (1963)	Wyoming bentonite	Na^+	Passed through series of exchange resins (OH, H, Na)	None	Achieved *ESP* of 85 %. Confirmed $AgNO_3$ test for Cl^- was negative.
	Belle Fourche bentonite	Na^+	Mixed once with NaCl solution	Washed by centrifugation and decantation	Achieved *ESP* of 82 %. Confirmed $AgNO_3$ test for Cl^- was negative.
	Utah bentonite				Achieved *ESP* of 40 %. Confirmed $AgNO_3$ test for Cl^- was negative.
	Aberdeen bentonite				Achieved *ESP* of 51 %. Confirmed $AgNO_3$ test for Cl^- was negative.
	Cheto bentonite	Na^+	Mixed 3x with NaCl solution		Achieved *ESP* of 86 %. Confirmed $AgNO_3$ test for Cl^- was negative.
Olson and Mesri (1970)	Wyoming bentonite	Na^+ Ca^{2+}	Multiple washes with NaCl or $CaCl_2$	None	Achieved ≥ 96 % of desired cation on exchange complex
Harter and Stotzky (1971)	Wyoming bentonite	Na^+, Ca^{2+}, H^+, Al^{3+}, La^{3+}, Th^{4+}	Centrifuged 3x with 0.5*N* appropriate chloride salt	Washed with DIW	Focus was formation of clay-protein complexes.
Hawthorne and Solomon (1972)	Kaolin	Na^+	Stirred for 10 hr with 1M NaCl and centrifuged, 2x	Washed or dialyzed with DIW	Washed with 300 mL DIW 5 – 10 times, for 15 min each wash. Otherwise, dialysis in DIW for 14 days
Mercier and Detellier (1994)	Smectite	Na^+	Soaked in NaCl solution	Dialysis	Focus was measurement of internal surface areas

Reference	Base Clay Type(s)	Desired Form(s)	Treatment to Homo-ionize	Soluble Salt Removal[1]	Additional Comments or Details Relevant to this Study
Churchman and Weismann (1995)	Various clays	Na^+	NaCl solution with sample inside dialysis tubing	Dialysis	Stopped DIW dialysis when dialysate $EC < 10$ μS/cm
Likos and Lu (2002)	Kaolinite-Smectite mixtures	Na^+	Saturated in 1.0 M NaCl 24 h, then centrifuged. Repeat 3 times.	Washed with distilled water	Washed with distilled water until no excess chlorides detected. Focus was water-sorption behavior.
Tarchitzky and Chen (2002)	Wyoming bentonite	Na^+ Ca^{2+}	Washed 3x with 1 M NaCl or $CaCl_2$	Washed with DIW	Washed with DIW until supernatant chloride concentration < 0.1mM.
Li et al. (2003)	Smectite clays	K^+ Ca^{2+}	Washed 4x with 0.5 M KCl or $CaCl_2$	Washed with Milli-Q water	Focus was sorption of pesticides by clays and humic-acid clay complexes.
Aydin et al. (2004)	Japan smectite Kazakhstan mica clay	Na^+ Ca^{2+}	Saturated with 0.5 M NaCl or 0.25 M $CaCl_2$	Centrifuged with ethyl alcohol	---
Lado et al. (2007)	Wyoming bentonite Fithian Illite Supreme kaolinite	Na^+ Ca^{2+}	Leached with 1M NaCl or $CaCl_2$	Washed with DIW, then ethanol-water	---
Kozaki et al. (2008)	Kunipia-F bentonite	Na^+	Immersed 3x in 1 M NaCl.	Dialysis with distilled water	Performed dialysis until Cl^- not detected with $AgNO_3$ test.
Bhardwaj et al. (2009)	Wyoming bentonite Fithian Illite Supreme kaolinite	Na^+ Ca^{2+}	Suspended in NaCl or $CaCl_2$ (0.5mol/kg) and centrifuged 3x	Washed with DIW, then ethanol-water	Followed similar preparation procedures as Harter and Stotzky (1971) and Lado et al. (2007)

Notes:
1. Water or de-ionized water was used, unless otherwise noted.
"-" = not reported
MMT = mineral montmorillonite

Table 3.2. Physical properties of sodium bentonite used to prepare specimens for membrane behavior and diffusion tests.

Property	Before Dialysis Treatment		After Dialysis Treatment (0.1 M NaCl, then DIW)
Soil Classification (ASTM D2487)	CH		CH
Specific Gravity [a] (ASTM D854)	2.71		
Clay (%) [a] (ASTM D422)	90		
Mineralogy (relative abundance %) [b]			
Quartz	2		
Plagioclase Feldspar	3		
Calcite	1		
Ferroan Dolomite	Trace		
Gypsum	1		
Illite / Mica	2		
Montmorillonite	91		
Liquid Limit, *LL* (%) (ASTM D4318)	428		871
Plasticity Index, *PI* (%) (ASTM D4318)	394		836
Cation exchange capacity ($cmol^+/kg$) [c] (ASTM D7503)	78.3		
Exchangeable Cations (molar ratio) (ASTM D7503)	[a]	[d]	[e]
Na^+	0.44	0.47	0.69
K^+	0.03	0.02	0.01
Ca^{2+}	0.41	0.36	0.20
Mg^{2+}	0.12	0.15	0.10

a. Average of 10 tests on bulk powder (Bohnhoff 2012).
b. Performed by Mineralogy, Inc. (Tulsa, OK).
c. Average of 6 tests (Soil, Water, and Plant Testing Laboratory, Colorado State University).
d. Average of 2 tests (Soil, Water, and Plant Testing Laboratory, Colorado State University).
e. Average of 4 tests (Soil, Water, and Plant Testing Laboratory, Colorado State University).

Table 3.3. Example properties of bentonite reported in literature.

Reference	Specific Gravity of Solids, G_s	Cation Exchange Capacity, *CEC* (meq/100g)	Liquid Limit, *LL* (%)	Plastic Limit, *PL* (%)	Plasticity Index, *PI* (%)	Activity, *A*	% Clay (< 2 μm)	Swell Index, *SI* (mL/2g)	% Montmor-illonite	Specific Surface, (m^2/g)
Kemper (1961)[a]	-----	94	-----	-----	-----	-----	-----	-----	-----	-----
Leonard and Low (1963)[a] Wyoming Belle Fourche Aberdeen Utah Cheto	-----	 87 85 84 111 112	-----	-----	-----	-----	(approx.) 98 97 95 68 87	-----	-----	 482 464 826 851 859
Olson and Mesri (1970)[b]	2.65 – 2.80	100	190 – 1160	31 - 47	-----	-----	-----	0.26 – 1.53	-----	500-700
Kemper and Quirk (1972)[b]	-----	80	-----	-----	-----	-----	-----	-----	-----	720
Kharaka and Berry (1973), Kharaka and Smalley (1976)[b]	2.7	88, 98	-----	-----	-----	-----	75	-----	92	-----
Fritz and Marine (1983)[c]	2.4	98	-----	-----	-----	-----	-----	-----	-----	-----
Demir (1988)[c]	-----	128	-----	-----	-----	-----	-----	-----	-----	-----
Barbour and Fredlund (1989)[c]	2.56	80 - 150	-----	-----	-----	-----	100	-----	-----	700 - 840
Kenney et al. (1992)	2.74	100	500	40	-----	-----	-----	25	-----	-----
Mercier and Detellier (1994), Ishiguro et al. (1995)[a]	2.72	83	-----	-----	-----	-----	>90	-----	-----	646
Komine and Ogata (1996)	-----	-----	474	27	447	6.9	64.5	-----	-----	-----
Di Maio (1996)[c]	-----	-----	400	80	320	-----	80	-----	-----	-----
Keijer et al. (1997)[b]	2.65	64	-----	-----	-----	-----	98	-----	-----	-----
Keijzer et al. (1999), Keijzer and Loch (2001)[b]	2.64	68.3 ± 1.3	-----	-----	-----	-----	98	-----	-----	556±13
Rowe et. al. (2000)[d]	-----	82 - 91	635	45	590	6.5	-----	-----	91	726
Likos and Lu (2002)[b]	-----	-----	485	32	453	-----	-----	-----	-----	-----
Malusis and Shackelford (2002a) Kang and Shackelford (2009)[e]	-----	47.7	478	39	439	-----	-----	-----	71	-----
Lloret et al. (2003)	-----	111 ± 9	102	53	49	-----	-----	-----	> 90	725
Shackelford and Lee (2003)[e]	-----	69.4	-----	-----	-----	-----	-----	-----	78	-----
Jo et al. (2005)	2.74 ±0.04	53 – 75	479 ±90	-----	441 ±86	-----	90	-----	-----	-----
Kolstad et al. (2004)	2.65	-----	-----	-----	-----	-----	90	35.5	-----	-----

Reference	Specific Gravity of Solids, G_s	Cation Exchange Capacity, *CEC* (meq/100g)	Liquid Limit, *LL* (%)	Plastic Limit, *PL* (%)	Plasticity Index, *PI* (%)	Activity, *A*	% Clay (< 2 μm)	Swell Index, *SI* (mL/2g)	% Montmor-illonite	Specific Surface, (m^2/g)
Lee and Shackelford (2005)	2.74 - 2.78	63.9 - 93.4	430 - 589	-----	393 – 548	-----	-----	27.5 – 30	77.2 – 86.0	-----
Ito (2006)[f]	2.66 - 2.72	62.7 - 79.7	399.3 - 767.8	23.3 - 30.1	376.1 - 737.7	-----	-----	-----	45 - 70	-----
Ito (2006)[b]	2.68 - 2.78	62.1 - 82.8	511.3 - 690.3	33 - 38.8	473.3 - 651.6	-----	-----	-----	60 - 71	-----
Katsumi et al. (2007)	-----	-----	619.5	51	-----	-----	-----	33	-----	-----
Meer and Benson (2007), Benson and Meer (2009)	-----	-----	504	-----	465	-----	87	34 - 36	-----	-----
Kozaki et al. (2008)[c]	-----	113	-----	-----	-----	-----	-----	-----	>98	-----
Guyonnet et al. (2009)[g]	-----	66.2 - 76.2	-----	-----	-----	-----	-----	-----	68.8 - 76.5	-----
Guyonnet et al. (2009)[d]	-----	33.7 - 72.5	-----	-----	-----	-----	-----	-----	29.6 - 76.8	-----
Sanchez et al. (2009)[d]	2.70	96 – 102	102 ± 4	53 ± 3	49	-----	67 ± 3	-----	>90	725
Malusis et al. (2010)[d]	-----	83.4	488	45	443	-----	93	-----	69	-----
Mishra et al. (2011)[h]	-----	61.0 6-29-95.6	119.4 - 678.0	43.9 - 64.1	67.1 - 622.7	2.1 - 7.2	32.4 - 85.7	6 - 29	-----	350.6 - 711.7

a Bentonite after purification (see Table 3.1)
b Wyoming bentonites
c Na-bentonite
d Ca-bentonite
e Na-bentonite as part of geosynthetic clay liner (GCL)
f Japanese bentonites
g Na-bentonite and Na-activated Ca-bentonite
h Ranges include 15 different bentonites.
Notes:
"-" = not reported

Table 3.4. Bulk diffusion models for leaching of contaminants from stabilized waste forms used to calculate apparent diffusion coefficients of the bentonite paste.

Geometry of Waste	**Model***
Semi-infinite (Nathwani & Phillips 1980)	$$CFL = \frac{M_t}{M_\infty} = 2\left(\frac{S}{V}\right)\left(\frac{D_a t}{\pi}\right)^{1/2}$$ $$D_a = \frac{\pi}{t}\left(\frac{CFL}{2}\frac{V}{S}\right)^2$$
Finite cylindrical (Pescatore 1990)	Full solution: $$CFL = \frac{M_t}{M_\infty} = 1 - \frac{32}{\pi^2}\sum_{n=1}^{\infty}\frac{\exp\left[-((2n-1)\pi/H)^2 D_a t\right]}{(2n-1)^2}\sum_{m=1}^{\infty}\frac{\exp\left[-(\beta_m/R)^2 D_a t\right]}{\beta_m{}^2}$$ Truncated version used in this study (M = 20, N = 20): $$CFL = \frac{M_t}{M_\infty} = 1 - \frac{32}{\pi^2}\sum_{n=1}^{N}\frac{\exp\left[-((2n-1)\pi/H)^2 D_a t\right]}{(2n-1)^2}\sum_{m=1}^{M}\frac{\exp\left[-(\beta_m/R)^2 D_a t\right]}{\beta_m{}^2}$$

* CFL = cumulative fraction leached

D_a = apparent diffusion coefficient [L^2T^{-1}]

exp = exponential function (i.e., e^x)

H = height of cylinder [L]

M_t = cumulative mass of contaminant leached at time t [M]

M_∞ = total, initial mass of the contaminant in the waste [M]

R = radius of cylinder [L]

S = surface area exposed to the leachant [L^2]

t = elapsed time [T]

V = volume of the waste form [L^3]

β_m = m^{th} zero of the zero-order cylindrical Bessel function

Note: M = mass units; L = length units; T = time units

Table 3.5. Results of mass leaching analysis for dialyzed, bentonite paste using bulk diffusion models.

Test #	Initial NaCl Concentration, C_o (M) [a]	Dry Mass of Bentonite (g)	Total Duration of Leaching, t_f (d) [b]	Cumulative Fraction Leached at time t_f, *CFL*	Height, *H* (m)	Volume, *V* (mL) [c]		Apparent Diffusion Coefficient, D_a (x 10^{-10} m^2/s)		Finite Cylindrical D_a / Semi-infinite D_a
						Semi-infinite	Finite Cylindrical	Semi-infinite	Finite Cylindrical	
1	0.1	25	14	0.852	0.14	448	446	1.21	2.98	2.46
2				0.898				1.34	3.46	2.58
3				0.872				1.26	3.17	2.52
4				0.860				1.23	3.05	2.48
5				0.873	0.11	352	350	1.27	3.00	2.36
6				0.808				1.09	2.50	2.29
7			13	0.911	0.12	384	382	1.49	3.80	2.55
8				0.890				1.42	3.51	2.47
9				0.869				1.35	3.27	2.42
10				0.860	0.13	416	414	1.32	3.24	2.45
11	0.5		14	0.643	0.11	352	350	0.688	1.74	2.47
12	1.0			0.573				0.545	1.53	2.80
13		10		0.600				0.599	1.60	2.68

a. C_o = concentration used for NaCl treatment.
b. t_f = total duration of the de-ionized water dialysis stage.
c. The volume used in the semi-infinite model is the actual volume of paste in the dialysis bag. The volume used in the finite cylindrical model is an approximated, cylindrical volume based on the height (*H*) and radius (*R* = 31.83 mm). Values of surface area (*S*) were the same for both models (*S* = flat width x 2 x height = 100 mm x 2 x *H*).

Table 3.6. Measured molar ratios of exchangeable cations for bentonite before and after dialysis treatment, which included dialysis with NaCl solution, followed by dialysis with de-ionized water to remove excess salts.

Exchangeable Cation (molar ratio)	Before Dialysis		After Dialysis		
			Dialysis NaCl Concentration (M)		
			0.1	0.5	1.0
	[a]	[b]	[c]	[d]	[d]
Na^+	0.44	0.47	0.69	0.80	0.89
K^+	0.03	0.02	0.01	<0.01	<0.01
Ca^{2+}	0.41	0.36	0.20	0.15	0.08
Mg^{2+}	0.12	0.15	0.10	0.05	0.02

a. Average of 10 tests on bulk powder (Bohnhoff 2012).
b. Average of 2 tests (Soil, Water and Plant Testing Laboratory, Colorado State University).
c. Average of 4 tests (Soil, Water and Plant Testing Laboratory, Colorado State University).
d. Average of 2 tests (Soil, Water and Plant Testing Laboratory, Colorado State University).

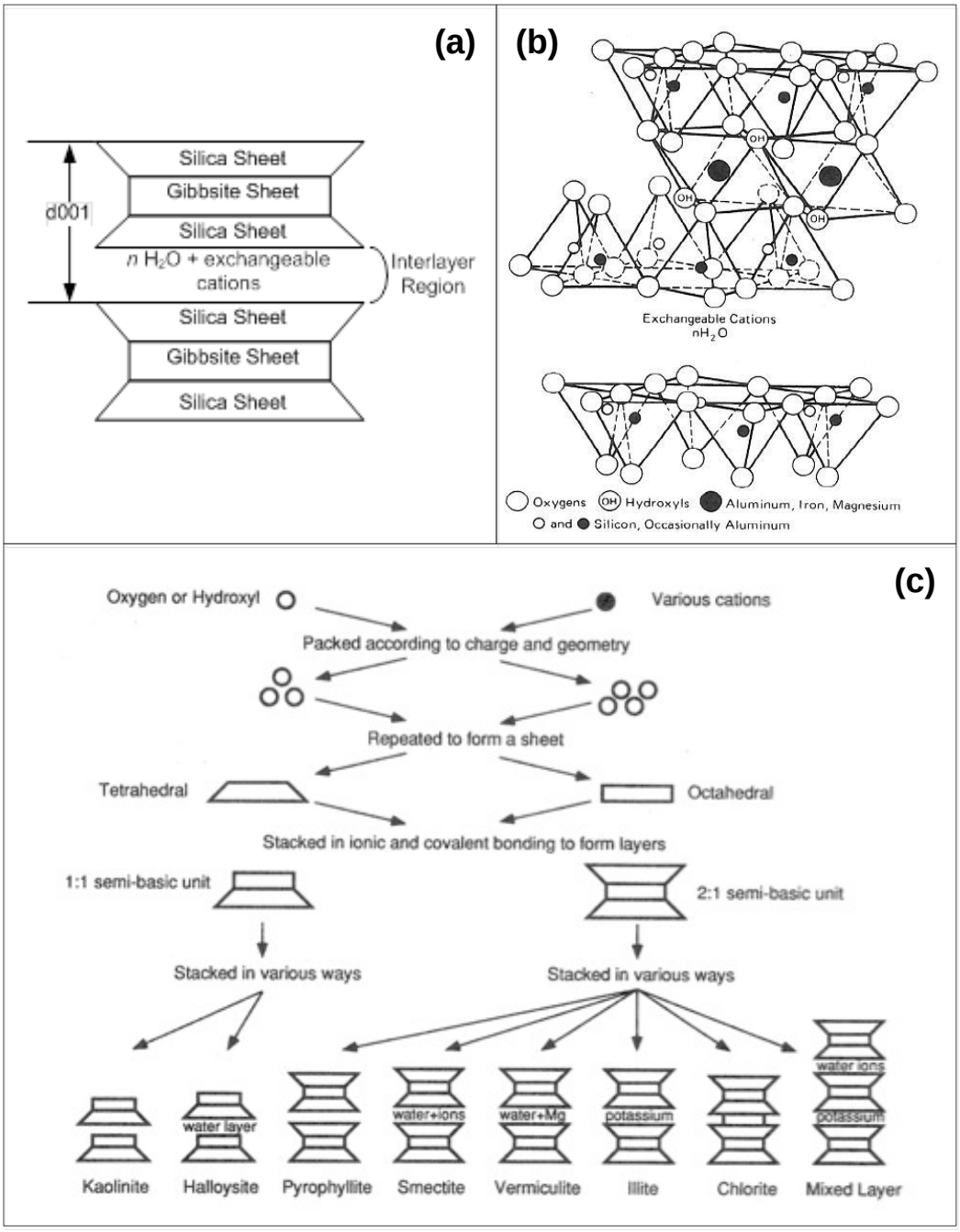

Figure 3.1. Schematic representation of the (a) structure of smectite minerals, (b) structure of montmorillonite, and (c) formation of clay minerals (all figures from Mitchell and Soga 2005).

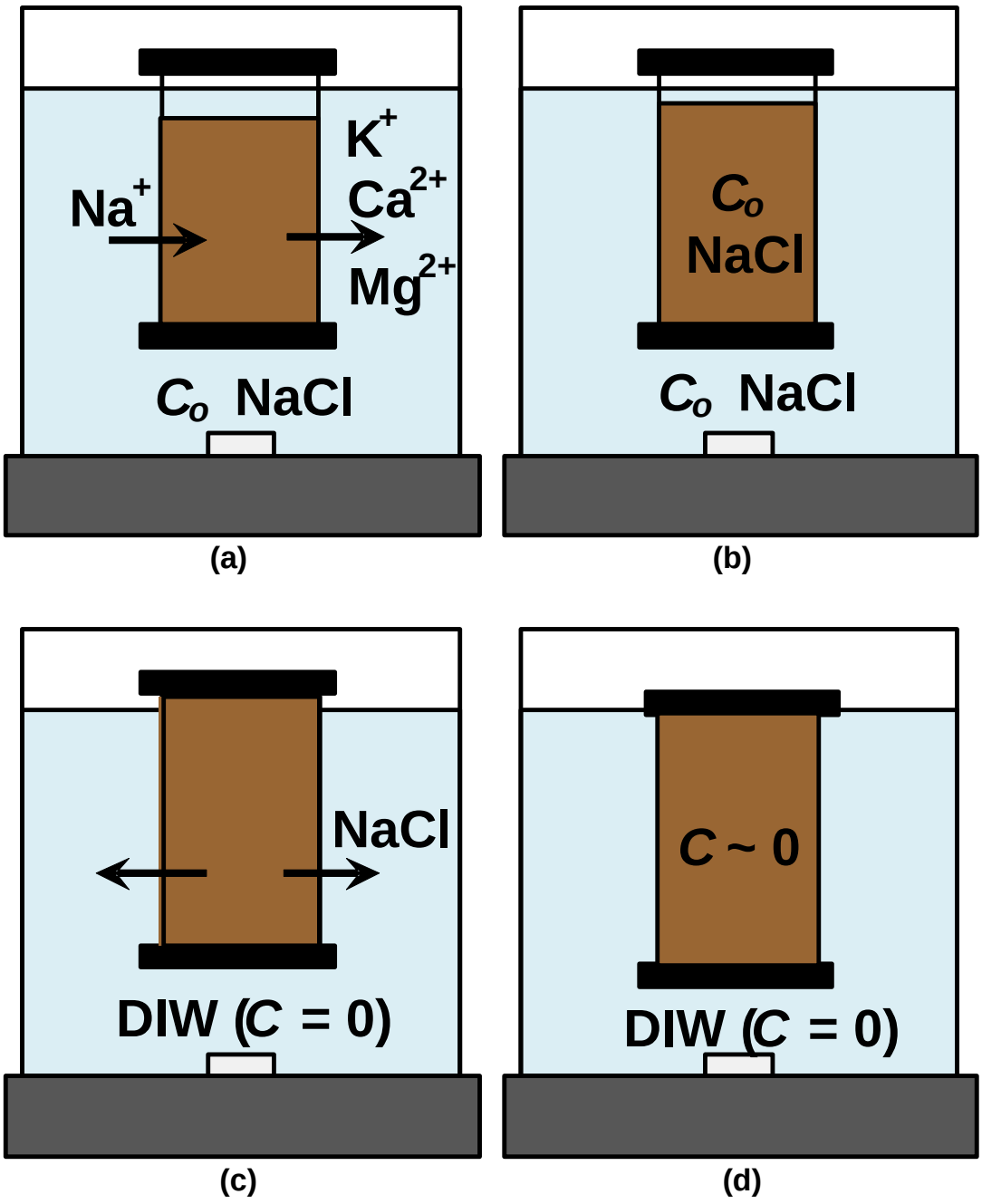

Figure 3.2. Schematic of dialysis method: (a) at the beginning of the NaCl treatment stage, (b) at the end of the NaCl treatment stage, (c) during the deionized water (DIW) stage, and (d) at the end of the DIW stage.

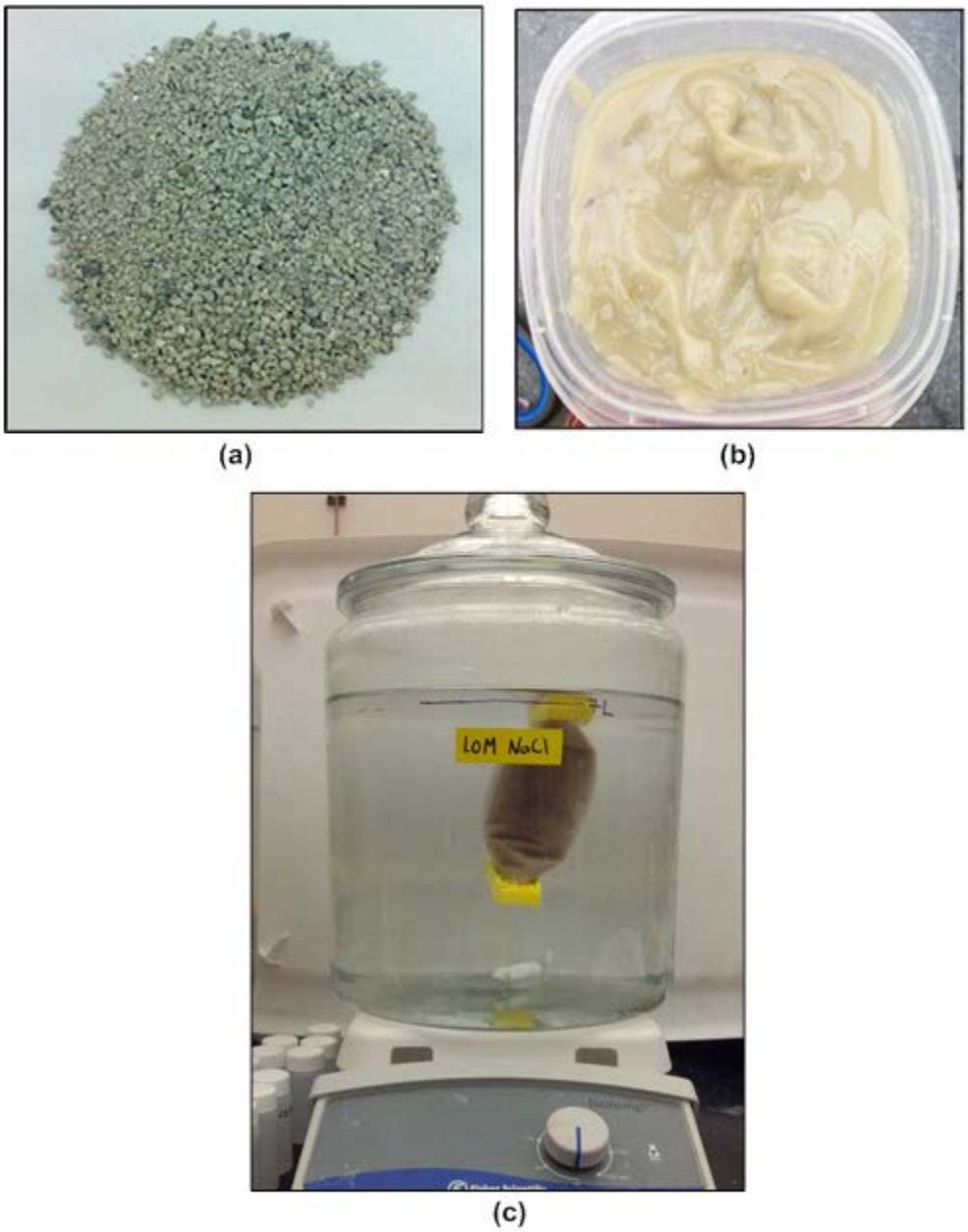

Figure 3.3. Photographs of bentonite (a) before and (b) after dialysis treatment, and (c) setup for dialysis treatment to increase the percentage of Na^+ on the exchange complex (using NaCl solution) and remove soluble salts (using de-ionized water).

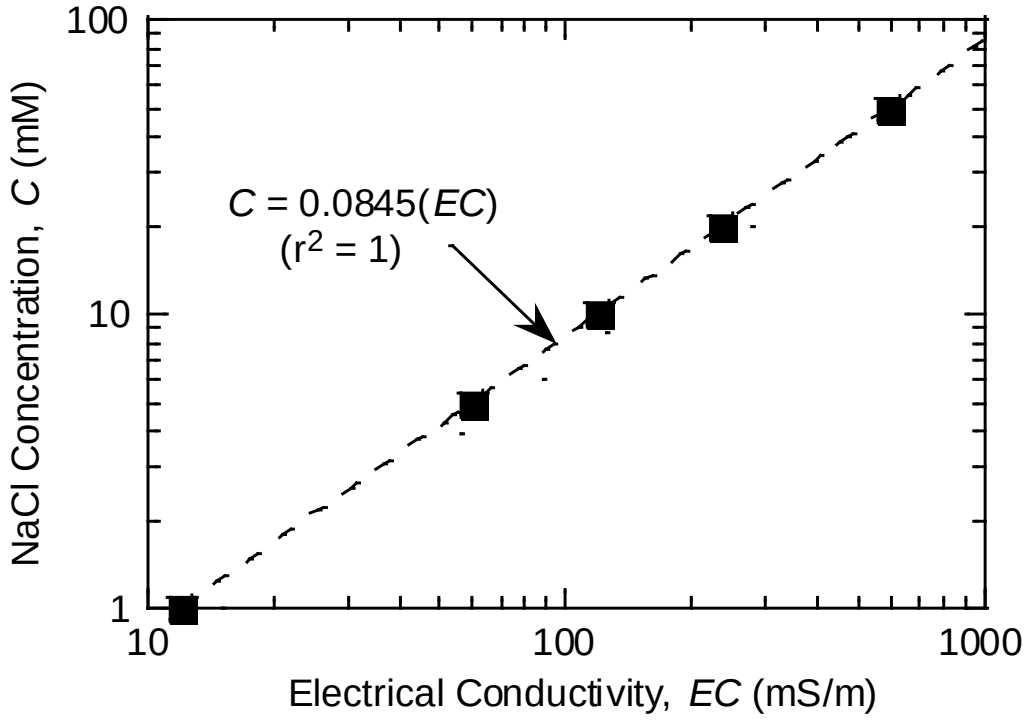

Figure 3.4. Correlation between NaCl concentration and electrical conductivity of the solution, *EC* (Malusis et al. 2013).

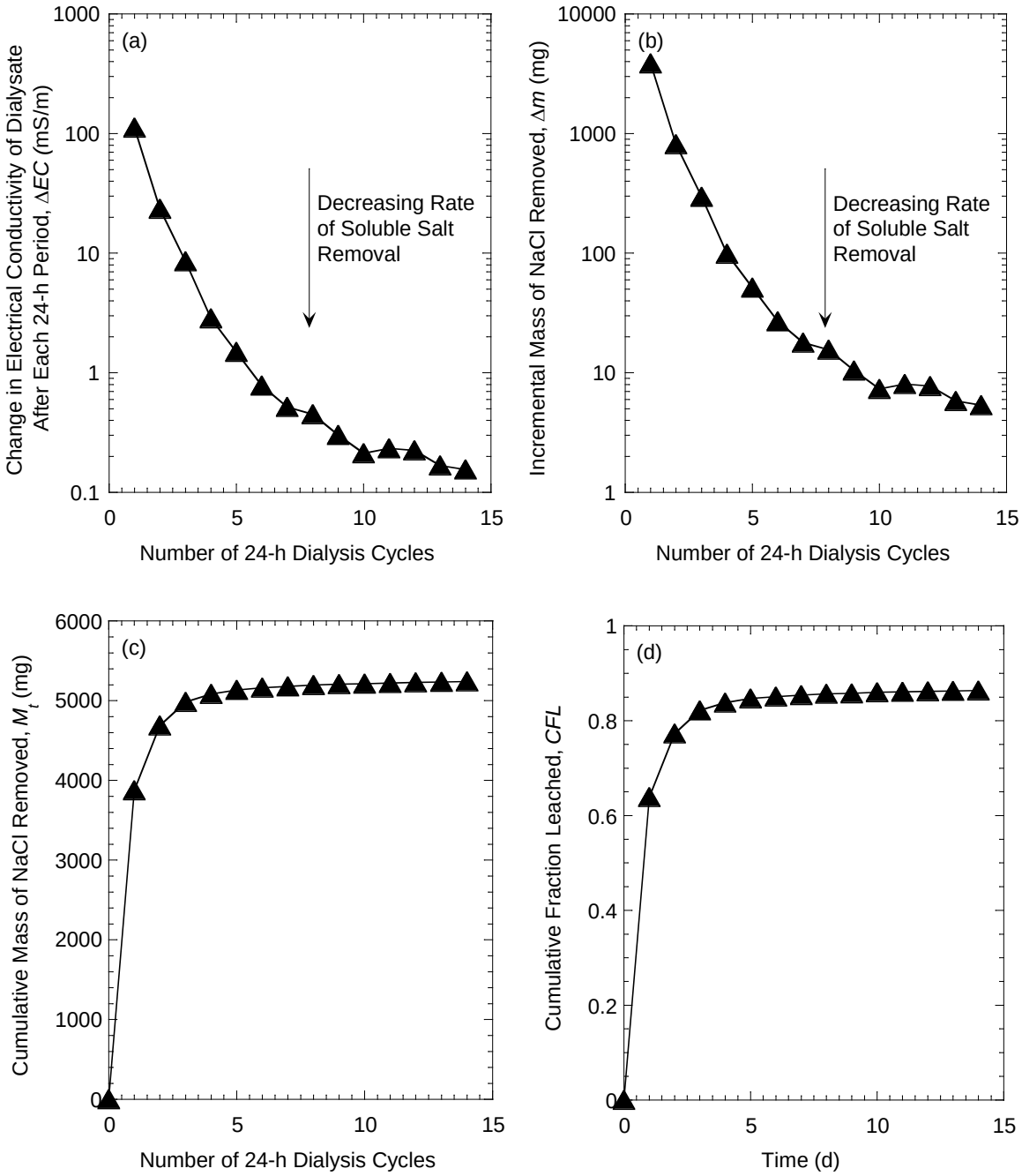

Figure 3.5. Example calculations for mass leaching analysis: (a) change in electrical conductivity of the dialysate after each 24-hour dialysis period, Δ*EC*, during the soluble salt removal stage; (b) incremental mass of NaCl removed from specimen (from Δ*EC*); (c) cumulative mass of NaCl removed from specimen; and (d) cumulative fraction leached (*CFL*). Results shown are for 0.5 M NaCl treatment and 25 g (dry mass) of bentonite.

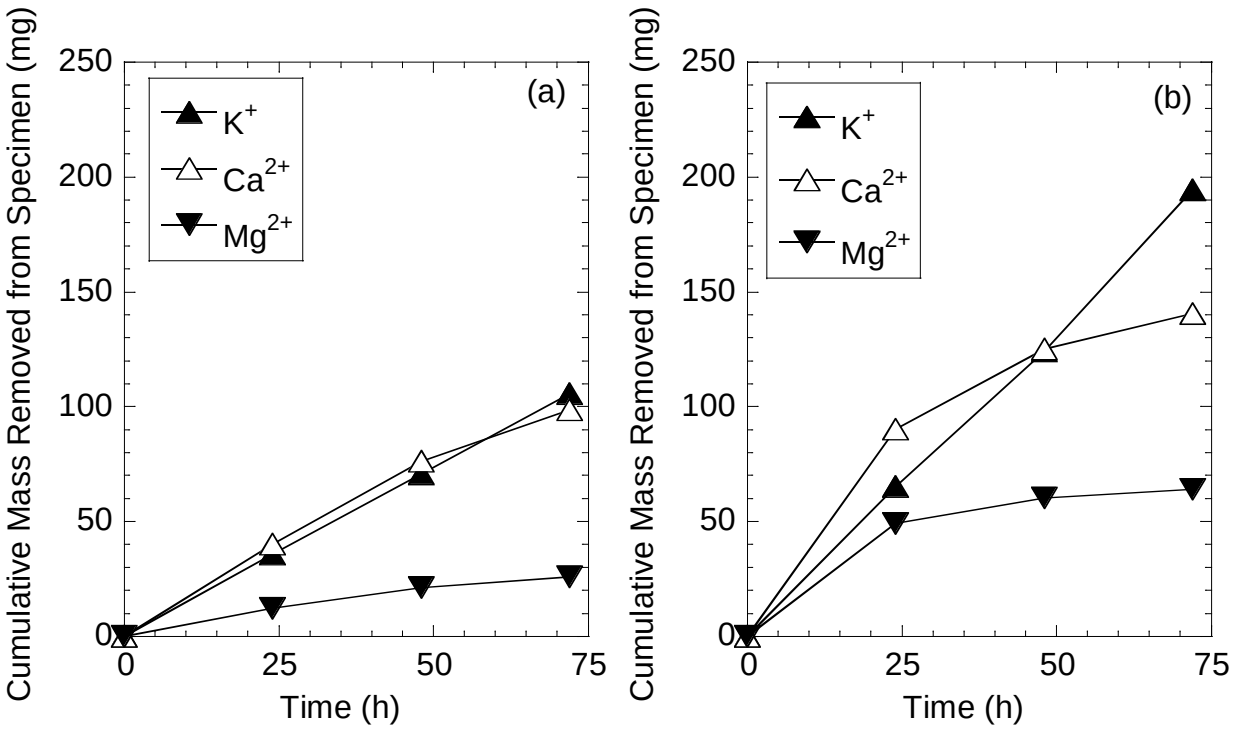

Figure 3.6. Cumulative masses of potassium (K^+), calcium (Ca^{2+}) and magnesium (Mg^{2+}) removed from 25-g (dry mass) specimens during NaCl treatment stage using (a) 0.5 M NaCl, and (b) 1.0 M NaCl.

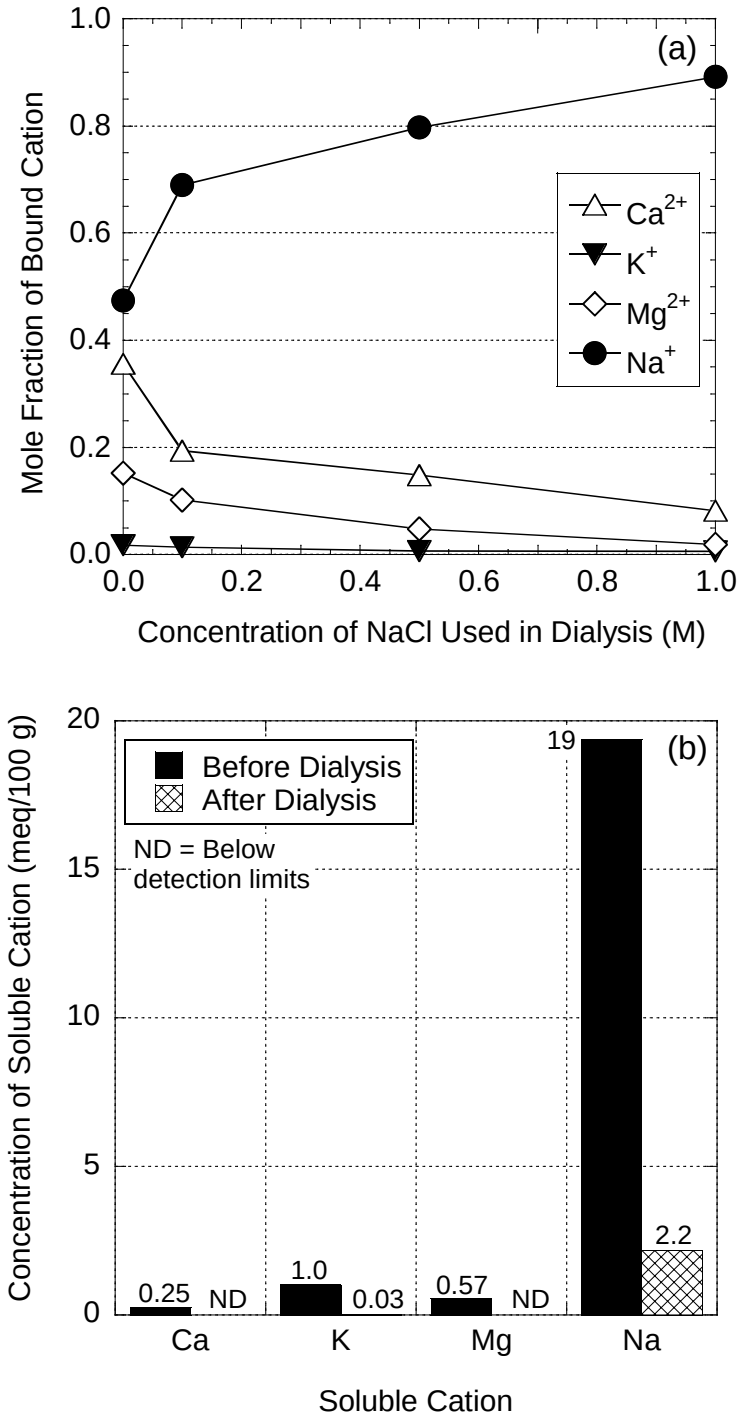

Figure 3.7. Bentonite properties before and after dialysis treatment: (a) mole fractions of cation species on the exchange complex; (b) concentrations of soluble cations.

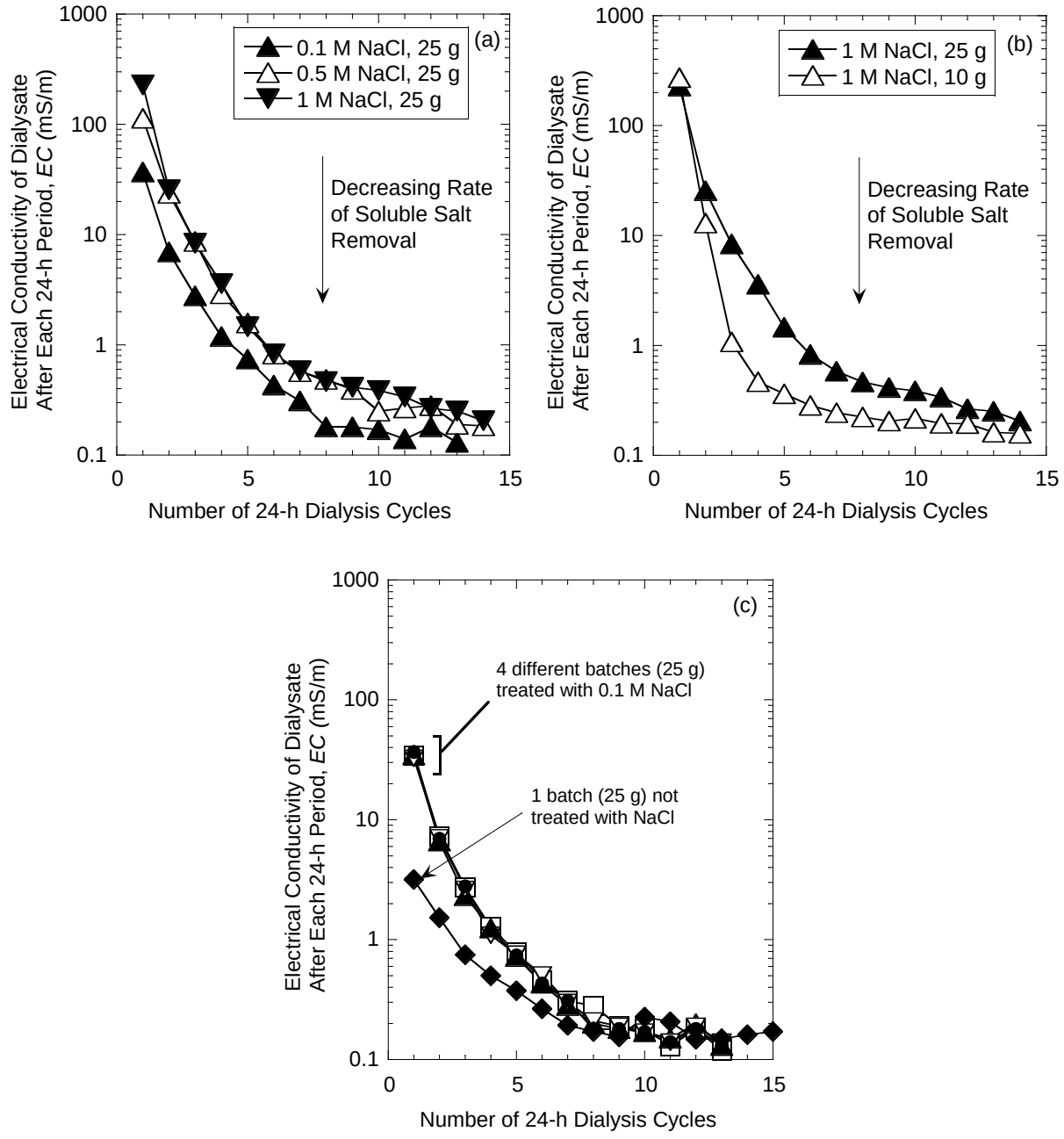

Figure 3.8. Electrical conductivity of the dialysate after each 24-hour dialysis period (prior to replacement with fresh dialysate) during the soluble salt removal stage for: (a) different concentrations of NaCl used during the cation treatment stage prior to soluble salt removal; (b) different batch sizes of treated bentonite (10 g or 25 g, dry mass); (c) bentonite that did and did not undergo cation treatment prior to soluble salt removal.

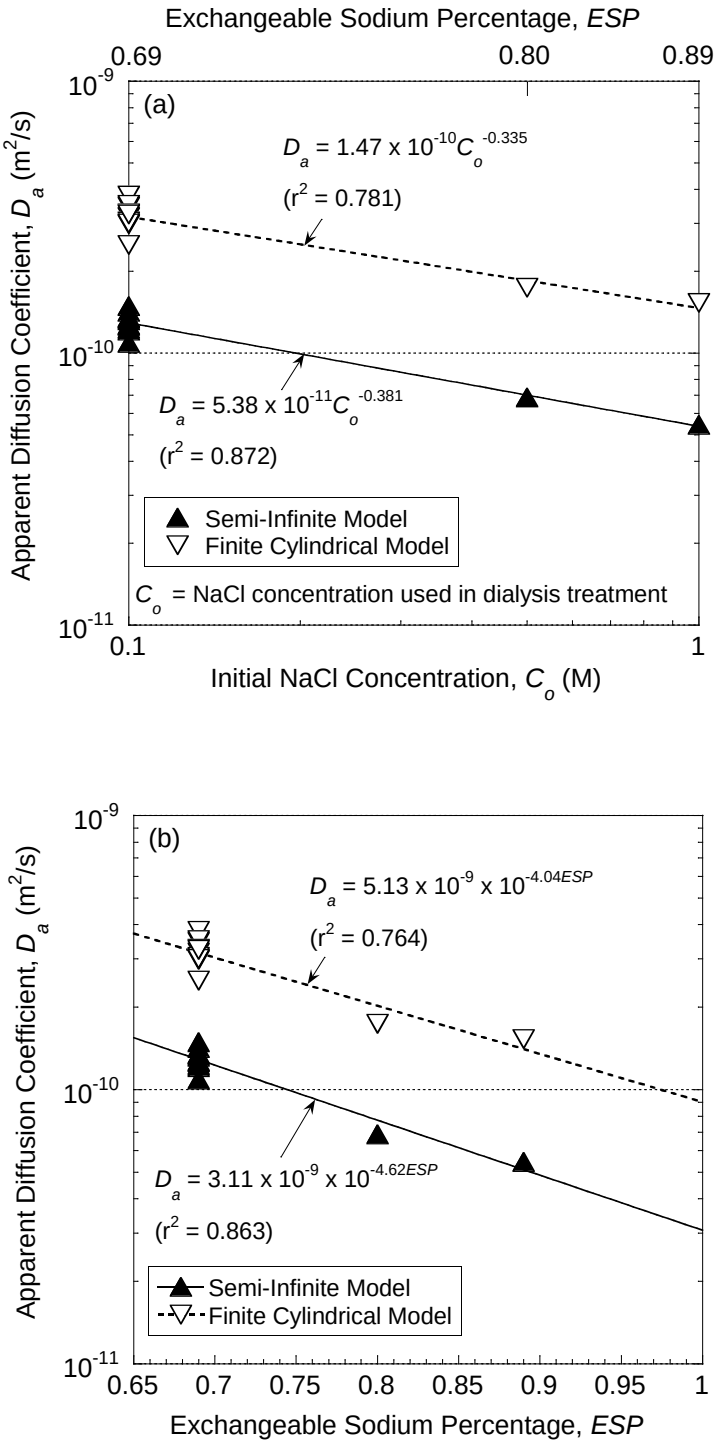

Figure 3.9. Relationship between apparent diffusion coefficients calculated from mass leaching models and (a) concentration of NaCl solution used to treat the bentonite prior to dialysis with de-ionized water, and (b) exchangeable sodium percentage.

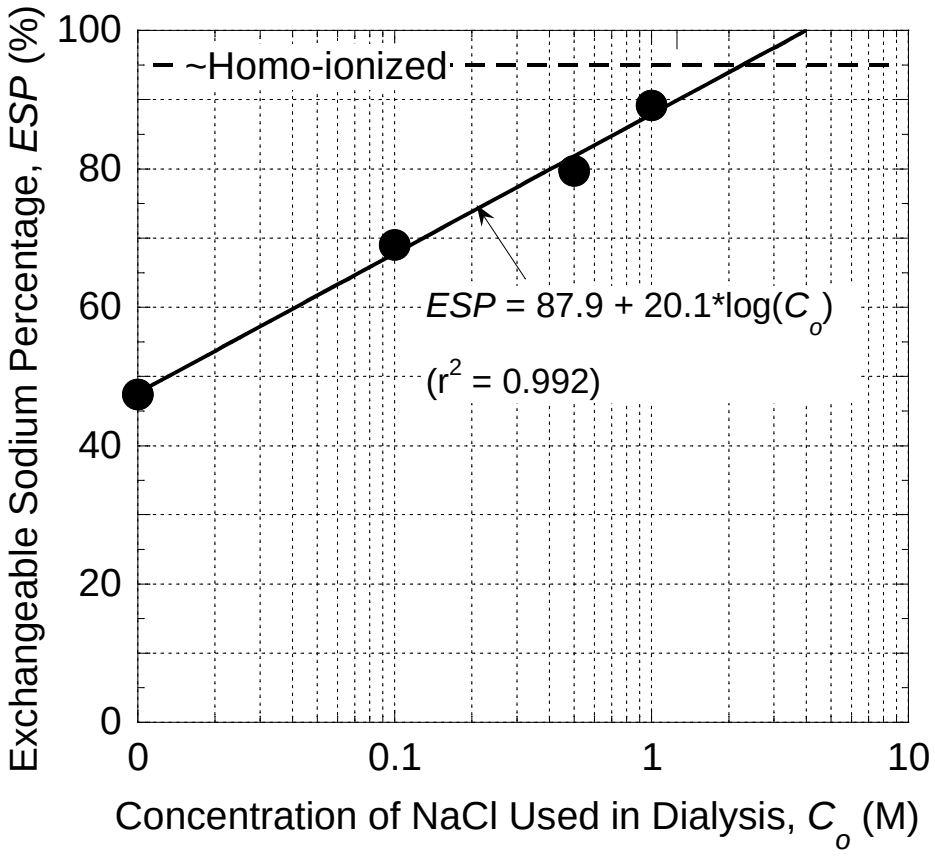

Figure 3.10. Measured exchangeable sodium percentage (*ESP*) of the bentonite as a function of the concentration of the NaCl solution used in the dialysis procedure.

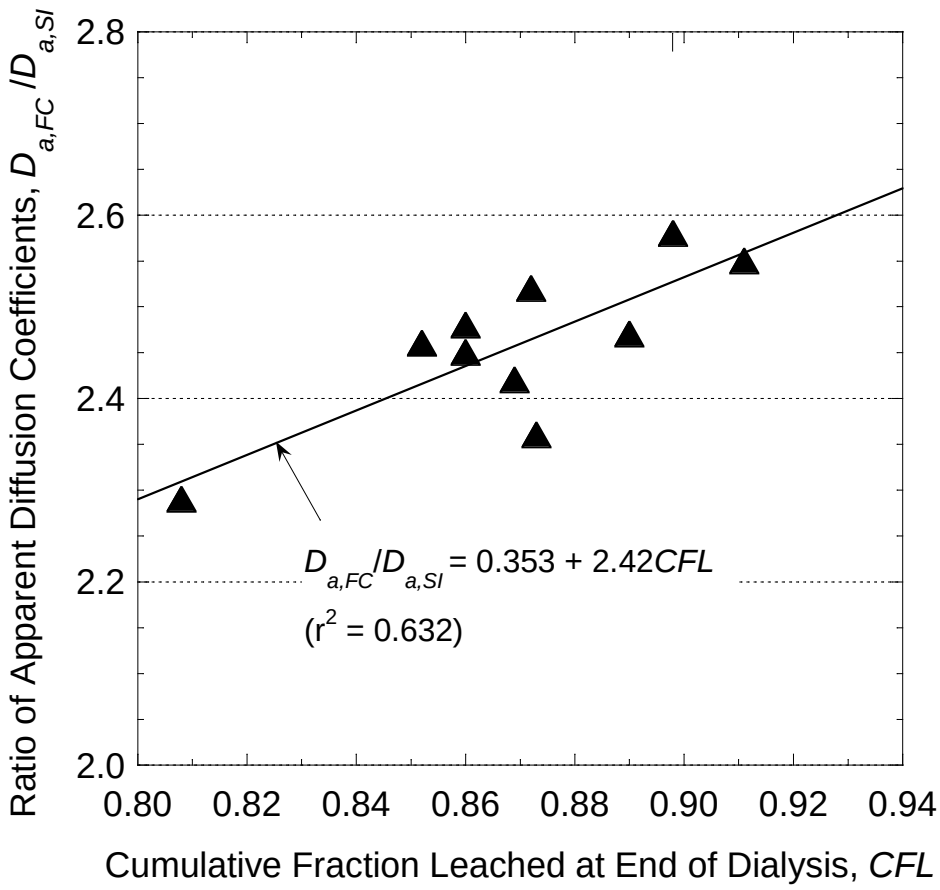

Figure 3.11. Ratio of apparent diffusion coefficients calculated from the finite-cylinder ($D_{a,FC}$) and semi-infinite ($D_{a,SI}$) leaching models versus the cumulative fraction leached (*CFL*) at the end of dialysis (i.e., the value of *CFL* used in the Equations shown in Table 3.4).

REFERENCES

Abd-el-aziz, M., and Taylor, S. (1965). "Simultaneous flow of water and salt through unsaturated porous media: I. Rate equations." *Proceedings of the Soil Science Society of America*, 29(2), 141-143.

Arasan S., and Yetimoglu, T. (2008). "Effect of inorganic salt solutions on the consistency limits of two clays." *Turkish Journal of Engineering and Environmental Sciences*, Vol. 32, 107-115.

ASTM (2008). "Standard test method for accelerated leach test for diffusive releases from solidified waste and a computer program to model diffusive, fractional leaching from cylindrical waste forms." *ASTM C1308*, ASTM International, West Conshohocken, PA.

ASTM (2010). "Standard test method for measuring the exchange complex and cation exchange capacity of inorganic fine-grained soils." *ASTM D7503*, ASTM International, West Conshohocken, PA.

Aydin, M., Yano, T., and Kilic, S. (2004). "Dependence of zeta potential and soil hydraulic conductivity on adsorbed cation and aqueous phase properties." *Proceedings of the Soil Science Society of America*, 68(2), 450-459.

Barbour, S., and Fredlund, D. (1989). "Mechanisms of osmotic flow and volume change in clay soils." *Canadian Geotechnical Journal*, 26(4), 551-562.

Baver, L. (1956). *Soil Physics*, 3rd ed., *John Wiley and Sons*, New York.

Benson, C., and Meer, S. (2009). "Relative abundance of monovalent and divalent cations and the impact of desiccation on geosynthetic clay liners." *Journal of Geotechnical and Geoenvironmental Engineering*, 135(3), 349-358.

Benzel, W., and Graf, D. (1984). "Studies of smectite membrane behavior: Importance of layer thickness and fabric in experiments at 20° C." *Geochimica et Cosmochimica Acta*, 48(9), 1769-1778.

Bhardwaj, A., McLaughlin, R., Shainberg, I., and Levy, G. (2009). "Hydraulic characteristics of depositional seals as affected by exchangeable cations, clay mineralogy, and polyacrylamide." *Proceedings of the Soil Science Society of America*, 73(3), 910-918.

Bohnhoff, G. (2012). *Membrane Behavior, Diffusion, and Compatibility of a Polymerized Bentonite for Containment Barrier Applications*. PhD Dissertation, Colorado State University, Fort Collins, CO.

Bohnhoff, G., Shackelford, C., and Sample-Lord, K. (2014) "Calcium-resistant membrane behavior of polymerized bentonite." *Journal of Geotechnical and Geoenvironmental Engineering*, 140(3), 040113029-1 – 04013029-12.

Brigatti, M., Galan, E., and Theng, B. (2006). "Chapter 2: Structures and mineralogy of clay minerals." *Handbook of Clay Science, Volume 1, Developments in Clay Science,* F. Bergaya, B. Theng and G. Lagaly., Eds., *Elsevier*, New York, NY.

Carrado, K., Decarreau, A., Petit, S., Bergaya, F., and Lagaly, G. (2006). "Chapter 4: Synthetic Clay Minerals and Purification of Natural Clays." *Handbook of Clay Science, Volume 1, Developments in Clay Science,* F. Bergaya, B. Theng and G. Lagaly., Eds., *Elsevier*, New York, NY.

Churchmann, G. and Weissman, D. (1995). "Separation of sub-micron particles from soils and sediments without mechanical disturbance." *Clays and Clay Minerals*, 43(1), 85-91.

Coplen, T., and Hanshaw, B. (1973). "Ultrafiltration by a compacted membrane – I. Oxygen and hydrogen isotope fractionation." *Geochimica et Cosmochimica Acta*, 37(10), 2205-2310.

Cornell University (1951). *Final Report on Soil Solidification Research,* Cornell University, Ithaca, NY.

Côté, P., Constable, T., and Moreira, A. (1987). "An evaluation of cement-based waste forms using the results of approximately two years of dynamic leaching." *Nuclear and Chemical Waste Management*, 7(2), 129-138.

Daniel, D., Bowders, J., Jr., and Gilbert, R. (1997). "Laboratory hydraulic conductivity testing of GCLs in flexible-wall permeameters." *Testing and Acceptance Criteria for Geosynthetic Clay Liners, ASTM STP 1308,* L.Well, Ed., West Conshohocken, PA, 208–226.

Deer, W., Howie, R., and Zussman, J. (1992). *An Introduction to the Rock-forming Minerals*, 2nd ed., *Addison Wesley Longman Limited*, Essex.

Demir, I. (1988). "Studies of smectite membrane behavior: Electrokinetic, osmotic, and isotopic fractionation processes at elevated pressures." *Geochimica et Cosmochimica Acta*, 52(3), 727-737.

Di Emidio, G. (2010). *Hydraulic and Chemico-Osmotic Performance of Polymer Treated Clay*. PhD Dissertation, University of Ghent, Ghent, Belgium.

Di Maio, C. (1996). "Exposure of bentonite to salt solution: osmotic and mechanical effects." *Géotechnique*, 46(4), 695-707.

Di Maio, C., Santoli, L., and Schiavone, P. (2004). "Volume change behavior of clays: the influence of mineral composition, pore fluid composition and stress state." *Mechanics of Materials*, 36(5-6), 435-451.

Dominijanni, A., Manassero, M., and Puma, S. (2013). "Coupled chemical-hydraulic-mechanical behavior of bentonite." *Géotechnique*, 63(3), 191-205.

Dufey, J., Banin, A., Laudelout, H., and Chen, Y. (1976). "Particle shape and sodium self-diffusion coefficient in mixed sodium-calcium montmorillonite." *Soil Science Society of America Journal*, 40(2), 310-314.

Dufey. J., Sheta, T., Gobran, G., and Laudelout, H. (1982). "Dispersion of chloride, sodium and calcium ions in soils as affected by exchangeable sodium." *Soil Science Society of America Journal*, 46(1), 47-50.

Elrick, D., Smiles, D., Baumgartner, N., and Groenevelt, P. (1976). "Coupling phenomena in saturated homo-ionic montmorillonite: I. Experimental." *Proceedings of the Soil Science Society of America*, 40(4), 490-491.

EPA (2013). "Method 1315: Mass transfer rates of constituents in monolithic or compacted granular materials using a semi-dynamic tank leaching procedure." *SW-846 Test Methods for Evaluating Solid Waste, Physical/Chemical Methods,* Environmental Protection Agency, USA.

Fritz, S., and Marine, W. (1983). "Experimental support for a predictive osmotic model of clay membranes." *Geochimica et Cosmochimica Acta*, 47(8), 1515-1522.

Gleason, M., Daniel, D., and Eykholt, G. (1997). "Calcium and sodium bentonite for hydraulic containment applications." *Journal of Geotechnical and Geoenvironmental Engineering*, 123(5), 438-445.

Godbee, H., Compere, E., Joy, D., Kibbey, A., Moore, J., Nestor, Jr., C., Anders, O., and Neilson, Jr., R. (1980). "Application of mass transport theory to the leaching of radionuclides from waste solids." *Nuclear and Chemical Waste Management*, 1(1), 29-35.

Grim, R. (1968). *Clay Mineralogy*, 2nd ed., *McGraw-Hill Book Company, Inc.*, New York.

Grim, R., and Güven, N. (1978). "Bentonites: geology, mineralogy, properties and uses." *Developments in Sedimentology*, Vol. 24, *Elsevier*, New York, NY.

Guyonnet, D., Touze-Foltz, N., Norotte, V., Pothier, C., Didier, G., Gailhanou, H., Blanc, P., and Warmont, F. (2009). "Performance-based indicators for controlling geosynthetic clay liners in landfill applications." *Geotextiles and Geomembranes*, 27(5), 321-333.

Hanshaw, B. (1962). *Membrane Properties of Compacted Clays*. PhD Dissertation, Harvard University, Cambridge, MA, USA

Hanshaw, B. and Coplen, T. (1973). "Ultrafiltration by a compacted clay membrane – II. Sodium ion exclusion at various ionic strengths." *Geochimica et Cosmochimica Acta*, 37(10), 2311-2327.

Harter, R. and Stotzky, G. (1971). "Formation of clay-protein complexes." *Proceedings of the Soil Science Society of America*, 35(3), 383-389.

Hawthorne, D., and Solomon, D. (1972). "Catalytic activity of sodium kaolinites." *Clays and Clay Minerals*, 20(2), 75-78.

Helfferich, F. (1962). *Ion Exchange*. *McGraw-Hill*, New York.

Ishiguro, M., Matsuura, T., and Detellier, C. (1995). "Reverse osmosis separation for a montmorillonite membrane." *Journal of Membrane Science*, 107(1-2), 87-92.

Ito, H. (2006). "Compaction properties of granular bentonites." *Applied Clay Science*, 31(1-2), 47-55.

Jo, H., Benson, C., Shackelford, C., Lee, J-M, and Edil, T. (2005). "Long-term hydraulic conductivity of a geosynthetic clay liner permeated with inorganic salt solutions." *Journal of Geotechnical and Geoenvironmental Engineering*, 131(4), 405-417.

Kang, J., and Shackelford, C. (2009). "Clay membrane testing using a flexible-wall cell under closed-system boundary conditions." *Applied Clay Science*, 44(1-2), 43-58.

Katsumi, T., Ishimori, H., Ogawa, A., Yoshikawa, K., Hanamoto, K., and Fukagawa, T. (2007). "Hydraulic conductivity of nonprehydrated geosynthetic clay liners permeated with inorganic solutions and waste leachates." *Soils and Foundations*, 47(1), 79-96.

Keijzer, T., Kleingeld, P., and Loch, J. (1997). "Chemical osmosis in compacted clayey material and the prediction of water transport." *Geoenvironmental Engineering, Contaminated Ground: Fate of Pollutants and Remediation*, R. Yong and H. Thomas, Eds., *Thomas Telford Publ.*, London, 199-204.

Keijzer, T., Kleingeld, P., and Loch, J. (1999) "Chemical osmosis in compacted clayey material and the prediction of water transport." *Engineering Geology*, 53(2), 151-159.

Keijer, T., and Loch, J. (2001). "Chemical osmosis in compacted dredging sludge." *Soil Science Society of America Journal*, 65(4), 1045-1055.

Kemper, W. (1961). "Movement of water as affected by free energy and pressure gradients: II. Experimental analysis of porous systems in which free energy and pressure gradients act in opposite directions." *Proceedings of the Soil Science Society of America*, 25(4), 260-265.

Kemper, W., and Massland, D. (1964). "Reduction in salt content of solution passing through thin films adjacent to charged surfaces." *Proceedings of the Soil Science Society of America*, 28(3), 318-323.

Kemper, W., Maasland, D., and Porter, L. (1964), "Mobility of water adjacent to mineral surface." *Proceedings of the Soil Science Society of America*, 28(2), 164-167.

Kemper, W., and Quirk, J. (1972). "Ion mobilities and electric charge of external clay surfaces inferred from potential differences and osmotic flow." *Soil Science Society of America Journal*, 36(3), 426-433.

Kemper, W. and Rollins, J. (1966). "Osmotic efficiency coefficients across compacted clays." *Proceedings of the Soil Science Society of America*, 30(5), 529-534.

Kemper, W., and van Schaik, J. (1966). "Diffusion of salts in clay-water systems." *Proceedings of the Soil Science Society of America*, 30(5), 534-540.

Kenney, T., Vanveen, W., Swallow, M., and Sungaila, M. (1992). "Hydraulic conductivity of compacted bentonite sand mixtures." *Canadian Geotechnical Journal*, 29(3), 364-374.

Kharaka, Y. and Berry, F. (1973). "Simultaneous flow of water and solutes through geologic membranes, I. Experimental investigation." *Geochimica et Cosmochimica Acta*, 37(12), 2577-2603.

Kharaka, Y., and Smalley, W. (1976). "Flow of water and solutes through compacted clays." *Bulletin of the American Association of Petroleum Geologists*, 60(6), 973-980.

Kim, J., Kim, C., and Chung, C. (2002). "Modeling of nuclide release from low-level radioactive paraffin waste: A comparison of simulated and real waste." *Journal of Hazardous Materials*, 94(2), 161-178.

Kolstad, D., Benson, C., and Edil, T. (2004) "Hydraulic conductivity and swell of nonprehydrated geosynthetic clay liners permeated with multispecies inorganic solutions." *Journal of Geotechnical and Geoenvironmental Engineering*, 130(12), 1236-1249.

Komine, K., and Ogata, N. (1996). "Prediction for swelling characteristics of compacted bentonite." *Canadian Geotechnical Journal*, 33(1), 11-22.

Kozaki, T., Fujishima, A., Saito, N., Sato, S., and Ohashi, H. (2005). "Effects of dry density and exchangeable cations on the diffusion process of sodium ions in compacted montmorrilonite." *Engineering Geology*, 81(3), 246-254.

Kozaki, T., Liu, J., and Sato, S. (2008). "Diffusion mechanism of sodium ions in compacted montmorillonite under different NaCl concentration." *Physics and Chemistry of Earth*, 33(14-16), 957-961.

Lado, M., Ben-Hur, M., and Shainberg, I. (2007). "Clay mineralogy, ionic composition, and pH effects on hydraulic properties of depositional seals." *Soil Science Society of America Journal*, 71(2), 314-321.

Lee, J.-M., and Shackelford, C. (2005). "Impact of bentonite quality on hydraulic conductivity of geosynthetic clay liners." *Journal of Geotechnical and Geoenvironmental Engineering*, 131(1), 64-77.

Leonard, R., and Low, P. (1963). "Effect of gelation on the properties of water in clay systems." *Clays and Clay Minerals*, 12(1), 311-325.

Li, H., Sheng, G., Teppen, B., Johnston, C., and Boyd, S. (2003). "Sorption and desorption of pesticides by clay minerals and humic acid-clay complexes." *Soil Science Society of America Journal*, 67(1), 122-131.

Likos, W., and Lu, N. (2002). "Water vapor sorption behavior of smectitie-kaolinite mixtures." *Clays and Clay Minerals*, 50(5), 553-561.

Lloret, A., Villar, M., Snachez, M., Gens, A., Pintado X., and Alonso, E. (2003). "Mechanical behavior of heavily compacted bentonite under high suction changes." *Géotechnique*, 53(1), 27-40.

Malusis, M., Maneval, J., Barben, E., Shackelford, C., and Daniels, E. (2010). "Influence of adsorption on phenol transport through soil-bentonite vertical barriers amended with activated carbon." *Journal of Contaminant Hydrology*, 116(1-4), 58-72.

Malusis, M., Kang, J., and Shackelford, C. (2014). "Restricted salt diffusion in a geosynthetic clay liner." *Environmental Geotechnics*, ICE, Thomas Telford Ltd., London (http://dx.doi.org/10.1680/envgeo.13.00080).

Malusis, M., Shackelford, C., and Olsen, H. (2001). "Flow and transport through clay membrane barriers." *Geoenvironmental Engineering, Geoenvironmental Impact Management*, R. Yong and H. Thomas, Eds., *Thomas Telford Publ*., London, UK, 334-341.

Malusis, M., and Shackelford, C. (2002a). "Chemico-osmotic efficiency of a geosynthetic clay liner." *Journal of Geotechnical and Geoenvironmental Engineering*, 128(2), 97-106.

Malusis, M., and Shackelford, C. (2002b) "Coupling effects during steady-state solute diffusion through a semipermeable clay membrane." *Environmental Science and Technology*, 36(6), 3212-1319.

McBride, M. (1994). *Environmental Chemistry of Soils*, Oxford University Press, New York.

Meer, S., and Benson, C. (2007). "Hydraulic conductivity of geosynthetics clay liners exhumed from landfill final covers." *Journal of Geotechnical and Geoenvironmental Engineering*, 133(5), 550-563.

Mercier, L., and Detellier, C. (1994). "Intercalation of tetraalkylammonium cations into smectites and its application to internal surface area measurements." *Clays and Clay Minerals*, 42(1), 71-76.

Mesri, G., and Olson, R. (1971). "Mechanisms controlling the permeability of clays." *Clays and Clay Minerals*, 19(3), 151-158.

McKelvey, J., and Milne, I. (1962). "The flow of salt solutions through compacted clay." *Proceedings of the 9th National Conference on Clays and Clay Minerals*, Pergamon Press, 248-259.

Mishra, A., Ohtsubo, M, Li, L., Higashi, T., and Park, J. (2009). "Effect of salt of various concentrations on liquid limit, and hydraulic conductivity of different soil-bentonite mixtures." *Environmental Geology*, 57(5), 1145-1153.

Mishra, A., Ohtsubo, M., Li, L., and Higashi, T. (2011). "Controlling factors of the swelling of various bentonites and their correlations with the hydraulic conductivity of soil-bentonite mixtures." *Applied Clay Science*, 52(1-2), 78-84.

Mitchell, J., and Soga, K. (2005). *Fundamentals of Soil Behavior*, 3rd ed. *John Wiley and Sons*, New York.

Mokady, R., and Low P. (1966). "Electrochemical determination of diffusion coefficients in clay-water systems." *Soil Science Society of America Journal*, 30(4), 438-442.

Mokady, R., and Low, P. (1968). "Simultaneous transport of water and salt through clays: I. Transport mechanisms." *Soil Science*, 105(2), 112-131.

Nathwani, J., and Phillips, C. (1978). "Rates of leaching of radium from contaminated soils: An experimental investigations of radium bearing soils from Port Hope, Ontario." *Water, Air, and Soil Pollution*, 9(4), 453-465.

Nathwani, J., and Phillips, C. (1980). "Leachability of Ra-226 from uranium mill tailings consolidated with naturally occurring materials and/or cement." *Water, Air, and Soil Pollution*, 14(1), 389-402.

Odom, I. (1984). "Smectite clay minerals: properties and uses." *Philosophical Transactions of the Royal Society of London. Series A, Mathematical and Physical Sciences*, 311(1517), 391-409.

Odour, P., and Whitworth, T. (2005). "Mechanistic interpretation of ionic azo dye flux decline through compacted Na-montmorillonite membrane." *Journal of Membrane Science*, 265(1-2), 85-93.

Olsen, H. (1969). "Simultaneous fluxes of liquid and charge in saturated kaolinite." *Proceedings of the Soil Science Society of America*, 33(3), 338-344.

Olsen, H. (1972). "Liquid movement through kaolinite under hydraulic, electric, and osmotic gradients." *American Association of Petroleum Geologists Bulletin*, 56(10), 2022-2028.

Olson, R., and Mesri, G. (1970). "Mechanisms controlling the compressibility of clays." *Journal of the Soil Mechanics and Foundations Division*, 96(6), 1863-1878.

Page, A., Miller, R., and Keeney, D. (1982). *Methods of Soil Analysis, Part 2. Chemical and Microbiological Properties.* 2nd ed., *American Society of Agronomy and Soil Science Society of America*, *Madison*, WI.

Patra, A., Sumesh, C., Mohapatra, S., Sahoo, S., Tripathi, R., and Puranik, V. (2011). "Long-term leaching of uranium from different waste matrices." *Journal of Environmental Management*, 92(3), 919-925.

Pescatore, C. (1990). "Improved expressions for modeling diffusive, fractional cumulative leaching from finite-size waste forms." *Waste Management*, 10(2), 155-159.

Rao, S., Sridharan, A., and Chandrakaran, S. (1993). "Consistency limits behavior of bentonites exposed to seawater." *Marine Georesources and Geotechnology*, 11(3), 213-227.

Rowe, R., Lake, C., Petrov, R. (2000). "Apparatus and procedures for assessing inorganic diffusion coefficients for geosynthetic clay liners." *Geotechnical Testing Journal*, 23(2), 206-214.

Salas, J., and Serratosa, J. (1953). "Compressibility of clays." *Proceedings of the Third International Conference on Soil Mechanics and Foundation Engineering*, Zurich, Vol. 1, 192-198.

Sánchez, M., Gens, A., and Olivella, S. (2010). "Effect of thermo-coupled processes on the behavior of a clay barrier submitted to heating and hydration." *Anais da Academia Brasileira de Ciências*, 82(1), 153-168.

Santamarina, J., Klein, K., Palomino, A., and Guimaraes, M. (2002). "Micro-scale aspects of chemical-mechanical coupling: Interparticle forces and fabrics." *Chemo-Mechanical Coupling in Clays: From Nano-scale to Engineering Applications*, C. Di Maio, T. Hueckel, and B. Lloret, Eds., *Swets & Zeitlinger*, Lisse, the Netherlands.

Sayre, W., Guy, H., and Chamberlain, A. (1963). "Uptake and transport of radionuclides by stream sediments." *Transport of Radionuclides by* Streams, Geological Survey Professional Paper 433-A.

Segad, M., Jöhsson, B., Åkesson, T., and Cabane, B. (2010). "Ca/Na montmorillonite: Structure, forces and swelling properties." *Langmuir*, 26(8), 5782-5790.

Shackelford, C. (1991). "Laboratory diffusion testing for waste disposal - A review." *Journal of Contaminant Hydrology*, Elsevier, Amsterdam, 7(3), 177-217.

Shackelford, C. (2013). "Membrane behavior in engineered bentonite-based containment barriers: State of the art." *Proceedings of Coupled Phenomena in Environmental Geotechnics (CPEG)*, M. Manassero, A. Dominijanni, S. Foti, and G. Musso, eds., July 1-3, Torino, Italy, CRC Press/Balkema, Taylor & Francis Group, London, 45-60.

Shackelford, C. (2014). "The ISSMGE Kerry Rowe Lecture: The role of diffusion in environmental geotechnics." *Canadian Geotechnical Journal*, NRC, 51(11), 1219-1242

Shackelford, C., Benson, C., Katsumi,T., Edil, T., and Lin,L. (2000). "Evaluating the hydraulic conductivity of GCLs permeated with non-standard liquids." *Geotextiles and Geomembranes*, 18(2–4), 133-161.

Shackelford, C., and Lee, J. (2003). "The destructive role of diffusion on clay membrane behavior." *Clays and Clay Minerals*, 51(2), 187-197.

Shackelford, C., and Sample-Lord, K. (2014). "Hydraulic conductivity and compatibility of bentonite for hydraulic containment applications." *From Soil Behavior Fundamentals to innovations in Geotechnical Engineering*, M. Iskander, J. Garlanger, and M. Hussein, Eds., Geotechnical Special Publication 233 Honoring Roy E. Olson, ASCE, Reston, VA, 370-387.

Shainberg, I. and Kemper, W. (1972). "Transport numbers and mobilities of ions in bentonite membranes." *Proc. Soil Science Society of America*, 36(4), 577-582.

Sharma, H.D. and Lewis, S.P. (1994). *Waste Containemnt Systems, Waste Stabilization, and Landfills*. John Wiley and Sons, Inc., New York.

Sherwood, J., and Craster, B. (2000). "Transport of water and ions through a clay membrane." *Journal of Colloid and Interface Science*, 230(2), 349-358.

Sparks, D. (2003). *Environmental Soil Chemistry*. Academic Press, San Diego, CA.

Spectrum Labs (2011). *Product Information for Standard Grade RC Membrane*, Spectrum Laboratories, Inc., Rancho Dominguez, CA.

Sridharan, A. (1991). "Engineering behaviour of clays: A fundamental approach." *Indian Geotechnical Journal*, 21(1), 1-136.

Sridharan, A., Rao, S., and Murthy, N. (1986). "Compressibility behavior of homoionized bentonite." *Géotechnique*, 36(4), 551-564.

Stern, O. (1924). "Zur theorie der elektrolytischen doppelschicht." *Zeitschrift für Elektrochemie*, 30(21-22), 508-516.

Tarchitzky, J., and Chen, Y. (2002). "Rheology of sodium-montmorillonite suspensions: Effects of humic substances and pH." *Soil Science Society of America Journal*, 66(2), 406-412.

van Schaik, J., and Kemper, W. (1966). "Chloride diffusion in clay-water systems." *Proc. Soil Science Society of America*, 30(1), 22-25.

van Schaik, J., Kemper, W., and Olsen, S. (1966). "Contribution of adsorbed cations to diffusion in clay-water systems." *Proc. Soil Science Society of America*, 30(1), 17-22.

van Olphen, H. (1963). *An Introduction to Clay Colloid Chemistry*. John Wiley & Sons, Inc., New York.

Whitworth, T., and Fritz, S. (1994). "Electrolyte-induced solute permeability effects in compacted smectite membranes." *Applied Geochemistry*, 9(5), 533-546.

Yeo, S., Shackelford, C., and Evans, L. (2005). "Membrane behavior of model soil-bentonite backfill mixtures." *Journal of Geotechnical and Geoenvironmental Engineering*, 131(4), 418-429.

Yukselen-Aksoy, Y., Kaya, A., and Oren, A. (2008). "Seawater effect on consistency limits and compressibility characteristics of clays." *Engineering Geology*, 102(1-2), 54-61.

CHAPTER 4. A THROUGH-DIFFUSION METHOD FOR EVALUATING SOLUTE DIFFUSION THROUGH UNSATURATED SODIUM BENTONITE

4.1 Introduction

Fine-grained soils with high swell and low hydraulic conductivity (e.g., bentonites) are used for natural and engineered barriers in chemical containment applications to limit advective (hydraulic) transport of contaminants into the environment (e.g., liners for waste containment systems, slurried vertical cutoff walls). Examples of these barriers include bentonite amended natural soils (e.g., compacted sand-bentonite mixtures and bentonite amended natural clays), geosynthetic clay liners (GCLs), soil-bentonite (SB) vertical cutoff walls, and highly-compacted bentonite buffers for high-level radioactive waste (HLRW) disposal (Shackelford 2013). Because the barriers used in these applications generally are regulated to achieve and maintain low hydraulic conductivity and/or low hydraulic gradient, advective transport of chemicals through the barriers typically is relatively minor such that diffusion becomes an important, if not dominant, chemical transport process (Goodall and Quigley 1977; Crooks and Quigley 1984; Quigley et al. 1987; Rowe 1987; Rowe et al., 1997, 2000; Shackelford 1988, 1989, 1991; Johnson et al. 1989; Muurinen 1990; Shackelford and Daniel 1991a; Kim et al. 1993; Bourg et al. 2003; Montes et al. 2005; Neville and Andrews 2006; Sleep et al. 2006; Kozaki et al. 2008; Glaus et al. 2010; Yong et al. 2010; Shackelford and Moore 2013; Shackelford 2014). Thus, a thorough understanding of the factors affecting diffusive transport for a proposed barrier material allows for improved design and performance of the containment system.

The majority of previous studies on diffusion of chemicals through barriers have focused on the situation where the barriers are water saturated, i.e., with a degree of water saturation, *S*,

of 100 % (Shackelford 2014). However, diffusion under unsaturated conditions (S < 100 %) also may be an important consideration for some containment applications.

For example, highly compacted bentonite (e.g., dry densities, ρ_d, $\geq$ 1.6 Mg/m^3 and porosities, n, < 0.5) has been considered extensively as a barrier in the subsurface disposal of HLRW to isolate or buffer canisters of HLRW from the surrounding environment (Yong et al. 1985; Bucher and Mayor 1989; Komine and Ogata 1996; Madsen 1998; Herbert and Moog 2000; Gens et al. 2002; Lloret et al. 2003; OECD 2003; Montes et al. 2005; Komine 2008; Sánchez et al. 2010; Yong et al. 2010; Ye et al. 2014). In this case, the compacted bentonite initially is unsaturated, and special precautions, such as locating the disposal above the water table and/or within a low moisture environment (e.g., within salt deposits) in order to minimize the likelihood of significant radionuclide migration, may allow for unsaturated conditions to exist in the bentonite for long periods of time (e.g., hundreds or thousands of years) (Herbert and Moog 2000; OECD 2003; Komine and Ogata 2004; Yong et al. 2010). Generation of heat by the decaying waste may cause an initial, thermally-induced redistribution of the pore water in the unsaturated bentonite buffer, resulting in desiccation in the hottest part (near the canister) and wetting in the colder, outer section of the buffer (Pusch and Yong 2006; do N. Guimarães et al. 2006). This heat also may tend to maintain or decrease the initial, overall degree of water saturation of the bentonite buffer (OECD 2003; Rutqvist et al. 2005; do N. Guimarães et al. 2006; Sánchez et al. 2010; Yong et al. 2010; Rutqvist et al. 2014). Over time, uptake of water from the host rock and backfill is expected to lead to full saturation of the bentonite buffer (referred to as maturation of the buffer), with the time required for the buffer to become saturated ranging from a decade for high water-bearing, crystalline host rock to thousands of years for argillaceous host rock (Yong et al. 2010). During this period, diffusion through the bentonite

buffer under unsaturated conditions is a key transport process (Herbert and Moog 2000; Montes et al. 2005).

Another example of a containment application where diffusion under unsaturated conditions may be a predominant consideration includes the use of bentonite based GCLs in cover systems. In this case, several studies have shown that the exchange of multivalent cations (e.g., Ca^{2+}) for monovalent cations, primarily sodium (Na^{+}) that initially is predominant on the exchange sites of the bentonite, can result in a reduced swelling capacity of the GCL upon rehydration, resulting in ultimate failure of the GCL in minimizing percolation of water through the cover (ATU 1992; James et al. 1997; Shackelford et al. 2000; Egloffstein 2001; Jo et al. 2001, 2004; Benson 2002; Shackelford 2005; Benson et al. 2007; Meer and Benson 2007; Scalia and Benson 2010). In this case, diffusion of the multivalent cations under unsaturated conditions from the surrounding soils into the GCL has been postulated as one of the mechanisms by which multivalent-for-monovalent cation exchange has been facilitated. To the author's knowledge, there is little to no published data for measured values of diffusion coefficients of unsaturated bentonite at porosities similar to those of a GCL (e.g., $n > 0.7$).

Based on the aforementioned considerations, a method was developed for measuring the diffusion of salts through fine-grained barrier materials under unsaturated conditions. The method was based on the through-diffusion technique, whereby different concentrations of diffusing solutes are maintained essentially constant at the boundaries of the soil specimen over sufficiently long periods so as to allow for the establishment of steady-state diffusion of the diffusing chemical species. The method was evaluated by considering the diffusion of a simple salt, i.e., potassium chloride (KCl), through a compacted sodium bentonite (Na-bentonite) at constant values of S ranging from 0.79 to 1.0. The advantages and disadvantages of the proposed

method based on the results of four experiments at different values of S are elucidated. Measured values of diffusion coefficients for K^+ and Cl^- are reported and compared with previously published values.

4.2 Background

4.2.1 Diffusion in clays

Diffusion is a fundamental, irreversible process whereby chemical species are transported from a region of higher chemical potential to a region of lower chemical potential (Crank 1975). The gradient in chemical potential driving diffusion may be represented by the concentration gradient of the chemical species. Fick's first law for solute mass flux due to one-dimensional diffusion in a porous medium may be written as follows (e.g., Porter et al. 1960; Shackelford and Daniel 1991a):

$$J_D = -\theta\tau_a D_o \frac{\partial C}{\partial x} = -\theta D^* \frac{\partial C}{\partial x} \tag{4.1}$$

where J_D is the diffusive solute mass flux, θ is the volumetric water content, τ_a is the apparent tortuosity factor, D_o is the aqueous-phase or free-solution diffusion coefficient, C is the aqueous-phase concentration of the chemical species, x is the direction of transport, and D^* (= $\tau_a D_o$) is the effective diffusion coefficient. In some cases, Equation 4.1 is written as follows (e.g., Shackelford and Moore 2013):

$$J_D = -D_e \frac{\partial C}{\partial x} \tag{4.2}$$

where D_e (= θD^*) also has been referred to as the "effective diffusion coefficient."

The volumetric water content is equal to the product of S and the porosity of the porous medium, n (i.e., $\theta = Sn$), such that Equation 4.1 also may be written as follows (Shackelford and Daniel 1991a):

$$J_D = -Sn\tau_a D_o \frac{\partial C}{\partial x} = -SnD^* \frac{\partial C}{\partial x} \tag{4.3}$$

Thus, for a saturated soil (S = 1), Equation 4.3 may be written as follows (e.g., Shackelford and Moore 2013):

$$J_D = -n\tau_a D_o \frac{\partial C}{\partial x} = -nD^* \frac{\partial C}{\partial x} \tag{4.4}$$

The apparent tortuosity factor has been defined as the product of the matrix (or geometric) tortuosity factor, τ_m, representing the geometry of interconnected pores in the porous medium, and a restrictive tortuosity factor, τ_r, that takes into account other factors that may reduce solute flux and contribute to τ_r including anion exclusion (membrane behavior) and solute drag near the surfaces of clay particles (Malusis and Shackelford 2002; Shackelford and Moore 2013), or:

$$\tau_a = \tau_m \tau_r = \tau_m (\tau_1 \tau_2 \ldots \tau_N) \tag{4.5}$$

where N is the number of factors other than the matrix tortuosity that contribute to reducing the diffusive solute mass flux.

The governing equation for transient diffusion is Fick's second law, which may be written for diffusion of non-decaying chemical species as follows (Shackelford and Daniel 1991a; Shackelford and Moore 2013; Shackelford 2014):

$$\frac{\partial C}{\partial t} = D_a \frac{\partial^2 C}{\partial x^2} \tag{4.6}$$

where D_a is defined as an apparent diffusion coefficient, or

$$D_a = \frac{D_o \tau_a}{R_d} = \frac{D^*}{R_d} \tag{4.7}$$

and R_d is the retardation factor that accounts for reduced diffusion due to linear, reversible, and instantaneous sorption of a chemical species onto the solid phase of the porous medium. Thus, in the case where a diffusing chemical species is subject to sorption, $R_d > 1$ such that $D_a < D^*$, resulting is slower diffusion relative to a non-sorbing chemical species with $R_d = 1$.

4.2.2 Measurement of diffusion in unsaturated soils

Several studies have measured diffusion coefficients for unsaturated soils (e.g., Klute and Letey 1958; Porter et al. 1960; Graham-Bryce 1963; Romkens and Bruce 1964; Rowell et al. 1967; Warncke and Barber 1972; Conca and Wright 1990; Barbour et al. 1996; Lim et al. 1998). However, diffusion testing of unsaturated soil generally is more challenging, costly and time consuming than testing of saturated soils (Lim et al. 1998). When testing unsaturated soils, control of the soil suction is desirable so as to avoid bulk liquid flow due to uncontrolled

gradients in matric suction (Barbour et al. 1996). Also, if the test is to be performed at constant or controlled θ, high air-entry (HAE) disks typically are required at the boundaries of the specimen to prevent flow of gas into or out of the specimen.

Saturated HAE disks will prevent passage of free air as long as the pressure does not exceed the air-entry pressure of the HAE disk. However, the potential for dissolved air to diffuse through the water in the disk and then to emerge from solution on the opposite boundary of the disk has been a common concern for unsaturated soils testing (Fredlund 1975; Lu and Likos 2004). For example, Fredlund and Rahardjo (1993) reported that air diffusion through HAE disks may occur in unsaturated soil testing with test durations as short as 1 d. Also, Padilla et al. (2006) measured air diffusion through HAE disks with air-entry pressures of 100 kPa (1 bar), 300 kPa (3 bar), 500 kPa (5 bar), and 1500 kPa (15 bar). The disks were tested against pressures that were 50 % and 95 % of the air-entry pressures. Padilla et al. (2006) concluded that the amount of air that diffused through the disks was negligible (i.e., not measurable) for the 1-bar and 3-bar disks, small ($\leq 1.16 \times 10^{-12}$ m^3/s) for the 5-bar disks, and large ($\leq 2.43 \times 10^{-12}$ m^3/s) for the 15-bar disks. Therefore, potential errors due to air diffusion through the HAE disks used in this research were assumed to be negligible because: 1) only 3-bar and 5-bar disks were used; 2) the applied air pressures did not exceed 70 % of the air-entry pressures of the disks; and 3) circulation of solutions with the closed-system apparatus described subsequently provided constantly flushing boundaries along the HAE disks.

Previous studies have reported decreasing values of D^* in clays with decreasing values of θ (e.g., Porter et al. 1960; Warncke and Barber 1972; Shackelford 1991). Thus, the diffusive solute mass flux of contaminants across a clay barrier typically is lower under unsaturated conditions than saturated conditions. This observation supports the use of simpler, saturated

testing conditions for conservative (i.e., high) estimates of diffusive transport. Therefore, experimental research focused on diffusion in saturated soils has been far more prevalent, relative to research performed on unsaturated soils, due to the greater challenges and limitations of laboratory methods for measurement of unsaturated diffusion and the conservative (high) estimates of diffusion coefficients under saturated conditions.

The most common methods used by soil scientists to measure diffusion in unsaturated soils have been transient methods, specifically the half-cell method (Klute and Letey 1958; Porter et al. 1960; Graham-Bryce 1963; Romkens and Bruce 1964; Rowell et al. 1967). In the half-cell method, two identical specimens of the same soil are equilibrated in two separate half cells with either two different salt solutions or the same salt solution with one cell spiked with an isotope tracer (Shackelford 1991; Barbour et al. 1996; Hu and Wang 2003). The cells then are placed against each other to allow diffusion of solutes from one half-cell to the other. The diffusion coefficient of the soil is calculated based on the change in the solute mass or tracer in each half cell at the end of the test. One challenge of the half-cell method is ensuring full contact between the faces of the two half-cells and interconnectivity of the liquid phase (Shackelford 1991). Another disadvantage of the half-cell method for testing unsaturated soils is the lack of control of the stress state of the soil, as the water content, soil structure and suction in each specimen typically are not controlled. Further, by not controlling the soil suction, solute mass flux may occur across the interface between the two half cells due to suction gradients versus only concentration gradients (Barbour et al. 1996).

To overcome some of the shortcomings of the half-cell method for diffusion testing of unsaturated soils, Barbour et al. (1996) developed a single-reservoir method that allowed for control of the stress state and matric suction, ψ_m, of the soil. The method used the axis-

translation technique and an HAE disk between the specimen and the source reservoir to control ψ_m throughout testing. In the axis-translation technique, air pressure in the soil is increased while the pore-water pressure is maintained at a reference value, typically atmospheric. This technique is useful for investigating a wide range of matric suctions, while remaining above negative water pressures at which cavitation would occur (Fredlund and Rahardjo 1993; Lu and Likos 2004). The source reservoir was maintained at a constant volume so that advection did not occur across the specimen during testing. The specimens used to evaluate the testing apparatus were Beaver Creek Sand, a uniform, fine to medium sand with 1.1 % fines content and a cation exchange capacity (CEC) of 1.3 meq/100g. The specimen thicknesses generally were ≤ 20 mm and saturations ranged from 0.1 to 1.0. The diffusion experiments were performed with KCl solutions with concentrations ranging from 20 mM to 23 mM. Changes in the source reservoir concentration with time were monitored via sampling of small volumes (< 1 mL) at regular time intervals. The results of the test program were subsequently discussed in Lim et al. (1998).

The single-reservoir diffusion experiments were assumed to have reached chemical equilibrium once the changes in the reservoir concentration became insignificant. At chemical equilibrium, the pore-water concentrations in the HAE disk and throughout the specimen were assumed to be constant and equal to the final concentration in the source reservoir. For the experiments where chemical equilibrium was achieved, D^* was determined by matching the predicted reservoir concentrations with the actual reservoir concentrations measured at regular intervals in elapsed time. The theoretical concentration-versus-time profile for the reservoir was generated with the finite element program CTRAN/W (Geo-Slope International Ltd, Calgary, Alberta). The value of D^* was adjusted until the theoretical curve best fit the measured values.

At the end of the test, the specimen was removed and the mass of adsorbed K^+ was determined by saturating the specimen with barium chloride solution (0.1 N) and extracting the fluid (i.e., using ion exchange to remove the adsorbed K^+). Freundlich adsorption coefficients were determined from 24-h batch experiments in accordance with ASTM D 4646-87.

Chemical equilibrium was not achieved in some of the experiments, even after long durations (> 50 d), particularly for K^+. In these experiments, both the diffusion and adsorption coefficients were unknown. To determine these properties, two separate regressions were performed simultaneously with the same input values using CTRAN/W, viz. (1) regressing the theoretical and measured profiles of the reservoir concentration versus time, as previously described, and (2) regressing the theoretical and measured concentration profiles versus depth in the soil specimen. Values of effective diffusion and adsorption coefficients were varied until the theoretical concentration profiles versus both time (reservoir) and depth (specimen) matched the respective experimental concentration profiles.

4.3 Materials and methods

4.3.1 Materials

The bentonite specimens were prepared from GCL-grade, granular bentonite (Colloid Environmental Technologies Co. (CETCO), Hoffman Estates, IL). Physical and mineralogical properties of the bentonite are provided in Chapter 3 (see Table 3.2). The bentonite contained 90 % clay-size particles (ASTM D 422) and classified as high plasticity clay (CH) according to the Unified Soil Classification System (ASTM D 2487). Mineralogical analyses conducted by Mineralogy, Inc. (Tulsa, OK) using x-ray diffraction indicated the relative abundance of montmorillonite was 91 %.

The liquids used in this study included de-ionized water (DIW) (pH = 7.35, electrical conductivity, *EC*, at 25 ^{o}C = 0.06 mS/m) and solutions of DIW with KCl (certified A.C.S.; Fisher Scientific, Fair Lawn, NJ) with target concentrations of 20 mM to 50 mM KCl. The actual measured concentrations of the KCl solutions ranged from 19 mM to 51 mM KCl. Concentrations of K^+ were measured using inductively coupled plasma-atomic emission spectrometry or ICP-AES (IRIS® Advantage/1000 ICAP Spectrometer, Thermo Jarrel Ash Co., Franklin, MA). Concentrations of chloride (Cl^-) were measured using ion chromatography or IC (Dionex® 4000i 131 IC Module, Dionex Co., Sunnyvale, CA). The measured pH of the KCl solutions ranged from 4.8 to 6.5 and the measured *EC* at 25 ^{o}C ranged from 280 mS/m to 683 mS/m.

During the long-term diffusion testing, if bio-activity in the unsaturated specimen was suspected (as indicated by erratic *EC* readings – see Section 4.3.6), biocide (DOWICIL QK-20 Antimicrobial, Dow Chemical Co., USA) was added to the KCl source solutions at a concentration of 500 ppm (Nelson 2000; Jo et al. 2005). Nelson (2000) performed hydraulic conductivity tests on paper sludges and determined that concentrations of DOWICIL QK-20 between 500 ppm and 2,000 ppm were effective in eliminating biological activity, but did not cause significant physicochemical changes that would alter the hydraulic conductivity. Based on the results of Nelson (2000), Jo et al. (2005) added 500 ppm of DOWICIL QK-20 to the permeant solution (5 mM $CaCl_2$) used in a long-term hydraulic conductivity test conducted on a GCL. The active ingredient in the biocide is 2,2-dibromo-3-nitrilopropionamide (commonly referred to as DBNPA), which provides broad-spectrum control of bacteria, fungi, and yeast (Dow Chemical Company 2000). The end products of the biocide after decomposition are carbon dioxide (CO_2), ammonia (NH_3) bromide (Br^-), and hydrogen (H^+). In this study, the

maximum change in pH and *EC* of the KCl solutions upon addition of 500 ppm of biocide was 10 % and 1 %, respectively.

4.3.2 Specimen preparation

The purpose of the research was to evaluate diffusion, as well as membrane behavior (anion exclusion), in unsaturated Na-bentonite. Therefore, control of the exchangeable cations on the bentonite was desired to allow for distinction between solutes that have diffused from solutions applied at the boundaries and through the specimen versus solutes initially within the pore water of the specimen (e.g., if Na^+ dominates the exchange complex, then K^+ and Cl^- can be distinguished relative to Na^+). In addition, amplification of membrane behavior by increasing the exchangeable sodium percentage of the bentonite was preferred to draw clearer, more confident conclusions regarding the relationship between membrane efficiency and degree of saturation (see Chapter 5). Therefore, the original GCL-grade bentonite was treated with a dialysis procedure to modify the exchange complex such that Na^+ occupied most (69 %) of the exchange sites and also to flush the bentonite of excess soluble salts. A detailed description of the dialysis procedure and relevant data are provided in Chapter 3. At the end of the dialysis procedure, the bentonite was in a paste form and the exchange complex of the bentonite consisted of 69 % Na^+, 1 % K^+, 20 % Ca^{2+}, and 10 % Mg^{2+} (by molar ratio), as determined by ASTM D 7503-10.

Consolidation of clay pastes and slurries using standard consolidation equipment (e.g. oedometer or triaxial cells) and procedures (e.g., ASTM D 2435, ASTM D 4767, ASTM D 7181) can be challenging due to issues such as material loss during incremental loading (for the oedometer cell) and difficulty assembling the test cell around the high-water content material.

Since the sole purpose of the consolidation stage was to prepare specimens to the desired value of n (or void ratio, e) for diffusion and membrane behavior testing (i.e., versus evaluating the consolidation behavior of the material), a simple column setup was designed to consolidate the bentonite paste with incremental loading. A detailed schematic and photographs of the column setup used for consolidation of the paste are provided in Appendix C.

The dialysized bentonite paste (~37 g dry mass of bentonite) was placed in an acrylic column with an inner diameter and thickness of 82.5 mm and 6.35 mm, respectively. The dry mass of 37 g provided sufficient bentonite to prepare one set of identical test specimens (same n and thickness) in the consolidation column, i.e., a consolidated specimen thick enough to be split into two thinner (< 10 mm) specimens for testing. Use of larger volumes of paste corresponding to a dry mass greater than 37 g was not desirable, as this would result in increased initial thicknesses of the paste specimens prior to consolidation and, therefore, longer durations for completion of primary consolidation due to increased drainage distances. Filter paper and geotextile along the top and bottom boundaries of the paste provided double-drained conditions during consolidation. The top of the column was covered with plastic wrap (Glad Products Company, Oakland, CA, USA) and the paste was allowed to sit for at least 24 hours before loading to allow self-weight consolidation to occur. Changes in specimen thickness with time were recorded manually and the period of self-weight consolidation was considered complete when the measured total deflection (or strain) of the specimen became constant (duration $\leq$ 7 d).

Upon completion of the self-weight consolidation stage, the specimen was consolidated further via incremental loading to achieve the desired n for diffusion and membrane testing. Prior to applying the first load, a porous disk was placed on top of the specimen. Loads were applied incrementally using tins of lead shot and steel plates (see Appendix C). A typical load

increment ratio (LIR) of one was used (i.e., doubling the load each increment), and the specimen deflections with time were manually recorded using a dial gauge (MHC Dial Indicator, Model No. 6605-4070, MHC Industrial Supply, China). For each load increment, the time required to achieve the end of primary consolidation, as indicated by the curve of deflection versus time for each load increment, typically was less than or equal to 7 d.

The curves of *e* versus vertical effective stress measured during consolidation of the four specimens used in the diffusion tests are provided in Figure 4.1a. The bentonite paste was consolidated to a final value of *n* ranging from 0.87 to 0.89, corresponding to values of *e* ranging from 6.7 to 8.1, respectively. This range of values of *n* allowed for comparison of the test results with data in the literature for diffusion and membrane behavior in saturated bentonite and GCL specimens (e.g., Malusis and Shackelford 2002; Malusis et al. 2014; Bohnhoff and Shackelford 2015). Although a thorough evaluation of the consolidation behavior of the dialysized, Na-bentonite was beyond the scope of this study, the compression results were compared with values reported by Olson and Mesri (1971), as shown in Figure 4.1b. The purpose of this comparison was mainly to confirm that the specimens prepared in the alternative consolidation equipment exhibited similar consolidation behavior to that of bentonite at high water contents consolidated using standard equipment and procedures. As expected, the compression curves measured for the dialysized bentonite with 69 % Na^+ on the exchange complex fell between the compression curves measured by Olson and Mesri (1970) for homo-ionized Na- and Ca-bentonites. This comparison confirmed that the basic compression measurements (e.g., deflection and strain) obtained with the alternative column setup were reasonable.

Following completion of consolidation, the loads were removed incrementally (using an LIR $\leq$ 2) to confirm that final value of *n* of the specimen remained within the desired range. The

specimen was removed from the column and the final thickness, diameter and weight of the specimen were recorded. The thickness of the consolidated specimens was 20 mm to 25 mm, which was sufficient to provide for a portion of the specimens to be used to measure water content and the remainder of the specimen to be split into two separate sub-specimens (each 7- to 10-mm thick) for testing.

After consolidation, the specimens essentially were fully saturated (S > 97 %). To prepare specimens at lower values of S for diffusion and membrane testing, the 7- to 10-mm thick specimens were placed in a pressure plate cell (15-bar Pressure Plate Extractor, Soilmoisture Equipment Corp., Santa Barabara, CA). The S and θ of the specimens were decreased by incrementally increasing ψ_m using axis translation, generally following the same procedure used to develop soil-water characteristic curves (SWCC) (ASTM D 6836). Every time that specimens were removed from the pressure plate and weighed to determine θ for the applied ψ_m the dimensions of the specimen were measured to account for changes in volume. Pictures of the pressure plate cell and associated equipment are provided in Appendix C.

The curves of ψ_m versus θ measured during preparation of the three unsaturated specimens used in the diffusion tests are provided in Figure 4.2. Comparison of the partial SWCCs measured for the specimens with commonly used mathematical models (e.g., Brooks and Corey 1964; van genuchten 1980; Fredlund and Xing 1994) was beyond the scope of this study, as the primary purpose was to prepare unsaturated specimens for diffusion and membrane testing. However, further evaluation of the soil-suction behavior of the Na-bentonite may provide additional insight regarding interpretation of the test results for unsaturated diffusion and membrane behavior, and should be addressed in future research.

To minimize changes to θ and *S* of the specimen after removal from the pressure plate, the specimen was immediately wrapped twice in plastic wrap, sealed in a plastic bag, and then placed inside another sealed container. Immediately prior to use in the diffusion and membrane testing, the dimensions and weights of all specimens were re-measured to ensure the values of *S* and *n* did not changed significantly during storage. However, the expectation of maintaining perfectly constant values of *n*, *S* and θ after removal of the specimen from the pressure plate, during temporary (< 1 d) storage (sealed as previously described), and during final assembly of the test cell at which time the specimen had to be uncovered briefly (< 20 min) without an applied air pressure, was not practical. As shown in Figure 4.2, some wetting of the specimen occurred, such that the final value of θ (and, therefore, *S*) at the start of the diffusion test was higher than the value of θ at the end of the saturation adjustment (pressure plate) stage. The tendency for θ of the specimen to increase during this time period was identified during initial testing trials and, therefore, measures were taken during the specimen preparation and assembly procedures to accommodate expected changes in the value of θ after removal from the pressure plate. For example, the specimens were prepared to lower θ (higher ψ_m) during the saturation adjustment stage than was needed for the diffusion and membrane testing, in anticipation of θ increasing slightly by the time the test began.

During the DIW circulation stage, after the test began but prior to circulation of KCl, measured values of suction at the specimen boundaries were used to confirm the final values of ψ_m of the specimen (see Chapter 5). Note that the values of all specimen properties listed for each diffusion test (e.g., *S*, *n*, θ) in Tables 4.1 to 4.3 refer to the actual properties of the specimen throughout the diffusion test, and not the values measured at the end of the saturation adjustment stage.

4.3.3 Experimental apparatus and boundary conditions

Diffusion properties of the bentonite specimens were measured with the through-diffusion method, also known as the time-lag or steady-state method (Shackelford 1991). The experimental apparatus and procedures used in this study are described in detail in Chapter 2. Briefly, the bentonite specimen is confined in a rigid-wall cell with a flexible membrane between the specimen perimeter and the sidewall of the rigid cell. The purpose of the flexible membrane is to prevent short circuiting of pressures during semipermeable membrane testing and solute mass flux during diffusion testing between the top and bottom boundaries of the specimen. To prevent uncontrolled changes in water content during diffusion testing (due to movement of gas into or out of the unsaturated bentonite specimen), HAE disks (Soilmoisture Equipment Corporation, Santa Barbara, CA), were placed above and below the specimen, as shown in Figure 4.3. The HAE disks are made of ceramic (formed from sintered kaolin), and the properties of the disks, including diffusion properties measured during calibration testing, were described in detail in Chapter 2. The cell was connected to a hydraulic control system consisting of a flow pump with two stainless-steel syringes. Chemical (electrolyte) solutions and DIW were circulated across the top and bottom boundaries of the test cell, respectively, via piston displacement from the syringes through stainless steel tubing. The syringe pumps allowed for circulation of the solutions and DIW at the same, constant flow rate. After each circulation cycle (typically every two days) whereby the liquid-holding capacity of the syringes (approximately 44 mL) had been exhausted, circulation was paused and the syringes were replenished with fresh solution or DIW from storage reservoirs.

Prior to diffusion testing, DIW was circulated through porous disks along both the top and bottom boundaries of the upper and lower HAE disks, respectively, to establish baseline

concentrations and remove remaining soluble salts from the specimen. For all experiments, the DIW stage was performed for 24 to 29 days and the final *EC* of the bottom effluent was less than 8 mS/m.

During diffusion testing, a concentration gradient was applied across the specimen by circulating a solution with an initial concentration of KCl ($C_{ot} > 0$) through the top porous disk and DIW ($C_{ob} \cong 0$) through the bottom porous disk. The experimental system was closed during testing, such that no liquid flow occurred through the specimen in order to maintain a constant volume. Since liquid flux was prevented, advective flux (J_A) and chemico-osmotic solute mass flux (J_π) could not occur (i.e., $J_A = J_\pi = 0$), such that the total solute mass flux through the layered porous media, J ($= J_A + J_\pi + J_D$) was equal to the diffusive flux, J_D.

Solutes diffused from higher concentration to lower concentration, i.e., from the top circulation boundary, through the upper HAE disk, the underlying specimen, and the lower HAE disk, and into the bottom circulation boundary. A schematic illustration of the development of the time-dependent concentration profiles within the porous media is shown in Figure 4.4a. The concentration profiles shown in this figure were generated by simulating a 20 mM KCl circulation stage using HYDRUS-1D (PC-Progress, Prague, Czech Republic). Since the experiments were performed in a closed system with essentially constant concentrations at the boundaries, the concentration profiles across each of the disks and the specimen become linear at steady-state diffusion (Malusis et al. 2012).

Development of linear concentration profiles at steady-state diffusion conditions is an important advantage of the closed-system testing method (Shackelford 2013). When the profile is linear, the change in concentration across the total length of the specimen ($\Delta C/L$) may be used in the calculation of D^* (see Section 4.3.5). In contrast, in open systems where chemico-osmotic

liquid flow (q_π) is allowed to occur, the resulting concentration profile at steady state is nonlinear, such that the assumption of a constant concentration difference (ΔC) across the porous medium is not valid (e.g., Dutt and Low 1962; Quigley et al. 1987; Muurinen 1990). Thus, the use of a closed system to prevent q_π from occurring in the specimen greatly simplifies the interpretation of the data.

4.3.4 Sampling and boundary concentrations

During refilling of the syringe pumps with fresh DIW and KCl solutions, the spent circulation fluid (effluent) was simultaneously collected in 50-mL vials. The pH and *EC* of the samples were measured immediately after collection, and portions of the samples were used for measurement of concentrations of all inorganic metals (e.g., K^+, Na^+) via ICP-AES, and anionic chemical species, principally chloride (Cl^-), via IC (same equipment as listed in Section 4.3.1).

Diffusion from the top boundary to the bottom boundary of the test system resulted in increased concentrations of Cl^- and K^+ in the circulation outflow collected from the bottom boundary, C_b (e.g., $C_b > C_{ob} \cong 0$). The concentrations of Cl^- and K^+ in the circulation outflow from the top boundary, C_t, were lower than those in the circulation inflow at the top boundary ($C_t < C_{ot}$) due to diffusion. The total concentration difference (ΔC_{total}) across the porous media (HAE disk-bentonite-HAE disk) was represented as the difference between the average concentrations at the boundaries (see Fig. 4.4b), or

$$\Delta C_{total} = C_{b,ave} - C_{t,ave} \tag{4.8}$$

where the average concentrations are determined from the measured concentrations of the inflows and outflows (effluent) at each boundary as follows:

$$C_{b,ave} = \left(\frac{C_{ob} + C_b}{2} \right); \; C_{t,ave} = \left(\frac{C_{ot} + C_t}{2} \right) \tag{4.9}$$

The concentrations of Cl^- and K^+ in C_b were monitored as a function of time to determine J_D required to calculate the effective diffusion coefficients, as discussed subsequently.

4.3.5 Diffusion analysis

The traditional through-diffusion method of analysis has been used to determine D^* values of saturated clays and clay mixtures in multiple studies using closed-system experiments to evaluate coupled diffusion and semipermeable membrane behavior (e.g., Malusis and Shackelford 2002; Di Emidio 2010; Dominijanni et al. 2013; Malusis et al. 2014; Bohnhoff and Shackelford 2015), as follows:

$$D^* = -\left(\frac{L}{n \left(C_{b,ave} - C_{t,ave} \right)} \right) J_{D,ss} \tag{4.10}$$

where L is the length of the specimen and $J_{D,ss}$ is J_D at steady state. If the specimen is unsaturated, such as in this study, the porosity in Equation 4.10 is replaced by the volumetric water content, θ, as follows:

$$D^* = -\left(\frac{L}{\theta\left(C_{b,ave} - C_{t,ave}\right)}\right) J_{D,ss} \tag{4.11}$$

For all of the diffusion experiments, $J_{D,ss}$ for each testing stage was determined based on the traditional through-diffusion analysis method using the cumulative solute mass, as follows (Shackelford 1991; Shackelford and Lee 2003; Shackelford and Moore 2013):

$$J_{D,ss} = \left.\frac{\Delta Q_t}{\Delta t}\right|_{steady-state} \tag{4.12}$$

where Q_t is the cumulative solute mass ($\Sigma\Delta m$) normalized with respect to the cross-sectional area of the specimen (A) (i.e., $Q_t = \Sigma\Delta m/A$, where Δm is the incremental mass of the chemical species in the sample withdrawn from the collection reservoir), and t is the elapsed time. The value of Δm is determined by multiplying the volume of the incrementally collected sample (ΔV) by the measured concentration of the species of interest in the sample (i.e., C_b). The plot of Q_t versus t generally is nonlinear at the beginning or transient stage of the test, followed by a linear portion corresponding to the establishment of steady-state diffusion for the individual chemical species through the specimen, as shown in Figure 4.5 (e.g., Shackelford 1991). The slope of the linear portion of the Q_t-versus-t data is assumed equal to $J_{D,ss}$ as shown in Equation 4.12. Thus, Equation 4.11 can be rewritten as follows:

$$D^* = -\left(\frac{L}{\theta\left(C_{b,ave} - C_{t,ave}\right)}\right)\left(\frac{\Delta Q_t}{\Delta t}\right)_{steady-state} \tag{4.13}$$

In this study, sequential linear regression was conducted to establish the number of measured data representing the steady-state diffusive mass flux, as described in Shackelford and Lee (2003). A linear regression was conducted on an increasing number of the Q_t-versus-t data. The value of t at which the coefficient of determination, r^2, of the linear regression deviated significantly from unity was considered to be the distinction between the transient and steady-state portions of the data. All of the plots used to determine the number of cumulative mass data required to estimate $J_{D,ss}$ for the experiments are provided in Appendix D. The values of $J_{D,ss}$ determined from this approach were used to calculate D^* values of the clay specimens using the traditional through-diffusion method applied to layered porous media under unsaturated conditions, as described subsequently.

The specimen sandwiched between two HAE disks in the test cell is similar to a layered soil system, consisting of three distinct layers (HAE disk-bentonite specimen-HAE disk). Therefore, Equation 4.11 may be modified as follows:

$$D^*_{clay} = -\left(\frac{L_{clay}}{\theta_{clay}\Delta C_{clay}}\right)\left(\frac{\Delta Q_t}{\Delta t}\right)_{steady-state} = -\left(\frac{L_{clay}}{\theta_{clay}\Delta C_{clay}}\right)J_{D,ss} \tag{4.14}$$

where D^*_{clay} is the effective diffusion coefficient for the clay specimen, L_{clay} and θ_{clay} are the thickness and volumetric water content of the clay specimen, respectively, and ΔC_{clay} is the concentration difference only across the clay specimen. To calculate D^*_{clay} using Equation 4.14, the value of ΔC_{clay} must be known. The value for ΔC_{clay} can be determined knowing the requirement that the concentration difference across the entire porous system is equal to the sums of the concentration differences across the two HAE disks and the clay (i.e., $\Delta C_{total} = \Delta C_{clay} +$

$2\Delta C_{HAE}$), and the requirement for continuity of solute mass flux across the porous system at steady state (i.e., $J_{D,ss} = J_{HAE,ss} = J_{clay,ss}$). Application of both of these requirements results in the following expression for D^*_{clay} (see Appendix D for details):

$$D^*_{clay} = \frac{L_{clay}}{\theta_{clay}\left(-\frac{\Delta C_{total}}{\Delta Q_t / \Delta t} - 2\frac{L_{HAE}}{D^*_{HAE}\theta_{HAE}}\right)} \tag{4.15}$$

where D^*_{HAE} is the effective diffusion coefficient of the HAE disk, and L_{HAE} and θ_{HAE} are the thickness and volumetric water content of each HAE disk, respectively. The values for all the independent variables in Equation 4.15 are either known or can be determined from the testing data using steady-state analysis methods as previously described (e.g., see Table 4.1). As described in Chapter 2, the D^* values of the HAE disks were 1.4 x 10^{-10} m^2/s to 1.6 x 10^{-10} m^2/s, which are similar to values reported for fine-grained soils (Shackelford 1991, 2014).

4.3.6 Experimental program

The experimental program consisted of four multistage diffusion experiments. These experiments were performed by sequentially circulating KCl solutions with increasingly higher source concentrations, C_{ot}, of KCl across the top circulation boundary. Each of the four experiments corresponded to a bentonite specimen with a different value of S that was maintained constant throughout the multistage test.

The values of S and θ for the four specimens ranged from 0.79 to 1.0 and 0.70 to 0.87, respectively. The range of S that could be evaluated was limited by time and equipment constraints. The time to reach steady-state diffusion (and thus, the required experimental

duration) increases as the diffusion coefficient of the clay decreases. The value of the effective diffusion coefficient of the clay, $D_{e,clay}$, is directly related to the volumetric water content ($D_{e,clay} = \theta D^*_{clay}$), such that $D_{e,clay}$ decreases as S and θ decrease. As a result, the time required to achieve steady-state diffusion increases as S decreases. In addition, specimens at lower S also will exhibit higher suction and, therefore, require the use of HAE disks with higher air-entry values (e.g., 15 bar rather than 3 or 5 bar). As the air-entry value of the HAE disk increases, the D^*_{HAE} likely will decrease as well (see Chapter 2), which in turn will further increase required test durations. As a result of these considerations and available soil-suction data obtained during specimen preparation (see Section 4.3.3), the minimum S evaluated in this study was set to 0.79 to allow use of HAE disks with a maximum air-entry value of 5 bar. Even with these considerations, the testing durations required for completion of each multistage test were lengthy, ranging from 280 to 330 d (see Table 4.1).

Also, based on budget, space, and available lab equipment, only two experiments could be performed concurrently, reducing the total number of experiments that could be completed within the project timeline. Four multistage experiments, each performed at a different constant value of S, were considered adequate to establish trends between diffusion coefficients and S or concentration.

4.4 Results

4.4.1 Electrical conductivity

The results of the *EC* measurements from circulation outflows collected at the top and bottom boundaries of the testing cell are shown for all of the diffusion experiments in Figure 4.7. Note that day 0 corresponds to the first day of circulation of KCl solution at the top boundary to

induce a concentration gradient across the specimen. Times prior to day 0 correspond to the initial DIW stage during which DIW was circulated at both the top and bottom boundaries to remove remaining soluble salts, and the diffusion test had not yet begun.

For all of the experiments, after the start of KCl circulation at the top boundary ($t > 0$), the *EC* of the outflow at the bottom boundary began to increase. This increase in *EC* was caused by increased salt concentration at the bottom boundary due to diffusion of solutes from the top boundary downward through the specimen. Subsequent changes in the *EC* of the bottom effluent were representative of changes in J_D through the bottom boundary. As expected, the *EC* of the bottom effluent increased with increasing source KCl concentration across the top boundary due to the greater concentration gradient and a correspondingly greater solute mass flux. For example, for the saturated bentonite specimen (S = 1.0, Figure 4.7a), as the source KCl concentration was increased from 20 mM to 30 mM and from 30 mM to 50 mM, the bottom *EC* increased from 23.6 mS/m to 38.4 mS/m and from 38.4 mS/m to 57.8 mS/m, respectively. Although these boundary *EC* values are useful (and simple) indicators of the boundary conditions for the experiments, these values cannot be used to determine solute diffusion coefficients because all ions in solution contribute to *EC* (e.g., Shackelford et al. 1999).

4.4.2 Ion concentrations, mass flux, and charge balances

Chemical analyses (ICP-AES and IC) were performed on samples of the bottom outflow to measure the concentrations of individual cations and anions. Although the samples were analyzed for 36 different cation species and 7 anion species, only three cation (K^+, Na^+, Ca^{2+}) and one anion species (Cl^-) were consistently measured above detection limits for all of the experiments. The measured concentrations of these four species throughout the diffusion

experiments are provided in Figure 4.7. As expected, the steady-state concentrations of K^+ and Cl^- increased as C_{ot} increased with each stage of the test (e.g, from 20 mM KCl to 30 mM KCl, from 30 mM to 50 mM). For example, for the specimen with S of 0.84 as the C_{ot} was increased from 30 mM to 50 mM KCl the steady-state K^+ and Cl^- concentrations in the bottom effluent both increased from 1.7 mM to 2.6 mM (see Figure 4.7c).

For all of the experiments, the initial Na^+ concentration in the bottom effluent was greater than the concentration of K^+. Therefore, the initial increase in EC at the start of diffusion testing (see Figure 4.6) can be attributed to diffusion of Na^+ and Cl^- from the specimen versus diffusion of K^+ from the top boundary through the specimen. Diffusion of Na^+ from the specimen at early times affects the rate of K^+ diffusion across the test system (see Section 4.5.3). In all of the experiments, the Na^+ concentration decreased to less than half of the K^+ concentration by the end of the first concentration stage (20 mM) and continued to decrease to values that ultimately were below the detection limit. Concentrations of Ca^{2+} in the bottom effluent remained relatively low ($\leq$ 0.2 mM) and constant during each test stage.

The diffusive fluxes (J_D) of Cl^-, K^+, Na^+, and Ca^{2+} are shown as a function of elapsed time in Figure 4.8. As expected, as the source concentration of KCl increased such that ΔC for K^+ and Cl^- across the test system increased, J_D of K^+ and Cl^- increased. For example, for the specimen at S of 0.84, as C_{ot} increased from 20 mM to 30 mM KCl, $J_{D,ss}$ of Cl^- and K^+ increased from 146 mg/m^2-d to 261 mg/m^2-d and from 156 mg/m^2-d to 282 mg/m^2-d, respectively (Figure 4.8c, Table 4.2). Note that the increase in $J_{D,ss}$ with increasing source concentration is not just a function of increasing ΔC, because an increase in D^* with increasing average concentration in the specimen also contributes to higher $J_{D,ss}$ (see Section 4.5.1).

To evaluate the charge balance of the effluent samples, the total charge equivalents of the anions and cations are plotted together as a function of time in Figure 4.9. Confirmation that the anion and cation charge equivalents are approximately equal (the charges in the sample are balanced) provides confidence that the chemical analyses were comprehensive and significant concentrations of ion species other than those measured were not present. For all of the diffusion experiments, the total charge equivalents of the cations generally were equal to or slightly greater than those of the anions. The cation charge equivalent may have been slightly greater than that of the anions due to excess Na^+ in the specimen or omission of a low concentration of any anionic species that were not measured as part of the IC analysis. Regardless, the values shown in Figure 4.9 generally indicate good agreement between the cationic and anionic charges (i.e., $1.0 \leq$ cation equivalents/anion equivalents ≤ 1.2) for the effluent samples at steady-state diffusion conditions.

4.4.3 Diffusion results

Steady-state diffusion for each concentration stage of the multistage experiments was evaluated following the procedure described in Section 4.3.5. The diffusion coefficients calculated for the clay specimens, viz. D^*_{clay} and $D_{e,clay}$ (= θD^*_{clay}), as well as the values of important parameters used in the analyses (e.g., $J_{D,ss}$), are summarized in Table 4.2. Plots of Q_t versus t for each multistage experiment are provided in Figure 4.10. For the through-diffusion analysis of the multistage experiments, the net values of Q_t and t, or Q_t' and t', respectively, pertaining to each concentration stage were used to determine the values for $J_{D,ss}$ and D^*_{clay} for each stage of the test, as follows (e.g., Bohnhoff and Shackelford 2015):

$$Q_t' = Q_{t,x+1} - Q_{t,x} \tag{4.15}$$

$$t' = t_{x+1} - t_x \tag{4.16}$$

where $Q_{t,x}$ and t_x are the final values of Q_t and t, respectively, from the previous stage of the experiment, and $Q_{t,x+1}$ and t_{x+1} are the corresponding values for the current stage of the experiment. Essentially, the use of Q_t' and t' resets the values for Q_t and t to zero at the start of each concentration stage (Bohnhoff and Shackelford 2015).

The plots of Q_t' versus t' for each experiment are shown in Figures 4.11 to 4.14, and the results of the analyses of these data are summarized in Table 4.2. The values of $J_{D,ss}$ for each stage of a given experiment (i.e., the slopes $\Delta Q_t'/\Delta t'$ resulting from linear regressions of the steady-state portions of the individual plots) ranged from 11 mg/m^2-d to 525 mg/m^2-d for Cl^- and from 11 mg/m^2-d to 552 mg/m^2-d for K^+. As expected, $J_{D,ss}$ increased with increasing source concentration (C_{ot}) due to the increasing concentration gradient. For example, for the specimen with S of 0.89, $J_{D,ss}$ for Cl^- was 203 mg/m^2-d, 342 mg/m^2-d and 525 mg/m^2-d for source concentrations of 20 mM, 30 mM, and 50 mM KCl, respectively. For the same multistage experiment, the $J_{D,ss}$ for K^+ was 179 mg/m^2-d, 232 mg/m^2-d and 544 mg/m^2-d for source concentrations of 20 mM, 30 mM, and 50 mM KCl, respectively.

For all of the bentonite specimens and source KCl concentrations, the steady-state values of D^*_{clay} ranged from 2.1 x 10^{-12} m^2/s to 4.1 x 10^{-10} m^2/s, whereas those for $D_{e,clay}$ ranged from 1.5 x 10^{-12} m^2/s to 3.6 x 10^{-10} m^2/s. These values of D^*_{clay} and $D_{e,clay}$ for Na-bentonite specimens are consistent with expectations based on available data in the literature, although literature values for diffusion coefficients of unsaturated bentonite specimens with high porosities (e.g., n > 0.7) is limited, at best.

For example, Rowe et al. (2000) performed double-reservoir diffusion experiments on saturated specimens of Na-bentonite (granular and powdered), as well as non-woven GCLs containing the same granular Na-bentonite. The source and collection reservoirs were filled with NaCl solution and DIW, respectively. The concentration of the NaCl solution was 56 mM for all of the diffusion experiments. In the diffusion experiments where the specimen volume was controlled throughout testing, the thickness of the bentonite ranged from 5.6 mm to 7.1 mm. The reported values of D^* for Cl^- ranged from 3.6 x 10^{-11} m^2/s to 2.1 x 10^{-10} m^2/s for porosities of 0.57 to 0.76, respectively. The values of D^* for Na^+ were slightly higher, ranging from 6.0 x 10^{-11} m^2/s to 3.5 x 10^{-10} m^2/s. The difference between the D^* values for Cl^- and Na^+ was attributed to initial concentrations of Na^+ in the pore water.

Also, Malusis and Shackelford (2002) reported diffusion coefficients for K^+ and Cl^- through a needle-punched, GCL containing granular, saturated Na-bentonite. A closed-system test apparatus was used to measure coupled diffusion and membrane behavior of the GCL. Solutions of KCl were circulated across the top boundary of the specimen, while processed tap water (EC = 0.32 mS/m) was circulated across the bottom boundary. The specimen was flushed to remove excess soluble salts prior to testing. The measured concentrations of KCl in the source solutions used in the multistage experiments were 3.9 mM, 8.7 mM, 20 mM, and 47 mM. For all specimens, $S > 0.96$ and $0.78 \leq n \leq 0.80$. The measured values of D^* for Cl^- and K^+ ranged from 7.1 x 10^{-11} m^2/s to 2.3 x 10^{-10} m^2/s, and from 4.4 x 10^{-11} m^2/s to 2.0 x 10^{-10} m^2/s, respectively.

Similar closed-system experiments to measure coupled diffusion and membrane behavior of GCLs were performed by Malusis et al. (2013). A needle-punched GCL was flushed of excess soluble salts prior to diffusion testing. The KCl measured concentrations used in the

multistage experiments were 3.9 mM, 6.0 mM, 8.7 mM, 20 mM, and 47 mM. A flexible-wall cell was used to control the effective stress (σ'), with σ' ranging from 34.5 kPa to 241 kPa. The thickness and porosity of the specimens ranged from 5.6 mm to 9.5 mm and from 0.66 to 0.81, respectively. The D^* values of the salt were estimated based on *EC* measurements of the effluent collected from the bottom boundary. The values of D^* for KCl ranged from 4.3 x 10^{-11} m^2/s to 2.8 x 10^{-10} m^2/s, with D^* decreasing with increasing effective stress.

Relative to published data for diffusion through high-porosity bentonite and GCLs, there is substantially more published data available for diffusion through highly compacted bentonite (dry density, $\rho_d \geq 1.6$ Mg/m^3) considered for use in radioactive waste disposal applications (see Shackelford and Moore 2013). As expected, the diffusion coefficients for the highly compacted Na-bentonite reported in the literature typically are lower than the values reported for GCLs, due to substantially lower porosity (e.g., n of 0.3 to 0.5) and greater tortuosity of the compacted specimens. For example, Kim et al. (1993) measured diffusion through compacted, saturated Na-bentonite with the back-to-back diffusion method (Torstenfelt et al. 1983). In the back-to-back method, a plane source impregnated with radionuclide is introduced at the mid-plane of a saturated soil specimen inside a diffusion cell. For anion diffusion, the authors assumed retardation was negligible (R_d = 1.0) and, therefore, $D_a = D_e$. The reported values of D_a (= D_e) for $^{36}Cl^-$ ranged from 5.0 x 10^{-12} m^2/s to 2.1 x 10^{-10} m^2/s for dry densities of 1.90 Mg/m^3 to 1.16 Mg/m^3, respectively. The volumetric water content of the specimens ranged from approximately 0.3 to 0.61.

Rosanne et al. (2003) measured diffusion of NaCl and potassium iodide (KI) through compacted Na-montmorillonite specimens (n = 0.41 to 0.59). Clay specimens were placed between two reservoirs of salt solution and brought to equilibrium with the desired solution for a

minimum of 200 h. Then the solution in one reservoir was replaced with a more or less concentrated solution, inducing diffusion across the specimen. The salt concentrations in the reservoirs with time were determined from *EC* measurements with conductivity probes. At an average NaCl concentration (C_{ave}) of 50 mM, the D^* values for NaCl ranged from 2.5 x 10^{-10} m^2/s to 1.5 x 10^{-9} m^2/s, whereas those for D_e ranged from 1.1 x 10^{-10} m^2/s to 9.0 x 10^{-10} m^2/s. For the potassium iodide, at C_{ave} of 55 mM KI, the D^* values for KI ranged from 1.2 x 10^{-10} m^2/s to 2.9 x 10^{-10} m^2/s, whereas those for D_e ranged from 1.2 x 10^{-10} m^2/s to 2.5 x 10^{-10} m^2/s.

Glaus et al. (2010) performed through-diffusion experiments with radioactive tracers (HTO, $^{22}Na^+$, $^{36}Cl^-$) in highly compacted (ρ_d = 1.90 ± 0.05 Mg/m^3), saturated specimens of kaolinite, Na-illite and Na-montmorillonite. The experiments were performed using 0.1 M, 0.5 M, 1.0 M, or 2.0 M $NaCl0_4$ solution. Prior to starting each diffusion test, the clay was saturated with the appropriate electrolyte solution for a minimum of four weeks. The experiments were performed in stages, with a new tracer started after the out-diffusion of the previous tracer was complete. For the Na-montmorillonite specimens, reported values of D_e for $^{22}Na^+$ and $^{36}Cl^-$ ranged from 3.6 x 10^{-11} m^2/s to 3.8 x 10^{-10} m^2/s and from 7.2 x 10^{-14} m^2/s to 7.2 x 10^{-13} m^2/s, respectively. The lower diffusion rate of the negatively charged tracer was attributed to anion exclusion effects.

In this study, the steady-state values of D^*_{clay} for K^+ (D^*_{clay,K^+}) generally were lower than those for Cl^- (D^*_{clay,Cl^-}). For example, for the saturated specimen (S = 1.0), D^*_{clay,K^+} ranged from 2.1 x 10^{-12} m^2/s to 3.1 x 10^{-10} m^2/s, while D^*_{clay,Cl^-} ranged from 2.3 x 10^{-12} m^2/s to 4.1 x 10^{-10} m^2/s. The possible reason(s) for these differences between the values of D^*_{clay,K^+} and D^*_{clay,Cl^-} measured in the diffusion experiments are discussed in further detail in Section 4.5.3.

4.5 Discussion

4.5.1 Effect of average pore-water concentration

The values of D^*_{clay} and $D_{e,clay}$ for both Cl^- and K^+ tended to increase with increasing average concentration in the specimen at steady-state diffusion (C_{ave}), as shown in Figures 4.15 and 4.16. This trend can be explained on the basis of classical diffuse double-layer (DDL) theory (e.g., Mitchell and Soga 2005). As C_{ot} increased, the average KCl concentration in the pore space of the specimen increased. As the salt concentration in the pore space of the bentonite increased, the thickness of the diffuse double layers surrounding the clay particles decreased, such that transport of charged ions was less restrictive and the diffusive flux of Cl^- and K^+ increased. For example, for the specimen at S of 0.84, as C_{ave} increased from 9.9 mM to 25.0 mM KCl, the values of D^*_{clay,Cl^-} and D^*_{clay,K^+} increased from 1.7 x 10^{-10} m^2/s to 3.1 x 10^{-10} m^2/s and from 1.3 x 10^{-10} m^2/s to 3.1 x 10^{-10} m^2/s, respectively.

As shown in Figure 4.17, the trend of increasing D^*_{clay} and $D_{e,clay}$ with increasing C_{ave} and C_{ot} also is consistent with results reported in the literature for bentonite at high porosities (n > 0.7) (Lake and Rowe 2000; Malusis and Shackelford 2002; Dominijanni et al. 2013; Malusis et al. 2014). For example, Dominijanni et al. (2013) measured diffusion of NaCl in specimens of powdered Na-bentonite prepared at an n of 0.81. As C_{ave} in the specimen increased from 10.3 mM to 109 mM NaCl, values of D^* for Cl^- increased from 2.5 x 10^{-10} m^2/s to 4.6 x 10^{-10} m^2/s,.

Increasing values of D^*_{clay} and $D_{e,clay}$ with increasing C_{ave} also have been observed for highly-compacted bentonites. For example, Rosanne et al. (2003) measured diffusion of NaCl through compacted Na-montmorillonite specimens at different average concentrations of NaCl. For specimens compacted to a n of 0.40 (ρ_d = 1.89 Mg/m^3), the D_e values increased from 2.0 x 10^{-11} m^2/s to 2.7 x 10^{-11} m^2/s as C_{ave} increased from 10 mM to 15.7 mM NaCl.

4.5.2 Effect of saturation and volumetric water content

The effects of S and θ on the measured values of D^*_{clay} and $D_{e,clay}$ were less obvious than the effects associated with pore-water concentration. As shown in Figures 4.18 and 4.19, the values of D^*_{clay} and $D_{e,clay}$ only decreased slightly, if at all, as S decreased from 1.0 to 0.84 and θ decreased from 0.87 to 0.74. For example, during circulation of 30 mM KCl, as θ decreased from 0.87 to 0.74, the values of D^*_{clay,Cl^-} and $D_{e,clay,Cl^-}$ decreased from 3.1×10^{-11} m^2/s to 3.0×10^{-11} m^2/s and from 2.8×10^{-11} m^2/s to 2.2×10^{-11} m^2/s, respectively.

Previous studies have reported decreasing values of effective diffusion coefficients with decreasing θ for a variety of soils (e.g., Porter et al. 1960; Romkens and Bruce 1964; Rowell et al. 1967; Warncke and Barber 1972; Lim et al. 1998). To the author's knowledge, there is no data available in the literature for changes in diffusion coefficients with water content at such high values of θ (> 0.7) for bentonite. However, the general trends for the specimens with $\theta \geq 0.74$ appear consistent with those reported by Porter et al. (1960) for Pierre clay ($\theta \leq 0.40$) and Conca et al. (1993) for Kunigel bentonite ($\theta \leq 0.66$) (Figure 4.20). For example, as the θ of the Kunigel bentonite was decreased from 0.66 to 0.20, the value of $D_{e,clay,Cl^-}$ decreased from approximately 2×10^{-9} m^2/s to 4×10^{-10} m^2/s for source concentrations of 100 mM KCl or NaCl.

The values of D^*_{clay} and $D_{e,clay}$ measured for the specimen with the lowest water content ($\theta = 0.74$) were significantly lower (> 1 order of magnitude) than the values from the other experiments (Figures 4.19 and 4.20). This significant decrease in D^*_{clay} and $D_{e,clay}$ as θ decreased from 0.74 to 0.70 was unexpected, based on the trends from the literature shown in Figure 4.20b. However, there were no indications of error in the data or that the test conditions had been compromised. Regrettably, due to limitations of the test equipment, D^*_{clay} and $D_{e,clay}$ values for $\theta < 0.70$ could not be measured to confirm the low values obtained for the test with θ of 0.74.

Multiple theoretical and empirical models have been developed to predict diffusion coefficients of unsaturated soils (e.g., Millington and Quirk 1961; Papendick and Campbell 1980; Sadeghi et al. 1989; Mehta et al. 1995; Olesen et al. 1996; Revil and Jougnot 2008). The relationships developed by Millington and Quirk (1961) and Sadeghi et al. (1989) are simple expressions based only on the soil *n* and/or θ. Other models (e.g., Papendick and Campbell 1980; Mehta et al. 1995; Olesen et al. 1996; Revil and Jougnot 2008) require fitting parameters and/or additional physical and chemical properties (e.g., air-entry suction, Archie's exponents, reflection coefficients). While the latter set of models may allow for more accurate estimates of diffusion coefficients, a detailed evaluation of such models and determination of appropriate fitting parameters was beyond the scope of this study. The Millington and Quirk (1961) model is one of the most widely used methods (Hu and Wang 2003) and, therefore, was chosen as the method to compare predicted and measured values of D^*_{clay} for the bentonite specimens.

The Millington and Quirk (1961) model originally was developed for gas diffusion, and later was modified for aqueous-phase diffusion, as follows:

$$D_e = \frac{\theta^{10/3}}{n^2} D_o \tag{4.17}$$

or in terms of D^*:

$$D^* = \frac{\theta^{7/3}}{n^2} D_o \tag{4.18}$$

Note that the diffusion coefficient is independent of soil type (aside from porosity) and the pore-water chemistry. The values of D^* and D_e calculated for the bentonite specimens using the Millington and Quirk (1961) model (D^*_{MQ} and $D_{e,MQ}$ respectively) are summarized in Table 4.3.

For all of the specimens, the Millington and Quirk (1961) method over-predicted the diffusion coefficients, with the ratio of the predicted to measured values, D^*_{MQ}/D^*_{clay} (= $D_{e,MQ}/D_{e,clay}$), ranging from 3.9 to 189. Over prediction of diffusion coefficients with the Millington and Quirk (1961) model may be due, in part, to the lack of consideration for double-layer effects (e.g., membrane behavior). The existence of membrane behavior in bentonites results in decreased values of D^*, with D^* approaching zero as membrane efficiency (ω) approaches 100 % or complete solute restriction (Shackelford 2014). Membrane behavior generally decreases as the average pore-water concentration (C_{ave}) in the bentonite increases, due to suppression of the diffuse double layers (Shackelford 2014; Meier et al. 2014). As shown in Figure 4.21, as the C_{ave} increased, the agreement between D^*_{MQ} and D^*_{clay} improved (i.e., the ratio decreased). For example, for the specimen with S of 0.84, the value of D^*_{MQ} / D^*_{clay} decreased from 7.3 to 3.9 as C_{ave} increased from 9.7 mM to 25.0 mM. The improved agreement between the predicted and measured diffusion coefficients as C_{ave} increased lends further support to the explanation that the difference between the values is attributed, in part, to membrane behavior effects. The membrane behavior of the bentonite specimens and the effects on measured values of D^* are discussed in further detail in Chapter 5.

4.5.3 Electroneutrality effects

For all of the experiments, the values of D^*_{clay} for K^+ were lower than or equal to those for Cl^- (see Table 4.2). The differences between the values of D^*_{clay,Cl^-} and D^*_{clay,K^+} generally

decreased with increasing source concentration (C_{ot}) and average concentration in the specimen (C_{ave}). For example, for the specimen with S of 0.84, D^*_{clay,Cl^-} was 1.8 x 10^{-10} m^2/s and D^*_{clay,K^+} was 1.4 x 10^{-10} m^2/s during circulation of 20 mM KCl , whereas D^*_{clay,Cl^-} and D^*_{clay,K^+} were both 3.1 x 10^{-10} m^2/s during circulation with 50 mM KCl.

At steady-state diffusion, electroneutrality requires charge balance between the anions and the cations diffusing through the system. The major chemical species present in the test system were Cl^- and K^+ from the source KCl solution, as well as Na^+ initially present in the bentonite specimen. The charge of the anions and cations must be balanced, as follows (Shackelford and Lee 2003; Bohnhoff and Shackelford 2015):

$$J_{D,Cl^-}(-z_{Cl^-}) = J_{D,K^+}(z_{K^+}) + J_{D,Na^+}(z_{Na^+}) \tag{4.19}$$

where J_D is the molar flux of the ionic species and z represents the charges of Cl^-, K^+, and Na^+ (-1, +1, and +1, respectively).

At early test stages (e.g., 20 mM KCl), Na^+ diffuses out of the specimen toward the top and bottom boundaries, while Cl^- and K^+ diffuse from the top boundary to the bottom boundary (see Figure 4.22). Over time, the Na^+ concentration in the test system decreases to negligible values (e.g., < 0.1 mM by the 50 mM stage). Confirmation of Na^+ initially in the test system and the subsequent decrease in Na^+ to negligible concentration values were presented in Section 4.4. The initial Na^+ concentration in the bentonite specimen, prior to being placed in the test cell, is assumed to be uniform, as shown in Figure 4.22. During early test stages flux of Na^+ toward the bottom boundary will result in the flux of K^+ being less than that of Cl^- ($J_{D,K^+} < J_{D,Cl^-}$), per Equation 4.19, and thus, $D^*_{clay,K^+} < D^*_{clay,Cl^-}$.

The ratios of chloride-to-potassium D^*_{clay} (= D^*_{clay,Cl^-} / D^*_{clay,K^+}) values are provided in Table 4.2. The maximum values of D^*_{clay,Cl^-} / D^*_{clay,K^+} occurred at early test stages (low C_{ave}), and the values decreased towards unity as C_{ave} increased. As shown in Figure 4.23, similar trends were observed by Malusis and Shackelford (2002). For example, for diffusion experiments on flushed GCLs Malusis and Shackelford (2002) reported values of D^*_{clay,Cl^-} / D^*_{clay,K^+} decreased from 1.61 to 1.18 as C_{ave} increased from 2.0 mM to 23.5 mM KCl.

4.6 Conclusions

A method was developed for measuring the diffusion of salts through unsaturated clays. The method was based on the through-diffusion technique, whereby different concentrations of diffusing solutes are maintained essentially constant at the boundaries of the specimen over sufficiently long periods so as to allow for the establishment of steady-state diffusion. Use of the described closed-system apparatus may provide several advantages for experimental evaluation of diffusion in unsaturated clays, such as:

- establishment of linear concentration profiles at steady-state diffusion, allowing for simpler diffusion analyses relative to open systems;
- ability to control and maintain constant values of matric suction, S and θ in the specimen throughout testing;
- constant circulation of solution that would remove air that, potentially, could collect at the boundaries after diffusing through the high air-entry disks (although diffusion of air through the HAE disks over the suction ranges evaluated in this research was considered negligible);

- capability to perform multistage (i.e., multiple concentration) diffusion tests to evaluate the effects of C_{ave} on values of D^*; and
- ability to concurrently measure membrane behavior (anion exclusion).

The apparatus and test method were evaluated by measuring the diffusion of KCl through Na-bentonite specimens at values of S ranging from 0.79 to 1.0. For all of the bentonite specimens and source KCl concentrations, the steady-state values of D^*_{clay} fell within the range of 2.1×10^{-12} m^2/s to 4.1×10^{-10} m^2/s, which was consistent with expectations based on available data in the literature. However, to the author's knowledge, there is little to no previously published data for measured values of diffusion coefficients of unsaturated bentonite at high porosities similar to those of a GCL (e.g., $n > 0.7$).

The values of D^*_{clay} for both Cl^- and K^+ tended to increase with increasing average concentration in the specimen, which was consistent with trends reported in the literature and could be explained on the basis of classical DDL theory. The effects of S and θ on the measured values of D^*_{clay} were less obvious, which may have been due to the limited range of S that could be evaluated in the research. Compared to the measured values of D^*_{clay}, the Millington and Quirk (1961) method over-predicted the diffusion coefficients, with the ratio of the predicted to measured values ranging from 3.9 to 189. Over-prediction of D^*_{clay} with the Millington and Quirk (1961) model may have been due, in part, to the lack of consideration for double-layer effects (e.g., membrane behavior). Finally, for all of the experiments, the values of D^*_{clay} for K^+ were lower than or equal to those for Cl^-, due to Na^+ initially present in the specimen.

Table 4.1. Test program for measurement of diffusion in sodium bentonite.

Properties of Bentonite Specimen				Test Duration (d)				
				Stage				Total
Degree of Saturation, *S*	Volumetric Water Content, θ	Porosity, *n*	Thickness, *L* (mm)	DIW	20 mM KCl	30 mM KCl	50 mM KCl	
1.0	0.87	0.87	6.6	29	122	108	76	335
0.89	0.79	0.89	5.7	24	74	74, 44[a]	64[a]	280
0.84	0.74	0.88	7.7	24	104, 34[a]	90[a]	72[a]	324
0.79	0.70	0.88	8.3	24	158, 50[a]	88[a]	NA	320

[a]Solution includes 500 ppm DOWICIL biocide.

Table 4.2. Results of through-diffusion analyses for sodium-bentonite specimens between high air-entry disks.

Properties of Clay Specimen	KCl C_{ot}		C_{ave,Cl^-} (mM)	Ion	Steady-State Diffusion Results			
	Target (mM)	Actual (mM)			$J_{D,ss} = \Delta Q_t/\Delta t$ (mg/d-m^2)	D^*_{clay} (m^2/s)	$D_{e,clay} = \theta D^*_{clay}$ (m^2/s)	$D^*_{clay,Cl^-}/D^*_{clay,K^+}$
S = 1 t = 6.6 mm n = 0.87 θ = 0.87	20	19	9.0	K^+	180	9.3 x 10^{-11}	8.1 x 10^{-11}	1.90
				Cl^-	172	1.8 x 10^{-10}	1.5 x 10^{-10}	
	30	30	15.0	K^+	325	1.9 x 10^{-10}	1.6 x 10^{-10}	1.68
				Cl^-	310	3.1 x 10^{-10}	2.8 x 10^{-10}	
	50	49	25.0	K^+	552	2.9 x 10^{-10}	2.5 x 10^{-10}	1.43
				Cl^-	502	4.1 x 10^{-10}	3.6 x 10^{-10}	
S = 0.89 t = 5.7 mm n = 0.89 θ = 0.79	20	21	10.5	K^+	179	6.0 x 10^{-11}	4.8 x 10^{-11}	3.04
				Cl^-	203	1.8 x 10^{-10}	1.5 x 10^{-10}	
	30	33	15.0	K^+	161	2.0 x 10^{-11}	1.6 x 10^{-11}	2.40
				Cl^-	216	4.8 x 10^{-11}	3.8 x 10^{-11}	
	30*	33*	16.5	K^+	232	3.4 x 10^{-11}	2.7 x 10^{-11}	9.95
				Cl^-	342	3.4 x 10^{-10}	2.7 x 10^{-10}	
	50*	51*	25.6	K^+	544	1.7 x 10^{-10}	1.3 x 10^{-10}	2.04
				Cl^-	525	3.4 x 10^{-10}	2.7 x 10^{-10}	
S = 0.84 t = 7.7 mm n = 0.88 θ = 0.74	20	20	9.7	K^+	155	1.3 x 10^{-10}	9.7 x 10^{-11}	1.29
				Cl^-	145	1.7 x 10^{-10}	1.3 x 10^{-10}	
	20*	20*	9.7	K^+	156	1.4 x 10^{-10}	1.0 x 10^{-10}	1.30
				Cl^-	146	1.8 x 10^{-10}	1.3 x 10^{-10}	
	30*	33*	16.5	K^+	282	2.4 x 10^{-10}	1.8 x 10^{-10}	1.28
				Cl^-	261	3.0 x 10^{-10}	2.2 x 10^{-10}	
	50*	50*	25.0	K^+	442	3.1 x 10^{-10}	2.3 x 10^{-10}	1.00
				Cl^-	398	3.1 x 10^{-10}	2.3 x 10^{-10}	
S = 0.79 t = 8.3 mm n = 0.88 θ = 0.70	20	20	9.9	K^+	11	2.1 x 10^{-12}	1.5 x 10^{-12}	1.11
				Cl^-	11	2.3 x 10^{-12}	1.6 x 10^{-12}	
	20*	20*	9.9	K^+	21	4.2 x 10^{-12}	2.9 x 10^{-12}	1.37
				Cl^-	25	5.7 x 10^{-12}	4.0 x 10^{-12}	
	30*	31*	15.2	K^+	44	6.0 x 10^{-12}	4.2 x 10^{-12}	1.06
				Cl^-	42	6.4 x 10^{-12}	4.4 x 10^{-12}	

Notes:

* Includes biocide.

Shaded = Results are questionable due to suspected bio-activity.

S = degree of water saturation; n = porosity; t = thickness; θ = volumetric water content.

C_{ot} = influent solute concentration at the top boundary of the top HAE disk.

C_{ave,Cl^-} = average Cl^- concentration in the specimen at steady-state diffusion.

$\Delta Q_t/\Delta t = J_{D,ss}$ = steady-state flux of solute determined from linear regression of steady-state data.

D^*_{clay} = effective diffusion coefficient of the clay specimen.

$D_{e,clay}$ = effective diffusion coefficient of the clay specimen = θD^*_{clay}.

Table 4.3. Comparison of diffusion coefficients for sodium-bentonite specimens calculated with through-diffusion analyses and Millington and Quirk (1961) model.

Properties of Clay Specimen	C_{ave} (mM)	$D_{o,KCl}$ (m^2/s)[a]	Through-diffusion		Millington & Quirk (1961)		$D^*_{MQ}/D^*_{clay,Cl^-}$
			D^*_{clay,Cl^-} (m^2/s)	$D_{e,clay,Cl^-}$ (m^2/s)	D^*_{MQ} (m^2/s)	$D_{e,MQ}$ (m^2/s)	
S = 1 n = 0.87 θ = 0.87	9.0	1.93×10^{-9}	1.8×10^{-10}	1.5×10^{-10}	1.9×10^{-9}	1.6×10^{-9}	10.5
	15	1.92×10^{-9}	3.2×10^{-10}	2.8×10^{-10}	1.8×10^{-9}	1.6×10^{-9}	5.8
	25.0	1.90×10^{-9}	4.1×10^{-10}	3.6×10^{-10}	1.8×10^{-9}	1.6×10^{-9}	4.4
S = 0.89 n = 0.89 θ = 0.79	10.5	1.93×10^{-9}	1.8×10^{-10}	1.5×10^{-10}	1.4×10^{-9}	1.1×10^{-9}	7.6
	16.5	1.92×10^{-9}	3.4×10^{-10}	2.7×10^{-10}	1.4×10^{-9}	1.1×10^{-9}	4.1
	25.6	1.90×10^{-9}	3.4×10^{-10}	2.7×10^{-10}	1.4×10^{-9}	1.1×10^{-9}	4.1
S = 0.84 n = 0.88 θ = 0.74	9.7	1.93×10^{-9}	1.7×10^{-10}	1.3×10^{-10}	1.2×10^{-9}	9.1×10^{-10}	7.3
	9.7	1.93×10^{-9}	1.8×10^{-10}	1.3×10^{-10}	1.2×10^{-9}	9.1×10^{-10}	6.9
	16.5	1.92×10^{-9}	3.0×10^{-10}	2.2×10^{-10}	1.2×10^{-9}	9.1×10^{-10}	4.0
	25.0	1.90×10^{-9}	3.1×10^{-10}	2.3×10^{-10}	1.2×10^{-9}	9.0×10^{-10}	3.9
S = 0.79 n = 0.88 θ = 0.70	9.9	1.93×10^{-9}	5.7×10^{-12}	4.0×10^{-12}	1.1×10^{-9}	7.6×10^{-10}	189
	15.2	1.92×10^{-9}	6.4×10^{-12}	4.4×10^{-12}	1.1×10^{-9}	7.5×10^{-10}	169

Notes:
[a] See Appendix D.
Shaded data in Table 4.2 has been omitted.

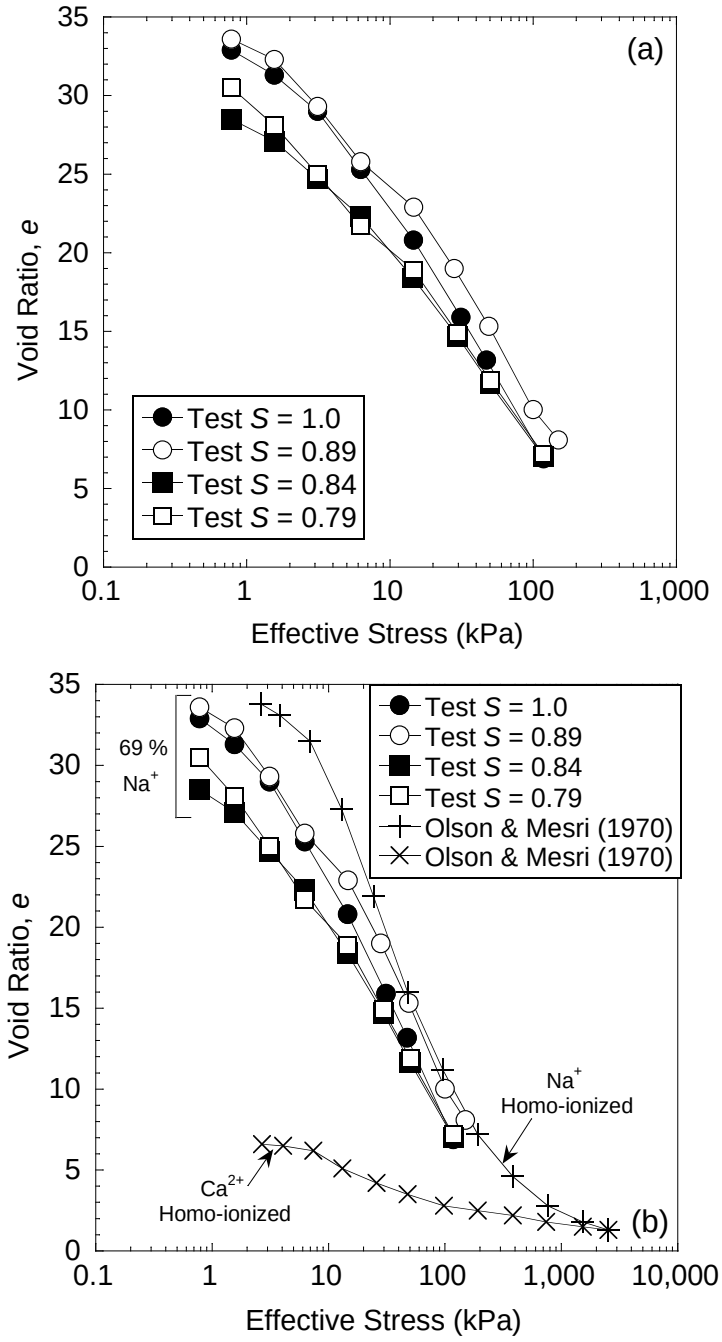

Figure 4.1. Measured void ratio as a function of effective stress during consolidation of bentonite paste: (a) bentonite specimens for diffusion and membrane behavior testing; (b) comparison with Olson and Mesri (1970) for homo-ionized clay specimens.

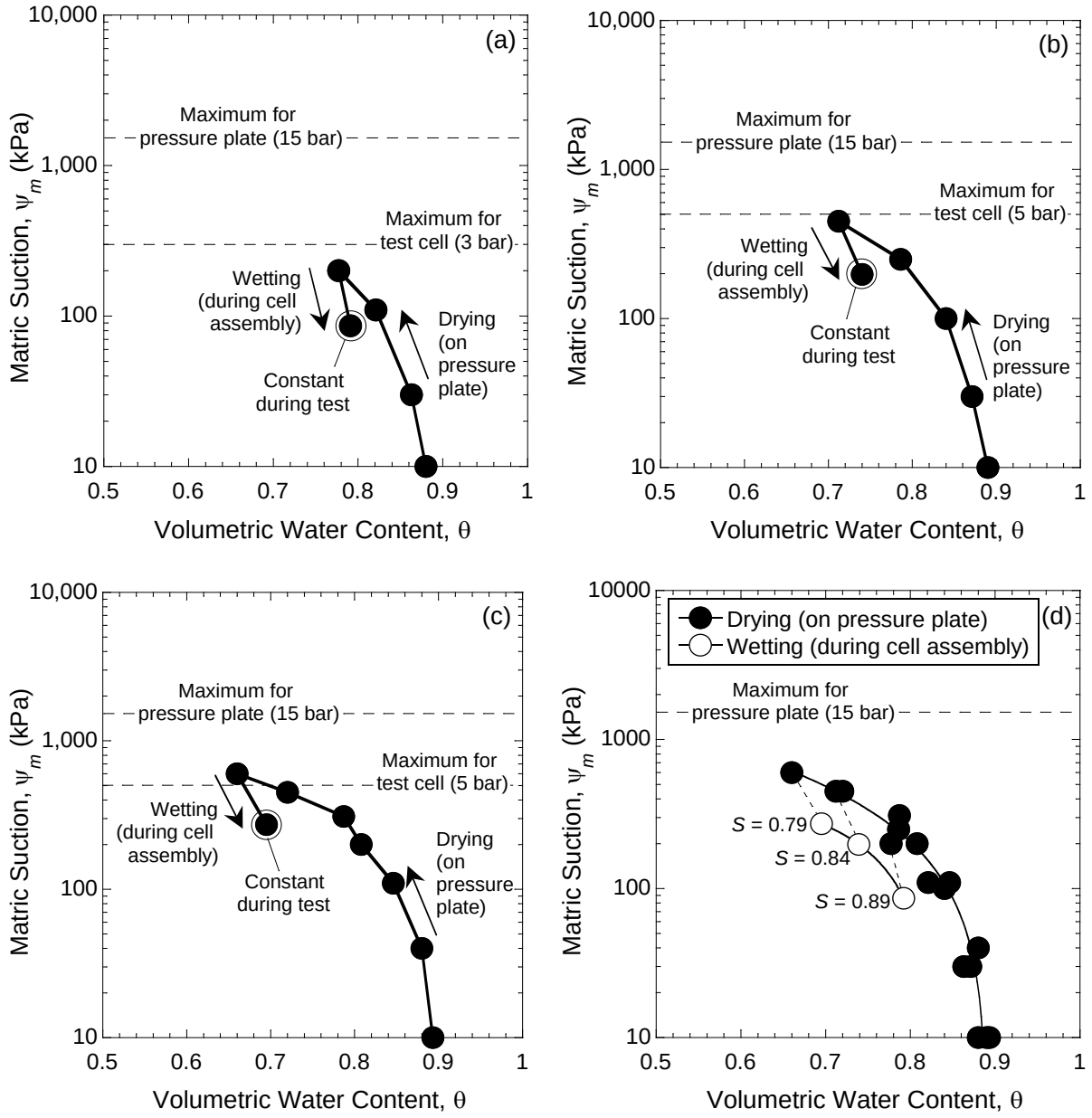

Figure 4.2. Matric suctions measured during preparation of unsaturated, sodium-bentonite specimens for diffusion and membrane behavior tests performed at constant degrees of saturation, *S*: (a) *S* = 0.89 (b) *S* = 0.84; (c) *S* = 0.79; (d) combined data from (a), (b), and (c).

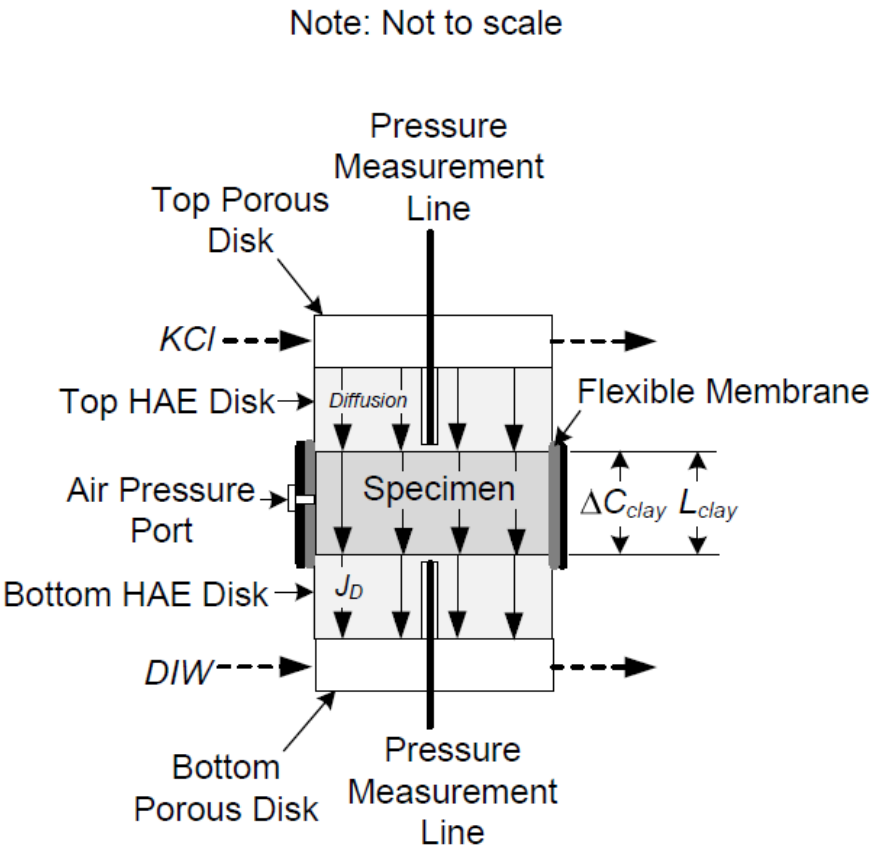

Figure 4.3. Schematic of diffusion through the rigid-wall cell used to measure coupled diffusion and membrane behavior of unsaturated, bentonite specimens (J_D = diffusive flux across the layer, ΔC_{clay} = concentration difference across the clay specimen, L_{clay} = length of clay specimen).

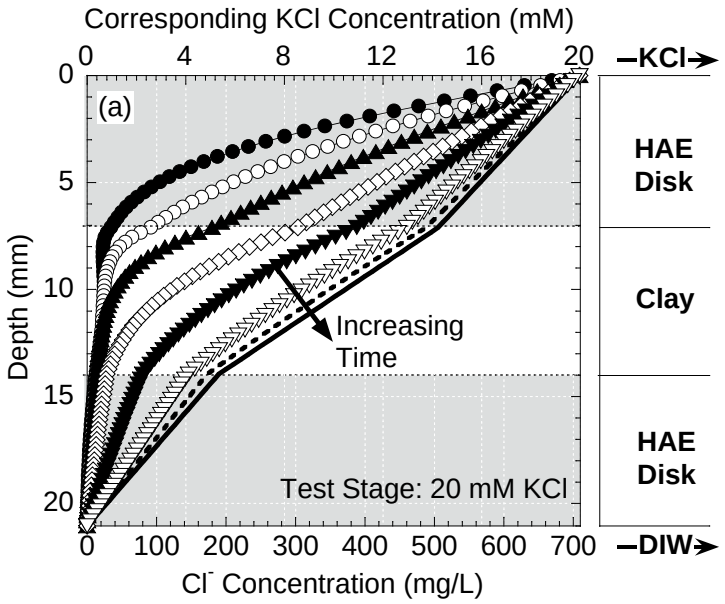

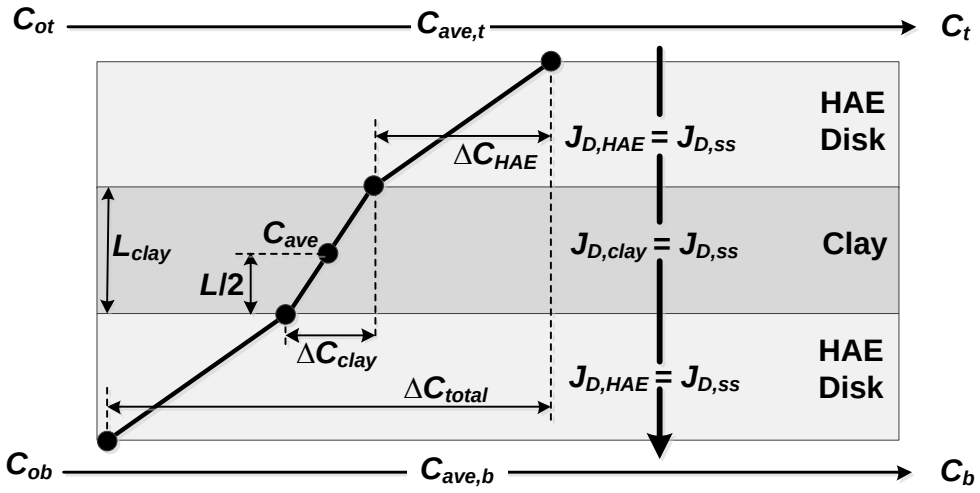

(b)

Notes:
n = porosity of the layer
D^* = effective diffusion coefficient of layer for solute
$J_{D,ss}$ = steady-state flux of solute across the layer (equal for all layers)
ΔC_{HAE} = solute concentration difference across the HAE disk
ΔC_{clay} = solute concentration difference across the specimen
C_{ave} = average solute concentration in the specimen
$C_{ave,t}$ = average solute concentration across the upper boundary of the top HAE disk
C_{ot} = influent solute concentration at the upper boundary of the top HAE disk
C_t = effluent solute concentration at the upper boundary of the top HAE disk
$C_{ave,b}$ = average solute concentration across the lower boundary of the top HAE disk
C_{ob} = influent solute concentration at the lower boundary of the bottom HAE disk (=0)
C_b = effluent solute concentration at the lower boundary of the bottom HAE disk (>0)

Figure 4.4. Schematic representations of (a) development of concentration profile across the test system with time, and (b) linear concentration profile and constant flux at steady-state diffusion conditions.

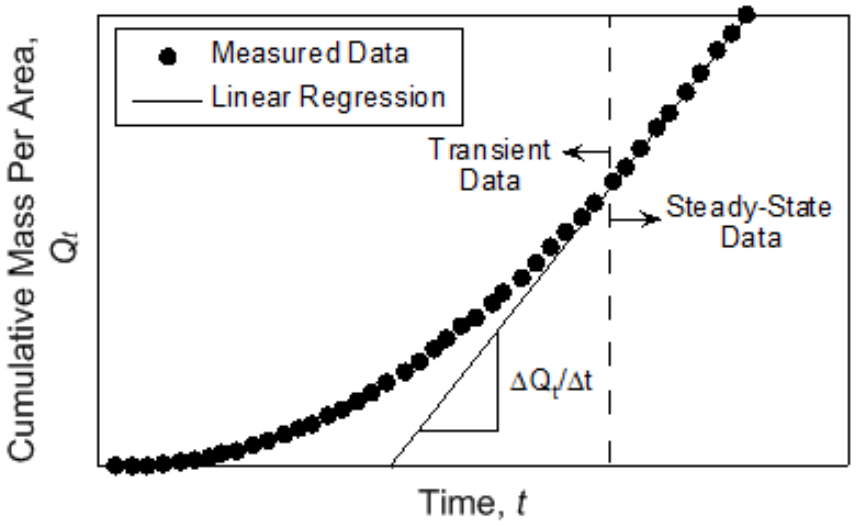

Figure 4.5. Schematic illustration of cumulative mass method for analysis of through-diffusion test data (adapted from Shackelford 2013).

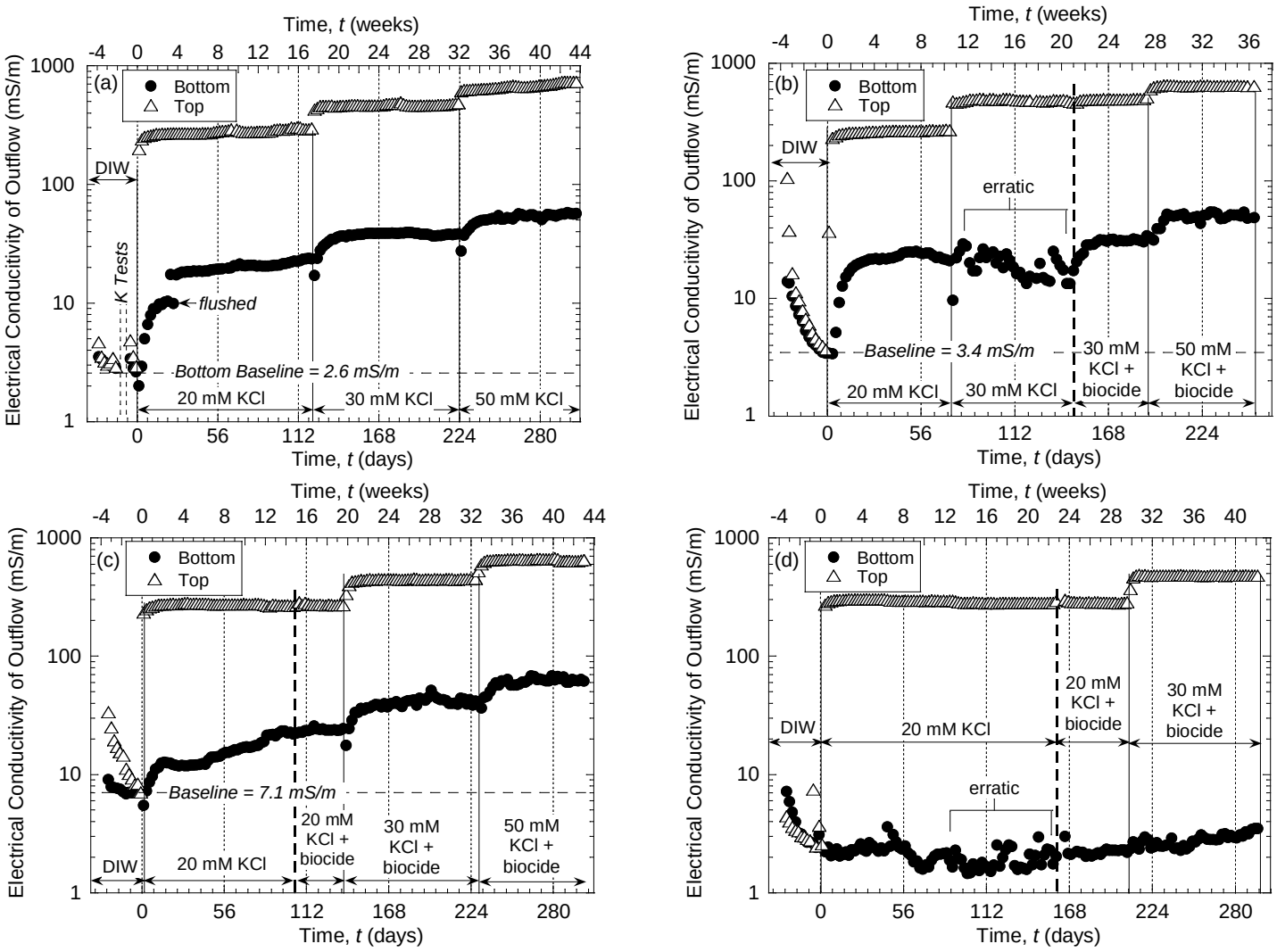

Figure 4.6. Measured electrical conductivity of the top and bottom outflows during diffusion testing of sodium bentonite: (a) S = 1.0; (b) S = 0.89; (c) S = 0.84; (d) S = 0.79.

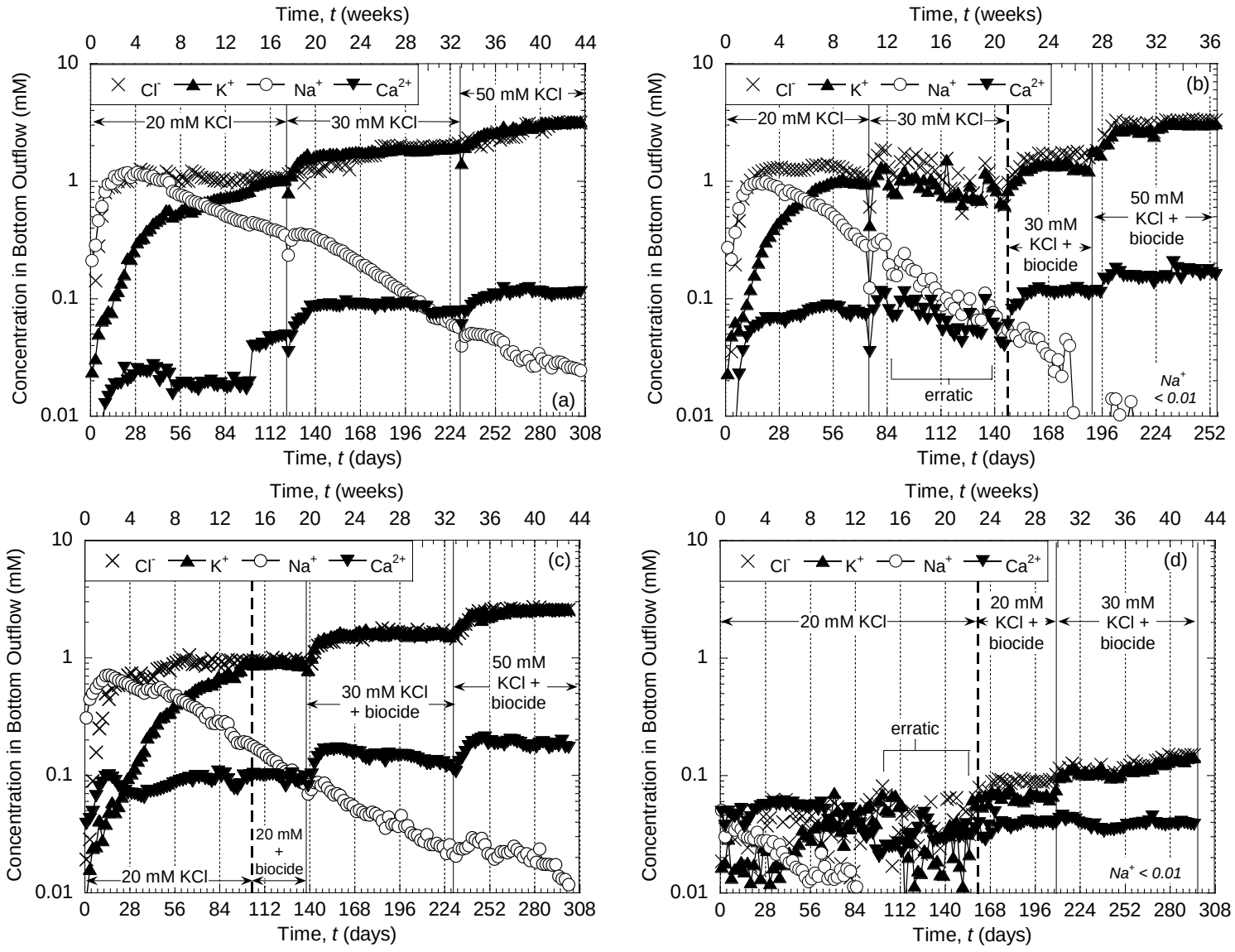

Figure 4.7. Bottom outflow concentrations as a function of time: (a) S = 1.0; (b) S = 0.89; (c) S = 0.84; (d) S = 0.79.

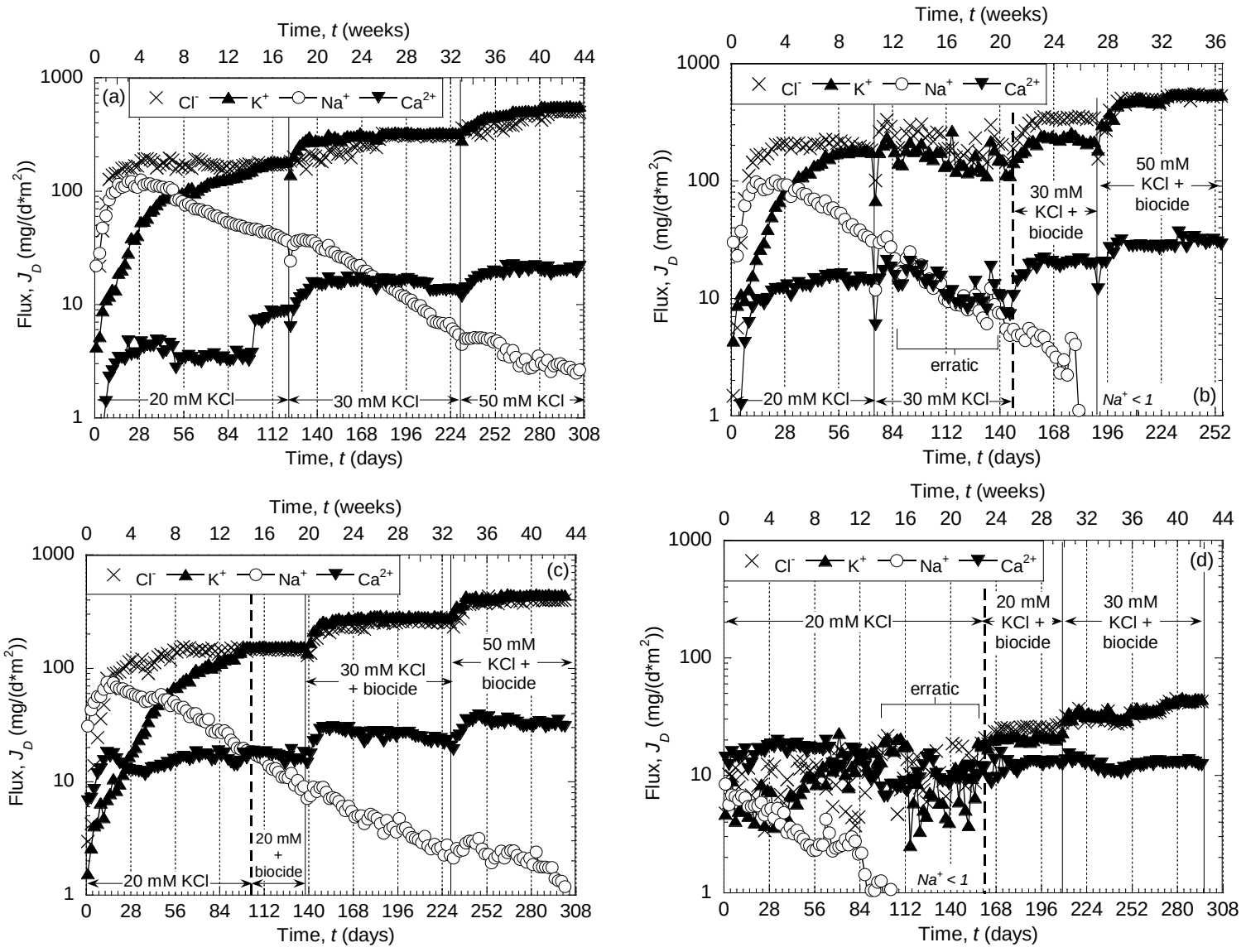

Figure 4.8. Solute flux through the bottom boundary of Na-bentonite specimens: (a) S = 1.0; (b) S = 0.89; (c) S = 0.84; (d) S = 0.79.

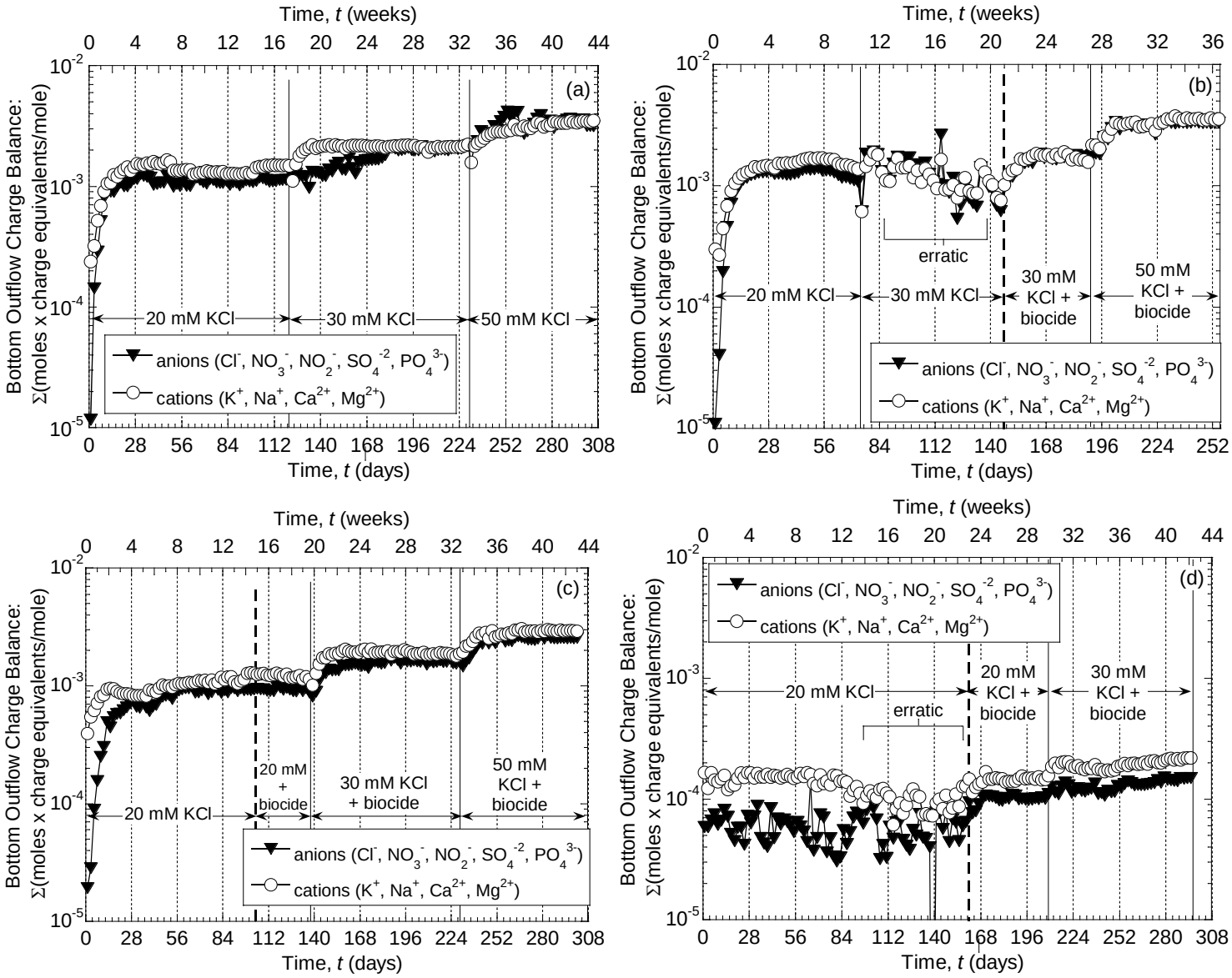

Figure 4.9. Charge balance for bottom outflow for Na-bentonite specimens: (a) S = 1.0; (b) S = 0.89; (c) S = 0.84; (d) S = 0.79.

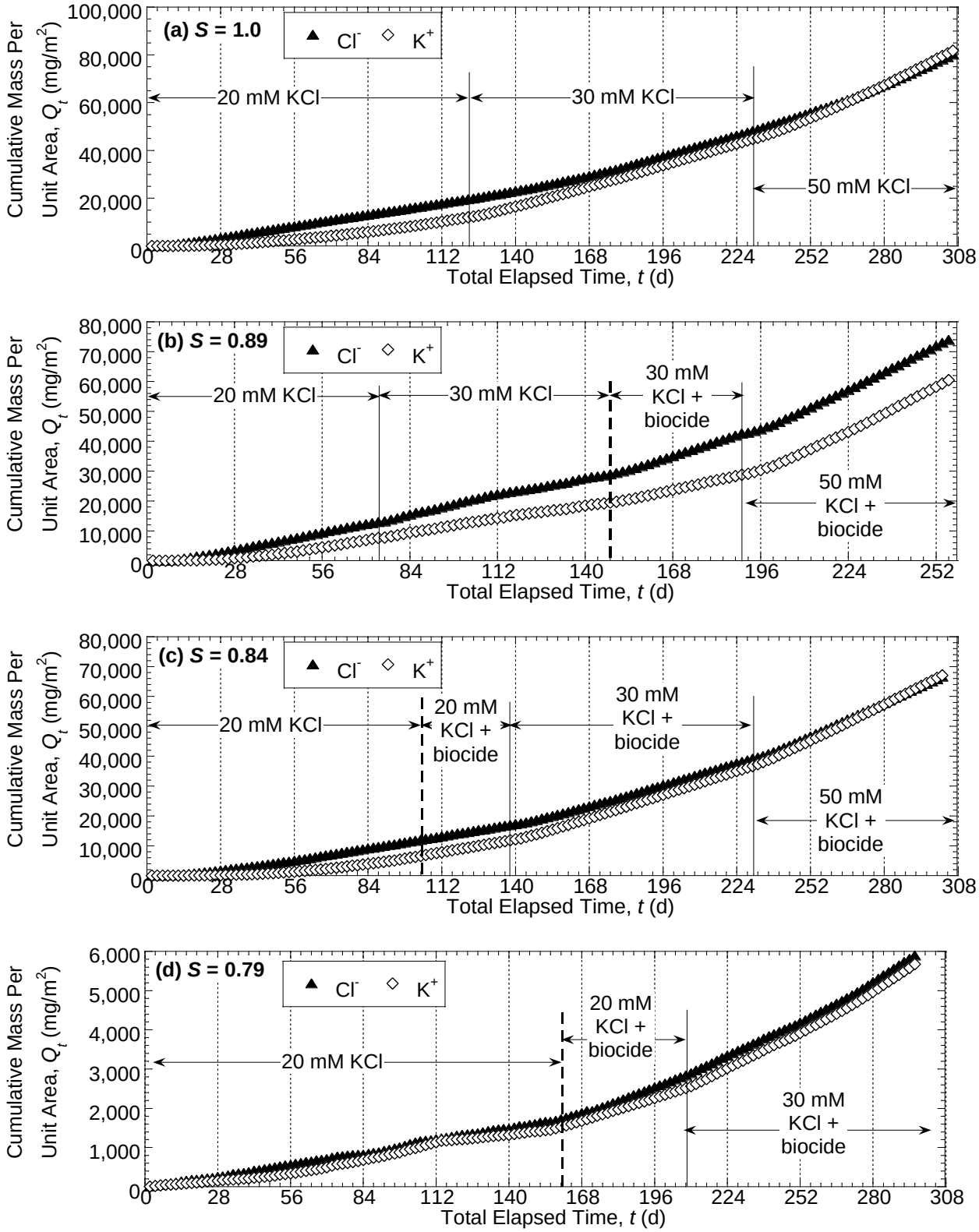

Figure 4.10. Diffusion results for multistage diffusion experiments on sodium-bentonite specimens.

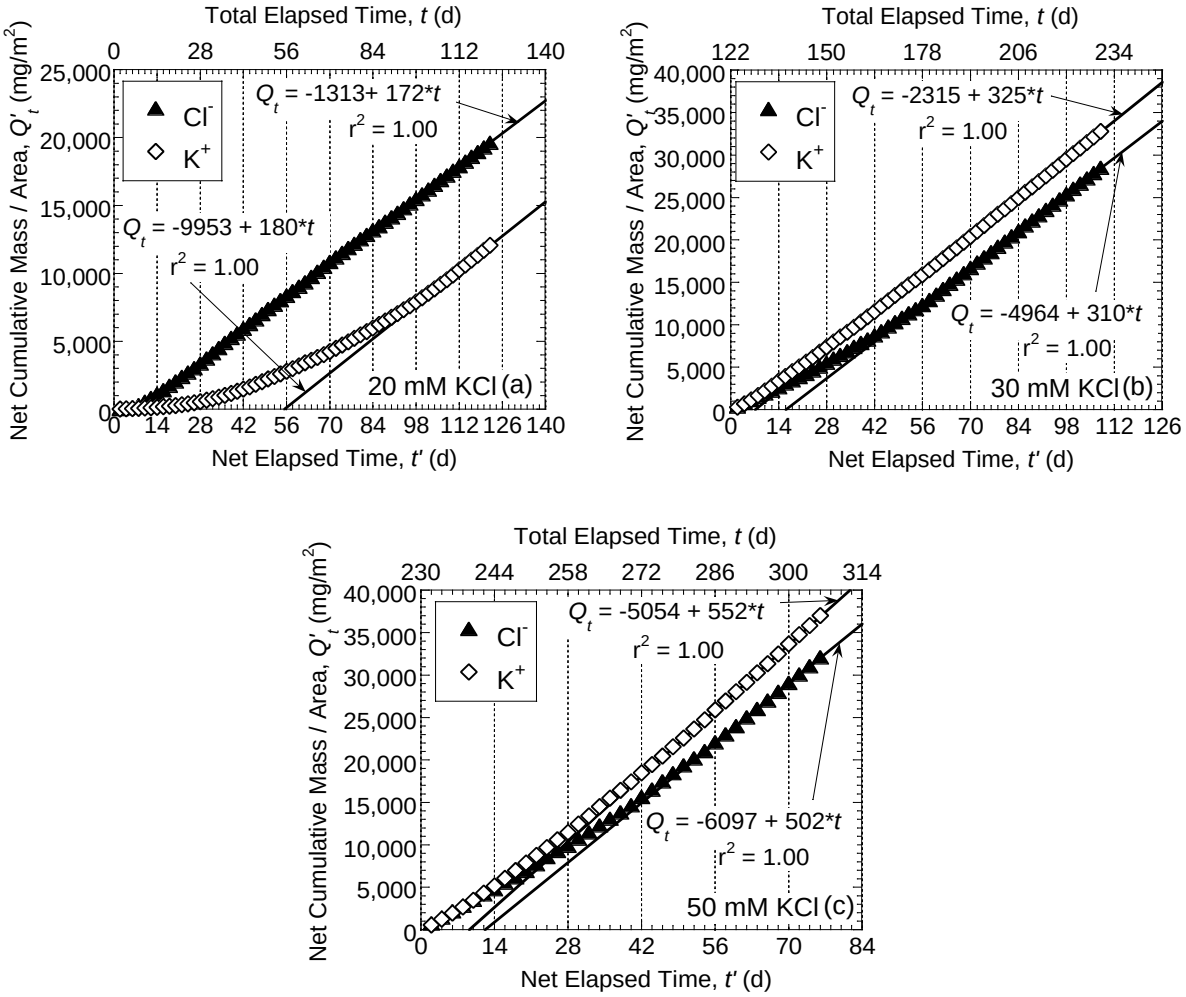

Figure 4.11. Diffusion results for each concentration stage for sodium bentonite with S = 1.0. Trendlines shown are linear-regressions of data at steady-state diffusion.

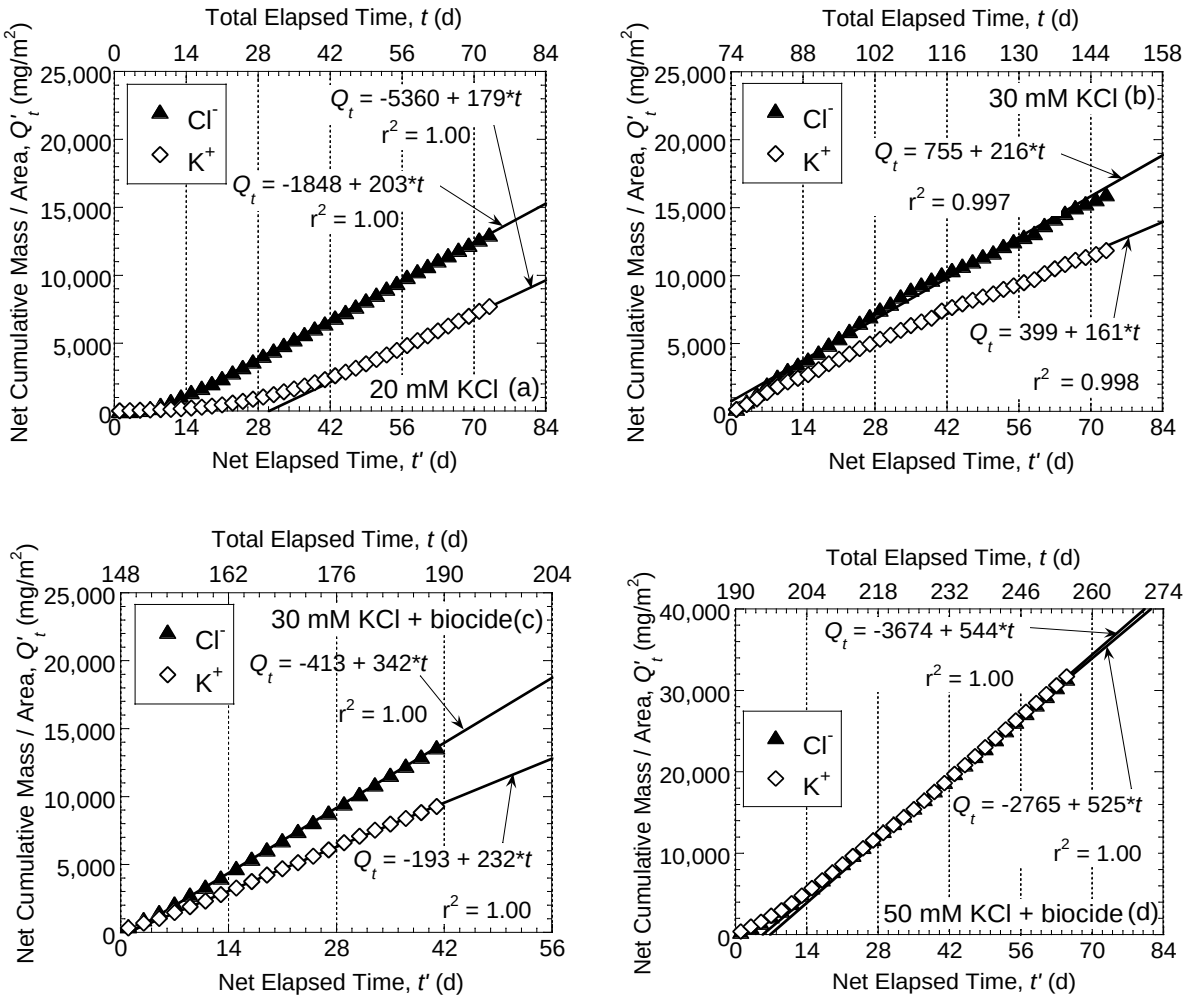

Figure 4.12. Diffusion results for each concentration stage for sodium bentonite with S = 0.89. Trendlines shown are linear-regressions of data at steady-state diffusion.

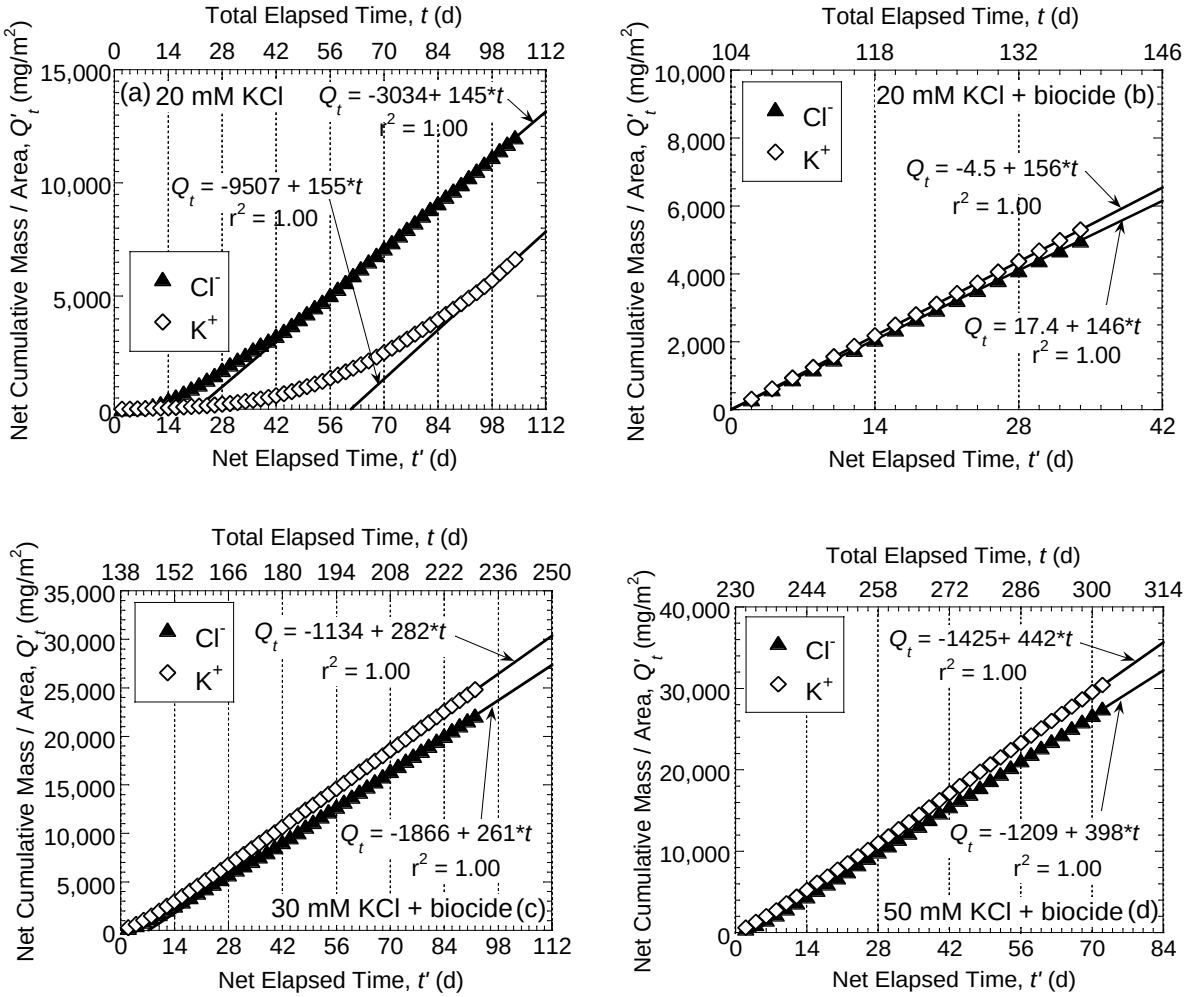

Figure 4.13. Diffusion results for each concentration stage for sodium bentonite with S = 0.84. Trendlines shown are linear-regressions of data at steady-state diffusion.

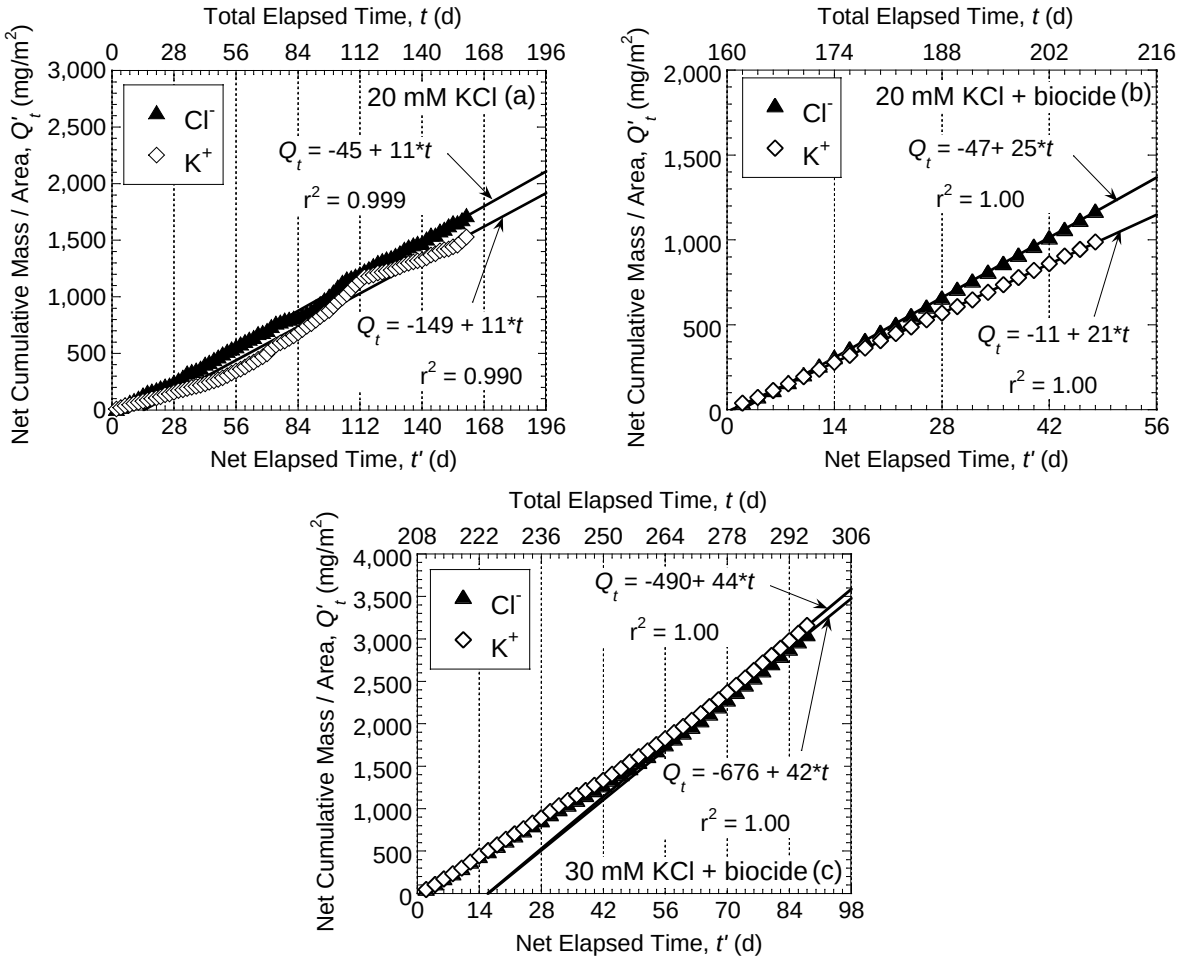

Figure 4.14. Diffusion results for each concentration stage for sodium bentonite with S = 0.79. Trendlines shown are linear-regressions of data at steady-state diffusion.

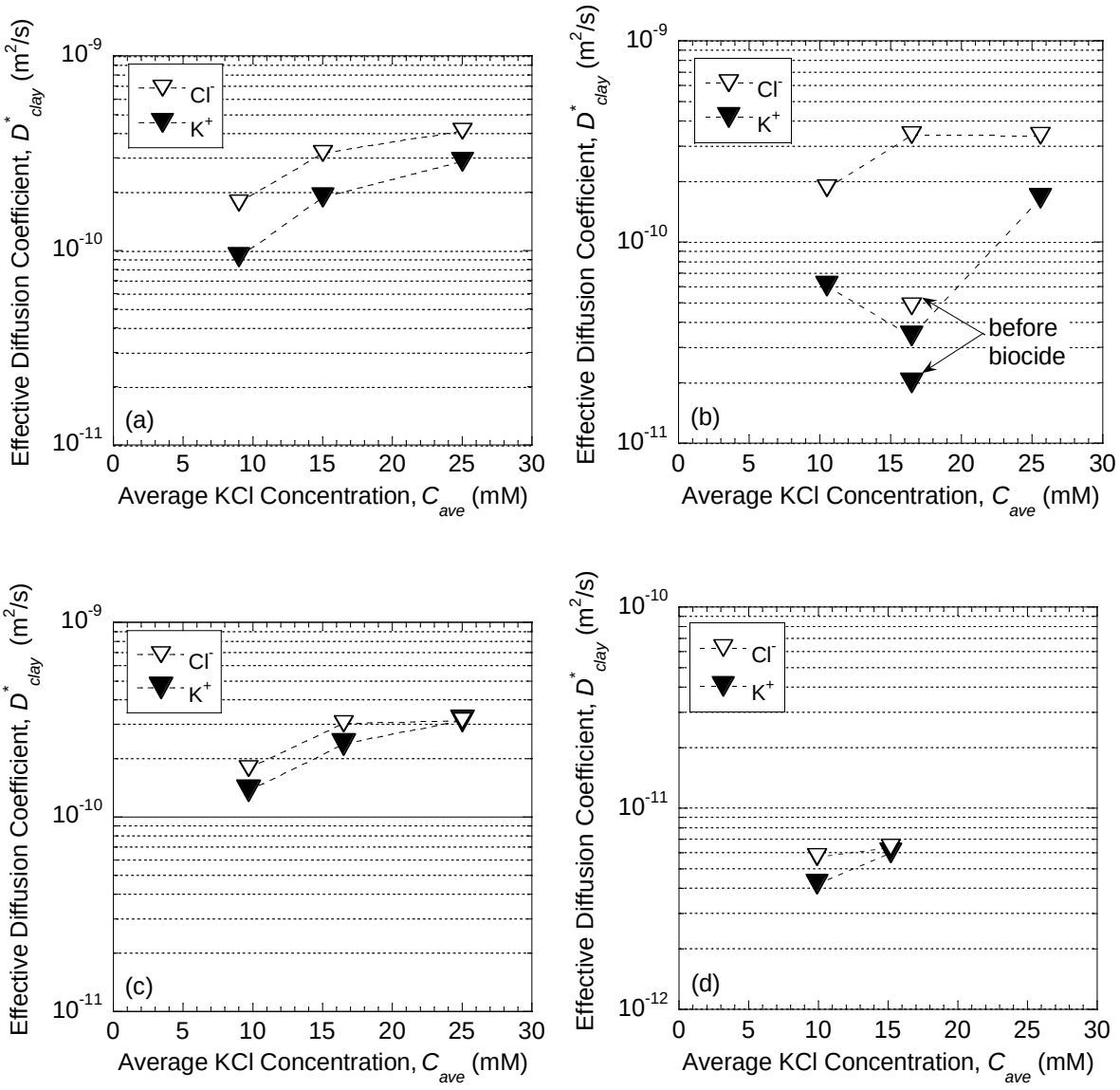

Figure 4.15. Effective diffusion coefficients of sodium bentonite (D^*_{clay}) versus average concentration in the specimen for: (a) S = 1.0; (b) S = 0.89; (c) S = 0.84; (d) S = 0.79.

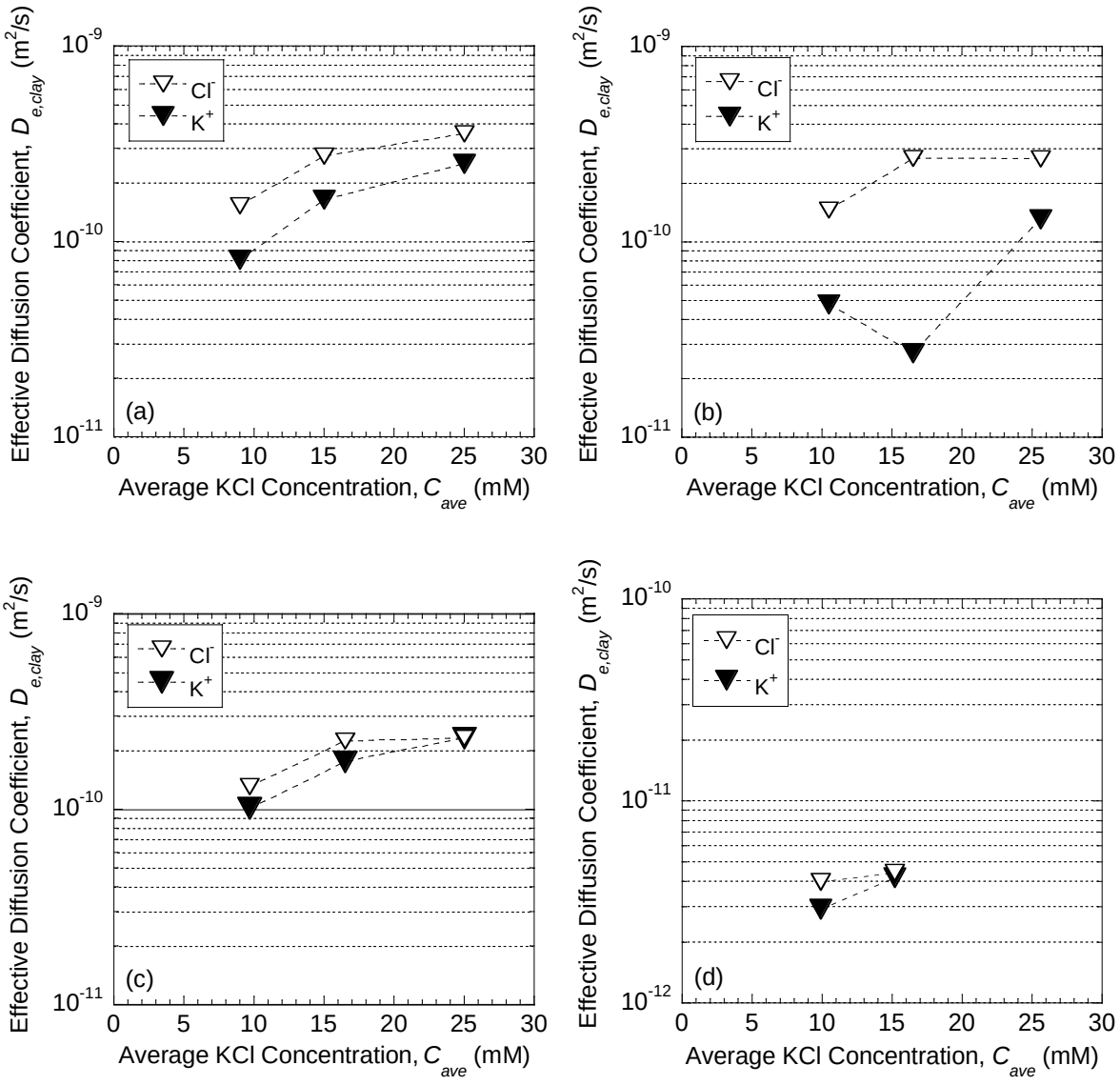

Figure 4.16. Effective diffusion coefficients of sodium bentonite ($D_{e,clay}$) versus average concentration in the specimen: (a) S = 1.0; (b) S = 0.89; (c) S = 0.84; (d) S = 0.79.

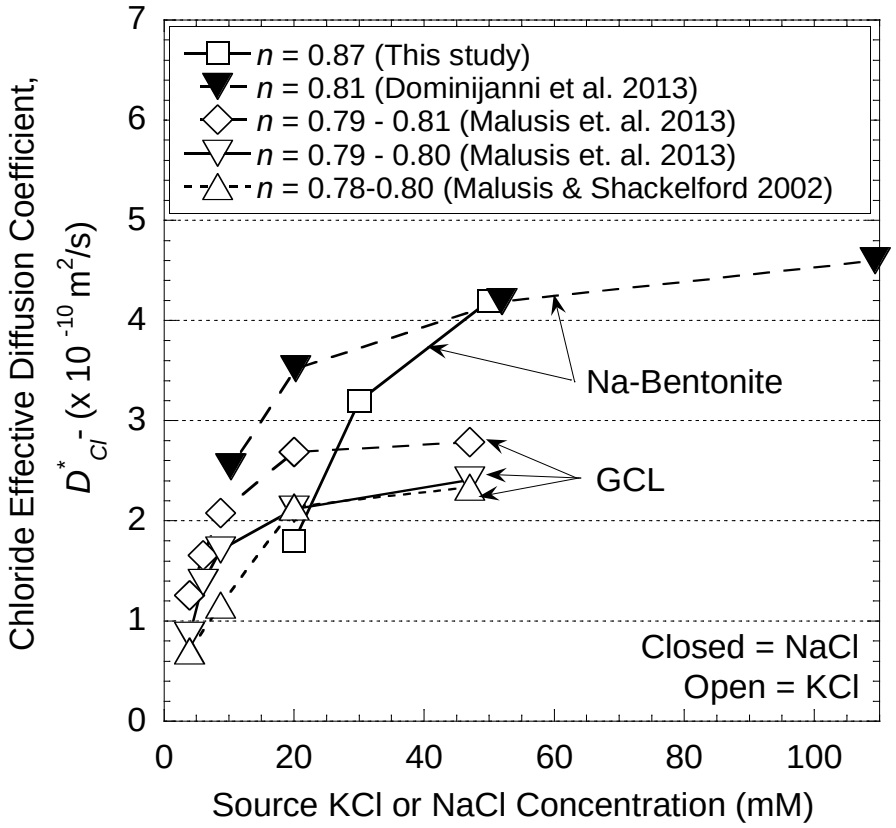

Figure 4.17. Chloride effective diffusion coefficients (D^*) for potassium chloride or sodium chloride source concentrations for saturated bentonite specimens. All values of D^* from the literature were determined using steady-state linear regressions.

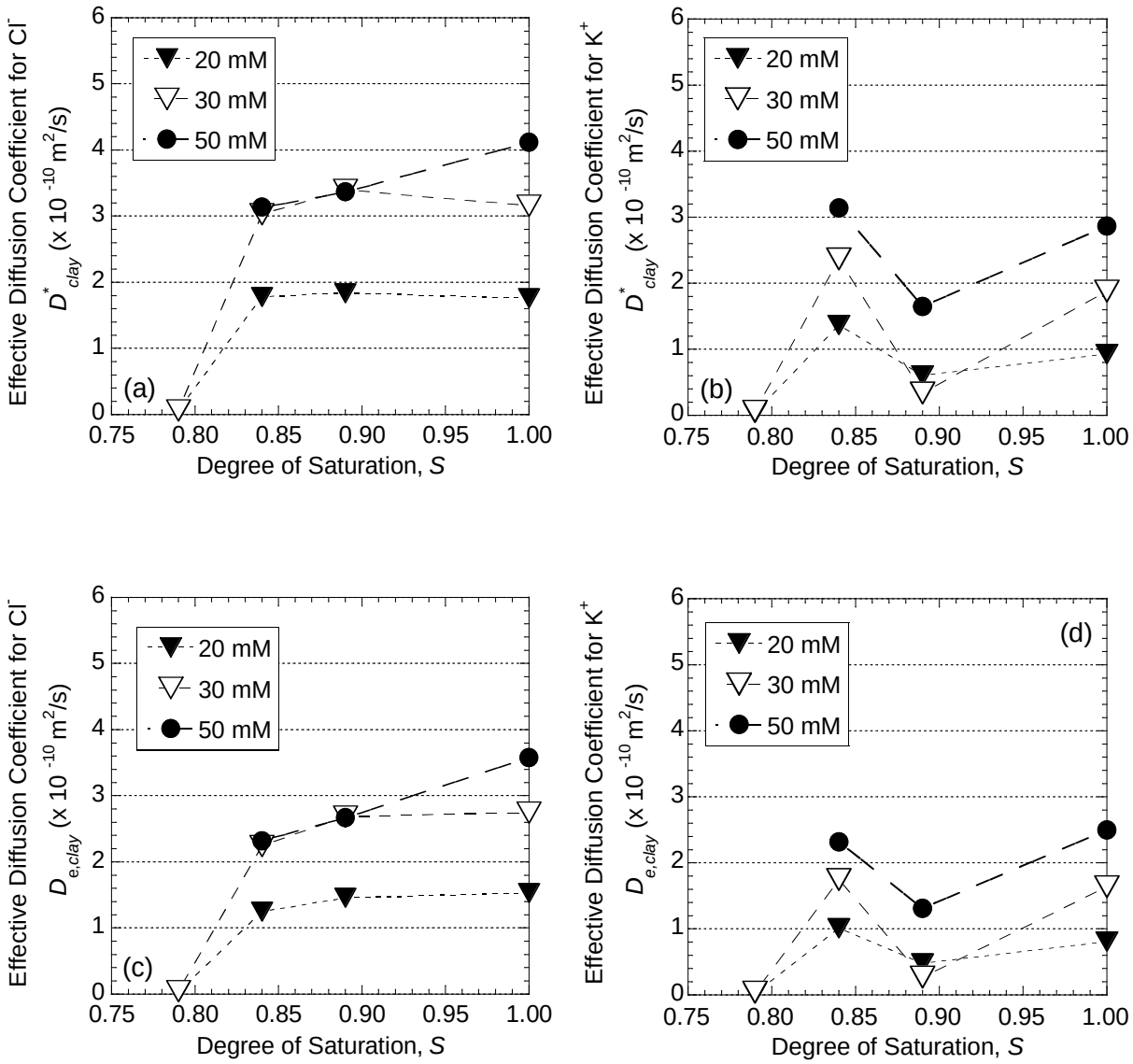

Figure 4.18. Effective diffusion coefficients of sodium bentonite versus degree of saturation: (a) D^*_{clay} for Cl^-; (b) D^*_{clay} for K^+; (c) $D_{e,clay}$ for Cl^-; (d) $D_{e,clay}$ for K^+.

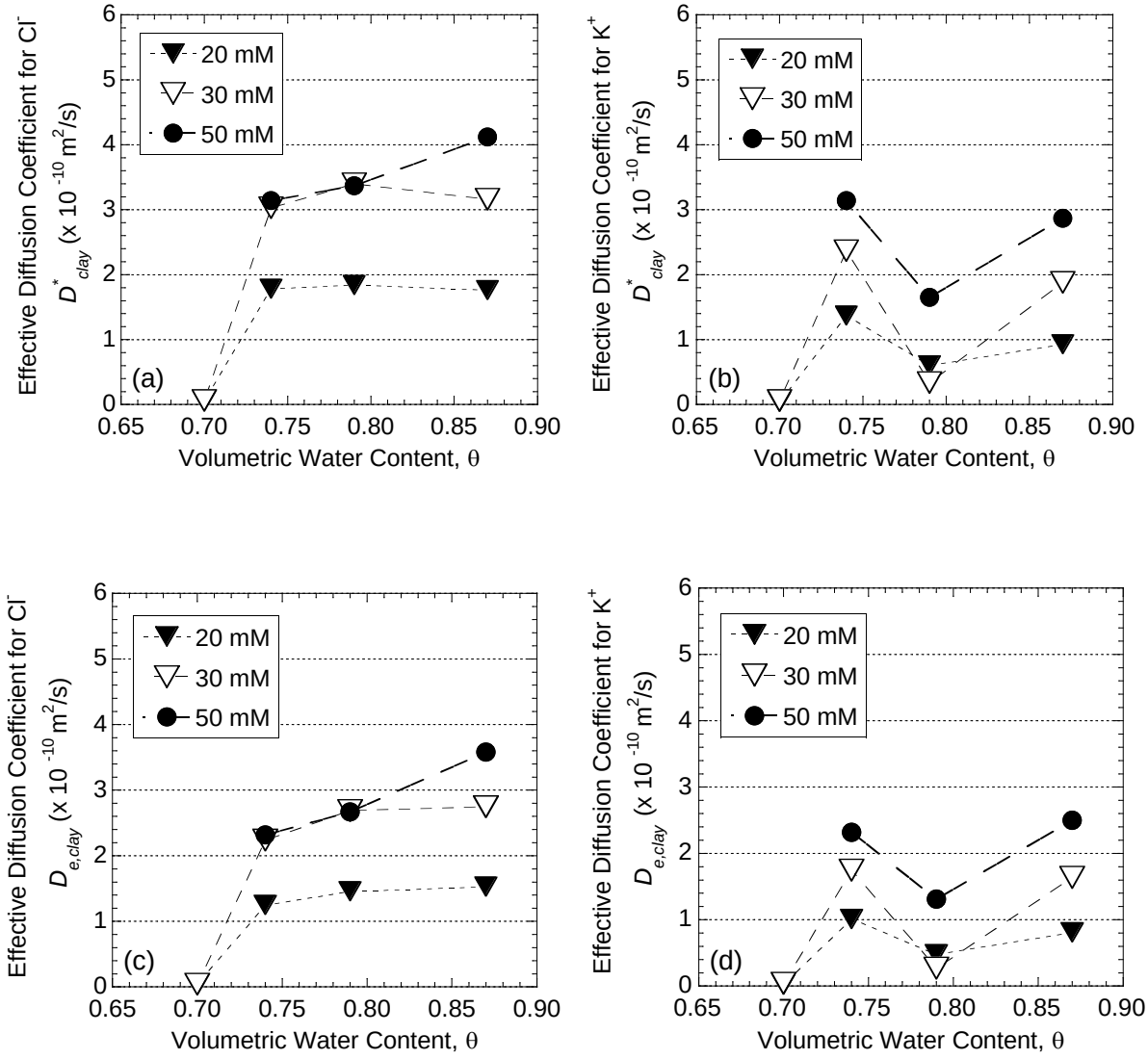

Figure 4.19. Effective diffusion coefficients of sodium bentonite versus volumetric water content: (a) D^*_{clay} for Cl^-; (b) D^*_{clay} for K^+; (c) $D_{e,clay}$ for Cl^-; (d) $D_{e,clay}$ for K^+.

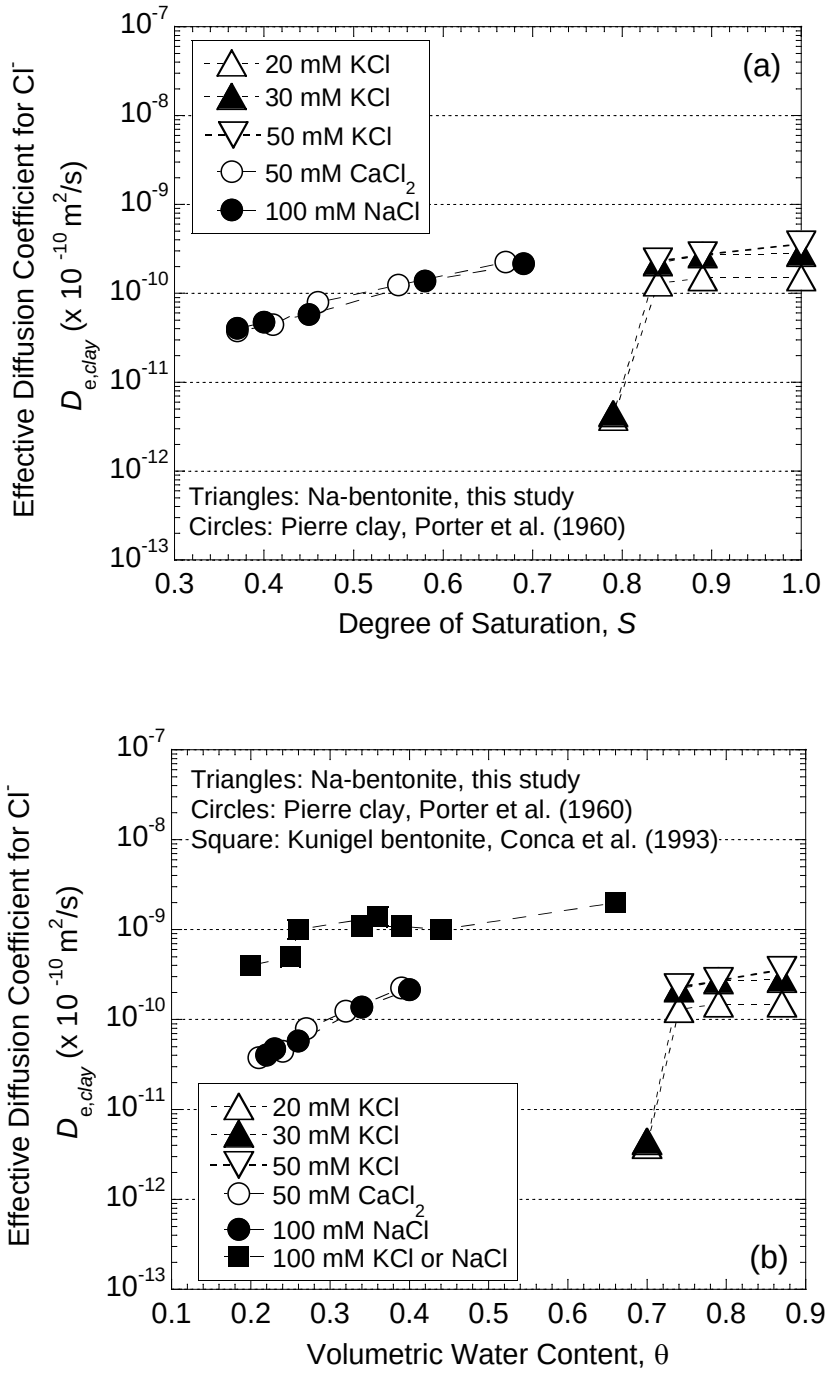

Figure 4.20. Comparison with literature for effective diffusion coefficients for Cl^- measured in clays versus degree of saturation. Legend indicates type and concentration of salt solution used as the source solution for diffusion testing.

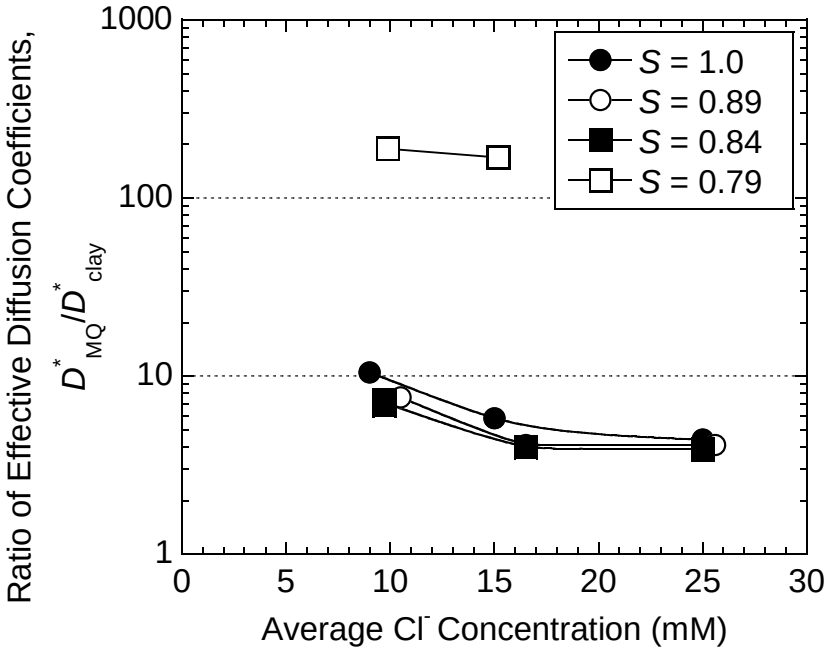

Figure 4.21. Ratio of effective diffusion coefficients calculated with the model from Millington and Quirk (1961) (D^*_{MQ}) to the values measured in the through-diffusion experiments (D^*_{clay}). [Note: values of D^*_{clay} are based on Cl^- results]

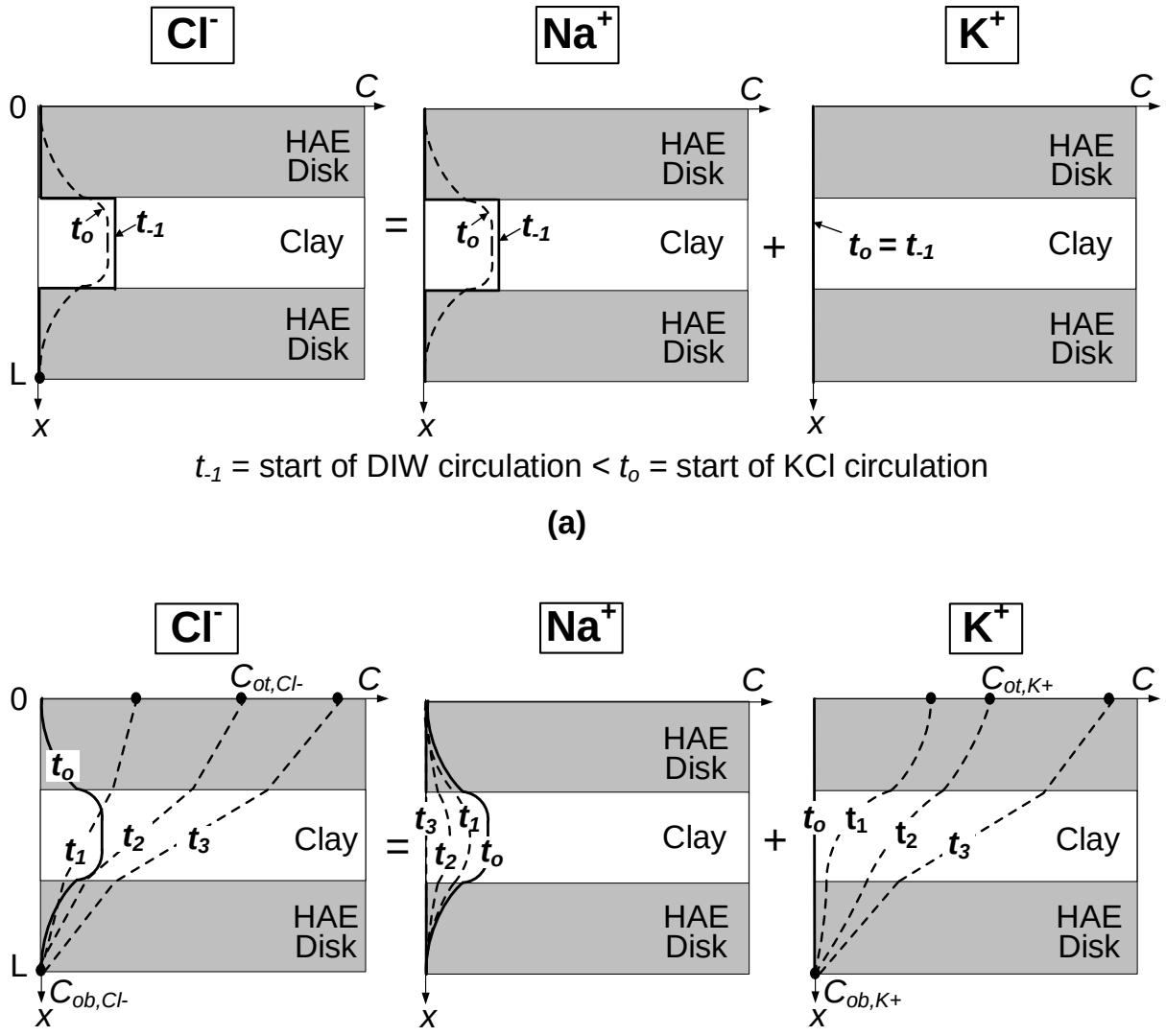

Figure 4.22. Conceptual illustration of diffusion of dominant ionic species in Na-bentonite specimens (a) during circulation of de-ionized water (DIW) at both boundaries, and (b) during multistage, through-diffusion experiments with KCl circulated at the top boundary. Times t_1, t_2, and t_3 correspond to the end of the 20-mM, 30-mM, and 50-mM concentration stages, respectively.

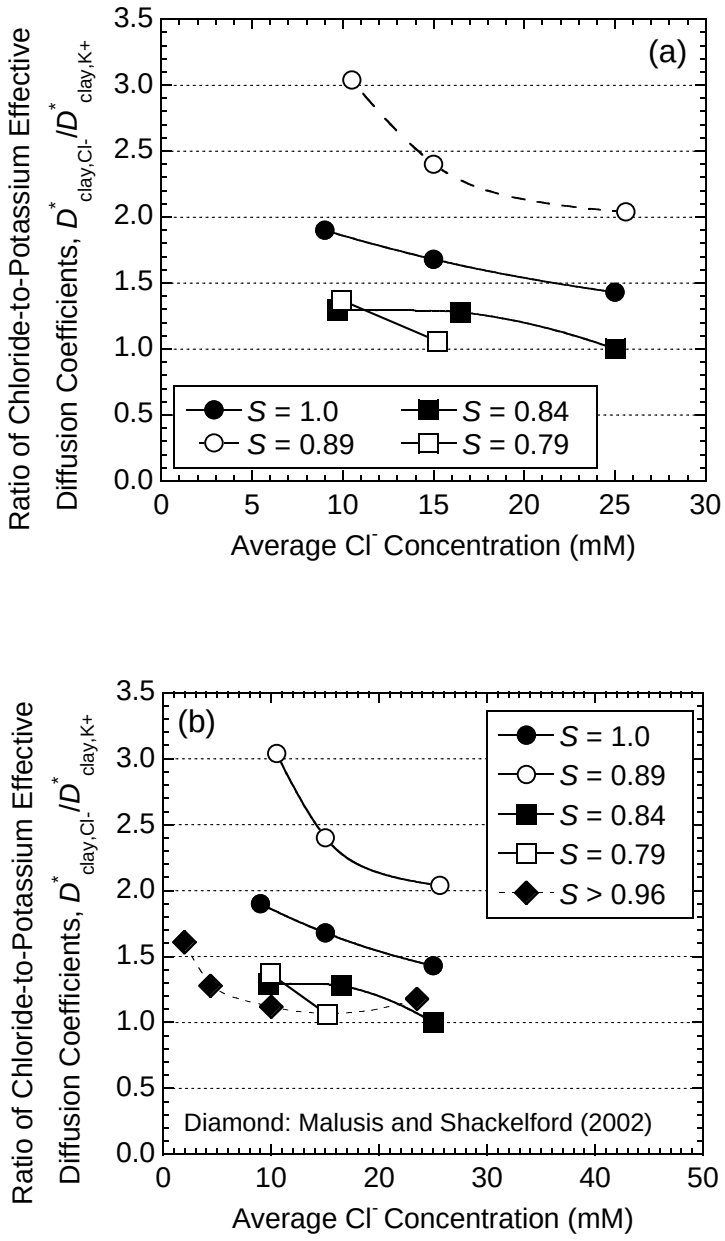

Figure 4.23. Ratio of chloride-to-potassium effective diffusion coefficients versus average KCl concentration for Na-bentonite: (a) results from this study; (b) comparison with other studies that used rigid-wall, through-diffusion experiments to measure diffusion in GCL-grade Na-bentonite.

REFERENCES

ATU (1992). "ClayMax sodium bentonite liner found degraded at New Jersey site." *Aboveground Tank Update*, 3(2), 1, 17-18.

Barbour, S., Lim, P., and Fredlund, D. (1996) "A new technique for diffusion testing of unsaturated soil." *Geotechnical Testing Journal*, 19(3), 247-258.

Benson, C. (2002). "Containment systems: lessons learned from North American failures." *Proceedings of the Fourth International Congress on Environmental Geotechnics*, Rio de Janeiro, Brazil, L. de Mello and M. Almeida, Eds., Swets & Zeitlinger, Lisse, The Netherlands, Vol. 2, 1095-1112.

Benson, C., Thorstad, P., Jo, H.-Y., and Rock, S. (2007). "Hydraulic performance of geosynthetic clay liners in a landfill final cover." *Journal of Geotechnical and Geoenvironmental Engineering*, 133(7), 814-827.

Bohnhoff, G., and Shackelford, C. (2015) "Salt diffusion through a bentonite-polymer composite." *Clays and Clay Minerals* (in re-review).

Bohnhoff, G., Shackelford, C., and Sample-Lord, K. (2014) "Calcium-resistant membrane behavior of polψμerized bentonite." *Journal of Geotechnical and Geoenvironmental Engineering*, 140(3), 040113029-1 – 04013029-12.

Bourg, I., Bourg, A., and Sposito, G. (2003). "Modeling diffusion and adsorption in compacted bentonite: A critical review." *Journal of Contaminant Hydrology*, 61, 293-302.

Brooks, R., and Corey, A. (1964). "Hydraulic properties of porous media." Hydrology Paper No. 3, March, Colorado State University, Fort Collins, CO.

Bucher, F., and Mayor, P. (1989). "Medium-scale experiments on highly-compacted bentonite." *Proceedings of the 12th International Conference on Soil Mechanics and Foundation Engineering*, Rio de Janeiro, Vol. 1, 583-585.

Conca, J., and Wright, J. (1990) "Diffusion coefficients in gravel under unsaturated conditions." *Water Resources Research*, 26(5), 1055-1066.

Conca, J., Apted, M., and Arthur, R. (1993). "Aqueous diffusion in repository and backfill environments." *Proceedings of the 16th International Symposium on the Scientific Basis for Nuclear Waste Management*, Boston, MA, C Interrante and R Pabalan, Eds., Cambridge University Press.,New York, NY, Vol. 294, 395-402.

Crank, J. (1975). *The Mathematics of Diffusion*, 2nd ed., Clarendon Press, Oxford, England.

Crooks, V., and Quigley, R. (1984). "Saline leachate migration through clay: A comparative laboratory and field investigation." *Canadian Geotechnical Journal*, 21(2), 349-362.

Di Emidio, G. (2010). *Hydraulic and Chemico-Osmotic Performance of Polymer Treated Clay*. PhD Dissertation, University of Ghent, Ghent, Belgium.

do N. Guimarães, Gens, A., Sánchez, M., and Olivella, S. (2006). "THM and reactive transport analysis of expansive clay barrier in radioactive waste isolation." *Communications in Numerical Methods in Engineering*, 22(8), 849-859.

Dominijanni, A., Manassero, M., and Puma, S. (2013) "Coupled chemical-hydraulic-mechanical behavior of bentonites." *Géotechnique*, 63(3), 191-205.

Dow Chemical Company (2000). "DOWICIL QK-20 Antimicrobial." Product Information, Form No. 253-01184-0100X/GW, Dow Chemical Company, Midland, MI.

Dutt, G., and Low, P. (1962) "Diffusion of alkali chlorides in clay-water systems." *Soil Science*, 93(4), 233-240.

Egloffstein, T. (2001). "Natural bentonites - influence of the ion exchange and partial desiccation on permeability and self-healing capacity of bentonites used in GCLs." *Geotextiles and Geomembranes*, 19(7), 427-444.

Fredlund, D. (1975). "A diffused air volume indicator for unsaturated soils." *Canadian Geotechnical Journal*, 12(4), 533-539.

Fredlund, D., and Rahardjo, H. (1993). *Soil Mechanics for Unsaturated Soils*, John Wiley & Sons, Inc., New York.

Fredlund, D., and Xing, A. (1994). "Equations for the soil-water characteristic curve." *Canadian Geotechnical Journal*, 31(4), 521-532.

Gens, A., do N. Guimarães, L., Garcia-Molina, A., and Alonso, E. (2002). "Factors controlling rock-clay buffer interaction in a radioactive waste repository." *Engineering Geology*, 64(2-3), 297-308.

Glaus, M., Frick, S., Rossé, R., and Van Loon, L. (2010) "Comparative study of tracer diffusion of HTO, $^{22}Na^{+}$ and $^{36}Cl^{-}$ in compacted kaolinite, illite and montmorillonite." *Geochimica et Cosmochimica Acta*, 74(7), 19991–2010.

Goodall, D., and Quigley, R. (1977). "Pollutant migration from two sanitary landfill sites near Sarnia, Ontario." *Canadian Geotechnical Journal*, 14(2), 223-236.

Graham-Bryce, I. (1963) "Effect of moisture content abd soil type on self diffusion of 86Rb in soils." *Journal of Agricultural Science*, 60(2), 239-244.

Herbert, H.-J., and Moog, H. (2000). "Modeling of saturation and swelling effects in clays under different saline conditions." *Proceedings of EUROSAFE Forum 2000,*Cologne, Germany, GRS, Köln, Germany.

Hu, G., and J., Wang (2003). "Aqueous-phase diffusion in unsaturated geologic media: A review." *Critical Reviews in Environmental Science and Technology*, 33(3), 275-297.

James, A., Fullerton, D., and Drake, R. (1997). "Field performance of GCL under ion exchange conditions." *Journal of Geotechnical and Geoenvironmental Engineering*, 123(10), 897-901.

Jo, H., Katsumi, T., Benson, C., and Edil, T. (2001). "Hydraulic conductivity and swelling of nonprehydrated GCLs permeated with single-species salt solutions." *Journal of Geotechnical and Geoenvironmental Engineering*. 127(7), 557–567.

Jo, H., Benson, C., and Edil, T. (2004). "Hydraulic conductivity and cation exchange in non-prehydrated and prehydrated bentonite permeated with weak inorganic salt solutions." *Clays and Clay Minerals*, 52(6), 661–679.

Jo, H., Benson, C., Shackelford, C., Lee, J-M., and Edil, T. (2005). "Long-term hydraulic conductivity of a geosynthetic clay liner permeated with inorganic salt solutions." *Journal of Geotechnical and Geoenvironmental Engineering*, 131(4), 405-417.

Johnson, R., Cherry, J., and Pankow, J. (1989) "Diffusive contaminant transport in natural clay: a field example and implications for clay-lined waste disposal sites." *Environmental Science and Technology*, 23(3), 340-349.

Kim, H., Suk, T., Park, S-H., and Lee, C-S. (1993). "Diffusivities for ions through compacted Na-bentonite with varying dry bulk density." *Waste Management*, 13(4), 303-308.

Klute, A., and Letey, J. (1958). "The dependence of ionic diffusion on the moisture content of non-adsorbing porous media." *Proceedings of the Soil Science Society of America*, 22(3), 213-215.

Komine, H. (2008). "Theoretical equations on hydraulic conductivities of bentonite-based buffer and backfill for underground disposal of radioactive wastes." *Journal of Geotechnical and Geoenvironmental Engineering*, 134(4), 497-508.

Komine, K., and Ogata, N. (1996). "Prediction for swelling characteristics of compacted bentonite." *Canadian Geotechnical Journal*, 33(1), 11-22.

Komine, K., and Ogata, N. (2004). "Predicting swelling characteristics of bentonites." *Journal of Geotechnical and Geoenvironmental Engineering*, 130(8), 818-829.

Kozaki, T., Liu, J., and Sato, S. (2008). "Diffusion mechanism of sodium ions in compacted montmorillonite under different NaCl concentration." *Physics and Chemistry of Earth*, 33(14-16), 957-961.

Lake, C., and Rowe, R. (2000). "Diffusion of sodium and chloride through geosynthetic clay liners." *Geotextiles and Geomembranes*, 18(2-4), 103-131.

Lambe, T., and Whitman, R. (1969) *Soil Mechanics*. Wiley, New York.

Lim, P., Barbour, S., and Fredlund, D. (1998) "The influence of degree of saturation on the coefficient of aqueous diffusion." *Canadian Geotechnical Journal*, 35(5), 811-827.

Lloret, A., Villar, M., Snachez, M., Gens, A., Pintado X., and Alonso, E. (2003). "Mechanical behavior of heavily compacted bentonite under high suction changes." *Geotechnique*, 53(1), 27-40.

Lu, N., and Likos, W. (2004) *Unsaturated Soil Mechanics.* John Wiley & Sons, Inc., Hoboken, NJ.

Madsen, F. (1998). "Clay mineralogical investigations related to nuclear waste disposal." *Clay Minerals*, 33(1), 109-129.

Malusis, M., Kang, J., and Shackelford, C. (2014) "Restricted salt diffusion in a geosyntheti clay liner." *Environmental Geotechnics*, ICE, Thomas Telford Ltd., London.

Malusis, M., Shackelford, C., and Olsen, H. (2001). "A laboratory apparatus to measure chemico-osmotic efficiency coefficients for clay soils." *Geotechnical Testing Journal*, 24(3), 229-242.

Malusis, M., and Shackelford, C. (2002). "Coupling effects during steady-state solute diffusion through a semipermeable clay membrane." *Environmental Science and Technology*, 36(6), 3212-1319.

Malusis, M., Shackelford, C., and Maneval, J. (2012). "Critical review of coupled flux formations for clay membranes based on nonequilibrium thermodynamics." *Journal of Contaminant Hydrology*, Vol. 138-139, 40-59.

Millington, R., and Quirk, J. (1961) "Permeability of porous solids." *Transactions of the Faraday Society*, Vol. 57, 1200-1207.

Meer, S., and Benson, C. (2007). "Hydraulic conductivity of geosynthetic clay liners exhumed from landfill final covers." *Journal of Geotechnical and Geoenvironmental Engineering*, 133(5), 550-563.

Mehta, B., Shiozawa, S., and Nakano, M. (1995) "Measurement of molecular diffusion of salt in unsaturated soils." *Soil Science*, 159(2), 115-121.

Meier, A., Sample-Lord, K., Castelbaum, D., Kallase, S., Moran, B., Ray, T., and Shackelford, C. (2014) "Persistence of semipermeable membrane behavior for a geosynthetic clay liner." *Proceedings, 7th International Conference on Environmental Geotechnics*, A. Bouazza, S. Yuen, and B. Brown, Eds., Nov. 10-14, 2014, Melbourne, Australia (ISBN 978-1-922107-23-7), 496-503.

Mitchell, J., and Soga, K. (2005). *Fundamentals of Soil Behavior*, 3rd ed., *John Wiley and Sons*, New York.

Montes, G., Marty, N., Fritz, B., Clement, A., and Michau, N. (2005). "Modelling of long-term diffusion-reaction in a bentonite barrier for radioactive waste confinement." *Applied Clay Science*, 30(3-4), 181-198.

Muurinen, A. (1990). "Diffusion of uranium in compacted sodium bentonite." *Engineering Geology*, 28(3-4), 359-367.

Nelson, M. (2000). *Hydraulic Conductivity of Paper Sludges*. M.S. Thesis, Dept. of Civil and Environmental Engineering, University of Wisconsin-Madison, Madison, WI.

Neville, C., and Andrews, C. (2006) "Containment criterion for contaminant isolation by cutoff walls." *Ground Water*, 44(5), 682-686.

OECD (2003). *Workshop Proceedings on Engineered Barrier Systems (EBS) in the Context of the Entire Safety Case*. Nuclear Energy Agency, Organization for Economic Co-Operation and Development (OECD), Oxford, United Kingdom, September 25-27, 2002.

Olesen, T., Moldrup, P., Henriksen, K., and Petersen, L. (1996) "Modeling diffusion and reaction in soils: IV. New models for predicting ion diffusivity." *Soil Science*, 161(10), 633-645.

Olson, R., and Mesri, G. (1970). "Mechanisms controlling the compressibility of clays." *Journal of the Soil Mechanics and Foundations Division*, 96(6), 1863-1878.

Padilla, J., Perera, Y., Houston, W., Perez, N., and Fredlund, D. (2006). "Quantification of air diffusion through high air-entry disks." *Proceedings of the 4th International Conference on Unsaturated Soils*, Carefree, AZ, April 2-6, G. Miller, Ed., ASCE, Reston, VA, Vol. 2, 1852-1863.

Papendick, R., and Campbell, G. (1980) "Theory and measurement of water potential." *Water Potential Relations in Soil Microbiology*, Special Publication 9, SSSA, Madison, WI.

Porter, L., Kemper, W., Jackson, R., and Stewart, B. (1960) "Chloride diffusion in soils as influenced by moisture content." *Proceedings of the Soil Science Society of America*, 24(6), 460-463.

Pusch, R., and Yong, R. (2006) *Microstructure of Smectite Clays and Engineering Performance*. Taylor & Francis, London.

Quigley, R., Yanful, E., and Fernandez, F. (1987) "Ion transfer by diffusion through clayey barriers." *Geotechnical Practice for Waste Disposal, Special Publication No. 13*, R. Woods, Ed., ASCE, New York, 137-158.

Revil, A., and Jougnot, D. (2008) "Diffusion of ions in unsaturated porous materials." *Journal of Colloid and Interface Science*, 319(1), 226-235.

Romkens, M., and Bruce, R. (1964) "Nitrate diffusivity in realtion to moisture content of non-adsorbing porous media." *Soil Science*, 98(5), 332-337.

Rosanne, M.,Mammar, N., Koudina, N., Prunet-Foch, B., Thovert, J-F., Tevissen, E., and Adler, P. (2003) "Transport properties of compact clays: II. Diffusion." *Journal of Colloid and Interface Science*, 260(1), 195-203.

Rowe, R. (1987) "Pollutant transport through barriers." *Geotechnical practice for waste disposal, Special Publication No. 13*, R. Woods, Ed., ASCE, New York, NY, 159-181.

Rowe, R., Lake, C., Petrov, R. (2000) "Apparatus and procedures for assessing inorganic diffusion coefficients for geosynthetic clay liners." *Geotechnical Testing Journal*, 23(2), 206-214.

Rowe, R., Lake, C., von Maubeuge, K., and Stweart, D. (1997) "Implications of diffusion of chloride through geosynthetic clay liners." *Geoenvironment '97*, Melbourne, Australia, November 26-28, M. Bouazza, J. Kodikara and R. Parker, Eds., Balkema, Netherlands, 295-300.

Rowe, R., Quigley, R., and Booker, J. (1995) *Clayey barrier systems for waste disposal facilities*. E&FN Spon, New York, NY.

Rowell, D., Martin, M., and Nye, P. (1967) "The measurement and mechanism of ion diffusion in soils. III. The effect of moisture content and soil solution concentration on the self diffusion of ions in soils." *Journal of Soil Science*, 18(2), 204-222.

Rutqvist, J., Chijimatsu, M., Jing, L., Millard, A., Nguyen, T., Rejeb, A., Sugita, Y., and Tsang, C. (2005) "A numerical study of THM effects on the near-field safety of a hypothetical nuclear waste repository – BMT1 of the DECOVALEX III project. Part 3: Effects of THM coupling in sparsely fractured rocks." *International Journal of Rock Mechanics and Mining Sciences*, 42(5-6), 745-755.

Rutqvist, J., Zheng, L., Chen, F., Liu, H-H., Birkholzer, J. (2014) "Modeling of coupled thermos-hydro-mechanical processes with links to geochemistry associated with bentonite-backfilled repository tunnels in clay formations." *Rock Mechanics and Rock Engineering*, 47(1), 167-186.

Sadeghi, A., Kissel, D., and Cabrera, M. (1989) "Estimating molecular diffusion coefficients of urea in unsaturated soil." *Soil Science Society of America*, 53(1), 15-18.

Sánchez, M., Gens, A., and Olivella, S. (2010). "Effect of thermos-coupled processes on the behavior of a clay barrier submitted to heating and hydration." *Anais da Academia Brasileira de Ciências*, 82(1), 153-168.

Scalia, J., and Benson, C. (2010). "Effect of permeant water on the hydraulic conductivity of exhumed GCLs." *Geotechnical Testing Journal*, 33(3), 1-11.

Shackelford, C. (1988). "Diffusion as a transport process in fine-grained barrier materials." *Geotechnical News*, Bi-Tech Publishers, Vancouver, B.C., 6(2), 24-27.

Shackelford, C. (1989). "Diffusion of contaminants through waste containment barriers." Transportation Research Record 1219, *Geotechnical Engineering 1989*, TRB, NRC, National Academy Press, Washington, DC, 169-182.

Shackelford, C. (1991). "Laboratory diffusion testing for waste disposal - A review." *Journal of Contaminant Hydrology*, 7(3), 177-217.

Shackelford, C. (2005). "Environmental issues in geotechnical engineering." *16th International Conference on Soil Mechanics and Geotechnical Engineering*, Osaka, Japan, Sept. 12-16, 2005, Millpress, Rotterdam, The Netherlands, Vol. 1, 95-122.

Shackelford, C. (2013). "Membrane behavior in engineered bentonite-based containment barriers: State of the art." *Proceedings of Coupled Phenomena in Environmental Geotechnics (CPEG)*, M. Manassero, A. Dominijanni, S. Foti, and G. Musso, eds., July 1-3, Torino, Italy, CRC Press/Balkema, Taylor & Francis Group, London, 45-60.

Shackelford, C. (2013). "The role of diffusion in environmental geotechnics." *Proceedings, 18th International Conference on Soil Mechanics and Geotechnical Engineering-Challenges and Innovations in Geotechnics*, P. Delage, J. Desrues, R. Frank, A. Puech, F. Schlosser, Eds., Presses des Ponts, Paris, Vol. 1, 127-150.

Shackelford, C., Benson, C., Katsumi,T., Edil, T., and Lin,L. (2000). "Evaluating the hydraulic conductivity of GCLs permeated with non-standard liquids." *Geotextiles and Geomembranes*, 18(2–4), 133-161.

Shackelford, C., and Daniel, D. (1991a). "Diffusion in saturated soil. 1. Background." *Journal of Geotechnical Engineering*, 117(3), 467-484.

Shackelford, C., and Daniel, D. (1991b). "Diffusion in saturated soil: II. Results for compacted clay." *Journal of Geotechnical Engineering*, 117(3), 485-506.

Shackelford, C., and Lee, J. (2003). "The destructive role of diffusion on clay membrane behavior." *Clays and Clay Minerals*, 51(2), 186-196.

Shackelford, C., Malusis, M., Majeski, M., and Stern, R. (1999). "Electrical conductivity breakthrough curves." *Journal of Geotechnical and Geoenvironmental Engineering*, 125(4), 260-270.

Shackelford, C., and Moore, S. (2013). "Fickian diffusion of radionuclides for engineered containment barriers: Diffusion coefficients, porosities, and complicating issues." *Engineering Geology*, Elsevier, Amsterdam, 152(1), 133-147.

Sleep, B., Shackelford, C., and Parker, J. (2006) "Modeling of fluid transport through barriers (Chapter 2)." *Barrier Systems for Environmental Contaminant Containment and Treatment*, C.C. Chien, H.I. Inyang, and L.G. Everett, Eds., CRC Press, Taylor and Francis Group, LLC, Boca Raton, FL, 71-141.

Torstenfelt, B., AIlard, B., Andersson, K., Kipatsi, H., Eliasson, L., Olofsson, U., and Persson, H. (1983). "Radionuclide diffusion and mobilities in compacted bentonite." *KBS Technical Report 83-34*, Swedish Nuclear Fuel and Waste Management Co., Stockholm, Sweden.

van Genuchten, M. (1980). "A closed form equation for predicting the hydraulic conductivity of unsaturated soils." *Soil Science Society of America Journal*, 44(5), 892-898.

Warncke, D., and Barber, S. (1972) "Diffusion of zinc in soil: I. The influence of soil moisture." *Proceedings of the Soil Science Society of America*, 36(1), 39-42.

Ye, W., Zhang, F., Chen, B., Chen, Y., Wang, Q., and Cui, Y. (2014). "Effects of salt solutions on the hydro-mechanical behavior of compacted GMZ01 bentonite." *Environmental Earth Science*, 72(7), 2621-2630.

Yong, R., Boonsinsuk, R., and Yiotis, D. (1985). "Creep behavior of a buffer materials for nuclear fuel waste vault." *Canadian Geotechnical Journal*, 22(4), 541-550.

Yong, R., Pusch, R., and Nakano, M. (2010) *Containment of High-level Radioactive and Hazardous Solid Wastes with Clay Barriers*. Spon Press, New York.

CHAPTER 5. MEMBRANE BEHAVIOR OF UNSATURATED SODIUM BENTONITE

5.1 Introduction

Membrane behavior refers to the ability of a soil to selectively restrict the passage of dissolved chemical species (solutes) in pore water. The electric fields associated with clay particles result in electrostatic repulsion of charged solutes, such that a phenomenon commonly referred to as anion exclusion occurs when particles are sufficiently close so as to cause these electric fields to overlap (Figure 5.1). Exclusion of anions from passage through the pore space leads to similar restriction of the cations in the solution due to the electroneutrality requirement. Under such conditions, chemico-osmosis also may occur, whereby water flows from higher water activity (lower solute concentration) to lower water activity (Shackelford et al. 2003).

Although the effects of membrane behavior and related processes have been documented historically by soil scientists and geologists (e.g., Kemper 1961; McKelvey and Milne 1962; Kemper and Massland 1964; Young and Low 1965; Kemper and Rollins 1966; Groenevelt and Bolt 1969; Olsen 1969, 1972; Letey et al. 1969; Bresler 1973; Kharaka and Berry 1973; Marine and Fritz 1981), significant advancement in the evaluation and quantification of the phenomenon has occurred within the past 15 years (Shackelford 2013). In particular, the results of several studies have shown that membrane behavior can affect contaminant transport across bentonite-based barriers commonly used for waste containment, such as geosynthetic clay liners (GCLs), soil-bentonite (SB) cutoff walls, and bentonite-amended compacted clay (e.g., Malusis et al. 2001; Manassero and Dominijanni 2003; Evans et al. 2008; Kang and Shackelford 2010, 2011; Shackelford 2013; Tang et al. 2014, 2015). Also, the occurrence of solute restriction and chemico-osmosis due to membrane behavior enhances the containment function of a clay barrier

(Shackelford 2013). However, current design and evaluation of such barriers neglect membrane behavior, largely due to a lack of fundamental knowledge of the phenomenon.

For significant membrane behavior or solute restriction to exist, the pore sizes in the clay must be sufficiently small to allow for interaction of the electric fields of adjacent clay particles. Generally, this requirement is achieved only in clays such as sodium bentonite (Na-bentonite) that contain highly active clay minerals, such as the smectites (e.g., montmorillonite). Membrane behavior also has been shown to increase with increasing dry density (decreasing void ratio), increasing effective stress, and increasing bentonite content of the clay (Shackelford et al. 2003; Shackelford 2013).

Experimental research to date has focused on membrane behavior and diffusion almost exclusively under saturated conditions (i.e., degree of water saturation, *S*, of the specimen of 100 %), partly due to the increased complexity of testing systems required for unsaturated conditions. However, clay barriers may exist at various percentages of saturation in field applications, such as in landfill covers and engineered and natural barriers for high-level radioactive waste (HLRW) disposal (see Chapter 4). Based on our current, conceptual understanding of the phenomenon, membrane behavior under unsaturated conditions should be more significant than under saturated conditions (Sample-Lord and Shackelford 2014).

As a result of the aforementioned considerations, a research program was undertaken to determine the extent and magnitude of membrane behavior of Na-bentonite under unsaturated conditions. The purpose of the research was to: (1) advance our understanding of membrane behavior in clays; and (2) contribute to the knowledge base that must be established prior to incorporating membrane behavior effects in the design of barriers for waste containment facilities. The results of this research program are presented, and the measured membrane

efficiencies are correlated with degree of saturation, as well as with the diffusion properties of the Na-bentonite previously described in Chapter 4.

5.2 Background

5.2.1 Anion exclusion and membrane behavior in saturated clays

Bentonite is highly plastic clay composed primarily of the clay minerals montmorillonite and beidellite, both of which are dioctahedral smectites (Grim 1968; Grim and Güven 1978; Deer et al. 1992). The smectite structure consists of an octahedral sheet sandwiched between two silica sheets, referred to as a 2:1 layered alumino-silicate (Grim 1968; Grim and Güven 1978). Isomorphic substitution within the crystalline structure of montmorillonite during formation of the clay results in a net negative charge. This charge deficiency is balanced by exchangeable cations within the interlayer regions of the crystalline structure, referred to as interlayer cations (Mitchell and Soga 2005), as well as on the external surfaces of individual clay particles. The interlayer bonding within the 2:1 smectite mineral is weak, permitting interlayer separation. The interlayer spacing (d_{001}) can vary from 0.96 nm to more than 2 nm, based on hydration and the types of exchangeable cations that are present (Norrish 1954; van Olphen 1963; Deer et al. 1992).

Interlayer swelling within clay particles occurs due to both crystalline swelling and osmotic (double-layer) swelling (McBride 1994; Yong et al. 2010). Crystalline swelling is attributed to initial hydration of dry clay due to penetration of water molecules (H_2O) into the interlayer regions as a result of a gradient in matric suction (van Olphen 1963; Rao et al. 2013). For montmorillonite, crystalline swelling may increase the interlayer spacing from approximately 1 nm (for dry clay) to 2 nm (i.e., double the volume) (Norrish 1954). Interlayer

swelling beyond 2 nm typically is associated with osmotic or double-layer swelling. Osmotic swelling occurs due to repulsion between the electrical double layers of adjacent clay particles. When the liquid in the interlayer space consists of monovalent cations (e.g., K^+, Na^+) at a low ionic strength, significant osmotic swelling may occur, resulting in increased interlayer spacing (e.g., > 12 nm, Norrish 1954) and thicker diffuse-double layers (DDLs), and decreased free (i.e., bulk) pore space between particles (Norrish 1954; Norrish and Quirk 1954; McBride 1994; Kolstad et al. 2004). In contrast, when the interlayer liquid contains multivalent cations (e.g., Ca^{2+}, Mg^{2+}, Al^{3+}) or is of high ionic strength, the osmotic swell is limited (e.g., interlayer spacing $\leq$ 2 nm), resulting in increased bulk pore space between particles (Kolstad et al. 2004).

The phenomenon of anion exclusion (membrane behavior) may be explained based on solute restriction occurring along two different pathways of transport: 1) through the interlayer space between individual clay particles, and 2) through the pore space between clods or assemblages of clay particles (Figures 5.1 and 5.2, respectively). Anion exclusion in the interlayer space between adjacent clay particles is attributed to overlapping fields of negative electrical potential (Ψ) of the DDLs surrounding each clay particle, as shown in Figure 5.1. The electrostatic double-layer thickness is represented by Zone 1 in Figure 5.1, while the bulk solution in the pore space is represented by Zone 2. Anion repulsion occurs within Zone 1 due to negative Ψ, and the thickness of this region is controlled by osmotic swelling. Thus, factors that would reduce osmotic swelling, such as an increase in ionic strength or the presence of multivalent cations, would decrease the degree of solute restriction in the pore space and the associated membrane behavior of the clay.

Under conditions of high osmotic swell, the pathway for solute transport between clods (granules or assemblages) of clay particles becomes more tortuous such that a higher degree of

anion exclusion is expected. As osmotic swell decreases, the pore space between the clods of clay particles increases such that solute transport through the clay is less restricted, resulting in a decrease in the membrane behavior of the clay (as shown in Figure 5.2a).

Membrane behavior typically is quantified in terms of a membrane efficiency coefficient, ω, where values of ω range from 0 for no membrane behavior to 1.0 representing 100 % solute restriction corresponding to a perfect membrane (Shackelford et al. 2003; Shackelford 2013). Most natural clays that exhibit membrane behavior are nonideal or imperfect, such that values of ω are between 0 and 1 because of the variation in pore sizes. The terms chemico-osmotic efficiency coefficient or reflection coefficient, represented by the symbol σ, also have been used to describe membrane efficiency in the literature. However, the symbol ω was preferred in this study to represent membrane efficiency, since σ commonly is used to represent stress in the engineering literature (Shackelford 2013).

Membrane behavior research is still at a fundamental level of study and, therefore, chemical solutions used in laboratory testing typically have been comprised of simple salt solutions (e.g., KCl, NaCl, $CaCl_2$) versus, for example, the more complex chemical solutions commonly encountered in natural groundwaters (e.g., Tremosa et al. 2012) or in practical applications involving the use of clays for containment of contaminants (e.g., Fang and Evans 1988; Ruhl and Daniel 1997; Kolstad et al. 2004; Bradshaw and Benson 2014; Chen et al. 2014). In bentonite-based materials, increased concentration of monovalent salt solutions (e.g., KCl, NaCl) generally correlates with decreased membrane behavior (e.g., Kemper and Rollins 1966; Kemper and Quirk 1972; Fritz and Marine 1983; Malusis et al. 2001; Shackelford et al. 2003; Kang and Shackelford 2009). Multivalent salt solutions (e.g., $CaCl_2$) have been shown to result in partial degradation or complete destruction of membrane behavior (e.g., Kemper and Rollins

1966; Shackelford and Lee 2003; Allred 2008), which is consistent with the osmotic swell mechanisms described previously.

5.2.2 Membrane behavior under unsaturated conditions

Based on our current conceptual understanding of the phenomenon, membrane behavior under unsaturated conditions should be more significant (Sample-Lord and Shackelford 2014). For example, for a specimen that is initially water saturated (S = 1), as shown in Figures 5.1a-b, a decrease in S would result in an initial reduction in the thickness of Zone 2 (Figures 5.1c-d). For a bulk solution of given chemistry and ionic strength, the thickness of Zone 1 would remain constant as S decreases, provided that saturation remains sufficiently high to allow for full development of the double layer (James and Rubin 1986). Thus, as a specimen becomes increasingly more unsaturated, the percentage of the liquid-filled pore space within which anion repulsion occurs (Zone 1/[Zone 1 + Zone 2]) increases (James and Rubin 1986; Allred 2007; Sample-Lord and Shackelford 2014), such that the effects of solute exclusion should be enhanced. Consequently, the potential advantages of clays exhibiting membrane behavior (e.g., enhanced containment due to reduced diffusion and chemico-osmotic flow) are likely to be more significant when such clays exist under unsaturated conditions, i.e., since pores that are accessible for saturated solute migration (Figure 5.1a) would become less accessible (Figure 5.1c).

As S decreases, membrane behavior also is expected to increase with increasing matric suction, ψ_m (= $P_{air} - u_w$, where P_{air} = pore-air pressure and u_w = pore-water pressure). As air enters the larger pores between the clay clods, the volumetric water content (θ) decreases and ψ_m increases, resulting in an increase in effective stress (Lu et al. 2010). If volume change is

allowed to occur, the increase in effective stress (σ') will lead to a decrease in the porosity (n) and, therefore, a decrease in the accessible pore width. In previous experimental studies, membrane behavior of saturated bentonite has been shown to increase with decreasing n or increasing dry density, ρ_d, and increasing σ' (Shackelford et al. 2003; Kang and Shackelford 2011; Shackelford 2013).

Although limited, some previous studies have focused on membrane behavior in unsaturated soils (e.g., Letey et al. 1969; Bresler 1973; Bresler and Laufer 1974; James and Rubin 1986; Allred 2007). However, conclusions regarding the relationship between observed membrane behavior and degree of saturation have been mixed. To the author's knowledge, there is no data available for membrane behavior of bentonite specimens maintained under unsaturated conditions.

For example, Letey et al. (1969) performed transient and steady-state experiments on fine sandy loam and clay loam specimens. The experiments were conducted as open-system tests, such that chemico-osmotic flow was allowed to occur through the specimen. In the transient experiments, the soil was placed in 49-mm-diameter and 5-mm-thick metal cylinders on top of ceramic plates (large high-air entry disks). The soil then was soaked in NaCl solution (ranging in concentration from 10 mM to 110 mM) for several hours. After soaking, the specimens were placed in a pressure plate and an air pressure ranging from 10 kPa to 1500 kPa was applied to bring the specimen to the desired θ and ψ_m. The specimens then were removed from the cylinders, placed in contact with other specimens of different NaCl concentrations, and sealed together in a cell. Water movement across the soil sections due to the osmotic pressure gradients caused by the concentration differences was determined by weighing the sections at the end of the test.

For the steady-state experiments, 10-mm-thick soil specimens ($1.03 \leq \rho_d \leq 1.26$ Mg/m^3) were placed in a cylinder between two ceramic plates. Calibration tests were performed to confirm that the ceramic plates did not exhibit membrane behavior and to measure the diffusion coefficients of the plates (although the values of the diffusion coefficients of the plates were not reported). Air pressure was applied to the specimen through small holes in the cylinder wall. NaCl solutions were placed in the two compartments (reservoirs) adjacent to the outer boundaries of each ceramic plate. The NaCl concentrations used in the study were 10, 30, 80, and 100 mM. Water flow across the specimen due to the concentration gradient between the reservoirs (chemico-osmotic flow) was measured by reading capillary tubes attached to each reservoir. After measuring the chemico-osmotic flow, a hydraulic pressure gradient was applied and the flow was measured again. The air pressure then was increased to decrease the saturation of the specimen and the procedure was repeated. Although the concentration difference across the whole system (the soil specimen and two ceramic plates) was known, the concentration difference across only the soil specimen (ΔC) initially was not known. The diffusion results from the tests and the known diffusion coefficients of the plates were used to calculate ΔC, and the resulting theoretical osmotic pressure difference ($\Delta\pi$) across the soil. However, Letey et al. (1969) concluded that the impedance to salt flow in the ceramic plates was negligible relative to the soil specimen and, therefore, $\Delta\pi$ across the system was approximately equal to $\Delta\pi$ across the specimen.

The results of the steady-state and transient tests reported by Letey et al. (1969) for specimens of Ascalon sandy loam, Fort Collins loam, and Pine River clay loam indicated that ω generally increased as ψ_m increased (i.e., as S decreased). However, the highest value of ψ_m for which ω could be measured was 66 kPa due to issues caused by air diffusion through the ceramic

plates. The diffusion of air through the plates suggests that the air-entry pressure of the plates was quite low (e.g., $\leq$ 60 kPa), which may explain why the diffusion coefficient of the plate was high enough that $\Delta\pi$ across the plate could be assumed negligible. The reported values of ω were low, ranging from 0.006 to 0.157, with the maximum ω occurring at the highest ψ_m (66 kPa) for the Fort Collins loam.

Unsaturated column experiments also have been performed to evaluate anion exclusion effects by measuring the effective percentage of pore water unavailable for transport of anions (e.g., Bresler 1973; James and Rubin 1986; Allred 2007). For example, Bresler (1973) evaluated anion exclusion in a loam soil (48 % sand, 20 % clay) using column tests conducted under conditions of infiltration and evaporation. The air-dried soil was packed in a 0.45-m-long column at a ρ_d of 1.4 Mg/m^3. The columns were infiltrated with a solution of 10 mN $CaCl_2$ and then divided into sections ranging in thickness from 10 mm to 20 mm to measure salt concentration, water content, and bulk (dry) density. Some of the columns were sealed after the infiltration stage, maintained sealed and undisturbed for four days, and then uncovered and exposed to a fan for 10 days to induce evaporation. For all of the tests, Bresler (1973) determined that, for the loam soil and the test conditions that were evaluated, the effects of anion exclusion on the transport of Cl^- were not significant. Although the loam was reported to consist of 20 % clay, most of which was montmorillonite, the reported *CEC* of the soil was only 14 meq/100 g, and 93 % of the exchange complex was occupied by Ca^{2+}. Based on the *CEC* and the presence of primarily divalent cations on the exchange complex, the interlayer swell was likely low (relative to a Na-bentonite), resulting in insignificant membrane behavior (see Section 5.2.1).

James and Rubin (1986) performed vertical, constant-flow column tests on saturated and unsaturated samples of Dehli sand (90 % sand, 7 % silt and 3 % clay) to evaluate anion exclusion effects on Cl^- transport. The unsaturated samples were packed into 0.485-m-long columns at a ρ_d of 1.6 Mg/m^3. A syringe pump was used to deliver $CaCl_2$ solutions to the column inlet at a constant flow rate. Suction was applied to the outlet end of the column to maintain a lower water content at the bottom of the column. At the end of the test, the column was sliced into sections ranging in thickness from 11.4 mm to 22.8 mm to determine the θ and Cl^- concentration profiles with depth. The value of θ in the soil columns was relatively constant with depth in the upper 0.4 m of the column, and ranged from 0.17 to 0.22 (S = 0.41 to 0.55, respectively) for the four unsaturated tests. The volumetric water content within which Cl^- was excluded (θ_{ex}) was compared with the total θ of the column. The relationship between anion exclusion as represented by the ratio of θ_{ex}/θ (or as shown in Figure 5.1, Zone 1/(Zone 1 + Zone 2)) and the θ (or S) of the soil was inconsistent. At saturated conditions, the value of θ_{ex}/θ was 0.05. As S of the columns decreased to values of 0.55 and 0.46, the value of θ_{ex}/θ increased to 0.09 and 0.12, respectively, as expected. However, for the column with the lowest value of S of 0.41, the value of θ_{ex}/θ was 0.09, which was inconsistent with the rest of the data where θ_{ex}/θ increased as S decreased. These inconsistencies in the results may be due to the relatively narrow range of S evaluated for the unsaturated columns (0.41 to 0.55) and the measurement error associated with the θ_{ex} values ($\pm$ 0.004 to 0.008, or 2 % to 4 % of the reported θ_{ex} values).

Allred (2007) performed transient column experiments on unsaturated soils to evaluate the effect of clay mineralogy on anion exclusion of nitrate (NO_3^-). The soils included quartz sand, two natural loam soils, and mixtures of sand and kaolinite, illite, and montmorillonite. The soils were prepared in the columns at values of ρ_d ranging from 1.6 to 1.9 Mg/m^3 and total

lengths of 0.12 m to 0.26 m. Anion exclusion effects were evaluated in terms of the ratio of the volumetric water content at the column inlet where NO_3^- was excluded (θ_{ex}) to the total θ at the column inlet, or θ_{ex}/θ. Since the soil at the column inlet was saturated, the ratio θ_{ex}/θ was equivalent to n_{ex}/n, where n_{ex} is the porosity of the excluded volume of liquid in the pores. The values of θ_{ex}/θ were determined by comparing the measured concentration of NO_3^- near the column inlet with the concentration of the solution initially injected in the column. As the wetting front advanced through the column, saturated conditions were maintained at the inlet boundary, but the water content of the rest of the column was not controlled. Based on the ratio of θ_{ex}/θ calculated for the inlet boundary, anion exclusion of NO_3^- was most prevalent (θ_{ex}/θ = 0.20) in the soil mixture with the highest percentage of montmorrillonite (25 % by dry mass). Although anion exclusion occurred under unsaturated conditions in the column as the wetting front advanced during testing, the value of θ_{ex}/θ was only quantified at the saturated inlet boundary.

5.3 Materials and methods

5.3.1 Materials and specimen preparation

The materials used in the study, including the bentonite, and the specimen preparation procedures are described in detail in Chapter 4 (Section 4.3). Physical and mineralogical properties of the bentonite, before and after dialysis treatment, are provided in Chapter 3 (Table 3.2). The liquids used in this study included de-ionized water (DIW) (pH = 7.35, electrical conductivity, *EC* = 0.06 mS/m) and solutions of DIW with potassium chloride (KCl) (certified A.C.S.; Fisher Scientific, Fair Lawn, NJ) with target concentrations of 20 mM to 50 mM KCl.

The actual measured concentrations of the KCl solutions ranged from 19 mM to 51 mM KCl (i.e., the same solutions used in the diffusion tests as described in Chapter 4).

5.3.2 Test procedure

Membrane behavior of the bentonite specimens was measured with the testing apparatus described in detail in Chapter 2. The bentonite specimens were confined between two high air-entry (HAE) disks in a rigid-wall cell with a flexible membrane between the specimen perimeter and the sidewall of the rigid cell. Both 3-bar and 5-bar HAE disks were used to accommodate specimens with suctions up to 300 kPa and 500 kPa, respectively. Chemical (electrolyte) solutions and DIW were circulated across the top and bottom boundaries of the test cell, respectively, at a constant rate with syringe pumps. Each circulation system (top and bottom) represents a closed loop, such that the amount of liquid contained in each circulation system remained constant (e.g., see Malusis et al. 2001). As a result, there was no volume change during circulation of the solutions (i.e., the system was closed), such that liquid flow through the specimen during this stage could not occur despite the difference in concentrations at each boundary. Therefore, the testing apparatus used in this study was unlike the previously noted studies involving evaluation of unsaturated membrane behavior using open systems (see Chapter 2 for details). If the specimen behaved as a semipermeable membrane, then a chemico-osmotic pressure difference (ΔP) developed across the length of the specimen (L) due to the applied concentration difference (ΔC). The ΔP across the specimen was measured via differential pressure transducers (Omega Engineering Inc., Models PX26 and PX209, Stamford, CT), as described in Chapter 2. Calibration tests performed on the HAE disks confirmed that the disks

did not exhibit any measurable membrane behavior (i.e., $\Delta P = 0$) and, therefore, did not affect the ΔP measurements (see Chapter 2).

In order to maintain positive pore-water pressures, u, under unsaturated conditions and avoid potential cavitation during testing of specimens at low S (high suction), a constant air pressure (P_{air}) greater than the matric suction of the specimen was applied during testing via an opening in the rigid cell (see Chapter 2 for details). The suctions at the top and bottom boundaries of the specimen ($\psi_{T,top}$ and $\psi_{T,bottom}$, respectively) were monitored with differential pressure transducers (same models as previously noted) as the difference between P_{air} and the water pressures at the top and bottom boundaries (u_{top} and u_{bottom}, respectively).

The testing was performed in stages, where the first stage consisted of circulating DIW across both top and bottom boundaries to establish the baseline value of ΔP. Once steady baseline pressures were established, the DIW at the top boundary was switched to an electrolyte solution (KCl), inducing a buildup of ΔP. After both steady-state ΔP and steady-state diffusion conditions (see Chapter 4) were established, the ΔC was increased via circulation of solution with a higher source concentration (C_o) at the top boundary, beginning a new stage of the same test. For the tests in this study, KCl was used as the solution for the top boundary to allow for comparison with previously published data. The target concentrations of KCl corresponding to the different stages of the multistage experiments were 20 mM, 30 mM and 50 mM KCl, as summarized in Table 5.1.

At the end of the circulation stage with DIW, and prior to circulation with electrolyte solutions, a constant-flow hydraulic conductivity (k) test could be performed utilizing the flow pump, if desired (see Chapter 2 for details). During the k testing stage, one syringe on the flow pump forced freshly de-aired, DIW through the specimen and HAE disks at a constant-flow rate,

q. The specimen was permeated from the bottom upward and the pressure difference across the specimen, Δu (=u_{top} - u_{bottom}), was measured with the same pressure transducers used to measure ΔP during the membrane test. The Δu due to the difference in elevation head between the top and bottom boundaries of the specimen was considered negligible ($\leq$ 0.08 kPa). Once a steady value of Δu was achieved, *k* was calculated based on Darcy's law, as described in Chapter 2. Due to time constraints, the *k* test was performed only for the saturated specimen (S = 1). The time that would be required for ψ_m and θ to return to equilibrium conditions throughout the unsaturated specimens after the *k* test were unknown, such that this optional step was not undertaken to minimize the total test durations for the unsaturated specimens.

5.3.3 Measurement of membrane efficiency

Under closed-system conditions, ω is calculated using the following (Groenevelt and Elrick 1976; Malusis et al. 2001):

$$\omega = \frac{\Delta P}{\Delta \pi} \tag{4.1}$$

where $\Delta\pi$ is the theoretical, maximum chemico-osmotic pressure difference across an ideal semipermeable membrane (i.e., ω = 1.0) associated with an applied concentration difference across the specimen (ΔC), which can be calculated based on the van't Hoff expression, as follows (Barbour and Fredlund 1989):

$$\Delta \pi = \nu RT \Delta C \tag{4.2}$$

where ν is the number of ions from one molecule of salt (e.g., $\nu = 2$ for KCl), R is the universal gas constant (8.314 J $mol^{-1}K^{-1}$), and T is the absolute temperature in Kelvin. Values of π for a range of concentrations for different salt solutions (e.g., KCl, NaCl) are tabulated in Appendix E.

To evaluate the membrane efficiency of the clay specimen, the value of ΔC across just the clay (ΔC_{clay}) must be used in Equation 4.2. However, ΔC_{clay} cannot be directly controlled or measured, due to the presence of HAE disks along the top and bottom boundaries of the specimen to maintain a constant value of θ of the clay during circulation of the solutions. Therefore, the steady-state values of ΔC_{clay} were determined via diffusion modeling as described in detail in Chapter 4, and the results are summarized in Table 5.2.

One challenge encountered in this study was that, even with the use of high source concentrations at the top boundary (e.g., 50 mM KCl), application of a large ΔC_{clay} (e.g., > 20 mM) was difficult in the unsaturated test apparatus, due to the presence of the HAE disks. The HAE disks have low diffusion coefficients (e.g., 1.6 x 10^{-10} m^2/s) and, therefore, a significant portion of the applied concentration difference across the test system occurred within the two HAE disks (i.e., 2 x $\Delta C_{HAE} > \Delta C_{clay}$). This issue was exacerbated as the source concentration was increased, since the diffusion coefficients of the clay increased with increasing average pore-water concentration (C_{ave}) due to DDL suppression (see Chapter 4), whereas the diffusion coefficients of the HAE disks remained constant with increasing C_{ave}. However, the membrane efficiency of the clay could still be evaluated over a wide range of C_{ave}, which directly affects membrane behavior as described previously.

5.3.4 Experimental program

The experimental program to evaluate membrane behavior of unsaturated Na-bentonite specimens consisted of four multistage experiments (see Tables 5.1 and 5.2). The only difference between the experimental program for the membrane testing and the diffusion testing described in Chapter 4 was that, for the specimen with S of 0.79, the concentration stage with a source solution of 30 mM KCl was not completed successfully for the membrane testing. At the start of the 30-mM stage in the multistage test for S of 0.79, the flexible membrane lost contact with the sidewall of the specimen after an adjustment in the air-pressure line. A portion of the thin space between the flexible membrane (which was confined by the outer rigid wall) and the perimeter of the specimen was filled with pressurized air, which made accurate measurement of ΔP across the specimen impossible. The diffusion results were still measurable, as diffusion only occurred through the pore water within the specimen. Thus, membrane behavior was quantified only for one concentration stage (20 mM KCl) for the specimen at S of 0.79.

5.4 Results

5.4.1 Boundary water pressures and total suction

The boundary water pressures measured at the top, u_{top}, and bottom, u_{bottom}, of the specimen during each multistage test are presented in Figure 5.3. The magnitudes of u_{top} and u_{bottom} were approximately equal (i.e., $u_{top} \approx u_{bottom}$) for all of the tests at the end of the initial test stage, when DIW was circulated across both the top and bottom specimen boundaries to establish the baseline pressure difference across the specimen (i.e., initial ΔP, or ΔP_o). Therefore, ΔP_o was negligible for all of the tests. To avoid potential cavitation in the water pressure lines of the unsaturated tests due to negative values of u_{top} and u_{bottom}, a value of P_{air} equal to the ψ_m of the

specimen determined during specimen preparation (see Chapter 4) was applied to the specimen throughout the duration of the multistage tests via a port in the sidewall (see Chapter 2).

For the saturated specimen only, two constant-flow *k* tests were performed at the end of the DIW stage. The first test was performed at a *q* of 1.13 x 10^{-10} m^3/s, which resulted in values of u_{bottom} that exceeded the limits of the pressure transducers. The *k* test was terminated (i.e., the flow pump was shut off), and the boundary pressures were allowed to dissipate before beginning a second *k* test at a lower value of *q*. The second *k* test was performed at a *q* of 4.80 x 10^{-11} m^3/s and steady values of u_{top} and u_{bottom} were achieved without exceeding the limits of the pressure transducers. All of the pressure data for both *k* tests are provided in Appendix E. Based on the results of the calibration testing (see Chapter 2), the measured value of Δu ($=u_{top} - u_{bottom}$) was corrected for the portion of Δu that was expected to occur across the HAE disks at the *q* used in the test. The value of *k* was calculated based on Darcy's law and the Δu that occurred across the clay specimen only, as described in Chapter 2. The *k* of the saturated, Na-bentonite specimen after the DIW circulation stage was 4.1 x 10^{-12} m/s. Due to time constraints, the constant-flow *k* test was performed only for the saturated specimen, and not for the unsaturated specimens, for reasons described previously.

At the start of circulation of the 20 mM KCl solution across the top boundary, the magnitude of u_{top} increased in all of the tests and became greater than u_{bottom}, such that the chemico-osmotic pressure difference across the specimen increased. The change in u_{bottom} at the start of circulation of KCl solution was inconsistent among the tests (although u_{bottom} was always $< u_{top}$). For example, for the test with the saturated specimen (S = 1.0), the magnitude of u_{bottom} did not increase relative to the values measured during circulation of DIW, and remained at a value of approximately zero throughout the test. In contrast, for the tests with *S* of 0.89 and *S* of

0.79, the values of u_{bottom} increased relative to those measured during the DIW stage, whereas for the test with the S of 0.84, the value of u_{bottom} decreased to negative values ($u_{bottom} < 0$). This inconsistency in the trends of measured values of u_{bottom} during closed-system, multistage membrane testing has been reported previously in the literature (e.g., Kang 2008; Bohnhoff 2012).

For example, Kang (2008) performed flexible-wall membrane tests on GCL specimens. For the tests performed at σ' of 34 kPa (5 psi) and 241 kPa (35 psi), the value of u_{bottom} generally increased above the applied back pressure of 172 kPa (25 psi), whereas for the tests performed at σ' of 103 kPa (15 psi) and 172 kPa (25 psi), the values of u_{bottom} generally decreased below the back pressure.

The total suctions at the top and bottom boundaries, or $\psi_{T,top}$ and $\psi_{T,bottom}$, respectively, which are defined as the difference between the supplied air pressure and the boundary water pressures (i.e., $\psi_T = P_{air} - u$), are shown in Figure 5.4. Since the value of P_{air} was constant throughout the test, changes in the value of $\psi_{T,top}$ and $\psi_{T,bottom}$ were due to changes in u_{top} and u_{bottom}, respectively. At the start of circulation of KCl solution across the top boundary, the values of $\psi_{T,top}$ decreased below the value of $\psi_{T,bottom}$ for all of the tests, due to the increase in u_{top} caused by the membrane behavior of the specimen.

The measured values of $\psi_{T,top}$ and $\psi_{T,bottom}$ included both matric and osmotic suction components. The HAE disks maintained the specimens at a constant value of θ and, therefore, ψ_m was assumed to remain constant throughout the test. Thus, changes in the values of $\psi_{T,top}$ and $\psi_{T,bottom}$ throughout the tests were attributed to changes in the osmotic suction due to membrane behavior (ψ_π), which were equal to the changes in u_{top} and u_{bottom} described previously.

5.4.2 Chemico-osmotic pressures

As previously described, when a specimen behaves as a semipermeable membrane in a closed-system testing apparatus, a chemico-osmotic pressure will develop at the top boundary causing an increase in u_{top}. In the membrane behavior literature, the positive x-direction typically is assumed downward from the top of the specimen (e.g., Kang and Shackelford 2009), such that calculation of the chemico-osmotic pressure difference across the clay, ΔP ($= u_{bottom} - u_{top}$) results in a negative value (i.e., $\Delta P < 0$, because $u_{bottom} < u_{top}$). Thus, values of $-\Delta P$ ($= u_{top} - u_{bottom}$) typically are provided in the literature to allow for easier discussion. The values of $-\Delta P$ measured for each of the multistage tests are shown in Figure 5.5.

The steady-state values of $-\Delta P$, or $-\Delta P_{ss}$, for each test stage were determined based on the steady values measured at the end of consecutive, two-day circulation cycles, as demonstrated in the example in Figure 5.6. The resulting values of $-\Delta P_{ss}$ measured for each test stage are summarized in Table 5.2. The values of $-\Delta P_{ss}$ for the test with S of 1.0 decreased from 7.2 kPa to 4.6 kPa as the source KCl concentration at the top boundary (C_{ot}) was increased from 20 mM to 50 mM KCl (see Figure 5.5a). A similar trend was observed in the test with S of 0.89, where $-\Delta P_{ss}$ decreased from 8.3 kPa to 6.9 kPa as C_{ot} increased from 20 mM to 50 mM. The decrease in the measured value of $-\Delta P_{ss}$ with increasing C_{ot} was due to decreasing ω resulting from compression of the diffuse double layers with increasing C_{ave} due to diffusion of KCl from the upper boundary (Fritz 1986; Shackelford et al. 2003). The decreasing values of $-\Delta P_{ss}$ with increasing salt concentration are consistent with trends previously reported by others for closed-system membrane tests (e.g., Malusis and Shackelford 2002a; Bohnhoff 2012). The values of $-\Delta P_{ss}$ measured in the unsaturated tests were higher than those measured in the saturated test. The

values of $-\Delta P_{ss}$ were 8.3 kPa to 6.9 kPa, 13.7 kPa to 21.1 kPa, and 62.1 kPa, for the tests with S of 0.89, 0.84 and 0.79, respectively.

5.4.3 Membrane efficiency coefficients

The values of ω for all of the membrane tests are summarized in Table 5.2 and shown as a function of C_{ave} in Figure 5.7. The values of ω ranged from 0.31 to 0.61, 0.34 to 0.66, 0.41 to 0.71, and 0.68 to 0.75 for the tests with S values of 1.0, 0.89, 0.84 and 0.79, respectively. These values of ω are comparable to those reported in the literature for Na-bentonites. For example, Malusis and Shackelford (2002a) used a closed-system, membrane testing apparatus to measure the membrane behavior of a GCL comprised of Na-bentonite exposed to KCl solutions. For the GCL specimen with n of 0.86, which was similar to the specimens in this study with n = 0.87 to 0.89, the values of ω ranged from 0.08 to 0.42 for C_{ave} of 23.5 mM to 4.4 mM KCl, respectively. Other comparisons with values of ω reported in the literature are discussed further throughout Section 5.5.

5.5 Discussion

5.5.1 Effect of average pore-water concentration

The effects of pore-water chemistry on the swelling behavior of clays dominated by montmorillonite are well documented in the soil science literature (e.g., Norrish 1954; Norrish and Quirk 1954; van Olphen 1963; Malik et al. 1992; Prost et al. 1998). As the ionic strength of the pore water increases, the interlayer swell of montmorillonite decreases, resulting in an increase in the zone of bulk (free) pore water within the interlayer space (i.e., Zone 2 in Figure 5.1) as well as between the clods of clay (Figure 5.2). For example, Norrish and Quirk (1954)

performed x-ray diffraction measurements on Na-montmorillonite immersed in solutions of NaCl. The value of d_{001} decreased from 4.0 nm to 1.5 nm as the concentration of the NaCl solution increased from 0.3 M to 4.0 M. Thus, as the zone of bulk pore water increases with increasing salt concentration due to suppression of the diffuse double layers and reduced swell of the clay, the restriction of solutes is expected to decrease, leading to decreased values of ω.

For all of the tests conducted in this study, the values of ω decreased with increasing C_{ave}, as expected (see Figure 5.6). This trend is consistent with other trends reported in the published literature on membrane behavior of clays exposed to salt solutions of KCl, NaCl, and $CaCl_2$ (Kemper and Rollins 1966; Malusis and Shackelford 2002a; Kang and Shackelford 2009; Di Emidio 2010; Dominijanni et al. 2013; Bohnhoff et al. 2014; Malusis et al. 2014; Meier et al. 2014). Previous studies have shown an approximately semi-log linear relationship between ω and C_{ave} (Shackelford et al. 2003). The actual trend between ω versus logarithm of C_{ave} likely becomes non semi-log linear as C_{ave} approaches the limiting concentrations (i.e., the concentrations at which $\omega \rightarrow 0$ and $\omega \rightarrow 1$, see Figure 5.8) (Sherwood and Craster 2000; Shackelford et al. 2003; Revil et al. 2011; Dominijanni et al. 2013; Manassero et al. 2014; Meier et al. 2014). However, the relationship between ω and log C_{ave} may be considered approximately semi-log linear for the concentration range evaluated in this research (C_{ave} = 9 mM to 25 mM KCl), as indicated by the high values of r^2 for the regressions shown in Figure 5.9 (r^2 = 0.97 to 1.0).

The aforementioned semi-log linear relationship is shown schematically in Figure 5.8, where the rate of decrease in ω with increasing C_{ave} (i.e., the slope of the semi-log linear trend line) is referred to as the membrane index, I_ω (Shackelford et al. 2003). The semi-log linear trend line also may be used to identify two limiting values of C_{ave} (Shackelford et al. 2003): (1)

the threshold concentration, $C_{ave,\omega}$, which is the concentration below which membrane behavior occurs (i.e., $\omega > 0$ for $C_{ave} < C_{ave,\omega}$); and (2) the perfect membrane concentration, $C_{ave,pm}$, which is the concentration below which the material behaves as a perfect membrane (i.e., $\omega = 1$ for $C_{ave} < C_{ave,pm}$). Finally, a reference membrane efficiency, ω_{ref}, also can be determined with the semi-log linear regression as the value of ω when $\log C_{ave} = 0$ (see Figure 5.8). The resulting values of I_ω, $C_{ave,\omega}$, $C_{ave,pm}$, and ω_{ref} obtained from the semi-log linear regressions are summarized in Table 5.3.

The semi-log linear regressions of the data for the saturated and unsaturated Na-bentonite specimens, excluding the test with S of 0.79 due to aforementioned inadequate data to perform a regression, are shown in Figure 5.9a. The values of $C_{ave,pm}$ were relatively similar among the tests, ranging only from 2.5 mM to 3.7 mM KCl. The values of I_ω also were relatively insensitive to S, ranging only from 0.70 to 0.72, with no identifiable trend between the values of S and I_ω. However, the values of $C_{ave,\omega}$ increased as S of the specimen decreased, indicating a higher threshold concentration for destruction of membrane behavior for the unsaturated specimens. As S decreased from 1.0 to 0.84, $C_{ave,\omega}$ increased from 63 mM to 91 mM KCl. Thus, a 16 % decrease in S resulted in a 43 % increase in $C_{ave,\omega}$. This trend suggests that, relative to saturated conditions, membrane behavior of bentonite may remain relevant over a wider range of salt concentrations under unsaturated conditions.

As discussed previously, the actual trend between ω versus logarithm of C_{ave} likely becomes nonlinear as C_{ave} approaches the limiting concentrations (i.e., $C_{ave,\omega}$ and $C_{ave,pm}$). For comparison with the semi-log linear regression, the data for the specimen with S of 1.0 is shown against the nonlinear theoretical model proposed by Revil et al. (2011) for saturated clays (Figure 5.9b). The Revil et al. (2011) model is based on n, cation exchange capacity (CEC), and

the density of the soil particles (ρ_s) in the specimen. As shown in Figure 5.9b, the values of C_{ave} evaluated in this research were not near the limiting concentration values, and fell within the approximately semi-log linear portion of the nonlinear model (resulting in the aforementioned high r^2 values for the semi-log linear fit). However, a comparison between the semi-log linear and nonlinear trend lines for the saturated specimen suggests that the semi-log linear fit results in conservative estimates of $C_{ave,\omega}$ (i.e., lower than the actual value of C_{ave} that results in complete destruction of membrane behavior) and unconservative estimates of $C_{ave,pm}$ (i.e., higher than the actual C_{ave} at which the clay would continue to behave as a perfect membrane). Further evaluation of the appropriateness of the semi-log linear versus nonlinear trendline fit is beyond the scope of this study.

The results from this study are compared in Figure 5.10 with those from previous experimental studies involving Na-bentonites. All of the data shown in Figure 5.10 are for saturated Na-bentonite specimens that were part of a GCL or were prepared at a high porosity similar to that of a GCL (e.g., n = 0.7 to 0.9). As shown in Figure 5.10, the rates of decrease in ω with increasing C_{ave} (i.e., I_ω) appear relatively similar up to a C_{ave} of approximately 25 mM KCl or NaCl among all of the data sets. The likely reasons for the differences in the magnitude of the ω values measured in this research relative to the other studies are discussed further in the following section.

5.5.2 Effect of exchangeable sodium

When monovalent cations occupy the exchange sites of a bentonite, the interlayer swelling is greater relative to when multivalent cations occupy the exchange complex (Norrish 1954; van Olphen 1966; Lambe and Whitman 1969; Kolstad et al. 2004). For example, in

calcium montmorillonite, the interlayer spacing, d_{001}, does not exceed 2 nm (Norrish and Quirk 1954). The d_{001} of Na-montmorillonite, however, may exceed 12 nm (Norrish 1954). Increased interlayer spacing results in a larger fraction of the total water bound to the clay and less bulk (free) pore space available for flow, and consequently, increased solute restriction (i.e., increased ω).

Typically, the bentonites used in GCLs have approximately equal fractions of Ca^{2+} and Na^{+} on the exchange complex after manufacture of the GCL (Shackelford et al. 2000). Therefore, the bentonite in a typical GCL is expected to exhibit less swell and lower ω than a Na-bentonite that has a higher percentage (e.g., > 60 %) of the exchange complex occupied by Na^{+}. As shown in Figure 5.10, relative to other studies that evaluated membrane behavior of GCLs and GCL-grade bentonite (Malusis and Shackelford 2002a; Dominijanni et al. 2013; Malusis et al. 2014; Meier et al. 2014), the highest values of ω were reported by Kemper and Rollins (1966) and in this study. For example, for C_{ave} between 9 mM and 10 mM, Dominijanni et al. (2013) reported an ω value of 0.33 for an Na-bentonite specimen with *n* of 0.81, whereas a higher ω value of 0.61 was measured for the saturated specimen in this study (despite the higher *n* of 0.87).

For all of the studies referenced in Figure 5.10, methods to reduce excess soluble salts in the bentonite (flushing via permeation, "squeezing" via consolidation, or dialysis with water) prior to testing were employed for the purpose of enhancing any observed membrane behavior. However, bentonite specimens in the study by Kemper and Rollins (1966) and in this study also were treated via dialysis to increase the percentage of Na^{+} on the exchange complex. Thus, the higher values of ω reported herein and by Kemper and Rolllins (1966) can be attributed, in part, to a likely greater percentage of Na^{+} on the exchange complex relative to the bentonites in the

other studies. Increases in the exchangeable sodium percentage (*ESP*) of a clay have been shown to result in decreased volume of pore space accessible to anions, i.e., increased ω (Dufey and Laudelout 1976).

For example, the bentonite in the GCL tested by Malusis and Shackelford (2002a), which was the same GCL used by Malusis et al. (2014) and Meier et al. (2014), had an *ESP* of 53 %. The *ESP* of the bentonite used in this study, after dialysis treatment with 0.1 M NaCl, was 70 % (see Chapter 3). Although the bentonite *ESP* was not reported in Kemper and Rollins (1966), the bentonite had been washed repeatedly with a strong (1 M) NaCl solution, such that the exchange complex was assumed to be saturated with Na^+ (i.e., $ESP \approx 100$ %). Thus, as expected, the value of ω increases as the prevalence of Na^+ on the exchange complex of the bentonite increases, i.e., all other factors (e.g., *S*, *n*) being the same.

5.5.3 Effect of saturation and volumetric water content

The values of ω are plotted as a function of *S* and θ in Figures 5.11a and b, respectively. For all values of C_{ot}, ω increased as *S* and θ decreased, as expected based on the concepts illustrated in Figures 5.1 and 5.2. The effect of *S* on the value of ω may be discussed in terms of the ratio of the ω measured in the unsaturated specimen relative to the value of ω measured in the saturated specimen (ω_{sat}) for the same C_{ot}. This ratio, Ω (= ω/ω_{sat}), ranged from 1.08 to 1.34 for the unsaturated tests (see Table 5.2). Values of Ω also are shown in Figure 5.12 as a function of C_{ot}. As C_{ot} increased and *S* decreased, the value of Ω increased. For example, as C_{ot} increased from 20 mM to 50 mM, the value of Ω for the specimen with *S* of 0.84 increased from 1.11 to 1.34.

The statistical significance of the effects of S and C_{ot} on values of ω were analyzed in Microsoft Excel (2010, Microsoft Office, Redmond, WA) using a two-way analysis of variance (ANOVA) without replication. A two-way ANOVA analysis can be used to evaluate the relationship between a dependent variable (e.g., ω) and two independent variables (in this case, S and C_{ot}). To perform the two-way ANOVA, the data sets must be of equal size, and, therefore, the partial data set from the test with S of 0.79, which consisted of only one concentration stage, was not included. The results of the analysis indicated that, at a 95 %-confidence level (i.e., p-value < 0.05), there was a significant difference in membrane behavior due to changes in S (p-value = 7.5 x 10^{-6}, $F = 230 > F_{critical} = 7.0$). Also, as expected, there was a significant effect of the concentration stage on the value of ω (p-value = 1.03 x 10^{-6}, $F = 1966 > F_{critical} = 7.0$). Thus, the results of the study indicate there is a statistically significant increase in membrane efficiency with decreases in S, even at the high values of S evaluated in this study (≥ 0.84).

The contour plot in Figure 5.13 depicts the combined effects of changes in S and C_{ot} on the value of ω. Conceptual diagrams of the expected influence of both S and C_{ot} on membrane behavior are shown in Figure 5.14. As expected, the highest value of ω was measured under the condition with the lowest values of both S and C_{ot} (ω = 0.75 for S = 0.79 and C_{ot} = 9.9 mM), whereas the lowest value of ω (= 0.31) was measured for the specimen with the highest S (= 1.0) at the highest value of C_{ot} (= 50 mM) during the test. Therefore, the results obtained in this study support the conceptual explanations shown in Figures 5.1, 5.2 and 5.14.

5.5.4 Effect of membrane behavior on solute diffusion

The concentration gradient imposed across the specimen during the membrane behavior testing resulted in solute diffusion across the specimen from the higher concentration boundary

to the lower concentration boundary. Diffusion analyses were performed for each concentration stage of the tests to determine the effective diffusion coefficients, D^*, for Cl^- and K^+ ($D^*_{Cl^-}$ and $D^*_{K^+}$, respectively) for the bentonite. The analysis method, which was based on the traditional through-diffusion method (Shackelford 1991), and all of the diffusion results are discussed in detail in Chapter 4.

The values of $D^*_{Cl^-}$ measured for each stage of the multistage tests are provided in Table 5.4 and plotted against values of ω and the complement of ω (1 - ω) in Figures 5.15a and b, respectively. As membrane behavior trends toward that of a perfect membrane (i.e., $\omega \rightarrow 1$), transport of Cl^- becomes increasingly more restricted due to the increased anion exclusion. Thus, the values of $D^*_{Cl^-}$ are expected to decrease with increasing ω, with $D^*_{Cl^-}$ approaching zero (no solute transport) as ω approaches unity (Malusis and Shackelford 2002b; Shackelford and Lee 2003). As shown in Figure 5.15, the values of $D^*_{Cl^-}$ decreased with increasing ω for all of the values of *S* that were evaluated, as expected. For example, for the specimen with *S* of 0.89, as ω increased from 0.39 to 0.66 the value of $D^*_{Cl^-}$ decreased from 3.4×10^{-10} m^2/s to 1.8×10^{-10} m^2/s. The trends of decreasing $D^*_{Cl^-}$ with increasing ω are consistent with data in the literature for saturated Na-bentonite and GCL specimens with similar porosities (n = 0.66 – 0.89), as shown in Figure 5.16.

As discussed previously (Chapter 4), D^* is defined as follows (Shackelford and Daniel 1991):

$$D^* = D_o \tau_a \tag{4.3}$$

where D_o is the aqueous-phase or free-solution diffusion coefficient of the solute, and τ_a is the apparent tortuosity factor ($0 \leq \tau_a \leq 1$). The apparent tortuosity factor is defined as (Shackelford and Moore 2013):

$$\tau_a = \tau_m \tau_r = \tau_m (\tau_1 \tau_2 \ldots \tau_N) \tag{4.4}$$

where τ_m is the matrix (or geometric) tortuosity factor representing the geometry of interconnected pores in the porous medium, τ_r is the restrictive tortuosity factor that takes into account other factors that may reduce solute flux (e.g., membrane behavior, solute drag near the surfaces of clay particles), and N is the number of factors other than τ_m that contribute to reducing the diffusive solute mass flux (Malusis et al. 2012; Shackelford and Moore 2013).

The value of τ_a, varies from zero when there are no interconnected pores corresponding to a perfect semipermeable membrane to unity when there is no porous medium (Shackelford and Daniel 1991). Based on Equation 4.3, values of τ_a were calculated by dividing $D^*_{Cl^-}$ by the D_o for KCl ($D_{o,KCl}$) corresponding to the average concentration in the specimen (C_{ave}) at steady-state diffusion. Values of $D_{o,KCl}$ for various KCl concentrations were tabulated in Appendix D. Values of $D_{o,KCl}$ were used to calculate τ_a,, rather than the D_o value for Cl^- alone, because Cl^- and K^+ were assumed to be diffusing in the same direction during the tests, corresponding to the case of salt (mutual) diffusion (Shackelford and Daniel 1991). As shown in Table 5.4 and Figure 5.17a, values of τ_a ranged from 0.10 to 0.22 and generally decreased as ω increased, as expected. For example, for the specimen with S of 1.0 as ω increased from 0.31 to 0.61 τ_a decreased from 0.22 to 0.10.

The value of τ_m generally is considered constant for a given arrangement of soil particles, whereas τ_r is a function of ω (Malusis et al. 2012). Under the limiting condition that ω approaches 0, the value of τ_r approaches unity, assuming other restrictive effects are insignificant. Thus, when ω is zero τ_m can be assumed to be equal to τ_a based on Equation 4.4 (Malusis et al. 2012; Dominijanni et al. 2013). Under the condition of zero membrane behavior, the value of $D^*_{Cl^-}$ is equal to the matrix or pore diffusion coefficient, D_p, defined as (Shackelford and Moore 2013):

$$D_p = D_o \tau_m \tag{4.5}$$

Values of D_p were determined by extrapolating the linear regressions shown previously in Figure 5.15b to the limit where ω is zero (i.e., $D^*_{Cl^-} = D_p$ when $1 - \omega = 1$). Thus, the slopes of the regressions shown in Figure 5.15b represent the values of D_p. Values of τ_m, calculated by dividing D_p by $D_{o,KCl}$, are shown in Figure 5.17b and Table 5.4. As expected, the values of τ_m for the bentonite specimens were essentially constant, varying only from 0.30 to 0.32, confirming good reproducibility for preparation of the bentonite specimens.

Values of τ_r were calculated by dividing $D^*_{Cl^-}$ by D_p based on Equations 4.3 and 4.4. As shown in Table 5.4 and Figure 5.17c, values of τ_r ranged from 0.30 to 0.74 and generally decreased as ω increased. The trend of decreasing τ_r with increasing ω (associated with decreasing C_{ave} as discussed previously) is due to a more restrictive (more tortuous) migration pathway caused by thicker diffuse double layers (Malusis and Shackelford 2002b). For the case where membrane behavior controls τ_r and other restrictive effects are insignificant, Manassero

and Dominijanni (2003) proposed the following relationship (based on concepts presented by Ferry (1935)):

$$\tau_r = 1 - \omega \tag{4.6}$$

As shown in Figure 5.17c, the values of τ_r measured for the bentonite specimens in this research show good agreement with the linear trend in Equation 4.6. In summary, for all specimens evaluated in this research, an increase in the measured membrane behavior resulted in a decrease in the value of τ_r and reduced rates of Cl^- diffusion across the specimen.

5.6 Conclusions

Experimental research to date has focused on membrane behavior and diffusion in clays almost exclusively under saturated conditions. However, membrane behavior under unsaturated conditions also may be an important consideration for some containment applications, such as in covers for landfills and engineered and natural barriers for HLRW disposal. The potential advantages of clays exhibiting membrane behavior (e.g., reduced contaminant flux through the barrier into the environment) are likely to be more significant when such clays exist under unsaturated conditions. Therefore, a research program was undertaken to evaluate the extent and magnitude of membrane behavior of unsaturated Na-bentonite.

The effect of saturation on membrane behavior of Na-bentonite was evaluated for values of *S* ranging from 0.79 to 1.0. The experimental program consisted of four multistage experiments with concentration stages of 20 mM, 30 mM, and 50 mM KCl. The values of ω ranged from 0.31 to 0.61, 0.34 to 0.66, 0.41 to 0.71, and 0.68 to 0.75 for the tests with *S* values

of 1.0, 0.89, 0.84 and 0.79, respectively. The measured values of ω were comparable to the ranges reported in the literature for saturated Na-bentonite specimens. Consistent with the current conceptual understanding of membrane behavior, values of ω increased with decreasing values of S, $C_{ave,}$ and $D^{*}_{Cl^-}$.

The research presented herein represents the first time membrane behavior has been measured for an unsaturated soil using a closed-system testing apparatus. In addition, to the author's knowledge, the data represent the first experimental results for membrane behavior of bentonite specimens maintained under unsaturated conditions. Increased membrane behavior in Na-bentonite due to a reduction in degree of saturation was verified experimentally, contributing to the knowledge base for contaminant transport mechanisms in clays that are commonly used in chemical containment applications.

Table 5.1. Test program for evaluation of membrane behavior in saturated and unsaturated sodium bentonite.

Properties of Bentonite Specimen				Test Duration (d)				
				Stage				Total
Degree of Saturation, S	Volumetric Water Content, θ	Porosity, n	Thickness, L (mm)	DIW	20 mM KCl	30 mM KCl	50 mM KCl	
1.0	0.87	0.87	6.6	29	122	108	76	335
0.89	0.79	0.89	5.7	24	74	74, 44[a]	64[a]	280
0.84	0.74	0.88	7.7	24	104, 34[a]	90[a]	72[a]	324
0.79	0.70	0.88	8.3	24	158, 50[a]	NA		232

[a] Solution includes 500 ppm DOWICIL biocide (see Chapter 4).

Table 5.2. Results of membrane testing on Na-bentonite specimens under saturated and unsaturated conditions. All values based on chloride data.

Properties of Bentonite Specimen [a]	Source KCl Concentration, C_{ot} (mM)		Average Concentration in Clay, C_{ave} [b] (mM)	Concentration Difference Across Clay, $-\Delta C_{clay}$ (mM)	Maximum Chemico-Osmotic Pressure Difference, $-\Delta\pi$ (kPa)	Steady-state Chemico-Osmotic Pressure Difference, $-\Delta P_{ss}$ (kPa)	Membrane Efficiency Coefficient, ω	Membrane Efficiency Ratio, Ω [c]
	Target	Actual						
S = 1 L = 6.6 mm n = 0.87 θ = 0.87	20	19	9.0	2.4	11.8	7.2	0.61	NA
	30	30	15.0	2.4	11.9	5.0	0.42	
	50	49	25.0	3.0	14.8	4.6	0.31	
S = 0.89 L = 5.7 mm n = 0.89 θ = 0.79	20	21	10.5	2.6	12.5	8.3	0.66	1.08
	30	33	15.0	10.5	51.4	17.2	0.34	0.80
	30*	33*	16.5	2.4	11.6	5.6	0.48	1.16
	50*	51*	25.6	3.6	17.8	6.9	0.39	1.26
S = 0.84 L = 7.7 mm n = 0.88 θ = 0.74	20	20	9.7	2.9	14.3	9.7	0.68	1.11
	20*	20*	9.7	2.8	13.7	9.7	0.71	1.15
	30*	33*	16.5	2.9	14.3	7.6	0.53	1.27
	50*	50*	25.0	4.3	21.1	8.7	0.41	1.34
S = 0.79 L = 8.3 mm n = 0.88 θ = 0.70	20	20	9.9	18.5	90.7	62.1	0.68	1.12
	20*	20*	9.9	17.0	83.2	62.1	0.75	1.22

[a] S = degree of water saturation; n = porosity; L = thickness; θ = volumetric water content.
[b] C_{ave} = average concentration in the bentonite specimen at steady-state diffusion.
[c] $\Omega = \omega / \omega_{sat}$, where ω_{sat} is the ω value measured for the same C_{ot} for the specimen with S = 1.
Shaded portions: results are questionable due to suspected bio-activity.

Table 5.3. Results of regression analyses of the membrane efficiency (ω) values for the sodium-bentonite specimens (see Fig. 5.8).

Degree of Saturation of Bentonite Specimen, S	Regression Results: $\omega = \omega_{ref} - I_{\omega} \cdot \log C_{ave}$ [(a)]			Limiting Average Concentrations (mM)	
	ω_{ref}	I_{ω}	r^2	@ $\omega = 0$, $C_{ave,\omega}$	@ $\omega = 1$, $C_{ave,pm}$
1.0	1.29	0.717	0.984	63	2.5
0.89	1.37	0.704	0.973	88	3.4
0.84	1.41	0.720	0.997	91	3.7

[(a)] ω_{ref} = reference membrane efficiency coefficient corresponding to log C_{ave} = 0; C_{ave} = average concentration in the specimen (mM); I_{ω} = the membrane index as defined by Shackelford et al. (2003) and illustrated schematically in Fig. 5.8.

Table 5.4. Results of membrane testing and diffusion analysis for sodium-bentonite specimens.

Degree of Saturation of Bentonite Specimen, S	Source KCl Concentration, C_{ot} (mM)		Membrane Efficiency Coefficient, ω	Ion	Effective Diffusion Coefficient, D^* (m^2/s)	Matrix Diffusion Coefficient for Cl^-, D_p (m^2/s)	Tortuosity factors			
	Target	Actual					τ_m [(a)]	τ_a [(b)]	τ_r [(c)]	τ_r [(d)]
1.0	20	19	0.61	Cl^-	1.8×10^{-10}	5.6×10^{-10}	0.30	0.10	0.32	0.31
				K^+	9.3×10^{-11}			-	-	-
	30	30	0.42	Cl^-	3.1×10^{-10}			0.17	0.57	0.56
				K^+	1.9×10^{-10}			-	-	-
	50	49	0.31	Cl^-	4.1×10^{-10}			0.22	0.74	0.73
				K^+	2.9×10^{-10}			-	-	-
0.89	20	21	0.66	Cl^-	1.8×10^{-10}	5.9×10^{-10}	0.32	0.10	0.32	0.31
				K^+	6.0×10^{-11}			-	-	-
	30	33	0.34	Cl^-	4.8×10^{-11}			0.03	0.08	0.08
				K^+	2.0×10^{-11}				-	-
	30*	33*	0.48	Cl^-	3.4×10^{-10}			0.18	0.58	0.56
				K^+	3.4×10^{-11}			-	-	-
	50*	51*	0.39	Cl^-	3.4×10^{-10}			0.18	0.58	0.56
				K^+	1.7×10^{-10}			-	-	-
0.84	20	20	0.68	Cl^-	1.7×10^{-10}	5.8×10^{-10}	0.31	0.09	0.29	0.28
				K^+	1.3×10^{-10}			-	-	-
	20*	20*	0.71	Cl^-	1.8×10^{-10}			0.10	0.31	0.30
				K^+	1.4×10^{-10}			-	-	-
	30*	33*	0.53	Cl^-	3.0×10^{-10}			0.16	0.52	0.51
				K^+	2.4×10^{-10}			-	-	-
	50*	50*	0.41	Cl^-	3.1×10^{-10}			0.17	0.54	0.53
				K^+	3.1×10^{-10}			-	-	-
0.79	20	20	0.68	Cl^-	2.3×10^{-12}	NA				
				K^+	2.1×10^{-12}					
	20*	20*	0.75	Cl^-	5.7×10^{-12}					
				K^+	4.2×10^{-12}					

* Includes biocide.

Shaded = Results are questionable due to suspected bio-activity.

(a) τ_m = matric tortuosity = $D_p / D_{o,KCl}$, where the value of $D_{o,KCl}$ corresponds to the concentration where $\omega = 0$ (i.e., $C_{ave,\omega}$).

(b) τ_a = apparent tortuosity = $D^*/D_{o,KCl}$, where values of $D_{o,KCl}$ were calculated as a function of average concentration.

(c) τ_r = restrictive tortuosity = D^*/D_p, where values of $D_{o,KCl}$ were assumed constant, and therefore D_p (= $\tau_m D_{o,KCl}$) was constant..

(d) $\tau_r = D^*/\tau_m D_{o,KCl}$, where values of $D_{o,KCl}$ were calculated as a function of average concentration (see Appendix D).

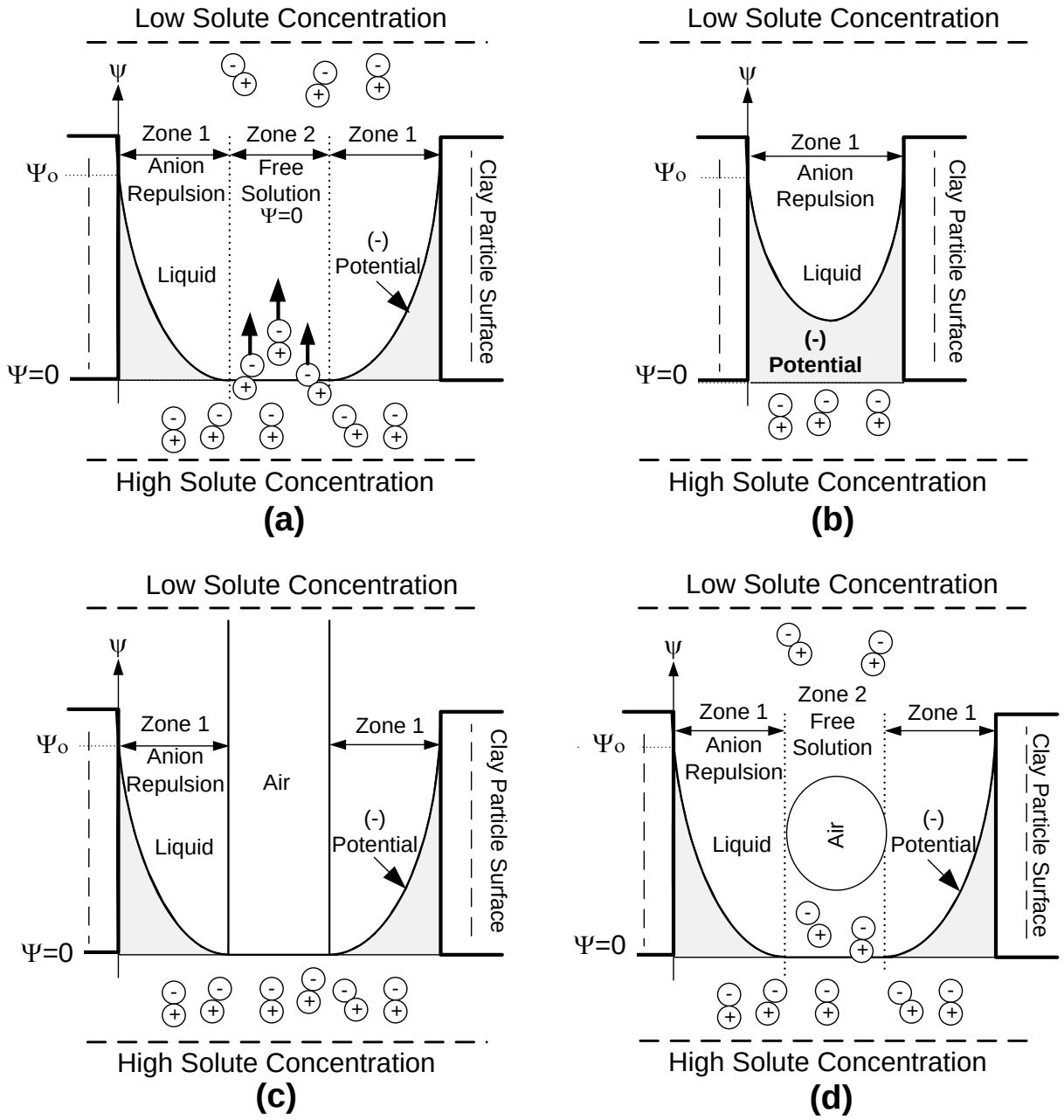

Figure 5.1. Conceptual schematics of influence of saturation conditions on solute restriction between clay particles: (a) water-saturated pores (S = 1) with no solute restriction; (b) S = 1 with complete solute restriction; (c) unsaturated pores (S < 1) with complete restriction from continuous air phase; (d) S < 1 with complete restriction from discontinuous (occluded) air.

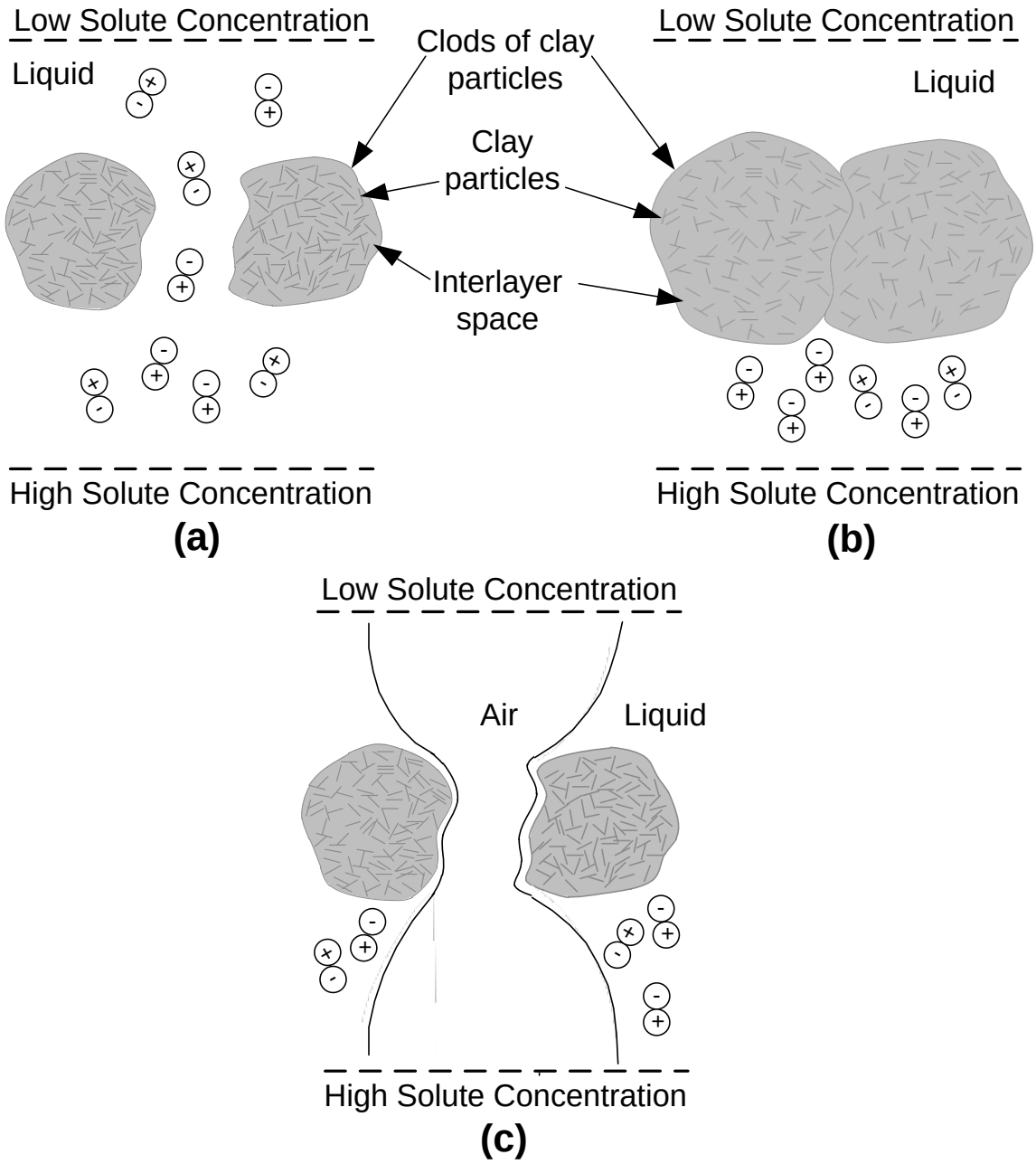

Figure 5.2. Conceptual schematics of influence of saturation conditions on solute restriction between clay clods: (a) water-saturated pores (S = 1) with crystalline swell only and no solute restriction; (b) S = 1 with crystalline and osmotic swell leading to complete solute restriction; and (c) unsaturated pores (S < 1) with crystalline swell only and complete restriction.

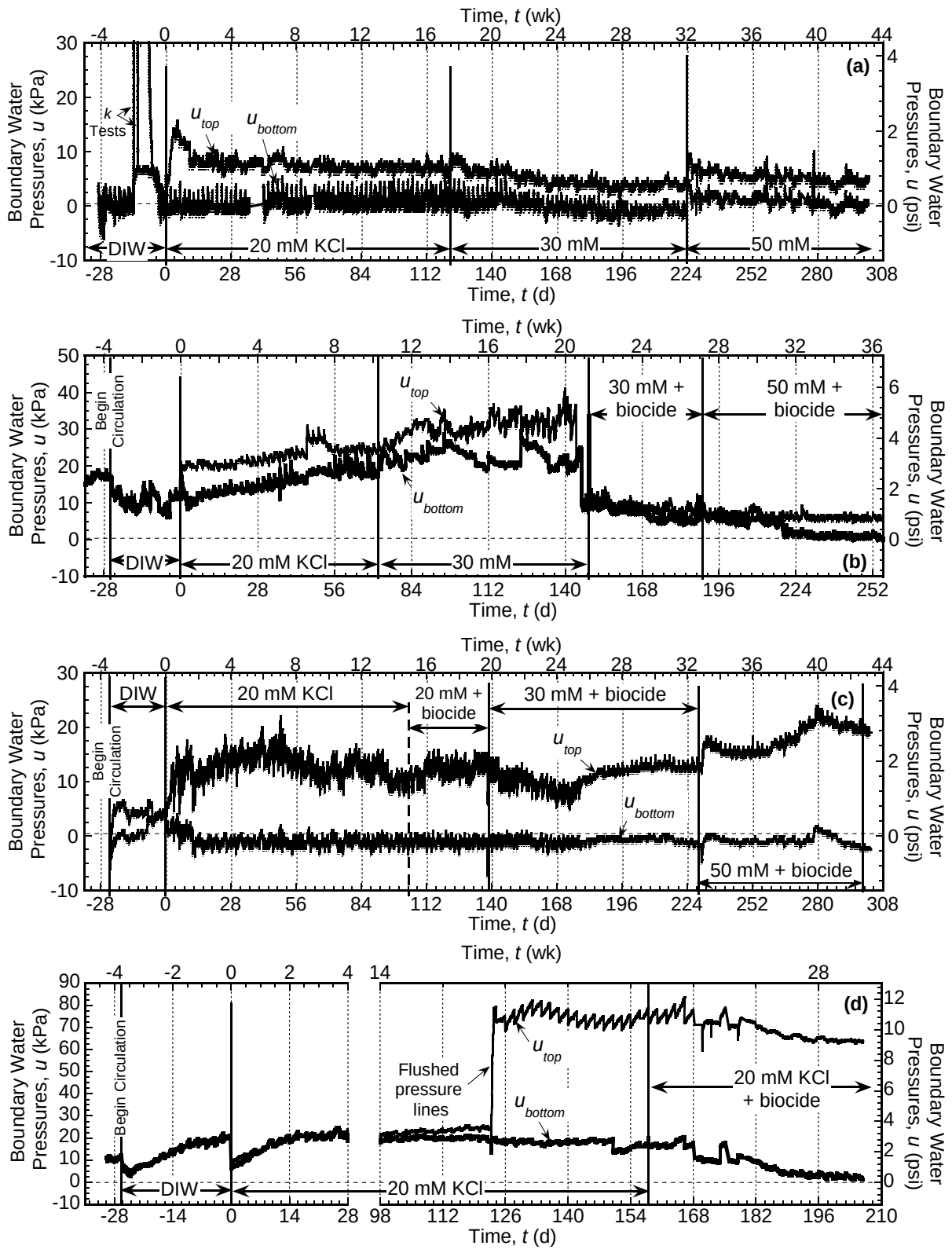

Figure 5.3. Boundary water pressures for Na-bentonite specimens during membrane testing: (a) S = 1.0; (b) S = 0.89; (c) S = 0.84; (d) S = 0.79.

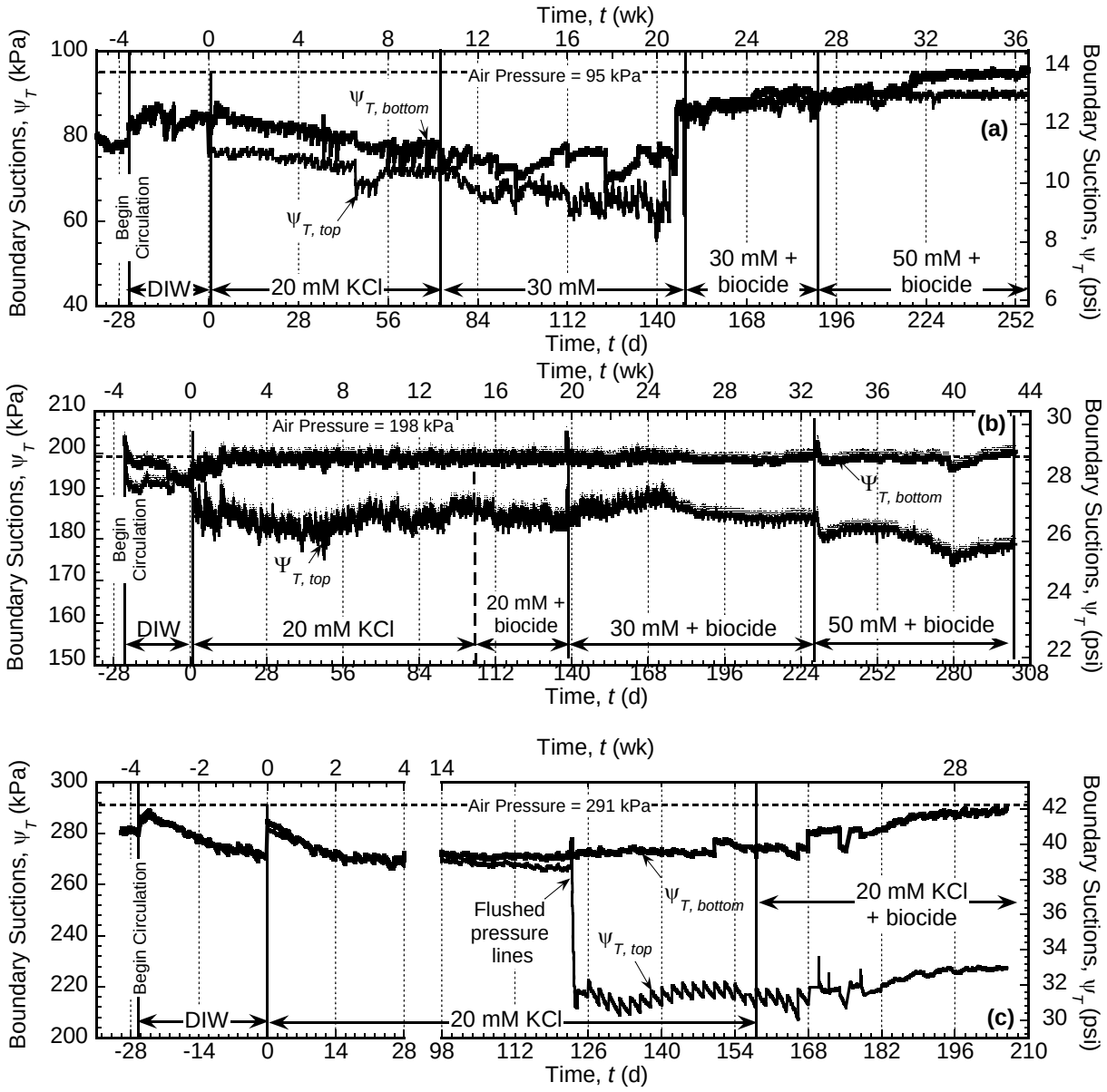

Figure 5.4. Measured total suctions at boundaries of Na-bentonite specimens during membrane testing: (a) S = 0.89; (b) S = 0.84; (c) S = 0.79.

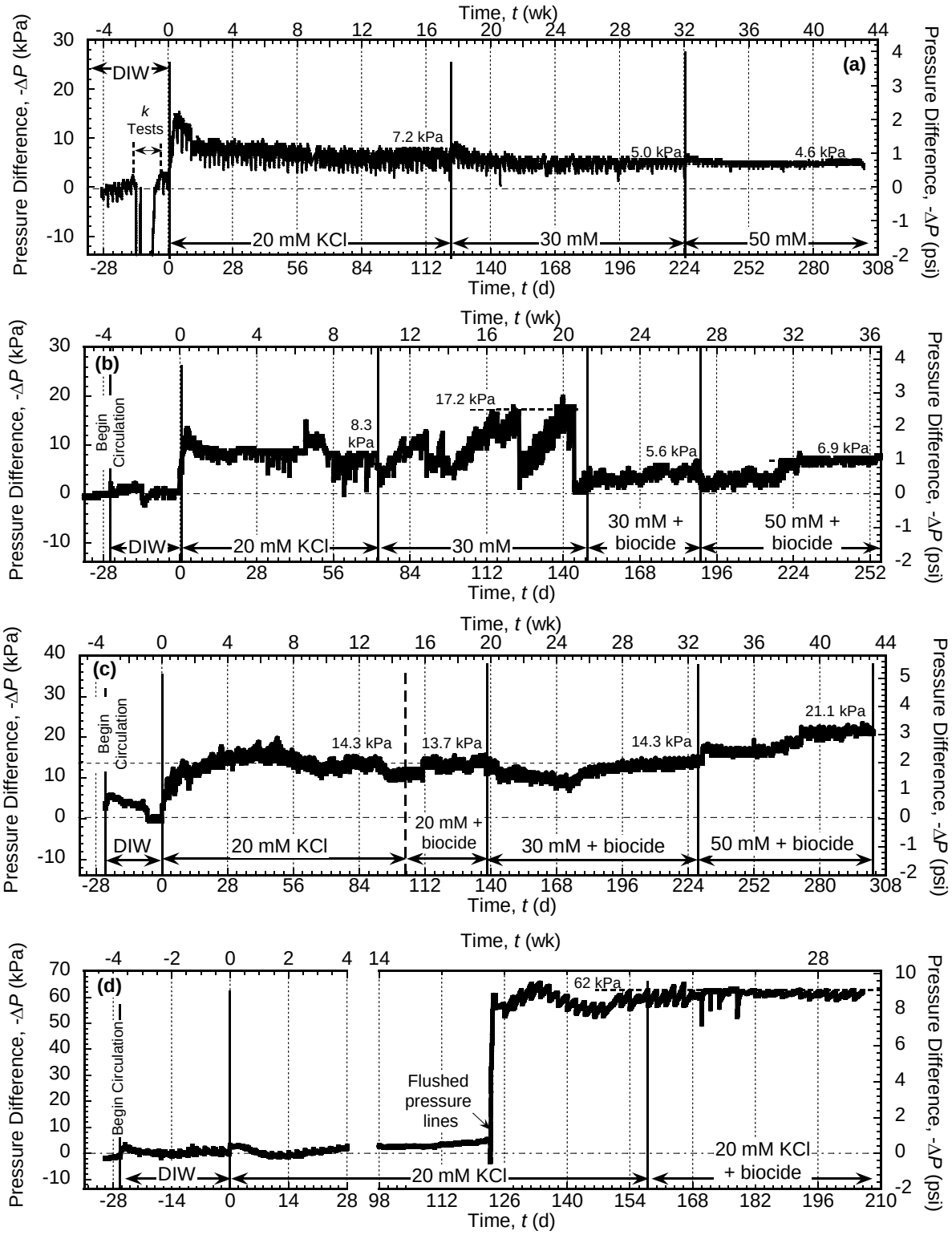

Figure 5.5. Measured chemico-osmotic pressure differences, -Δ*P*, across Na-bentonite specimens: (a) *S* = 1.0; (b) *S* = 0.89; (c) *S* = 0.84; (d) *S* = 0.79. [Values of -ΔP_{ss} are shown]

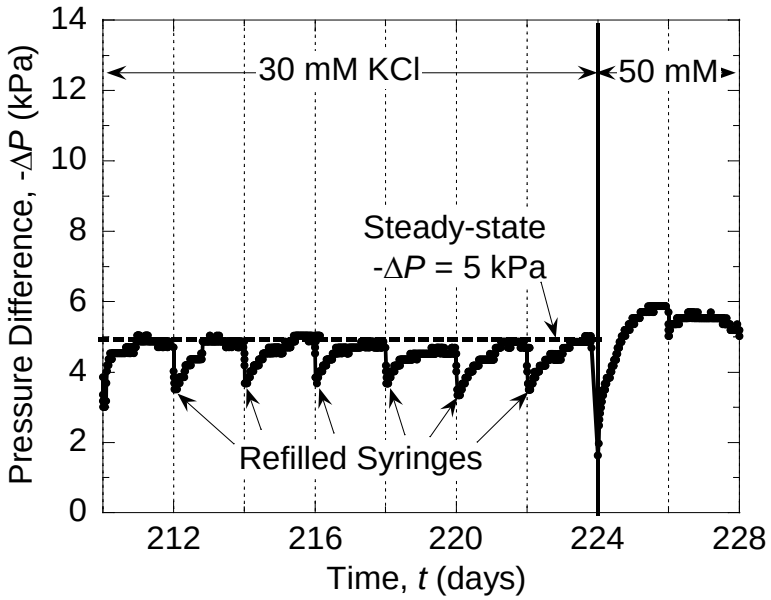

Figure 5.6. Typical example of chemico-osmotic pressure difference (-Δ*P*) during two-day circulation cycle and determination of steady-state -Δ*P* (-ΔP_{ss}) at the end of a concentration stage during membrane testing. Example data is for the 30 mM KCl stage of the Na-bentonite specimen with *S* of 1.0.

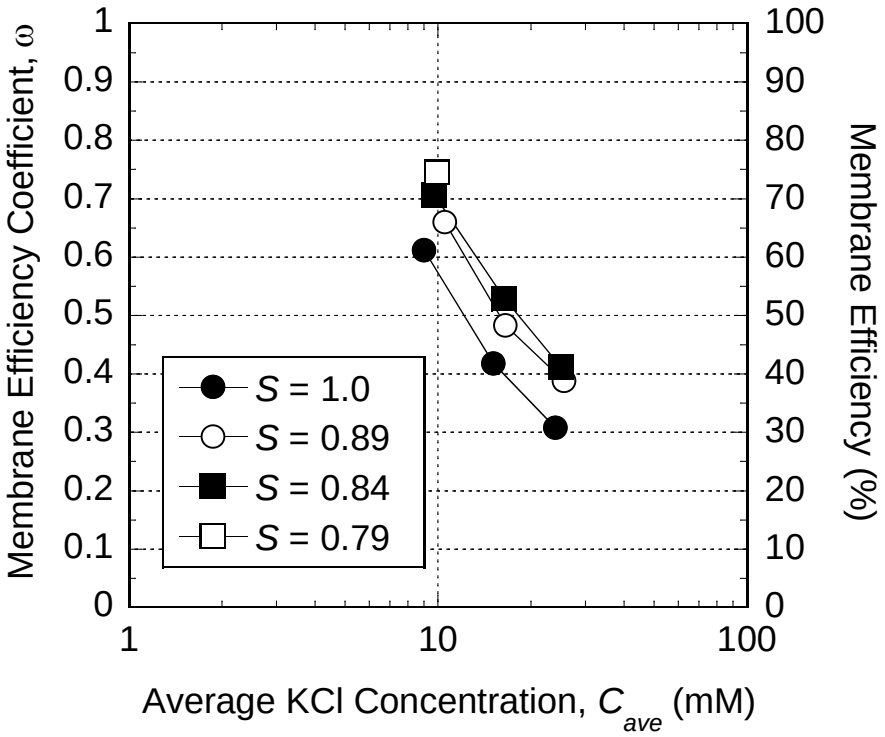

Figure 5.7. Steady-state membrane efficiency coefficients of Na-bentonite specimens during membrane testing as a function of average salt concentration in the specimen at steady-state diffusion. [*S* = degree of saturation]

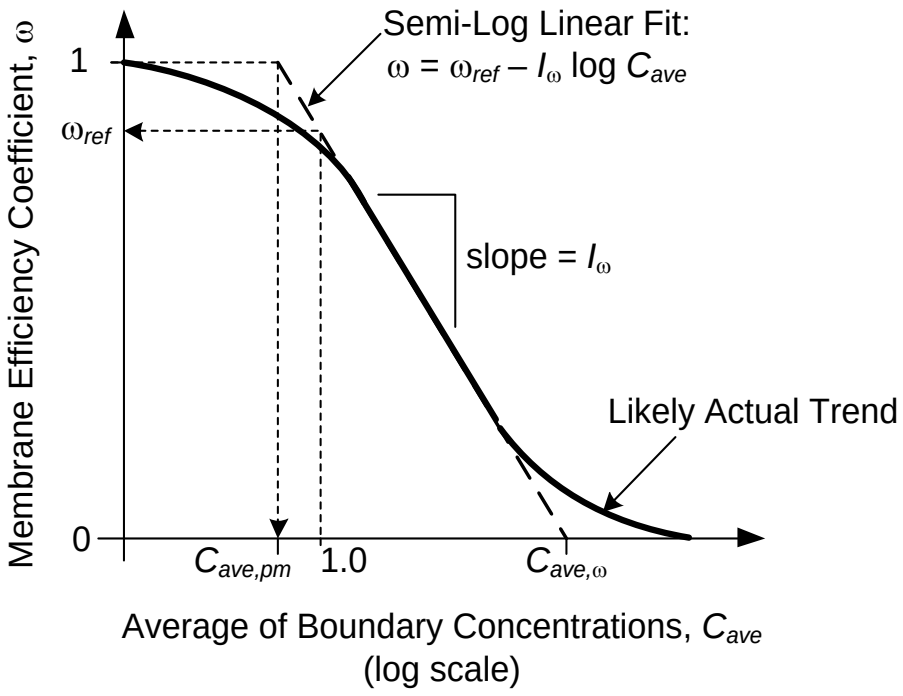

Figure 5.8. Schematic illustration of membrane efficiency, ω, versus average boundary salt concentration (after Shackelford et al. 2003) [ω_{ref} = reference membrane efficiency coefficient at log C_{ave} = 0; $C_{ave,\omega}$ = threshold concentration corresponding to ω = 0; $C_{ave,pm}$ = perfect membrane concentration corresponding to ω = 1; I_ω = membrane index].

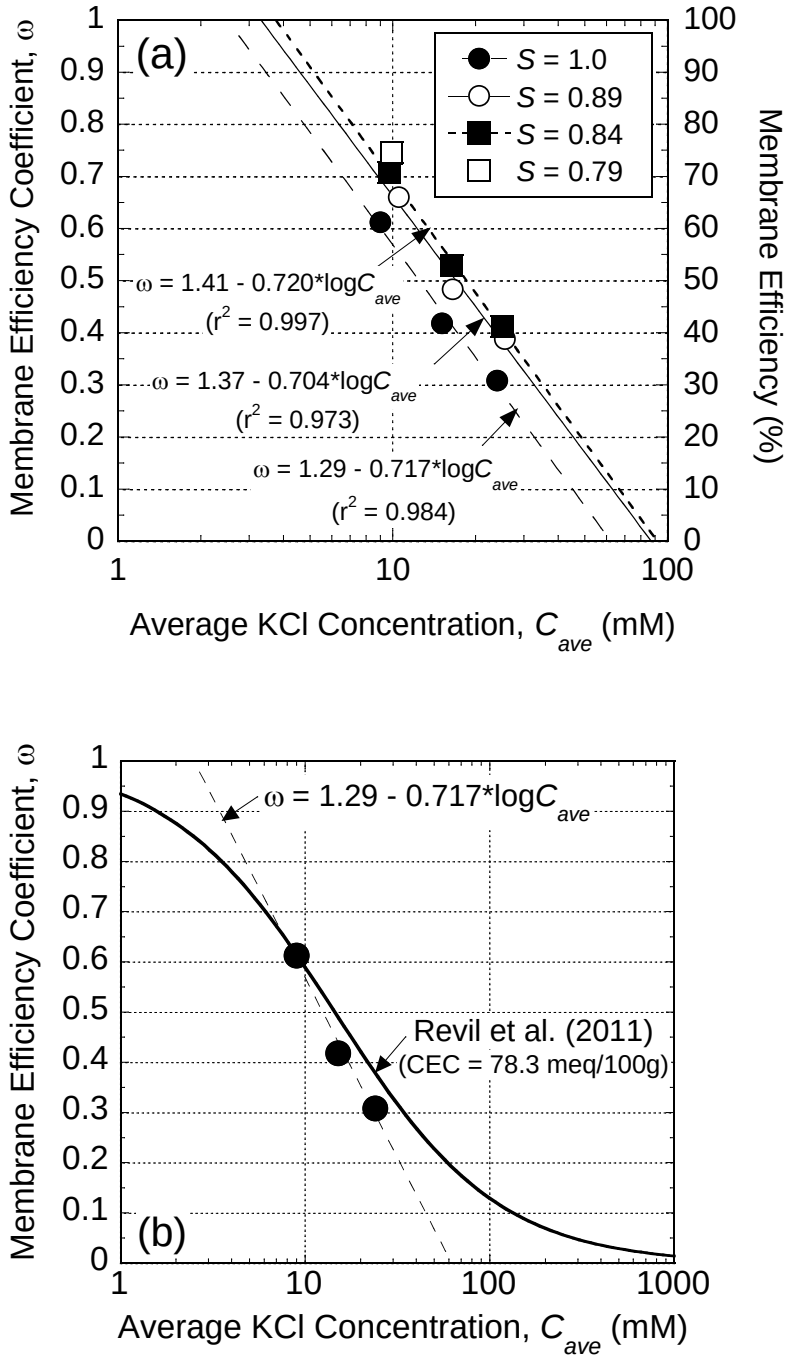

Figure 5.9. Membrane efficiency coefficients for Na-bentonite specimens as a function of average salt concentration in the specimen at steady-state diffusion: (a) semi-log linear regressions for all data; (b) comparison of data for saturated specimen with nonlinear theoretical model from Revil et al. (2011) for saturated clays. [CEC = measured cation exchange capacity of the bentonite]

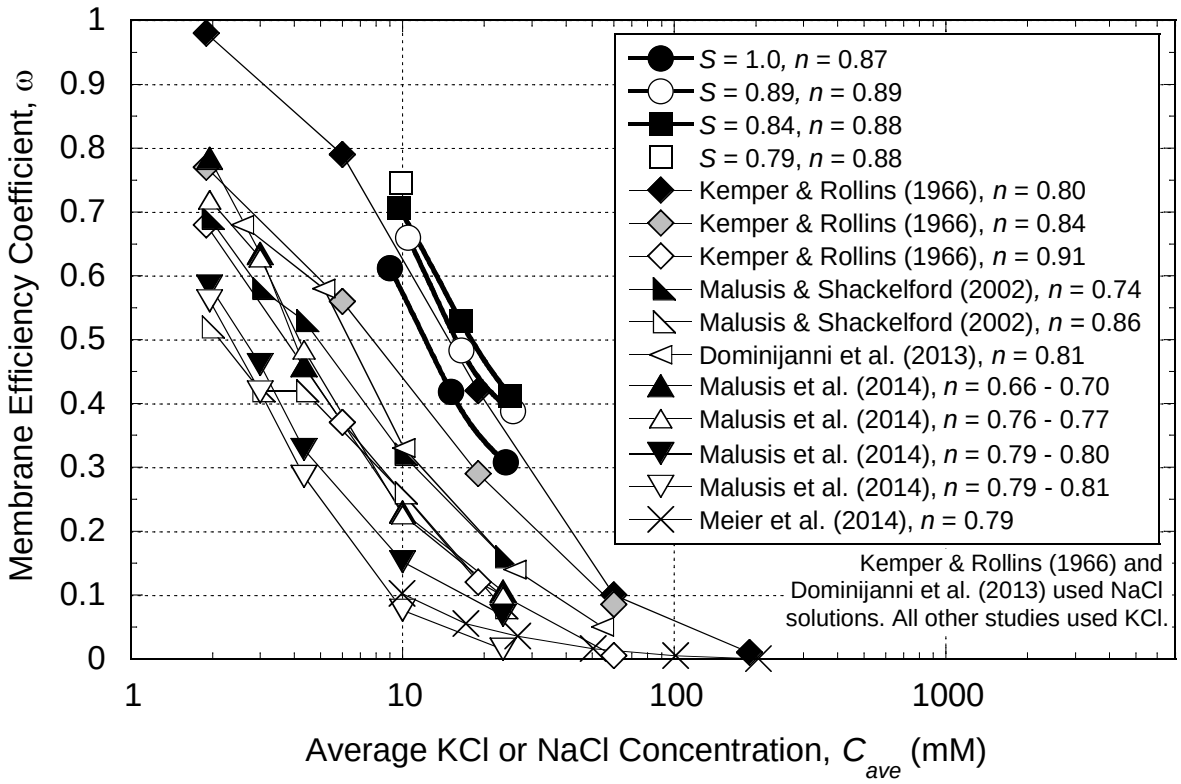

Figure 5.10. Comparison of membrane efficiency coefficients for Na-bentonite with published values for membrane tests on geosynthetic clay liners (GCLs) and Na-bentonite specimens subjected to KCl or NaCl solutions.

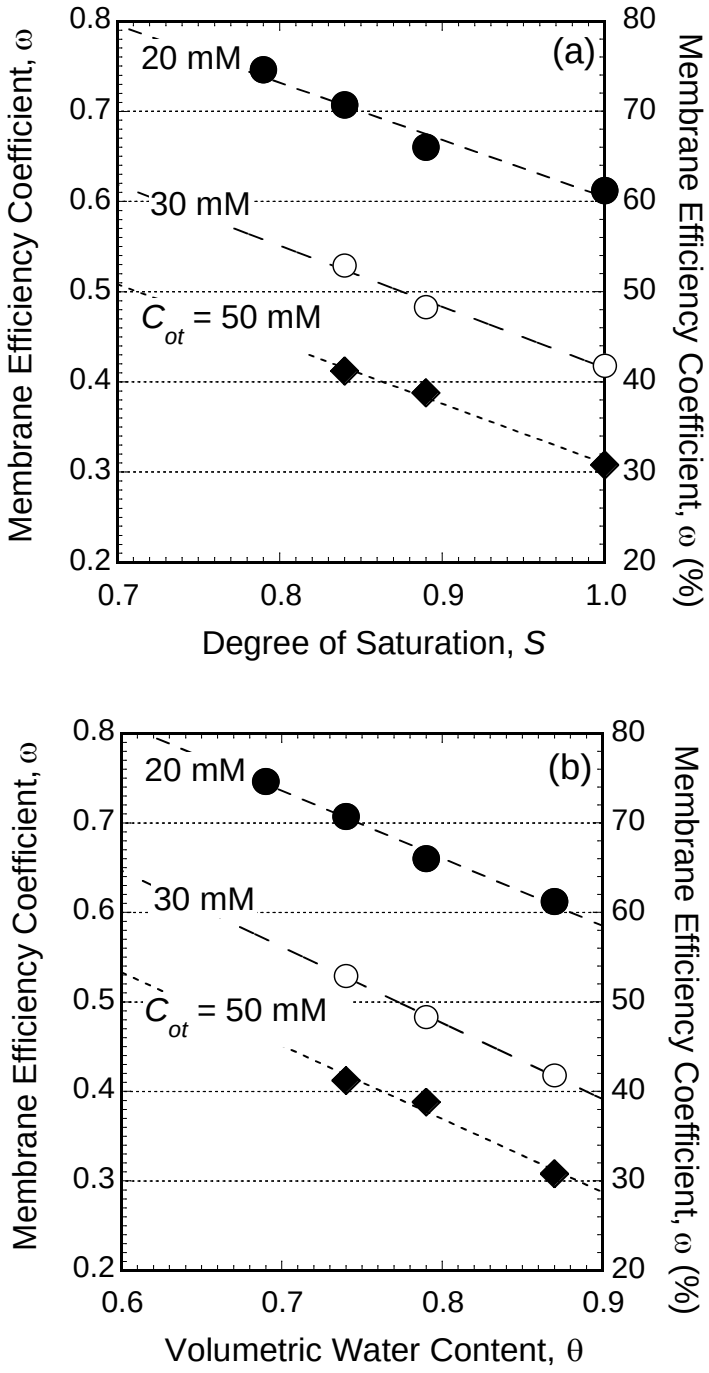

Figure 5.11. Membrane efficiency coefficients of Na-bentonite specimens as a function of (a) degree of saturation and (b) volumetric water content.

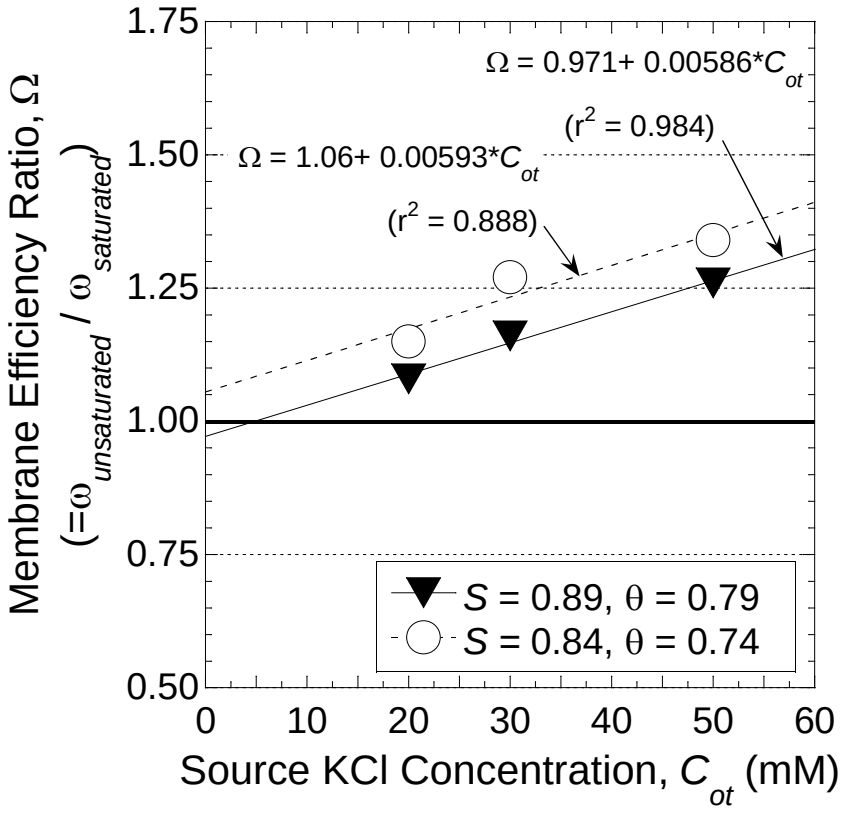

Figure 5.12. Membrane efficiency ratio, Ω, of Na-bentonite specimens as a function of source concentration of the circulation solution at the top boundary, C_{ot}.

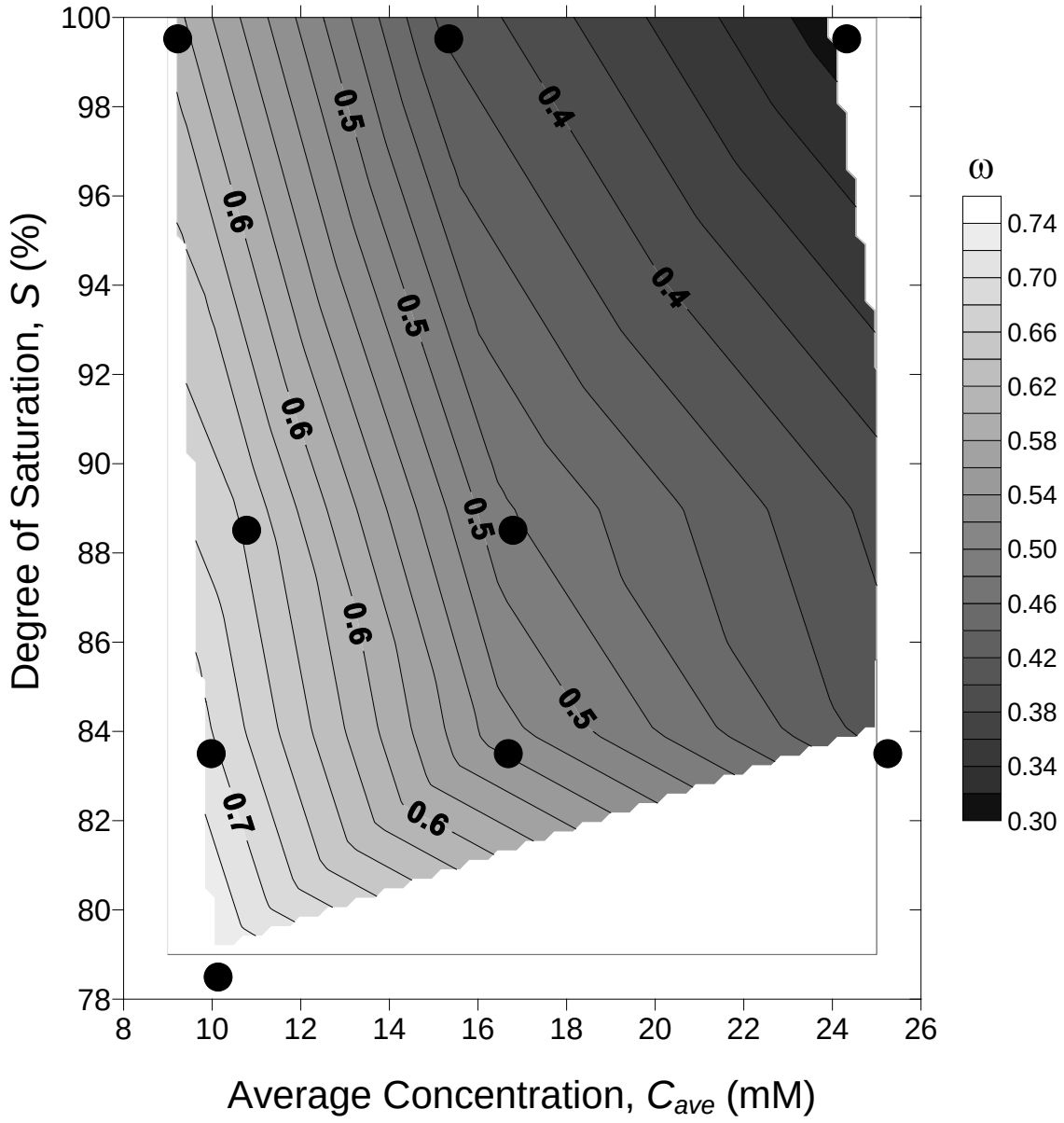

Figure 5.13. Contour plot of measured value of membrane efficiency (ω) as a function of average concentration in the specimen at steady-state diffusion (C_{ave}) and degree of saturation (S).

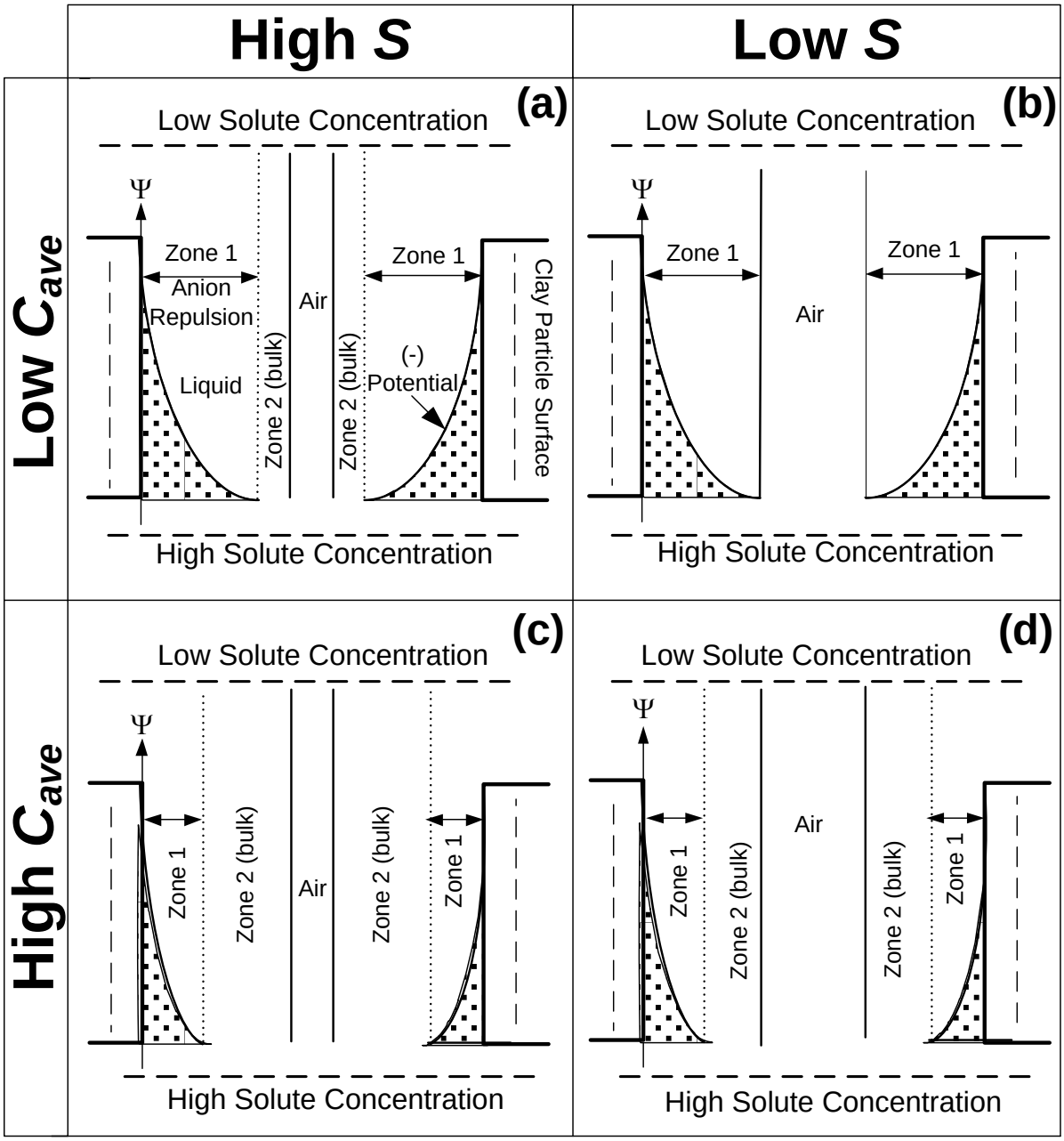

Figure 5.14. Conceptual examples of the coupled effects of degree of saturation, *S*, and average concentration in the pore space of the clay specimen, C_{ave}, on measured membrane efficiency of the clay: (a) high *S*, low C_{ave}; (b) low *S*, low C_{ave}; (c) high *S*, high C_{ave}; (d) low *S*, high C_{ave}.

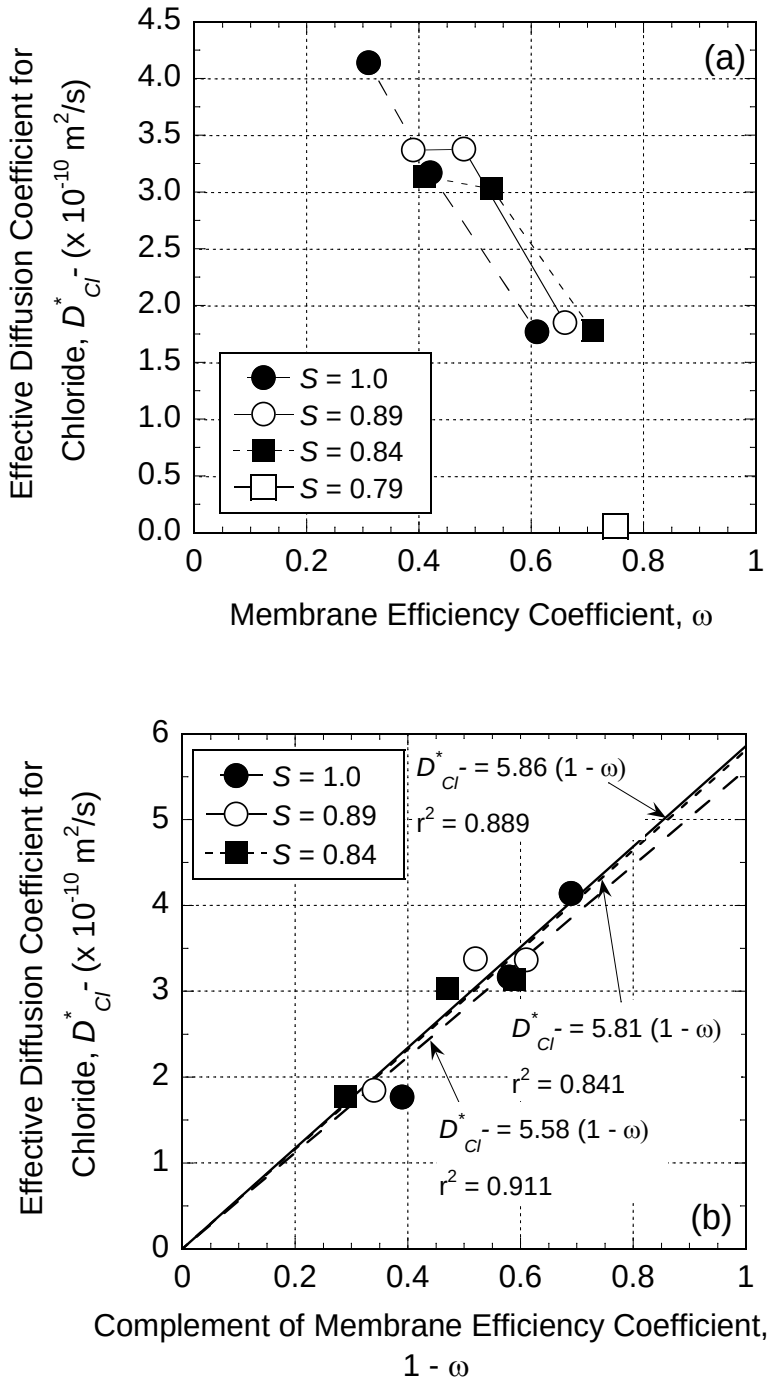

Figure 5.15. Effective diffusion coefficients as a function of membrane efficiency of Na-bentonite specimens: (a) all data; (b) linear regressions to determine the matrix diffusion coefficient (D_p) at ω = 0 (excludes S = 0.79 data point).

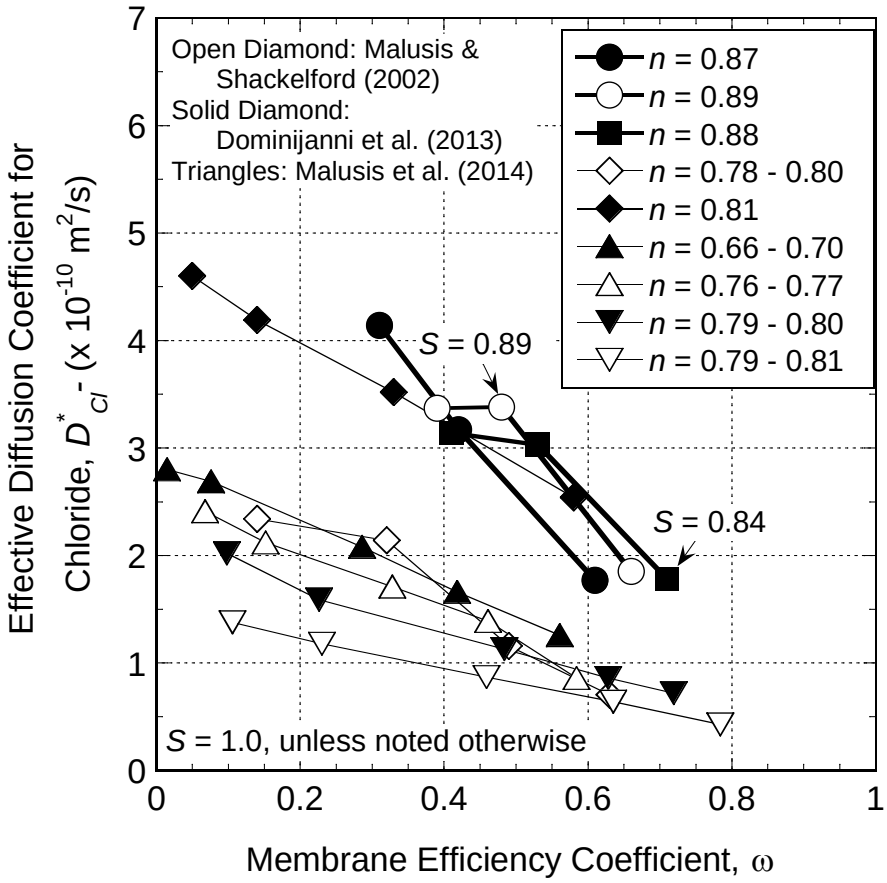

Figure 5.16. Comparison of effective diffusion coefficients for chloride for Na-bentonite specimens versus those for geosynthetic clay liners (GCLs) as a function of membrane efficiency.

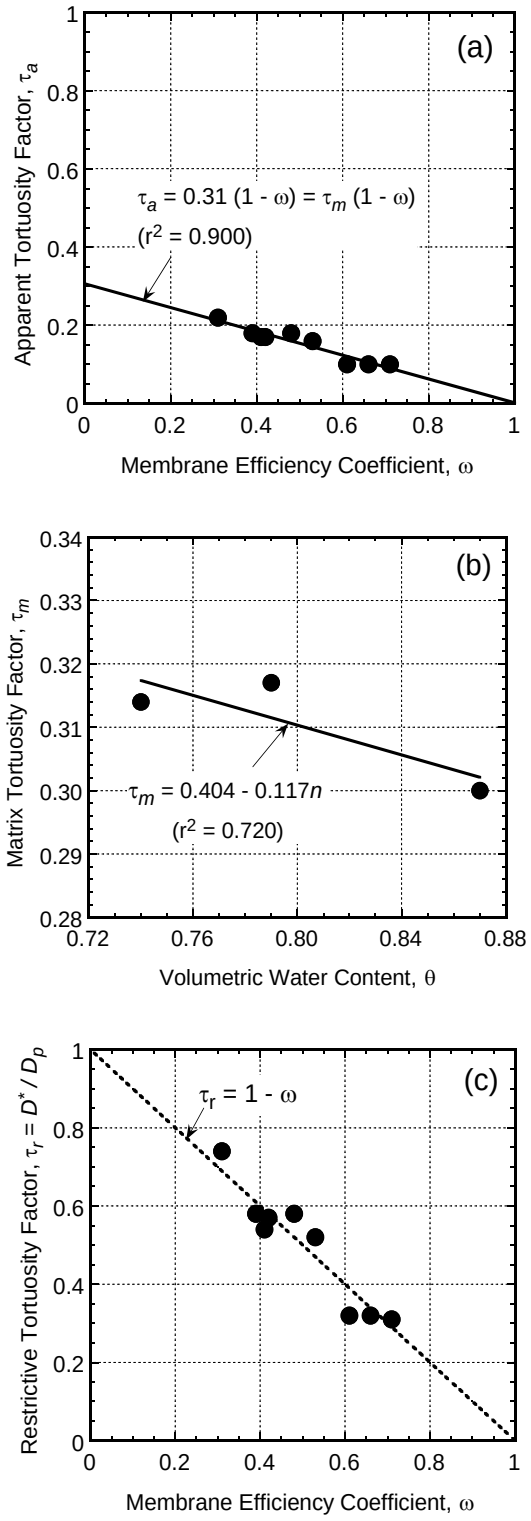

Figure 5.17. Factors for (a) apparent, (b) matrix, and (c) restrictive tortuosity for Na-bentonite specimens based on the membrane behavior and diffusion tests results for chloride.

REFERENCES

Allred, B. (2007). "Effects of nitrate concentration and ionic strength on nitrate anion exclusion under unsaturated flow conditions." *Soil Science*, 172(11), 842–860.

Allred, B. (2008). "Cation effects on nitrate mobility in an unsaturated soil." *Transactions of the American Society of Agricultural and Biological Engineers*, 51(6), 1997–2012.

Barbour, S., and Fredlund, D. (1989). "Mechanisms of osmotic flow and volume change in clay soils." *Canadian Geotechnical Journal*, 26(4), 551–562.

Bohnhoff, G. (2012). *Membrane Behavior, Diffusion, and Compatibility of a Polymerized Bentonite for Containment Barrier Applications*. PhD Dissertation, Colorado State University, Fort Collins, CO.

Bohnhoff, G., Shackelford, C., and Sample-Lord, K. (2014). "Calcium-resistant membrane behavior of polymerized bentonite." *Journal of Geotechnical and Geoenvironmental Engineering*, 140(3), 040113029-1– 04013029-12.

Bradshaw, S., and Benson, C. (2014). "Effect of municipal solid waste leachate on hydraulic conductivity and exchange complex of geosynthetic clay liners." *Journal of Geotechnical and Geoenvironmental Engineering*, 140(4), 04013038-1–04013038-17.

Bresler, E. (1973). "Anion exclusion and coupling effects in non-steady transport through unsaturated soils: II. Theory." *Proceedings of the Soil Science Society of America*, 37(5), 663–669.

Bresler, E., and Laufer, A. (1974). "Anion exclusion and coupling effects in non-steady transport through unsaturated soils: II. Laboratory and numerical experiments." *Proceedings of the Soil Science Society of America*, 38(2), 213-218.

Chen, J., Bradshaw, S., Likos, W., Benson, C., and Edil, T. (2014). "Hydraulic conductivity of geosynthetic clay liners to synthetic coal combustion product leachates." *Proceedings of Geo-Congress 2014: Geo-Characterization and Modeling for Sustainability*, M. Abu-Farsakh, X. Yu, and L.R. Hoyos, Eds., Geotechnical Special Publication 234, ASCE, Reston, VA, 334–342.

Deer, W., Howie, R., and Zussman, J. (1992). *An Introduction to the Rock-forming Minerals*, 2nd ed., *Addison Wesley Longman Limited*, Essex.

Di Emidio, G. (2010). *Hydraulic and Chemico-Osmotic Performance of Polymer Treated Clay*. PhD Dissertation, University of Ghent, Ghent, Belgium.

Dominijanni, A., Manassero, M., and Puma, S. (2013). "Coupled chemical-hydraulic-mechanical behavior of bentonites." *Géotechnique*, 63(3), 191–205.

Dufey, J., and Laudelout, H. (1976). "Hydration numbers of sodium-calcium montmorillonite." *Soil Science*, 121(2), 72–75.

Evans, J., Shackelford, C., Yeo, S., and Henning, J. (2008). "Membrane behavior of soil–bentonite slurry-trench cutoff walls." *Soil and Sediment Contamination*, 17(4), 316–322.

Fang, H.-Y., and Evans, J. (1988). "Long-term permeability tests using leachate on a compacted clayey liner material." *Groundwater Contamination: Field Methods, ASTM STP 963*, A. Collins and A. Johnson, Eds., Philadelphia, 397–404.

Ferry, J. (1935). "Statistical evaluation of sieve constants in ultrafiltration." *Journal of General Physiology*, 20(1), 95–104.

Fritz, S. (1986). "Ideality of clay membranes in osmotic processes: A review." *Clays and Clay Minerals*, 34(2), 214–223.

Fritz, S., and Marine, W. (1983). "Experimental support for a predictive osmotic model of clay membranes." *Geochimica et Cosmochimica Acta*, 47(8), 1515–1522.

Grim, R. (1968). *Clay Mineralogy*, 2nd ed., *McGraw-Hill Book Company, Inc.*, New York.

Grim, R., and Güven, N. (1978). "Bentonites: geology, mineralogy, properties and uses." *Developments in Sedimentology*, Vol. 24, *Elsevier*, New York, NY.

Groenevelt, P., and Bolt., G. (1969). "Non-equilibrium thermodynamics of the soil-water system." *Journal of Hydrology*, 7(4), 358–399.

Groenevelt, P. and Elrick, D. (1976). "Coupling phenomena in saturated homo-ionic montmorillonite: II. Theoretical." *Soil Science Society of America Journal*, 40(6), 820-823.

James, R. and Rubin, J. (1986). "Transport of chloride ion in a water-saturated soil exhibiting anion exclusion." *Soil Science Society of America Journal*, 50(5), 1142-1149.

Kang, J. (2008). *Membrane Behavior of Clay Liner Materials*. PhD Dissertation, Colorado State University, Fort Collins, CO.

Kang, J., and Shackelford, D. (2009). "Clay membrane testing using a flexible-wall cell under closed-system boundary conditions." *Applied Clay Science*, 44(1-2), 43–58.

Kang, J. and Shackelford, C. (2010). "Membrane behavior of compacted clay liners." *Journal of Geotechnical and Geoenvironmental Engineering*, 136(10), 1368–1382.

Kang, J. and Shackelford, C. (2011). "Consolidation enhanced behavior of a geosynthetic clay liner." *Geotextiles and Geomembranes*, 29(6), 544–556.

Kemper, W. (1961). "Movement of water as affected by free energy and pressure gradients: II. Experimental analysis of porous systems in which free energy and pressure gradients act in opposite directions." *Proceedings of the Soil Science Society of America*, 25(4), 260–265.

Kemper, W., and Massland, D. (1964). "Reduction in salt content of solution passing through thin films adjacent to charged surfaces." *Proceedings of the Soil Science Society of America*, 28(3), 318–323.

Kemper, W., and Quirk, J. (1972). "Ion mobilities and electric charge of external clay surfaces inferred from potential differences and osmotic flow." *Soil Science Society of America Journal*, 36(3), 426–433.

Kemper, W. and Rollins, J. (1966). "Osmotic efficiency coefficients across compacted clays." *Proceedings of the Soil Science Society of America*, 30(5), 529–534.

Kharaka, Y. and Berry, F. (1973). "Simultaneous flow of water and solutes through geologic membranes, I. Experimental investigation." *Geochimica et Cosmochimica Acta*, 37(12), 2577-2603.

Kolstad, D., Benson, C., and Edil, T. (2004). "Hydraulic conductivity and swell of nonprehydrated geosynthetic clay liners permeated with multispecies inorganic solutions." *Journal of Geotechnical and Geoenvironmental Engineering*, 130(12), 1236–1249.

Lambe, T., and Whitman, R. (1969). *Soil Mechanics*. Wiley, New York.

Letey, J., Kemper, W., and Noonan, L. (1969). "The effect of osmotic pressure gradients on water movement in unsaturated soil." *Proceedings of the Soil Science Society of America*, 33(1), 16–18.

Lu, N., Godt, J., and Wu, D. (2010). "A closed-form equation for effective stress in unsaturated soil." *Water Resources Research*, 46(5), 1–14.

Malik, M., Mustafa, M. A., and Letey, J. (1992). "Effect of mixed Na/Ca solutions on swelling, dispersion, and transient water flow in unsaturated montmorillonitic soils." *Geoderma*, 52(1-2), 17–28.

Malusis, M., Kang, J., and Shackelford, C. (2014). "Restricted salt diffusion in a geosynthetic clay liner." *Environmental Geotechnics*, ICE, Thomas Telford Ltd., London (http://dx.doi.org/10.1680/envgeo.13.00080).

Malusis, M., Shackelford, C., and Olsen, H. (2001). "A laboratory apparatus to measure chemico-osmotic efficiency coefficients for clay soils." *Geotechnical Testing Journal*, 24(3), 229–242.

Malusis, M., and Shackelford, C. (2002a). "Chemico-osmotic efficiency of a geosynthetic clay liner." *Journal of Geotechnical and Geoenvironmental Engineering*, 128(2), 97–106.

Malusis, M., and Shackelford, C. (2002b). "Coupling effects during steady-state solute diffusion through a semipermeable clay membrane." *Environmental Science and Technology*, 36(6), 3212–1319.

Malusis, M., Shackelford, C., and Maneval, J. (2012). "Critical review of coupled flux formations for clay membranes based on nonequilibrium thermodynamics." *Journal of Contaminant Hydrology*, Vol. 138–139, 40–59.

Manassero, M. and Dominijanni, A. (2003). "Modelling the osmosis effect on solute migration through porous media." *Géotechnique*, 53(5), 481–492.

Manassero, M., Dominijanni, A., Musso, G., and Puma, S. (2014). "Coupled phenomena in contaminant transport." *Proceedings, 7th International Conference on Environmental Geotechnics*, A. Bouazza, S. Yuen, and B. Brown, Eds., Nov. 10-14, 2014, Melbourne, Australia, 2014 Engineers Australia (ISBN 978-1-922107-23-7), *Proceedings of the 7th International Conference on Environmental Geotechnics*, A. Bouazza, S. Yuen, and B. Brown, Eds., Nov. 10-14, 2014, Melbourne, Australia, 2014 Engineers Australia (ISBN 978-1-922107-23-7).

Marine, I., and Fritz, S. (1981). "Osmotic model to explain anomalous hydraulic heads." *Water Resources Research*, 17(1), 73–82.

McBride, M. (1994). *Environmental Chemistry of Soils*, Oxford University Press, New York.

McKelvey, J., and Milne, I. (1962). "The flow of salt solutions through compacted clay." *Proceedings of the 9th National Conference on Clays and Clay Minerals*, Pergamon Press, 248–259.

Meier, A., Sample-Lord, K., Castelbaum, D., Kallase, S., Moran, B., Ray, T., and Shackelford, C. (2014) "Persistence of semipermeable membrane behavior for a geosynthetic clay liner." *Proceedings, 7th International Conference on Environmental Geotechnics*, A. Bouazza, S. Yuen, and B. Brown, Eds., Nov. 10-14, 2014, Melbourne, Australia (ISBN 978-1-922107-23-7), 496–503.

Mitchell, J., and Soga, K. (2005). *Fundamentals of Soil Behavior*, 3rd ed. *John Wiley and Sons*, New York.

Norrish, K. (1954). "Manner of swelling of montmorillonite." *Nature*, 173(4397), 256–257.

Norrish, K., and Quirk. J. (1954). "Crystalline swelling of montmorillonite, use of electrolytes to control swelling." *Nature*, 173(4397), 255–256.

Olsen, H. (1969). "Simultaneous fluxes of liquid and charge in saturated kaolinite." *Proceedings of the Soil Science Society of America*, 33(3), 338–344.

Olsen, H. (1972). "Liquid movement through kaolinite under hydraulic, electric, and osmotic gradients." *American Association of Petroleum Geologists Bulletin*, 56(10), 2022–2028.

Prost, R., Koutit, T., Benchara, A., and Huard, E. (1998). "State and location of water adsorbed on clay minerals: Consequences of the hydration and swelling-shrinkage phenomena." *Clays and Clay Minerals*, 46(2), 117–131.

Rao, S., Thyagaraj, T., and Rao, P. (2013). "Crystalline and osmotic swelling of an expansive clay inundated with sodium chloride solutions." *Geotechnical and Geological Engineering*, 31(4), 1399–1404.

Revil, A., Woodruff, W., and Lu, N. (2011). "Constitutive equations for coupled flows in clay materials." *Water Resources Research*, 47(5), W05548.

Ruhl, J., and Daniel, D. (1997). "Geosynthetic clay liners permeated with chemical solutions and leachate." *Journal of Geotechnical and Geoenvironmental Engineering*, 123(4), 369–381.

Sample-Lord, K., and Shackelford, C. (2014). "Membrane behavior of unsaturated bentonite barriers." *Proceedings of Geo-Congress 2014: Geo-Characterization and Modeling for Sustainability*, M. Abu-Farsakh, X. Yu, and L.R. Hoyos, Eds., Geotechnical Special Publication 234, ASCE, Reston, VA, 1900-1909.

Shackelford, C. (1991). "Laboratory diffusion testing for waste disposal - A review." *Journal of Contaminant Hydrology*, 7(3), 177–217.

Shackelford, C. (2013). "Membrane behavior in engineered bentonite-based containment barriers: State of the art." *Proceedings of Coupled Phenomena in Environmental Geotechnics (CPEG)*, M. Manassero, A. Dominijanni, S. Foti, and G. Musso, eds., July 1-3, Torino, Italy, CRC Press/Balkema, Taylor & Francis Group, London, 45–60.

Shackelford, C., Benson, C., Katsumi,T., Edil, T., and Lin,L. (2000). "Evaluating the hydraulic conductivity of GCLs permeated with non-standard liquids." *Geotextiles and Geomembranes*, 18(2–4), 133–161.

Shackelford, C., and Daniel, D. (1991). "Diffusion in saturated soil. 1. Background." *Journal of Geotechnical Engineering*, 117(3), 467–484.

Shackelford, C., and Lee, J. (2003). "The destructive role of diffusion on clay membrane behavior." *Clays and Clay Minerals*, 51(2), 186–196.

Shackelford, C., Malusis, M., and Olsen, H. (2003). "Clay membrane behavior for geoenvironmental containment." *Soil and Rock America Conference 2003*, P. J. Culligan, H. H. Einstein, and A. J. Whittle, Eds., Verlag Glückauf GMBH, Essen, Germany, 1, 767–774.

Shackelford, C., and Moore, S. (2013). "Fickian diffusion of radionuclides for engineered containment barriers: Diffusion coefficients, porosities, and complicating issues." *Engineering Geology*, Elsevier, Amsterdam, 152(1), 133–147.

Sherwood, J., and Craster, B. (2000). "Transport of water and ions through a clay membrane." *Journal of Colloid and Interface Science*, 230(2), 349–358.

Tang, Q., Katsumi, T., Inui, T., and Li, Zhenze (2014). "Membrane behavior of bentonite-amended compacted clay." *Soils and Foundations*, Japanese Geotechnical Society, 54(3), 329–344.

Tang, Q., Katsumi, T., Inui, T., and Li, Zhenze (2015). "Influence of pH on the membrane behavior of bentonite-amended Fukakusa clay." *Separation and Purification Technology*, Vol. 141, 132–142.

Tremosa, J., Gonçalvès, and Matray, J.-M. (2012). "Natural conditions for more limited osmotic abnormal fluid pressures in sedimentary basins." *Water Resources Research*, 48(4), W04530.

van Olphen, H. (1963). *An Introduction to Clay Colloid Chemistry*, 2nd ed., John Wiley & Sons, New York.

Yong, R., Pusch, R., and Nakano, M. (2010) *Containment of High-level Radioactive and Hazardous Solid Wastes with Clay Barriers*. Spon Press, New York.

Young, A., and Low, P. (1965). "Osmosis in argillaceous rocks." *American Association of Petroleum Geologists Bulletin*, 49(7), 1004–1007.

CHAPTER 6. SUMMARY AND CONCLUSIONS

6.1 Summary

The results of a study to evaluate the extent and magnitude of membrane behavior of Na-bentonite under unsaturated conditions and the effects of such membrane behavior on rates of diffusive transport were presented. A new testing apparatus to measure simultaneously both salt diffusion through and membrane behavior of unsaturated bentonite specimens was described. Four multistage experiments were performed on Na-bentonite specimens with degrees of saturation, *S*, ranging from 0.79 to 1.0 to measure membrane behavior and diffusive properties when exposed to solutions of potassium chloride (KCl) ranging in concentration from 20 mM to 50 mM. The results of the experiments were compared with membrane behavior literature for saturated Na-bentonite and conclusions were drawn regarding the significance of the effect of *S* on the solute restrictive behavior of Na-bentonite.

6.2 Conclusions

Based on the objectives and results presented in this document, the following conclusions can be drawn:

(1) The new, closed-system testing apparatus allows for simultaneous measurement of membrane behavior and diffusive transport in unsaturated bentonite. The membrane efficiencies (ω) and effective diffusion coefficients (D^*) of bentonite specimens with *S* values ranging from 0.79 to 1.0 were measured by performing four multistage tests using the apparatus. The results represent the first time membrane behavior of any soil under

unsaturated conditions has been measured using a closed-system testing apparatus. Use of the new apparatus for diffusion testing also may provide several advantages relative to current experimental methods to measure diffusion in unsaturated clays (see Chapter 4).

(2) The dialysis procedure is a simple and effective method for preparing Na-bentonite for membrane behavior and diffusion testing. The dialysis method was used to (1) increase the percentage of Na^+ on the exchange complex of bentonite, (2) remove excess soluble salts in the pore water of bentonite, and (3) estimate apparent diffusion coefficients (D_a) of the bentonite paste. The percentage of Na^+ on the exchange complex of the bentonite increased from 47 % to 69 % and 89 % after dialysis for 7 d in solutions of 0.1 M and 1.0 M NaCl, respectively. Subsequent dialysis in DIW for 14 d resulted in a significant reduction in soluble salts (e.g., Na^+ decreased from 19 meq/100g to 2.2 meq/100g), indicating dialysis provides a much faster method to flush specimens of soluble salts than those previously used in membrane behavior research (e.g., 14 d versus 6 months). The values of D_a measured for the bentonite paste ranged from 1.5 x 10^{-10} m^3/s to 3.8 x 10^{-10} m^3/s, which were comparable to values reported in the literature for Na-bentonites tested with traditional diffusion test methods.

(3) The steady-state values of D^* for the saturated and unsaturated bentonite specimens measured during the multistage tests ranged from 2.1 x 10^{-12} m^2/s to 4.1 x 10^{-10} m^2/s, which were consistent with expectations based on the limited data available in the literature for bentonite at high porosities (e.g., $n > 0.7$). The values of D^* for both Cl^- and K^+ tended to increase with increasing average salt concentration in the specimen (C_{ave}), which was consistent with trends reported in the literature and could be explained on the basis of classical diffuse-double-layer (DDL) theory. The effects of S and θ on the

measured values of D^* were less obvious, which may have been due to the limited range of S that could be evaluated in the study. For all of the experiments, the values of D^* for K^+ were lower than or equal to those for Cl^-, likely due to Na^+ initially present in the specimen. In agreement with previously reported results for Na-bentonite, the diffusive properties of the unsaturated specimens correlated well with the measured membrane behavior, with D^* decreasing with increasing ω.

(4) Membrane behavior in Na-bentonite increased as S decreased, providing experimental verification of the proposed hypothesis and achieving the goal of the study. The values of ω ranged from 0.31 to 0.61, 0.34 to 0.66, 0.41 to 0.71, and 0.68 to 0.75 for the tests with S values of 1.0, 0.89, 0.84 and 0.79, respectively. As expected, the values of ω decreased as C_{ave} increased. For example, for the specimen with S of 0.84 as C_{ave} increased from 9.7 mM to 25.0 mM KCl the value of ω decreased from 0.68 to 0.41. The results were in agreement with the current, conceptual understanding of membrane behavior as well as the proposed, conceptual explanations of the effects of saturation on solute restriction. The data represent the first experimental results for membrane behavior of Na-bentonite specimens maintained under unsaturated conditions.

6.3 Recommendations for future research

Recommendations for future research are as follows:

(1) Additional experimental work should be performed to measure membrane behavior of Na-bentonite specimens with values of S less than 0.79 in order to thoroughly evaluate the effect of S on ω. Experimental data over a wider range of S would allow for better

comparison of the results with available theoretical models and development of new models that include unsaturated membrane behavior. The range of saturations that could be evaluated in the study was limited due to the test durations required to reach steady-state diffusion, and, therefore, recommendations to reduce test durations are provided subsequently.

(2) To reduce the test durations required to achieve steady-state diffusion conditions in the test cell during unsaturated membrane testing, the following modifications to the testing apparatus and procedure should be considered:

- The use of thinner (e.g., $\leq$ 5 mm), high air-entry (HAE) disks in the test cell would reduce the time to reach steady-state diffusion across the test system. Thinner HAE disks also may allow for using HAE disks with higher air-entry values while maintaining reasonable test durations, making evaluation of specimens with greater matric suction (i.e., lower values of *S*) feasible.
- The use of thinner bentonite specimens (e.g., $\leq$ 5 mm) also would reduce required test durations to achieve steady-state diffusion.
- Performing transient diffusion modeling to analyze the data could eliminate the need to achieve steady-state diffusion in future testing.

(3) The scenario of combined diffusion of Na^+ initially in the pores of the bentonite and diffusion of K^+ due to the imposed gradient of KCl across the specimen should be modeled to confirm the observed diffusion behavior (i.e., values of D^*_{clay} for K^+ that were lower than or equal to those for Cl^-).

(4) Since unsaturated membrane behavior in Na-bentonite is relevant for the design of engineered barriers for high-level radioactive waste (HLRW) disposal, additional testing should be performed under conditions that are representative of such barriers. For example, testing should be performed on specimens of compacted bentonite or bentonite mixtures (dry density > 1.7 Mg/m^3) and under conditions of elevated temperature (e.g., 100° C).

(5) Additional dialysis testing should be performed to evaluate the dialysis procedure as a method to measure D_a for bentonite-based slurries and mixtures commonly used in soil-bentonite backfill applications, that otherwise may be difficult to evaluate using traditional laboratory equipment.

APPENDIX A. ADDITIONAL DETAILS OF APPARATUS DESIGN

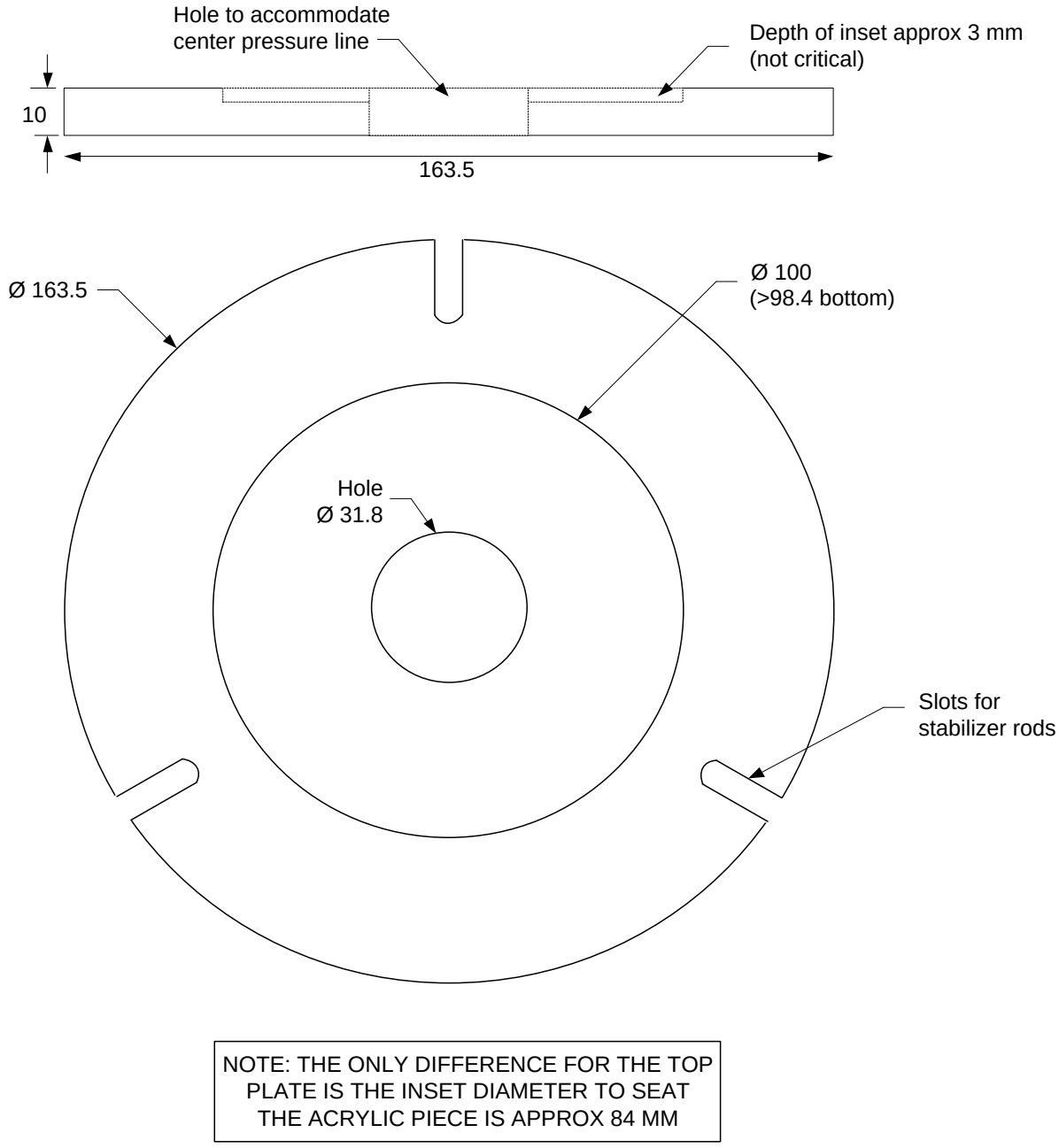

All dimensions in millimeters.

Figure A.1. Detailed design of stainless-steel, cell frame for Apparatus No. 1.

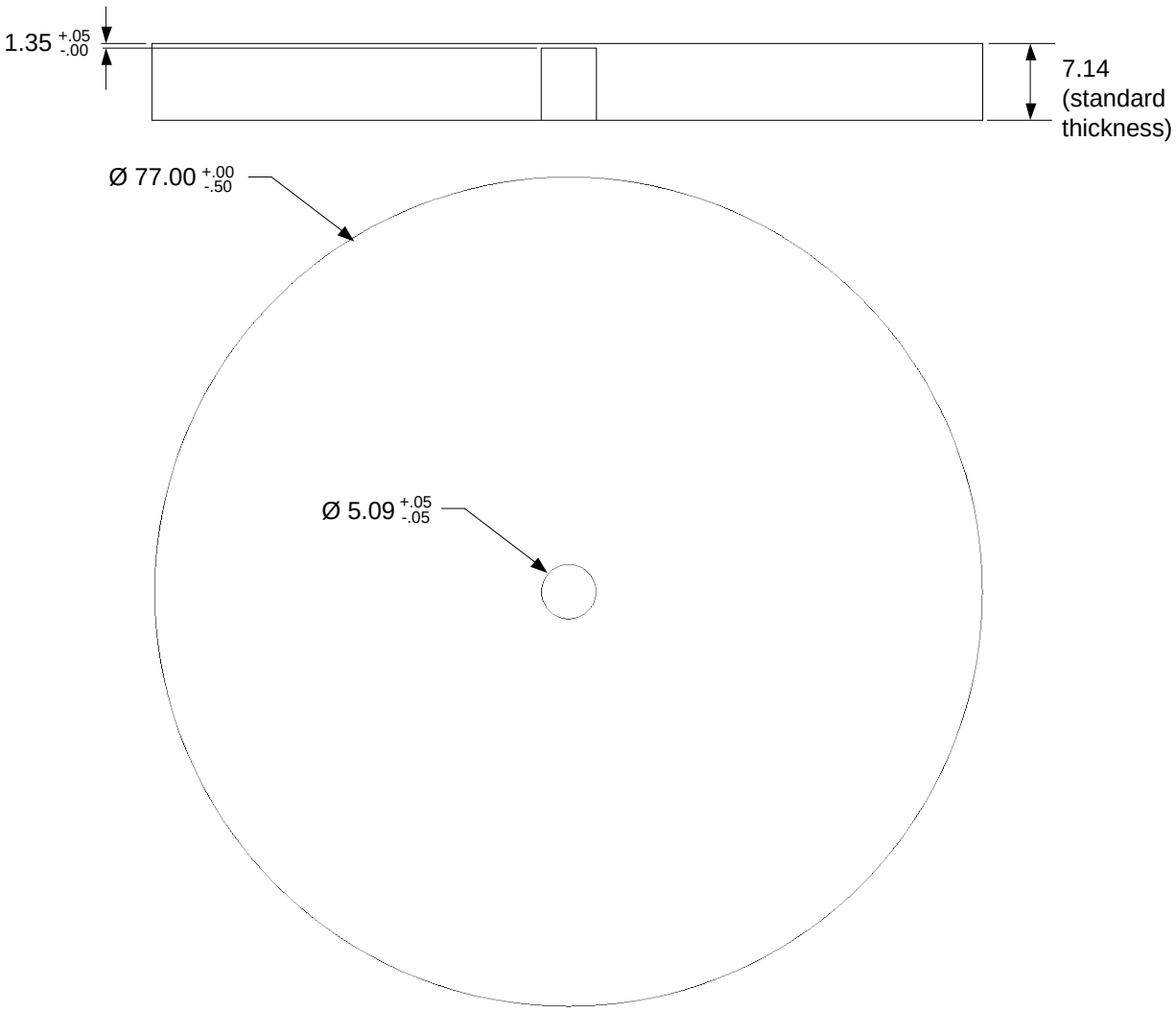

All dimensions in millimeters.

Figure A.2. Detailed design of ceramic, high air-entry disks for Apparatus No. 1.

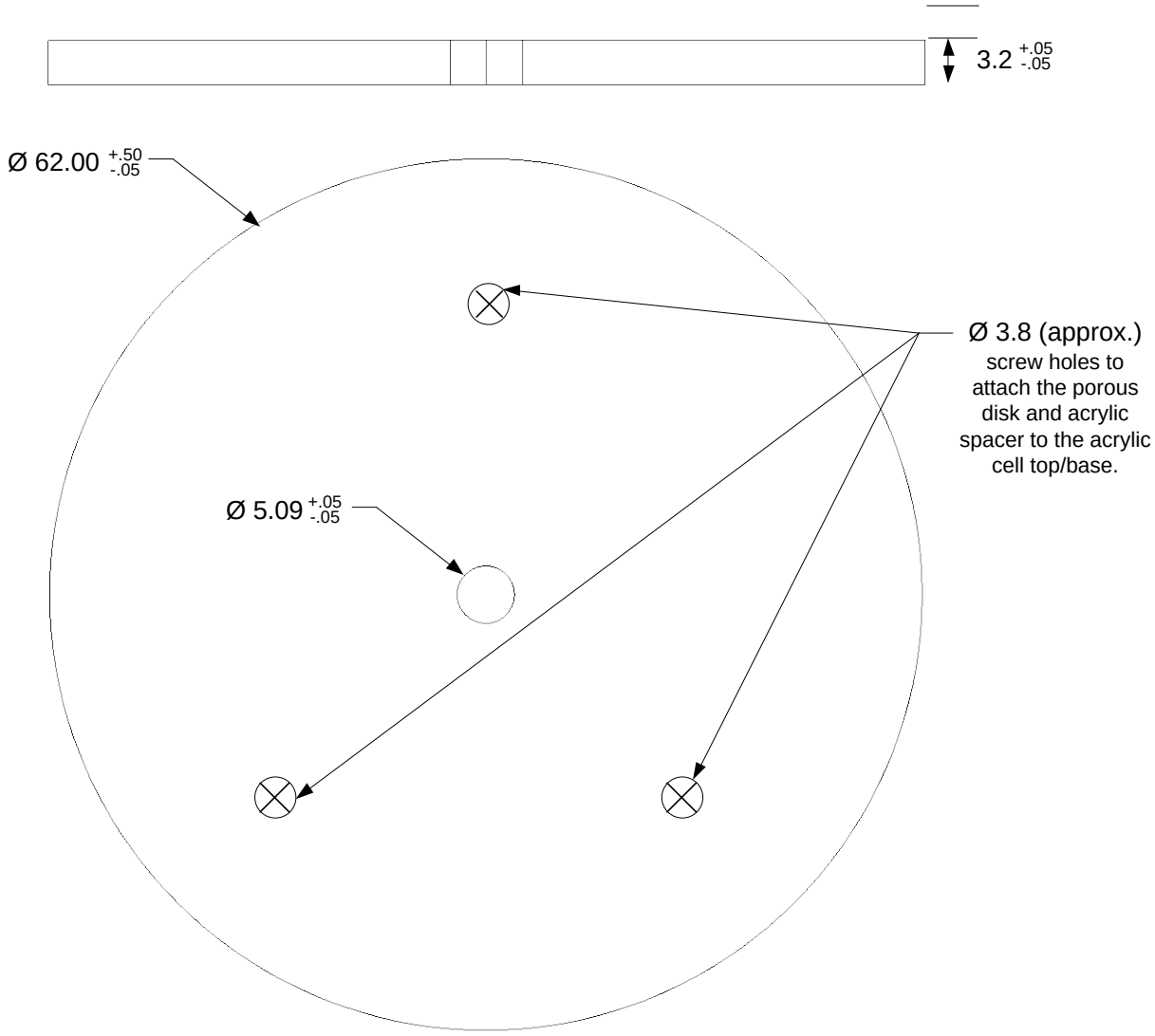

All dimensions in millimeters.

Figure A.3. Detailed design of plastic, porous disks for Apparatus No. 1.

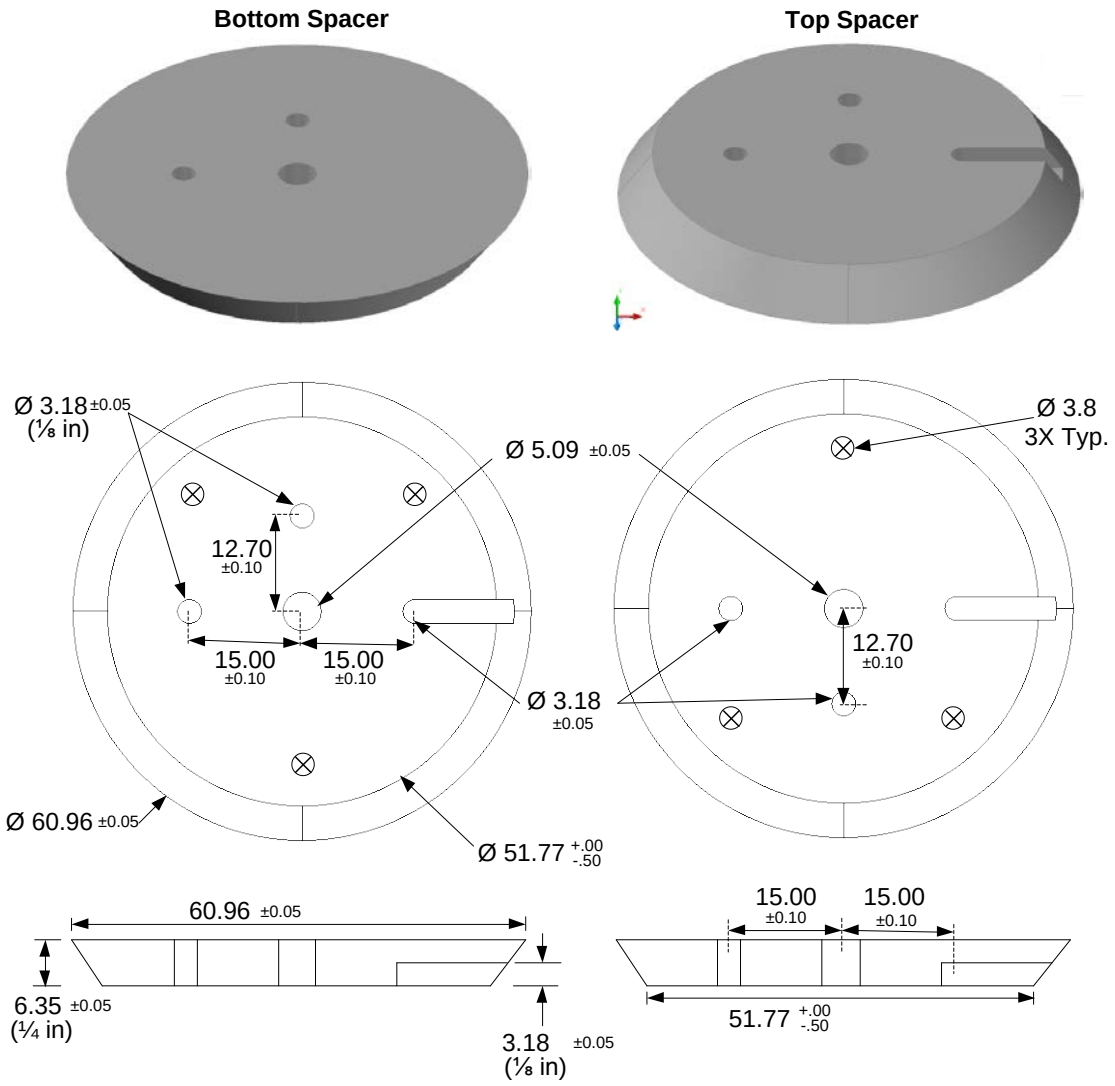

All dimensions in millimeters.

Figure A.4. Detailed design of top and bottom acrylic spacers for Apparatus No. 1.

APPENDIX B. DATA FOR MASS LEACHING ANALYSES

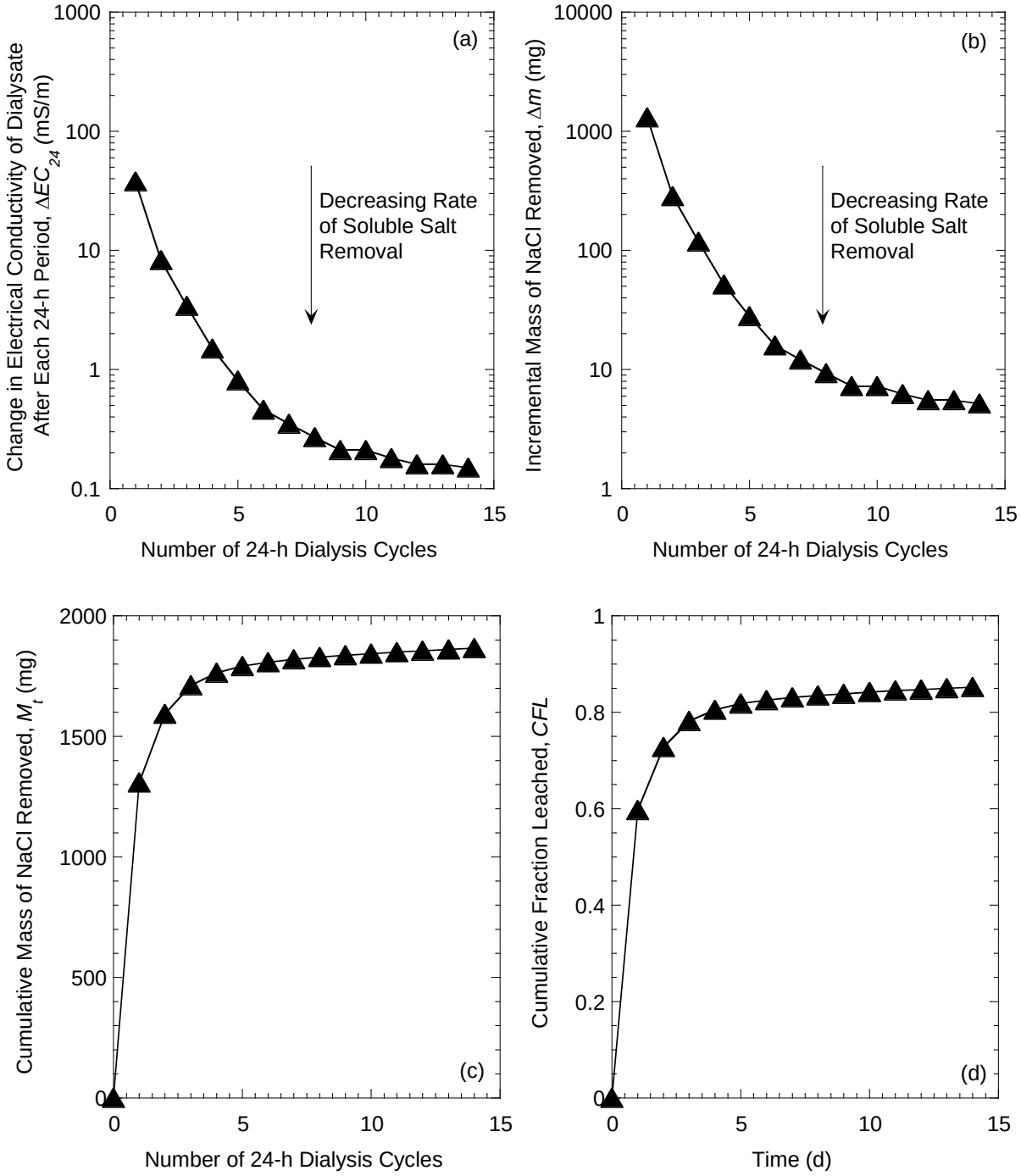

Figure B.1. Data for mass leaching analysis for Test No. 1: (a) change in electrical conductivity of the dialysate after each 24-hour dialysis period, ΔEC, during the soluble salt removal stage; (b) incremental mass of NaCl removed from specimen (from ΔEC); (c) cumulative mass of NaCl removed from specimen; and (d) cumulative fraction leached (CFL).

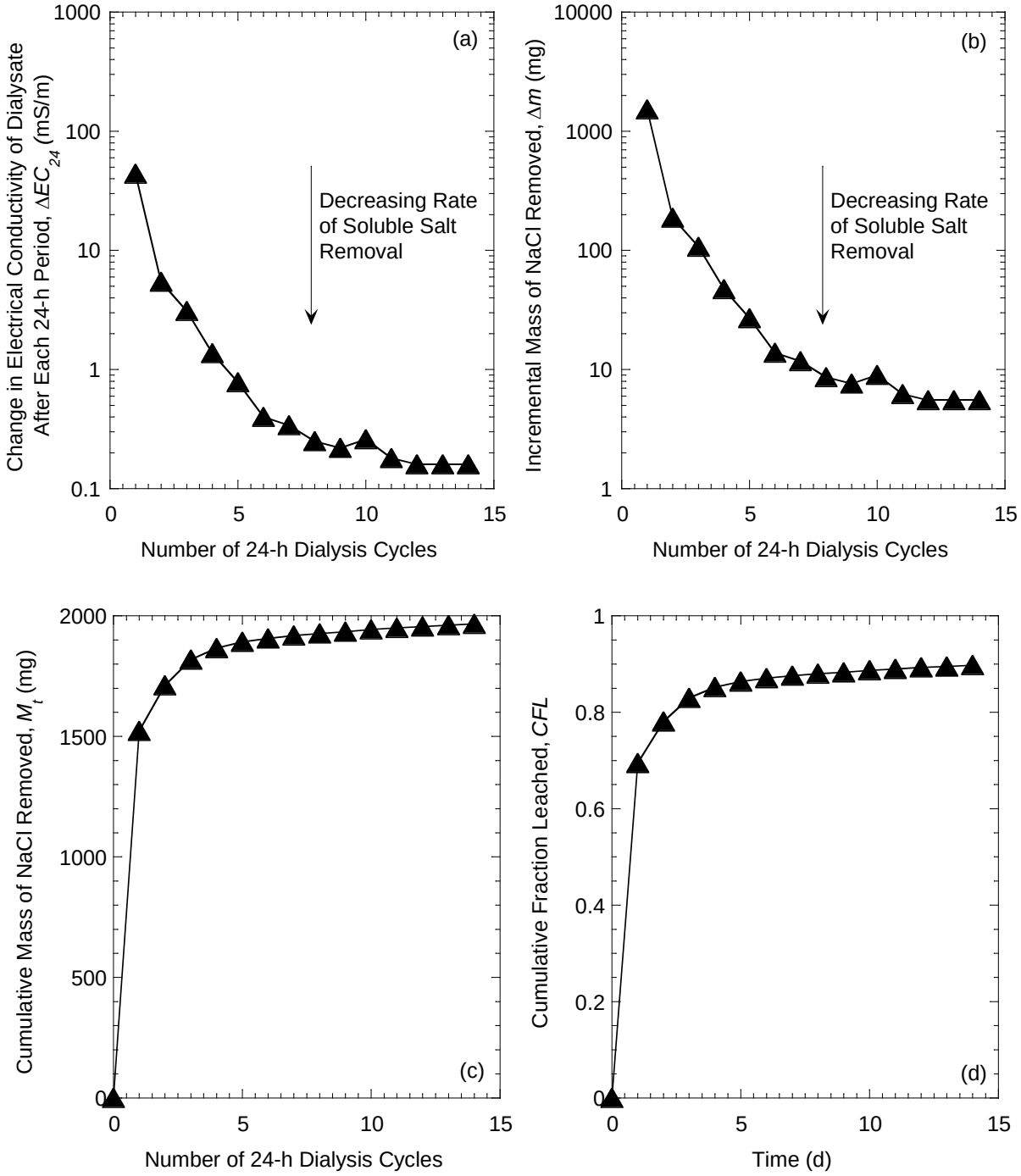

Figure B.2. Data for mass leaching analysis for Test No. 2: (a) change in electrical conductivity of the dialysate after each 24-hour dialysis period, ΔEC, during the soluble salt removal stage; (b) incremental mass of NaCl removed from specimen (from ΔEC); (c) cumulative mass of NaCl removed from specimen; and (d) cumulative fraction leached (CFL).

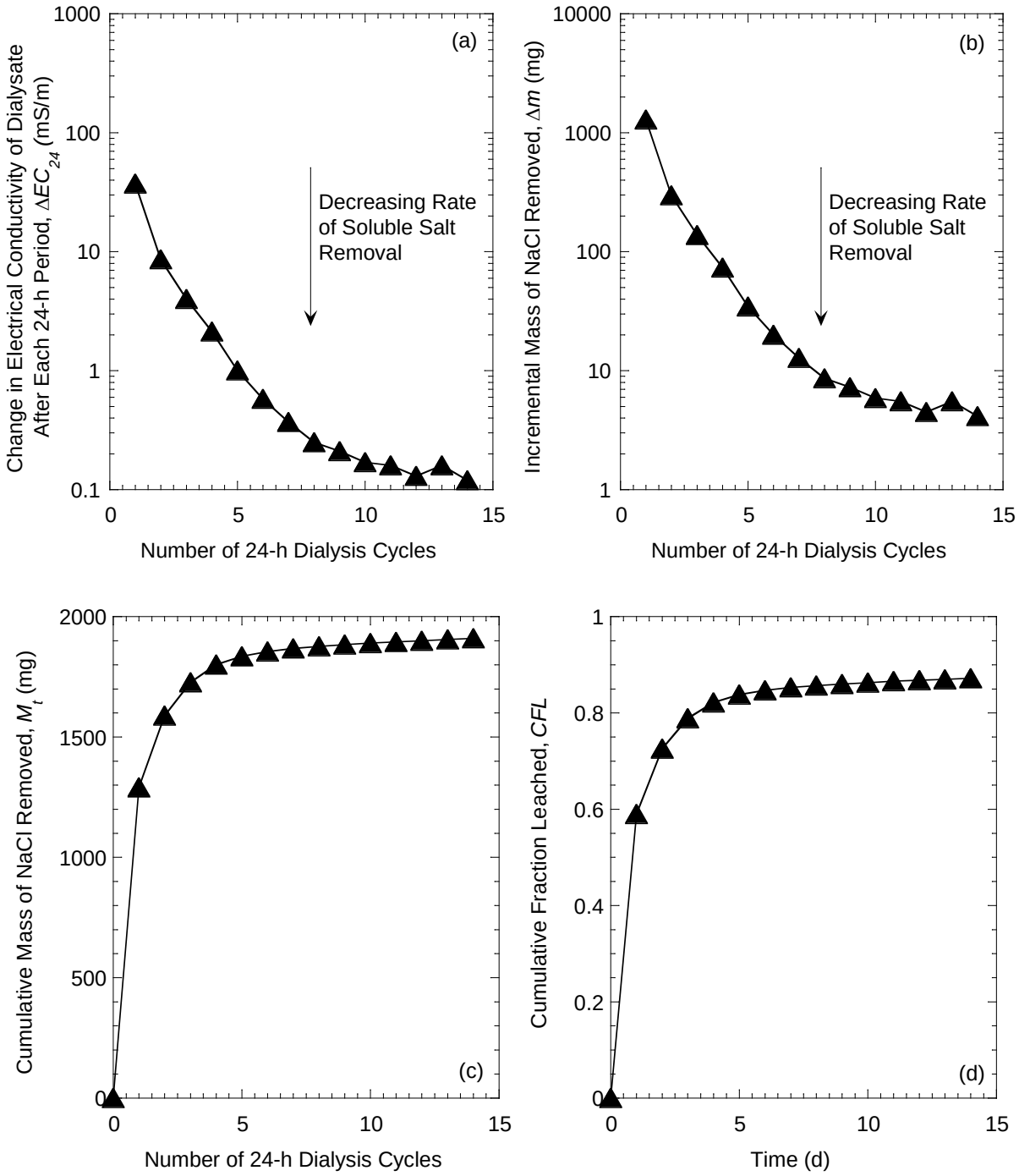

Figure B.3. Data for mass leaching analysis for Test No. 3: (a) change in electrical conductivity of the dialysate after each 24-hour dialysis period, ΔEC, during the soluble salt removal stage; (b) incremental mass of NaCl removed from specimen (from ΔEC); (c) cumulative mass of NaCl removed from specimen; and (d) cumulative fraction leached (CFL).

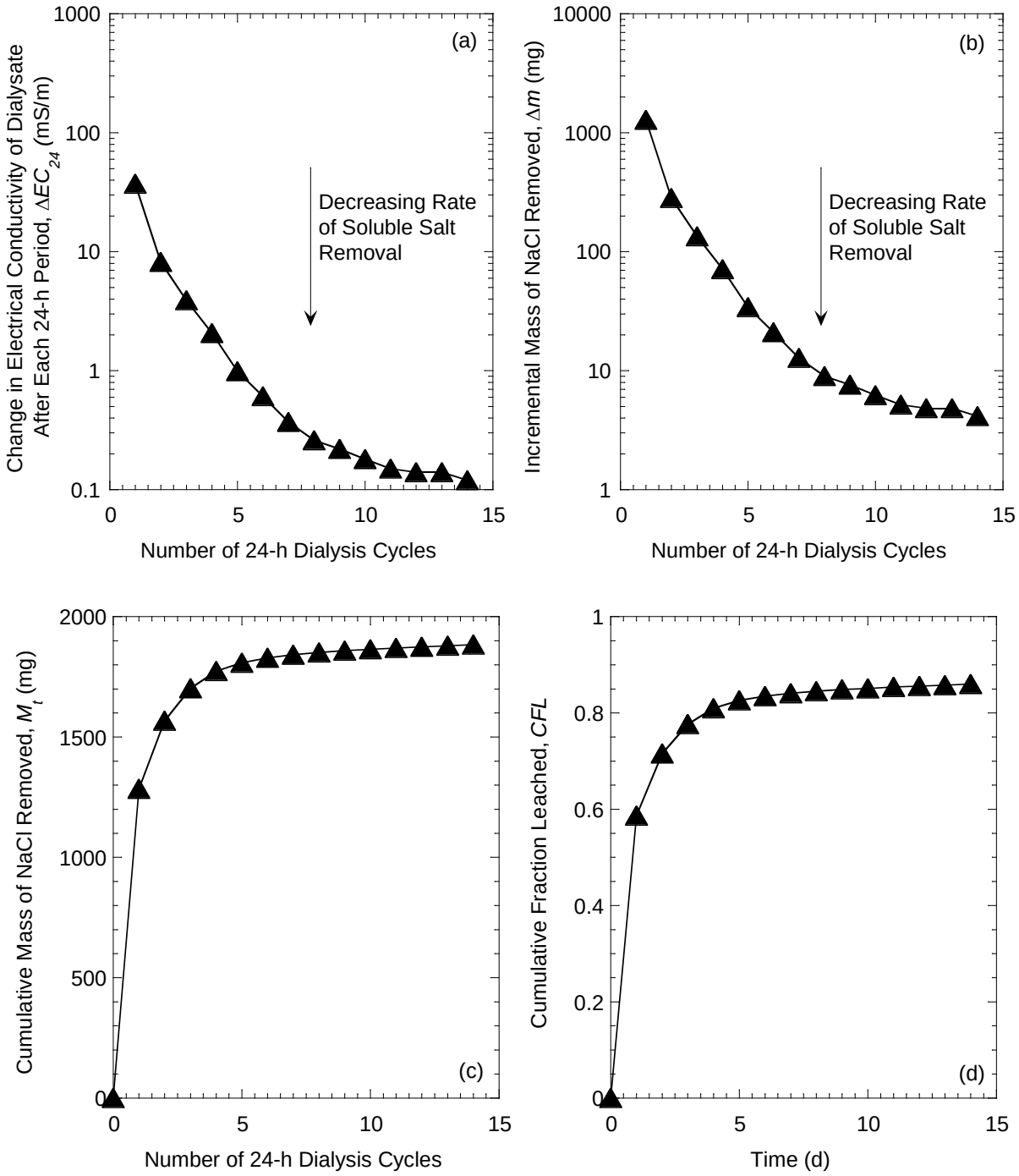

Figure B.4. Data for mass leaching analysis for Test No. 4: (a) change in electrical conductivity of the dialysate after each 24-hour dialysis period, ΔEC, during the soluble salt removal stage; (b) incremental mass of NaCl removed from specimen (from ΔEC); (c) cumulative mass of NaCl removed from specimen; and (d) cumulative fraction leached (CFL).

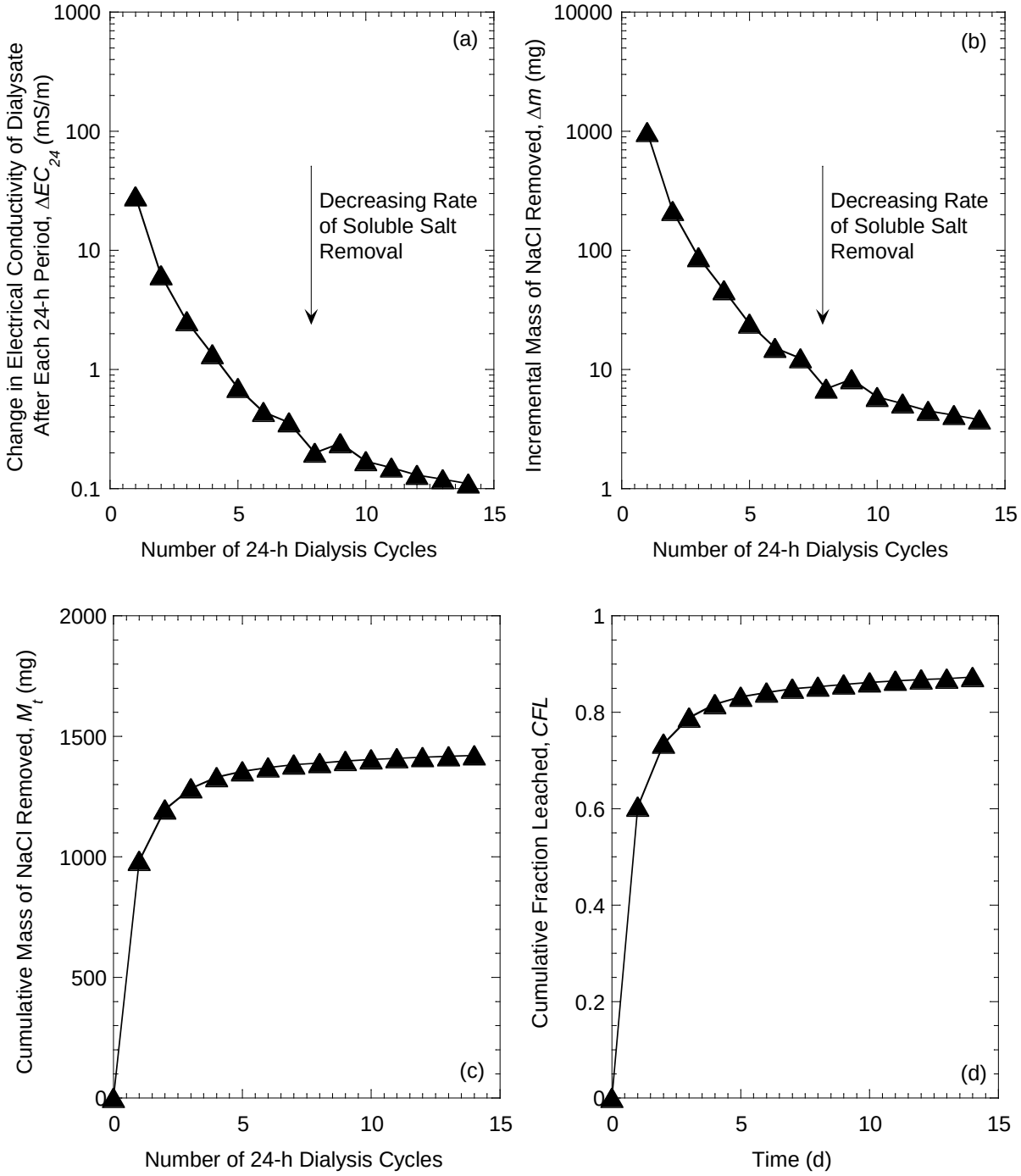

Figure B.5. Data for mass leaching analysis for Test No. 5: (a) change in electrical conductivity of the dialysate after each 24-hour dialysis period, ΔEC, during the soluble salt removal stage; (b) incremental mass of NaCl removed from specimen (from ΔEC); (c) cumulative mass of NaCl removed from specimen; and (d) cumulative fraction leached (*CFL*).

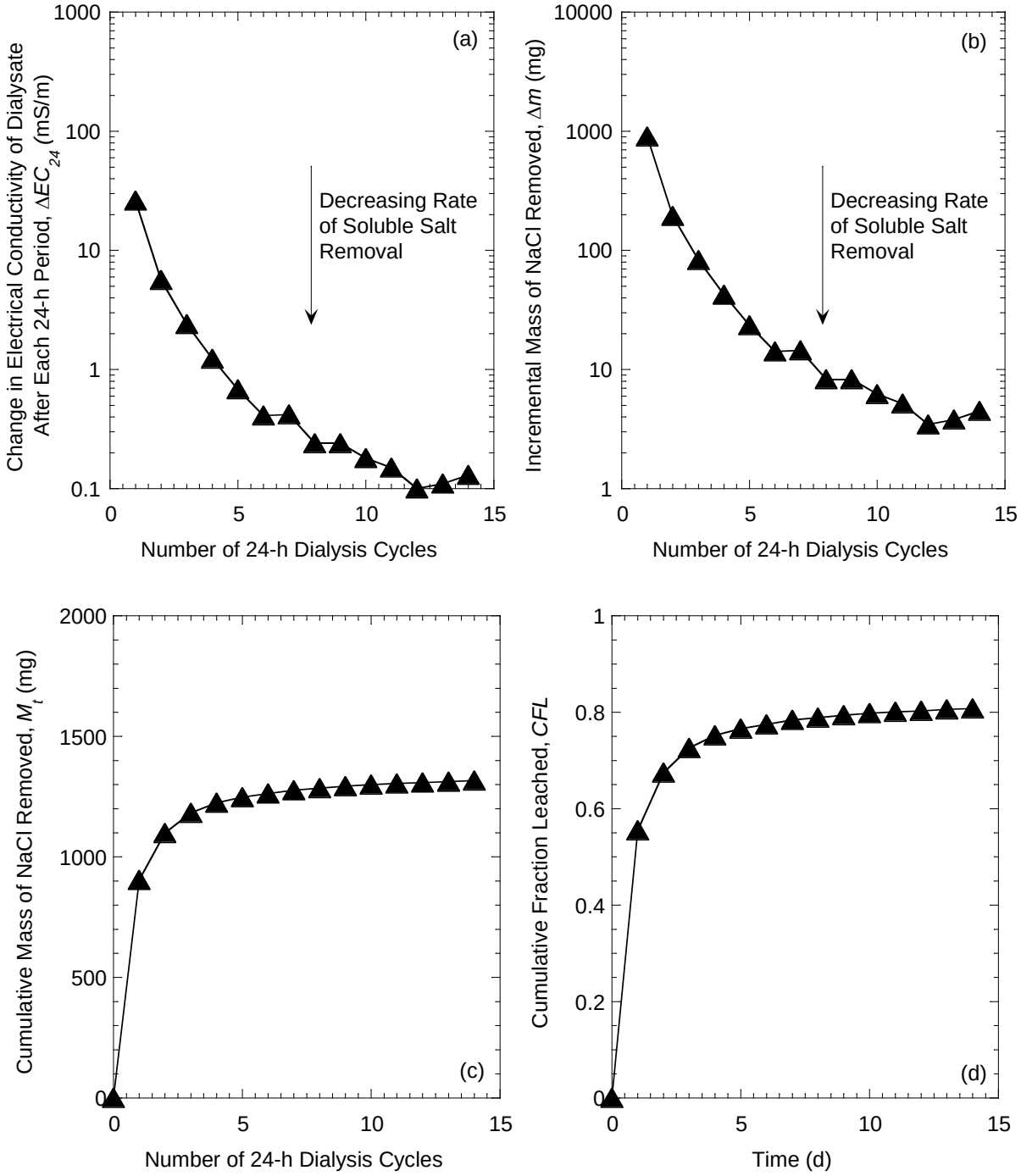

Figure B.6. Data for mass leaching analysis for Test No. 6: (a) change in electrical conductivity of the dialysate after each 24-hour dialysis period, ΔEC, during the soluble salt removal stage; (b) incremental mass of NaCl removed from specimen (from ΔEC); (c) cumulative mass of NaCl removed from specimen; and (d) cumulative fraction leached (CFL).

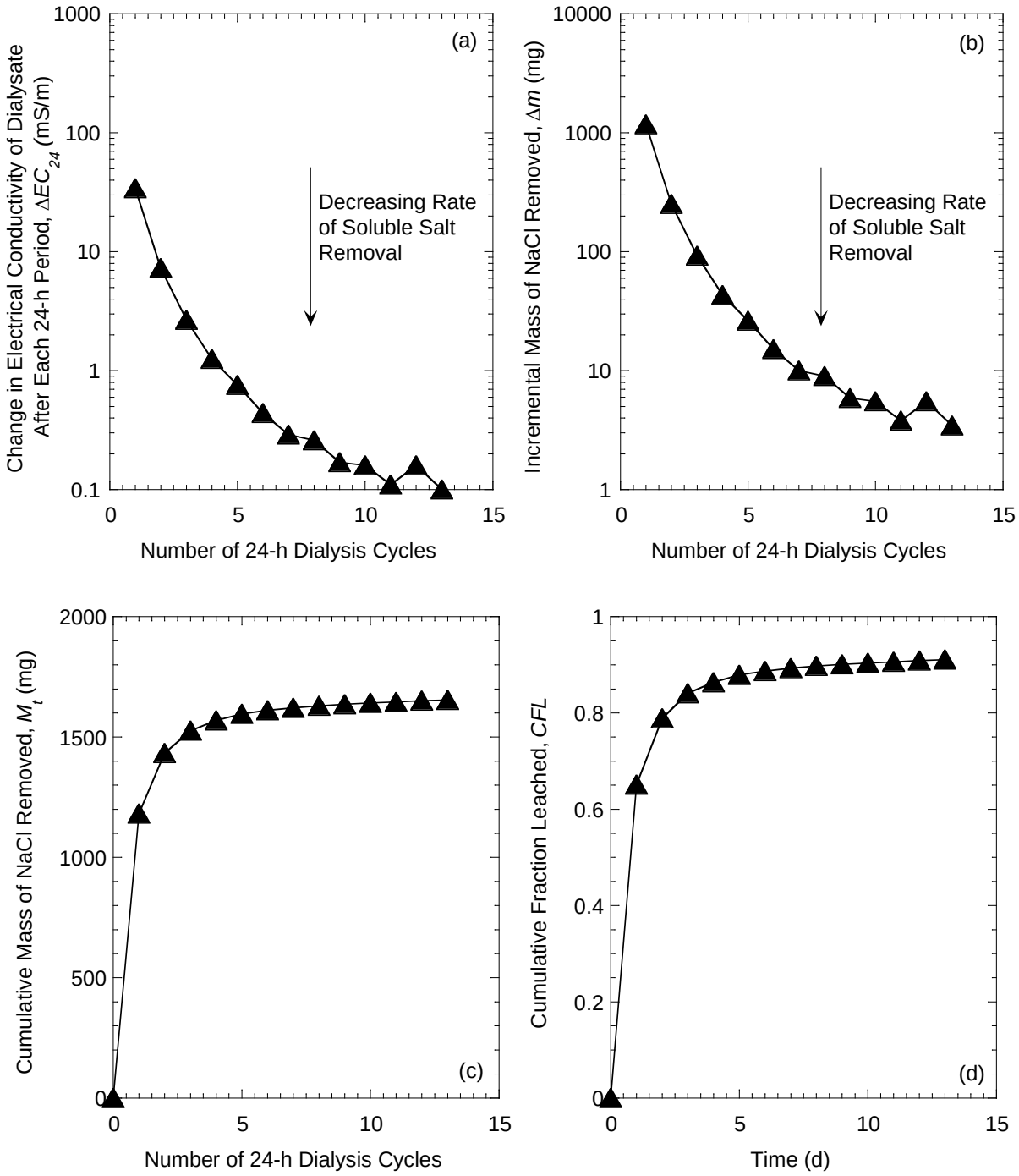

Figure B.7. Data for mass leaching analysis for Test No. 7: (a) change in electrical conductivity of the dialysate after each 24-hour dialysis period, ΔEC, during the soluble salt removal stage; (b) incremental mass of NaCl removed from specimen (from ΔEC); (c) cumulative mass of NaCl removed from specimen; and (d) cumulative fraction leached (CFL).

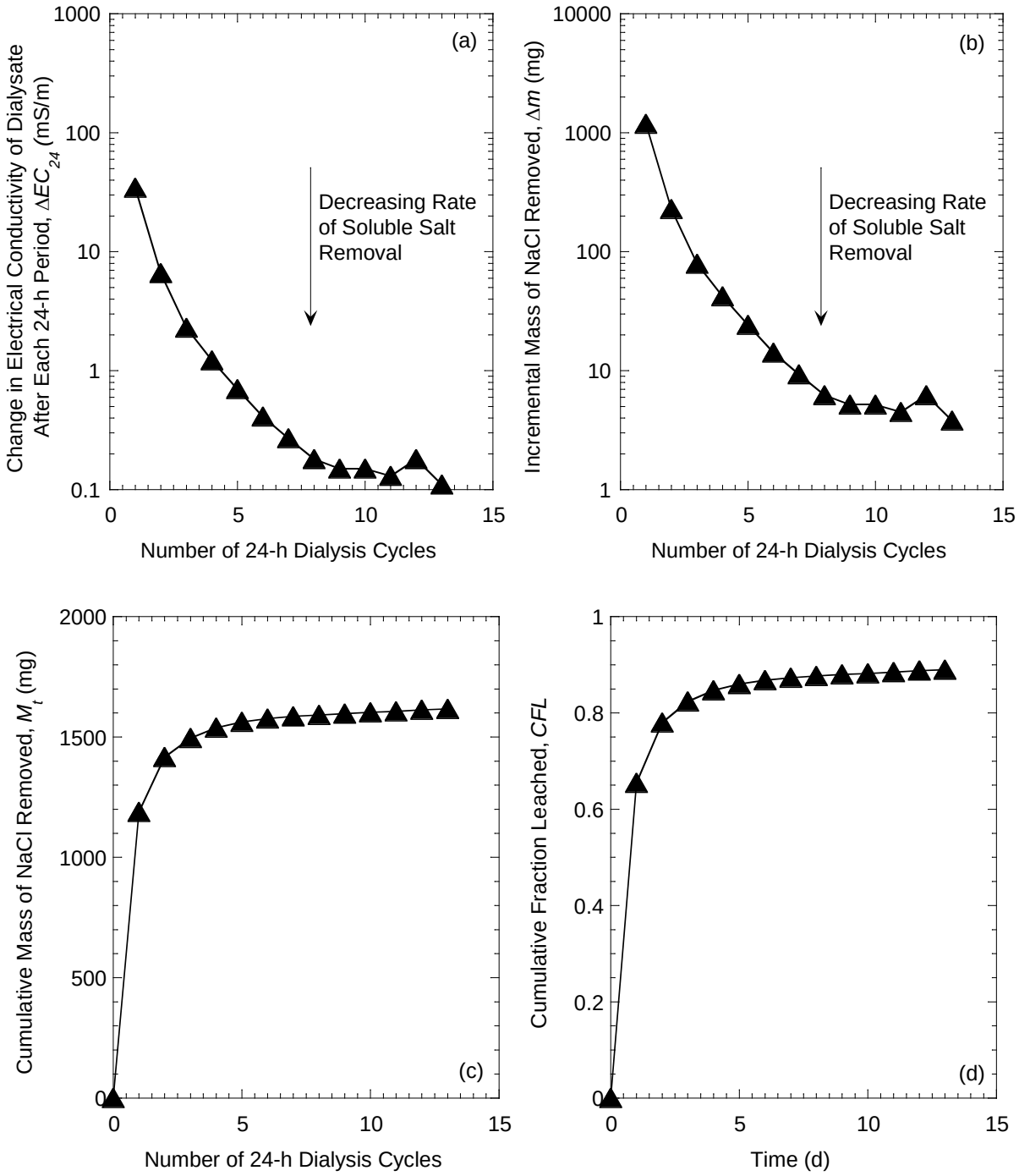

Figure B.8. Data for mass leaching analysis for Test No. 8: (a) change in electrical conductivity of the dialysate after each 24-hour dialysis period, Δ*EC*, during the soluble salt removal stage; (b) incremental mass of NaCl removed from specimen (from Δ*EC*); (c) cumulative mass of NaCl removed from specimen; and (d) cumulative fraction leached (*CFL*).

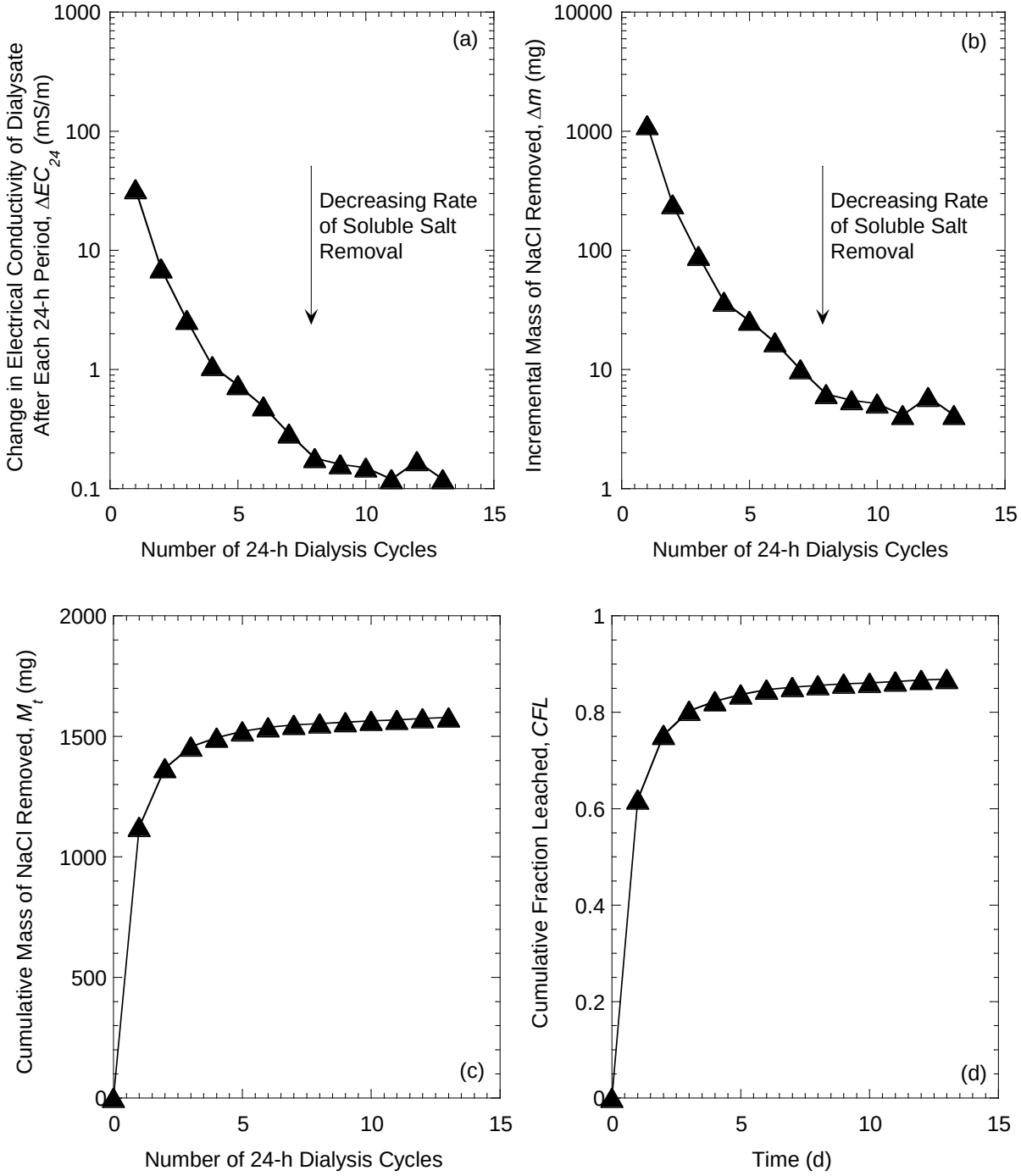

Figure B.9. Data for mass leaching analysis for Test No. 9: (a) change in electrical conductivity of the dialysate after each 24-hour dialysis period, ΔEC, during the soluble salt removal stage; (b) incremental mass of NaCl removed from specimen (from ΔEC); (c) cumulative mass of NaCl removed from specimen; and (d) cumulative fraction leached (CFL).

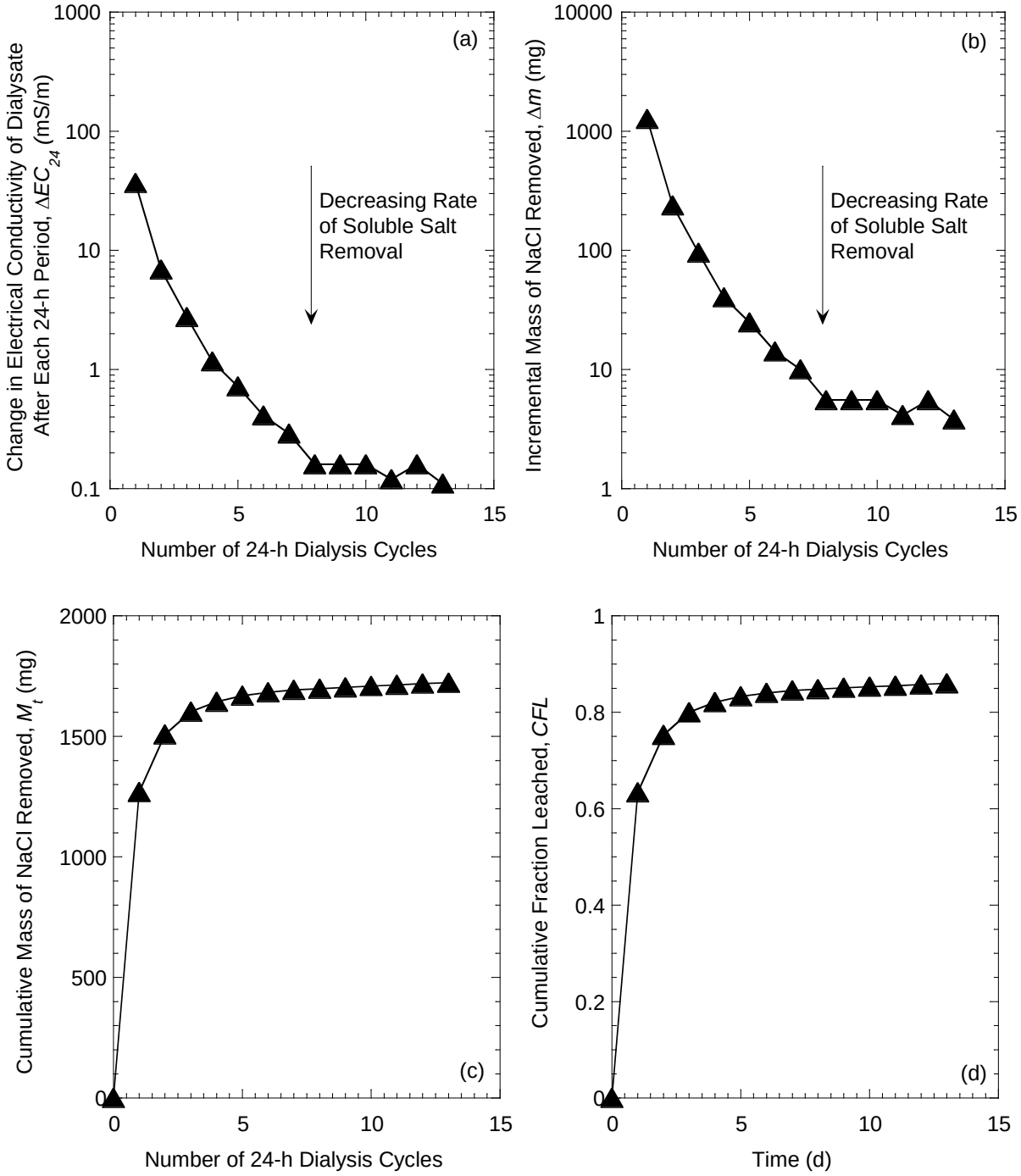

Figure B.10. Data for mass leaching analysis for Test No. 10: (a) change in electrical conductivity of the dialysate after each 24-hour dialysis period, ΔEC, during the soluble salt removal stage; (b) incremental mass of NaCl removed from specimen (from ΔEC); (c) cumulative mass of NaCl removed from specimen; and (d) cumulative fraction leached (CFL).

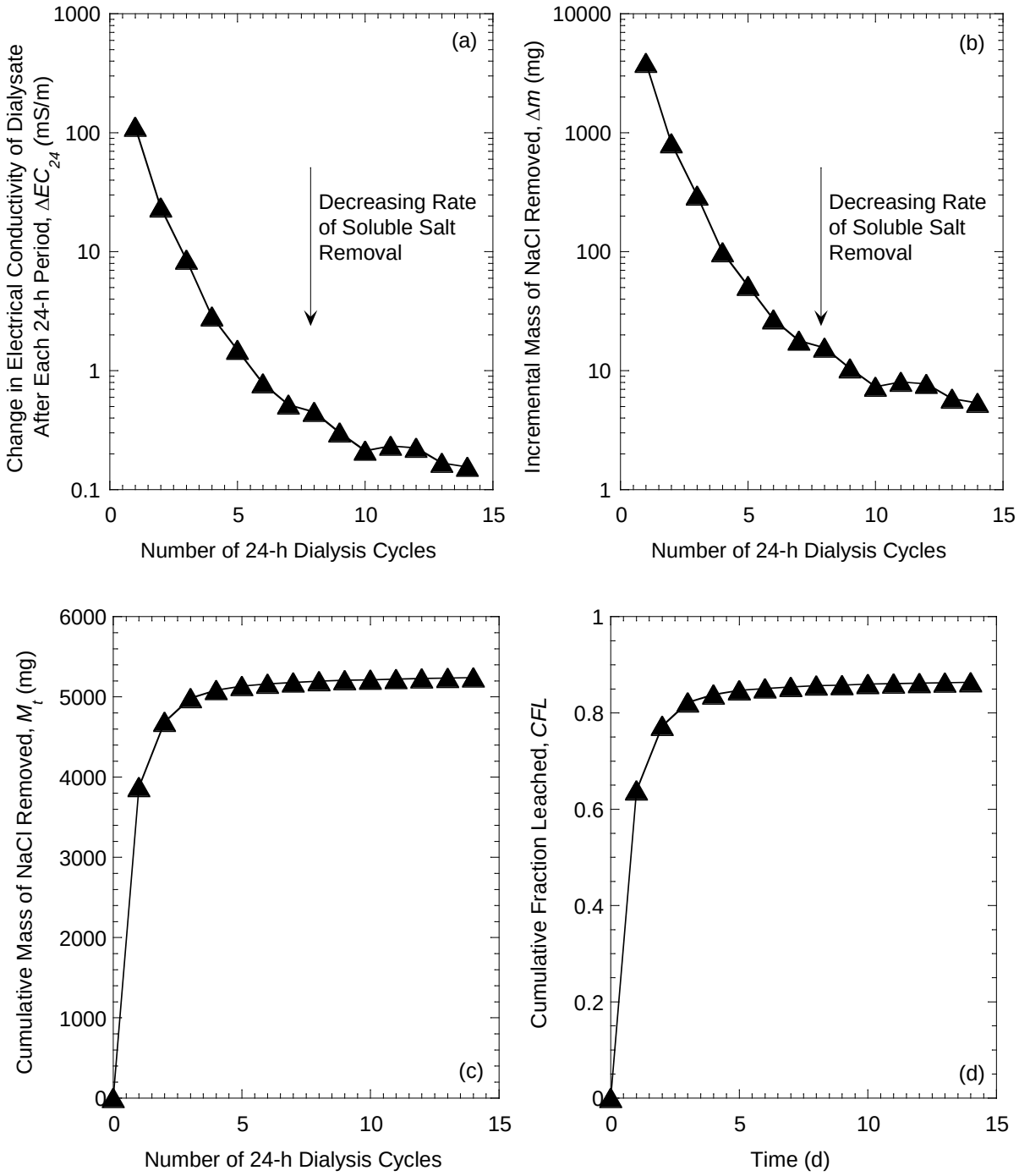

Figure B.11. Data for mass leaching analysis for Test No. 11: (a) change in electrical conductivity of the dialysate after each 24-hour dialysis period, Δ*EC*, during the soluble salt removal stage; (b) incremental mass of NaCl removed from specimen (from Δ*EC*); (c) cumulative mass of NaCl removed from specimen; and (d) cumulative fraction leached (*CFL*).

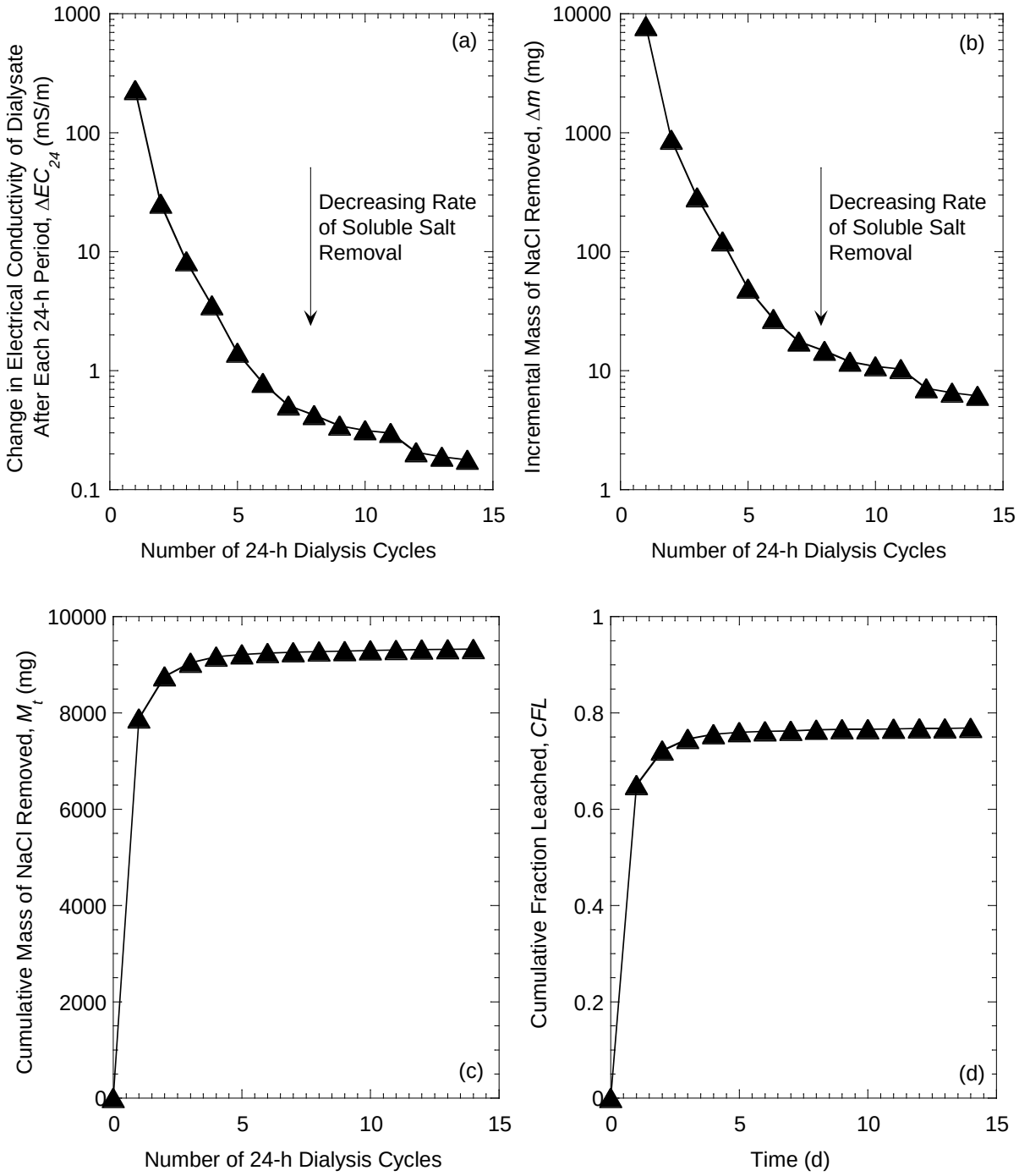

Figure B.12. Data for mass leaching analysis for Test No. 12: (a) change in electrical conductivity of the dialysate after each 24-hour dialysis period, ΔEC, during the soluble salt removal stage; (b) incremental mass of NaCl removed from specimen (from ΔEC); (c) cumulative mass of NaCl removed from specimen; and (d) cumulative fraction leached (CFL).

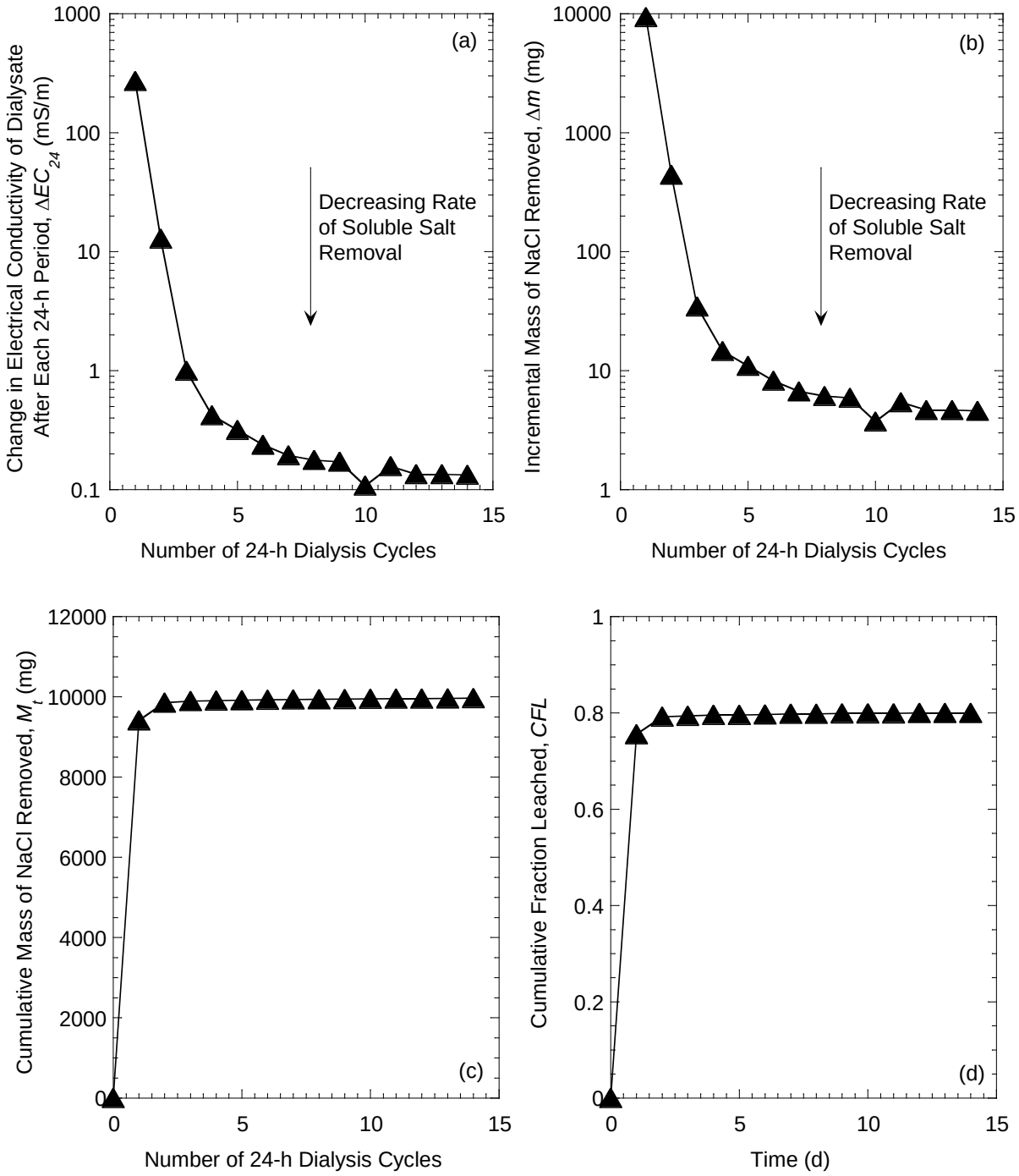

Figure B.13. Data for mass leaching analysis for Test No. 13: (a) change in electrical conductivity of the dialysate after each 24-hour dialysis period, ΔEC, during the soluble salt removal stage; (b) incremental mass of NaCl removed from specimen (from ΔEC); (c) cumulative mass of NaCl removed from specimen; and (d) cumulative fraction leached (CFL).

APPENDIX C. EQUIPMENT USED IN SPECIMEN PREPARATION

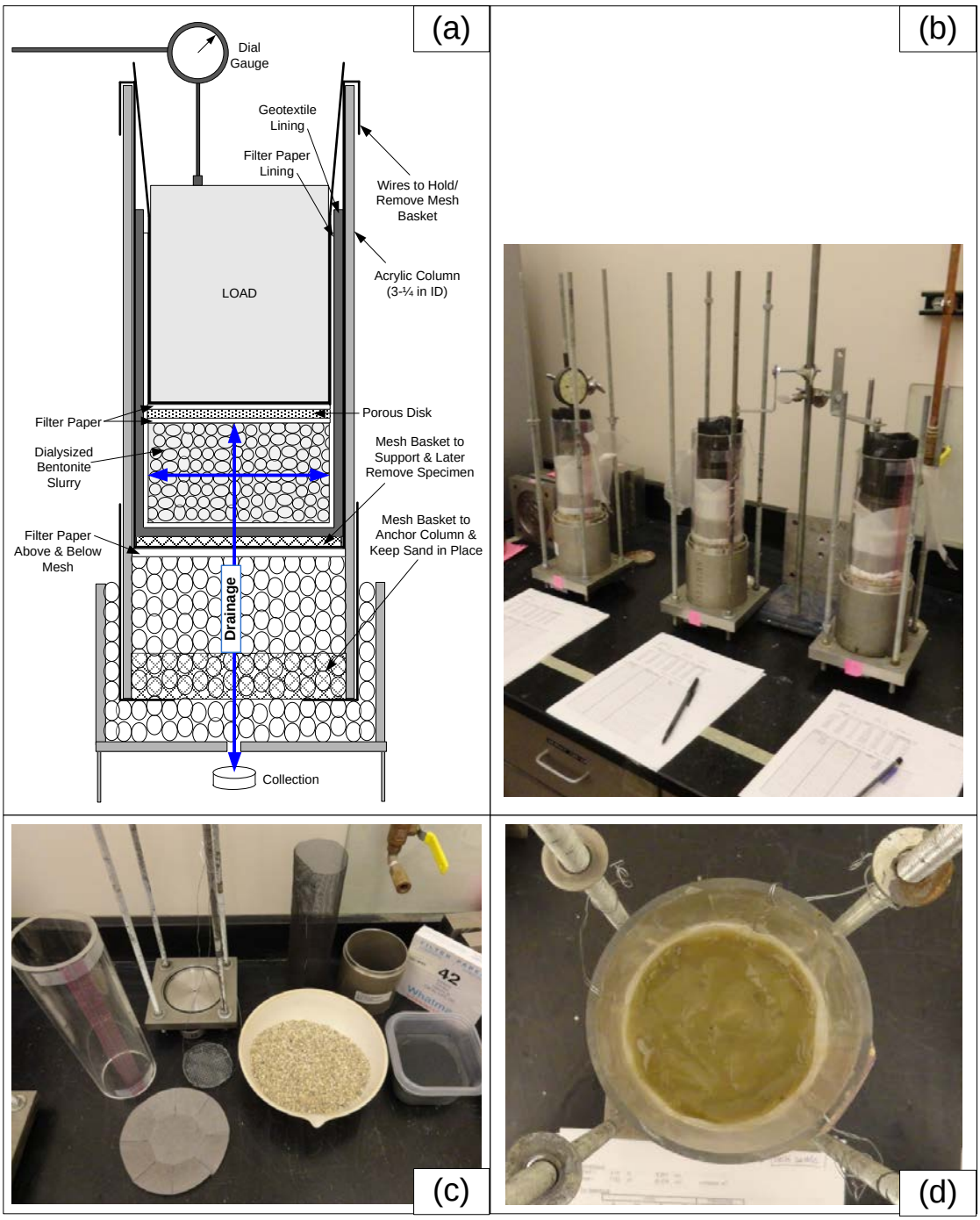

Figure C.1. Setup for slurry consolidation: (a) detailed schematic; (b) three consolidation columns being used concurrently to prepare specimens; (c) materials required to set up the column; (d) top view of the column after placing the bentonite slurry.

Figure C.2. Equipment used to adjust degree of saturation of bentonite specimens: (a) pressure-plate apparatus; (b) 15-bar, high air-entry disk used in pressure plate apparatus; (c) pressure gauge to adjust and monitor air pressure in the cell.

APPENDIX D. DIFFUSION MODELS AND SUPPLEMENTAL DATA

Appendix D-1

Supplemental Information for

Through-Diffusion Analysis Method

Derivation of Equations Used for Through-Diffusion Analysis:

List of parameters:

ΔC_{ave} = average concentration difference across the layer or system of interest;

ΔC_{clay} = concentration difference across the clay specimen;

ΔC_{total} = concentration difference across the whole layered system;

ΔQ_t = incremental change in cumulative mass of solute, per unit area, at steady-state diffusion;

Δt = time increment over which ΔQ_t considered;

θ = volumetric water content;

θ_{clay} = volumetric water content of the clay specimen;

θ_{HAE} = volumetric water content of the high-air entry disk;

C_b = outflow concentration at the bottom boundary;

$C_{b,ave}$ = average concentration at the bottom boundary;

C_{ob} = inflow concentration at the bottom boundary;

C_{ot} = inflow concentration at the top boundary;

C_t = outflow concentration at the top boundary;

$C_{t,ave}$ = average concentration at the top boundary;

D^* = effective diffusion coefficient = molecular diffusion coefficient x apparent tortuosity;

D^*_{clay} = effective diffusion coefficient of the clay specimen;

D^*_{HAE} = effective diffusion coefficient of the high-air entry disk;

D_e = effective diffusion coefficient = $D^*\theta$;

$D_{e,eq}$ = equivalent, effective diffusion coefficient for layered system;

$J_{D,ss}$ = steady-state, diffusive mass flux;

L = total length (thickness) of the specimen or layered system across which diffusion is occurring;

L_{clay} = length (thickness) of the clay specimen only;

L_{HAE} = length (thickness) of the high-air entry disk only; and

n = porosity of the layer.

Derivation for Through-Diffusion Analysis for Unsaturated, Layered Soil System:

Fick's first law for solute mass flux due to one-dimensional diffusion in a porous medium may be written as follows (e.g., Porter et al. 1960; Shackelford and Daniel 1991a):

$$J_{D,ss} = -\theta D^* \frac{\partial C}{\partial x} = -D_e \frac{\partial C}{\partial x} \tag{D.1}$$

Based on Fick's first law, the effective diffusion coefficient has been determined for saturated specimens ($n = \theta$) using the through-diffusion method and a closed-system testing apparatus, as follows (e.g., Malusis et al. 2013):

$$D^* = -\left(\frac{L}{n\,\Delta C_{ave}}\right)\left(\frac{\Delta Q_t}{\Delta t}\right)_{steady-state} = -\left(\frac{L}{n\,\left(C_{b,ave} - C_{t,ave}\right)}\right) J_{D,ss} \tag{D.2}$$

where:

$$C_{b,ave} = \left(\frac{C_{ob} + C_b}{2}\right);\ C_{t,ave} = \left(\frac{C_{ot} + C_t}{2}\right) \tag{D.3}$$

Replacing n with θ to accommodate unsaturated specimens, Equation D.2 becomes:

$$D^* = -\left(\frac{L}{\theta \Delta C_{ave}}\right)\left(\frac{\Delta Q_t}{\Delta t}\right) = -\left(\frac{L}{\theta\left(C_{b,ave} - C_{t,ave}\right)}\right) J_{D,ss} \tag{D.4}$$

In terms of D_e, Equation D.4 can be written:

$$D_e = -\left(\frac{L}{\Delta C_{ave}}\right)\left(\frac{\Delta Q_t}{\Delta t}\right) \tag{D.5}$$

For the test system used in this study, comprised of one clay specimen sandwiched between two high-air entry (HAE) disks, the assumption of continuity of solute mass flux across each layer at steady-state diffusion can be written as follows:

$$J_{D,ss} = J_{HAE,ss} = J_{clay,ss} \tag{D.6}$$

Expanding Equation D.5 for each of the layers and also for an equivalent layered system, based on Fick's first law, results in the following:

$$J_{D,ss} = -D_{e,HAE}\frac{\Delta C_{HAE}}{L_{HAE}} = -D_{e,clay}\frac{\Delta C_{clay}}{L_{clay}} = -D_{e,eq}\frac{\Delta C_{ave}}{L} \tag{D.7}$$

or in terms of D^* and θ for the clay and HAE disks:

$$J_{D,ss} = -\theta_{HAE} D^*_{HAE}\frac{\Delta C_{HAE}}{L_{HAE}} = -\theta_{clay} D^*_{clay}\frac{\Delta C_{clay}}{L_{clay}} \tag{D.8}$$

The concentration difference across the entire layered system (ΔC_{ave}) is equal to the sum of the concentration differences across each layer, as follows:

$$\Delta C_{ave} = \sum_i \Delta C_i = \Delta C_{HAE} + \Delta C_{clay} + \Delta C_{HAE} = \Delta C_{clay} + 2\Delta C_{HAE} \quad \text{(D.9)}$$

Inserting the relationships shown in Equation D.9 into Equations D.7 and D.8, and rearranging to solve for the equivalent D_e for the entire layered system, the relationship becomes (Foose et al. 1999):

$$D_{e,eq} = \frac{L}{2\left(\frac{L_{HAE}}{D^*_{HAE}\theta_{HAE}}\right) + \frac{L_{clay}}{D^*_{clay}\theta_{clay}}} \quad \text{(D.10)}$$

Finally, the effective diffusion coefficient of just the clay can be determined by setting Equation D.5 equal to Equation D.10, and solving for D^*_{clay}, as shown:

$$\boxed{D^*_{clay} = \frac{L_{clay}}{\theta_{clay}\left(-\frac{\Delta C_{ave}}{\Delta Q_t / \Delta t} - 2\frac{L_{HAE}}{D^*_{HAE}\theta_{HAE}}\right)}} \quad \text{(D.11)}$$

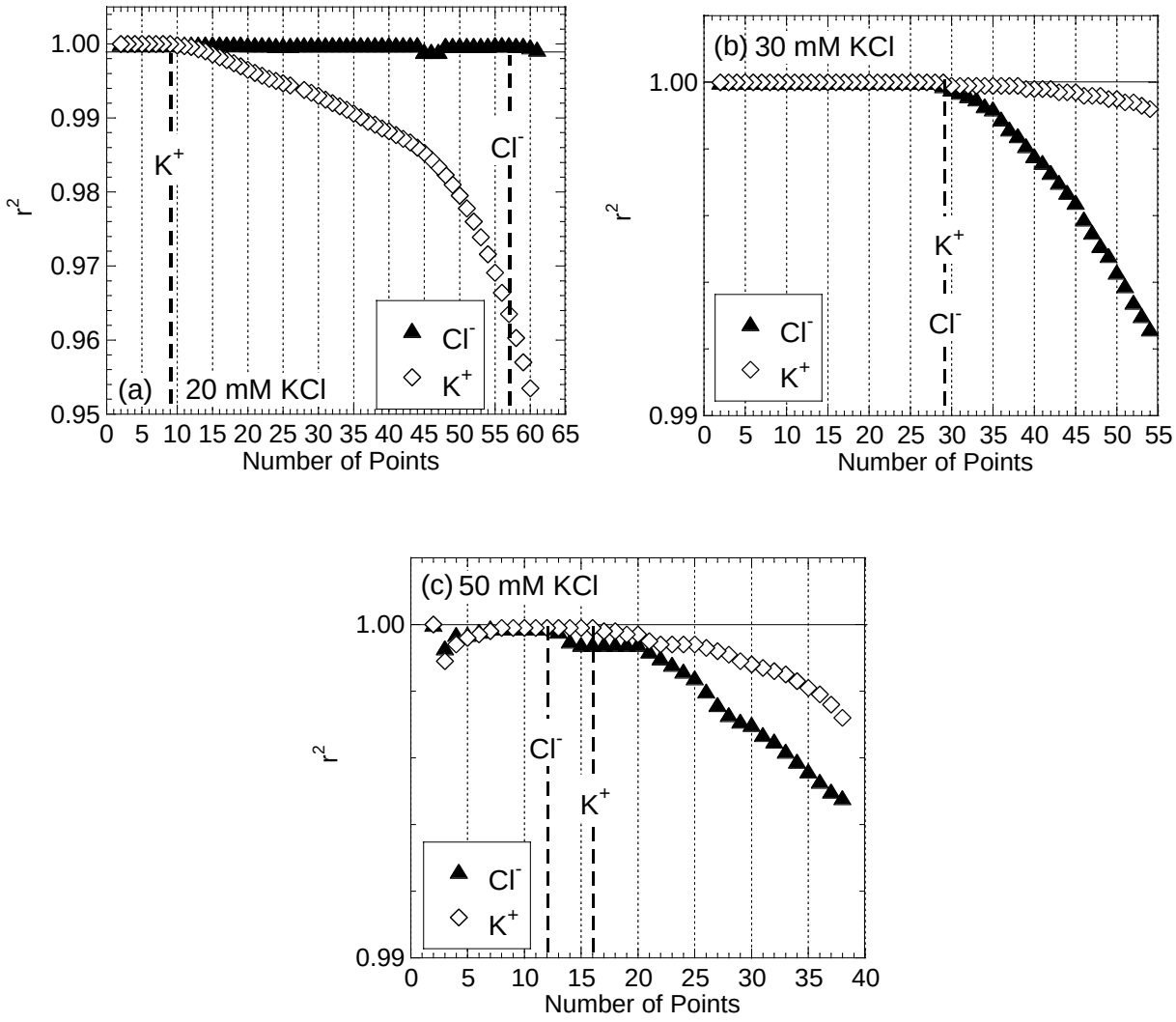

Figure D.1. Evaluation of number of data points to include in the steady-state linear regression of cumulative mass per area (Q_t) versus time (t) for the specimen with ***S* = 1.0.**

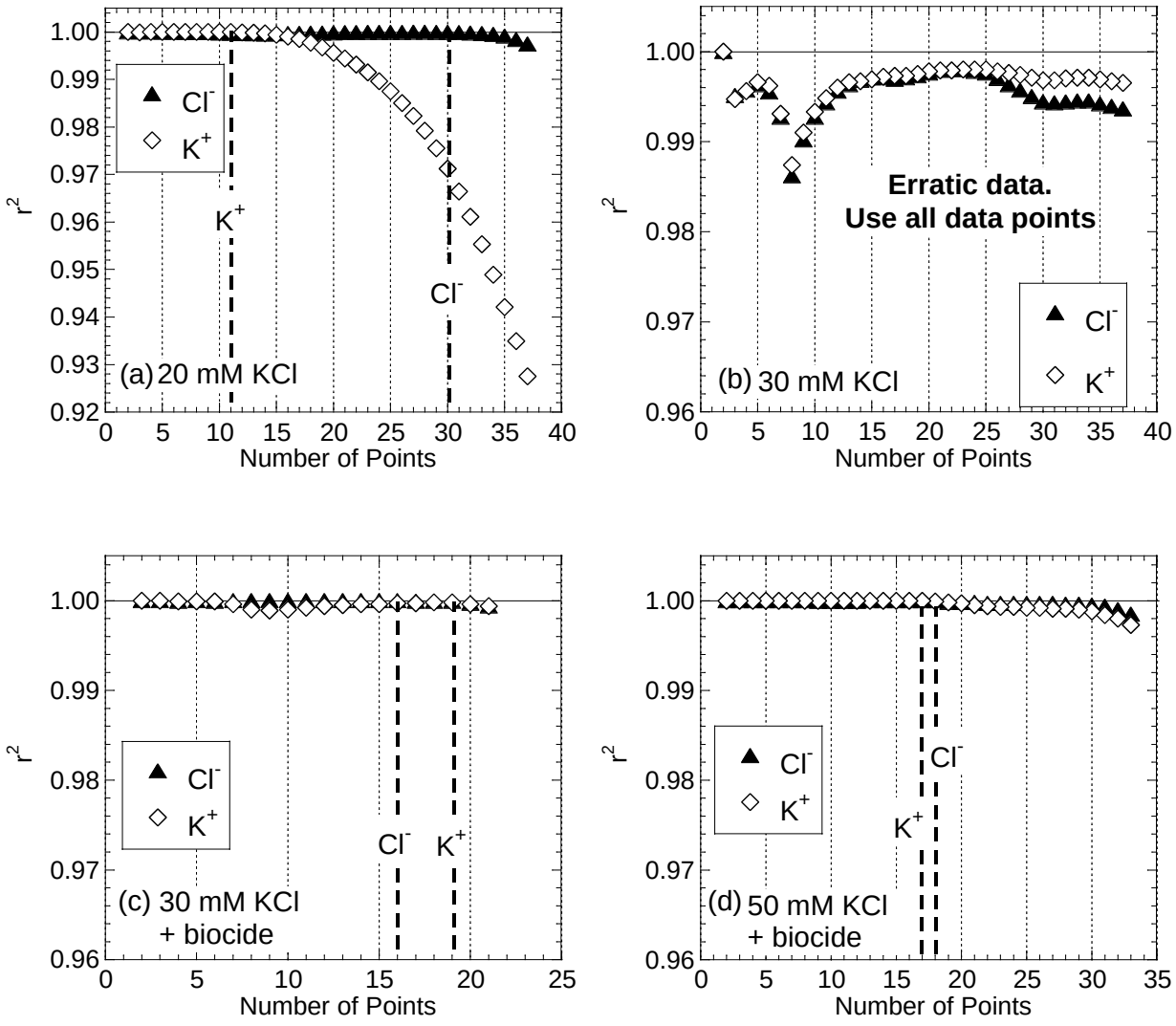

Figure D.2. Evaluation of number of data points to include in the steady-state linear regression of cumulative mass per area (Q_t) versus time (t) for the specimen with ***S* = 0.89.**

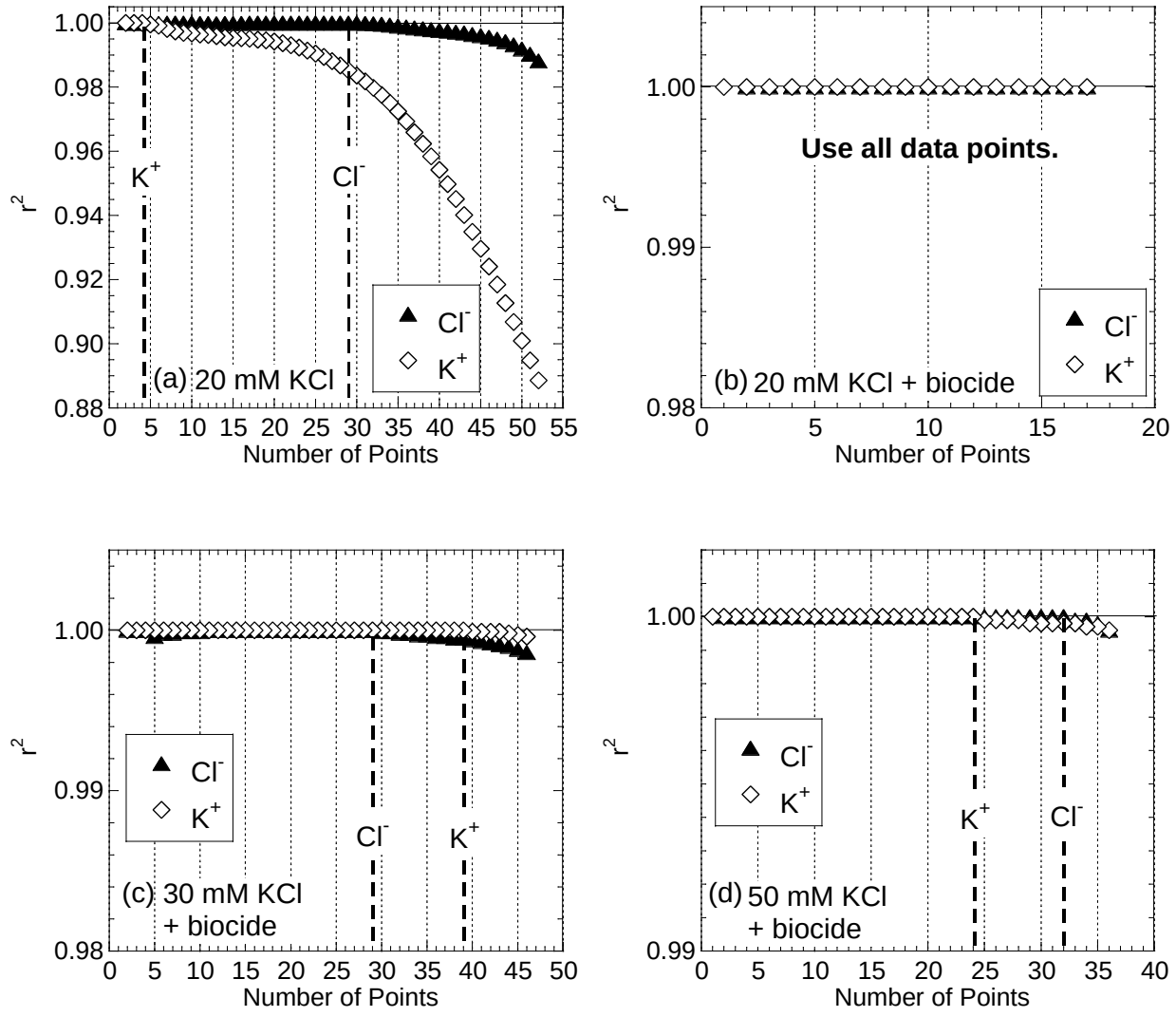

Figure D.3. Evaluation of number of data points to include in the steady-state linear regression of cumulative mass per area (Q_t) versus time (t) for the specimen with ***S* = 0.84.**

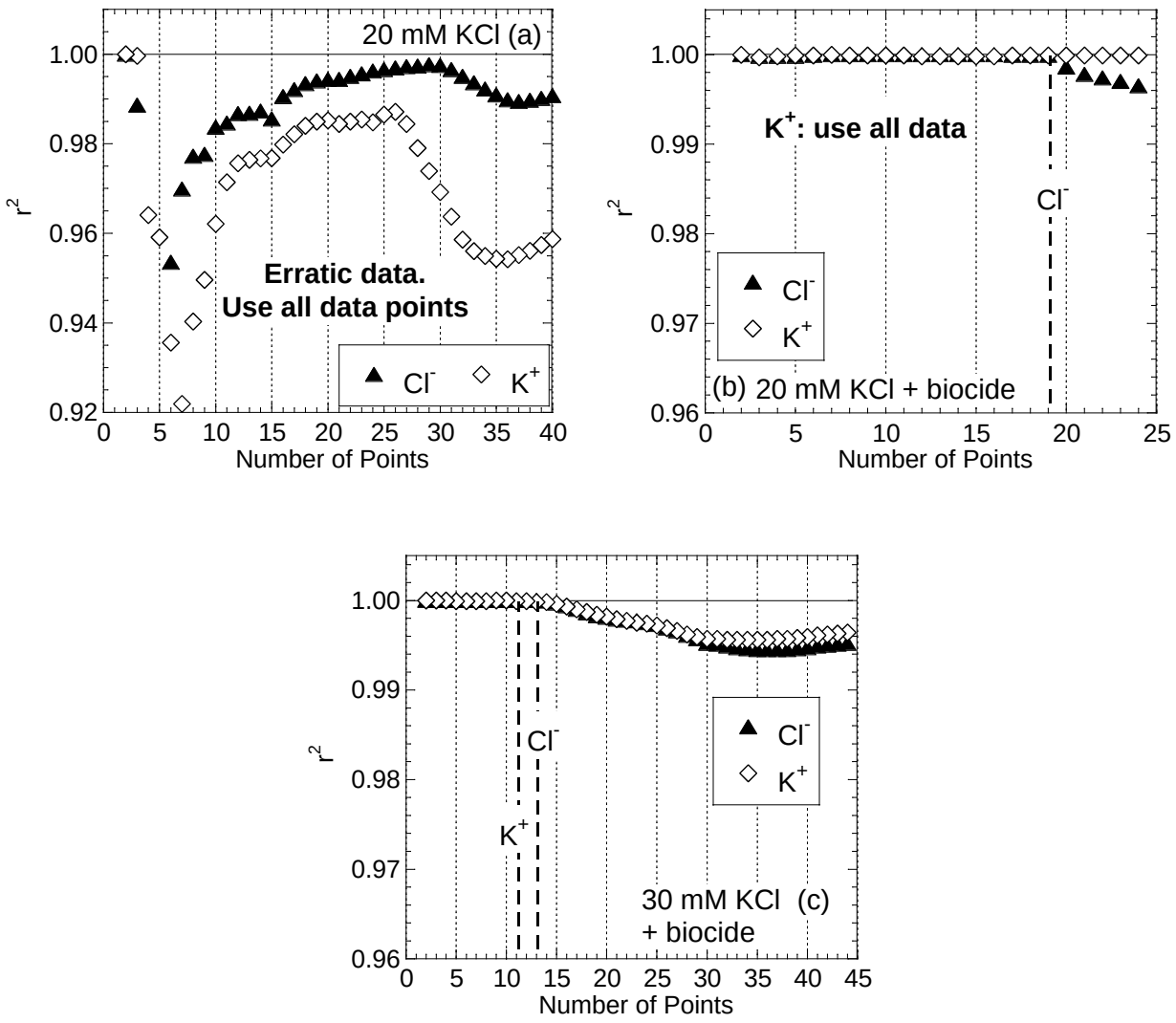

Figure D.4. Evaluation of number of data points to include in the steady-state linear regression of cumulative mass per area (Q_t) versus time (t) for the specimen with ***S* = 0.79.**

APPENDIX D-2

Supplemental Information for Empirical Relationships to Estimate Diffusion Coefficients of Unsaturated Porous Media

Table D-2.1. Aqueous diffusion coefficient (D_o) of KCl solution at 25 ° C (Robinson and Stokes 1959).

Concentration (M)	$\boldsymbol{D_{o,KCl}}$ **(m^2/s)**
0	1.99×10^{-9}
0.001	1.96×10^{-9}
0.002	1.95×10^{-9}
0.003	1.95×10^{-9}
0.005	$\mathbf{1.93 \times 10^{-9}}$
0.007	$\mathbf{1.93 \times 10^{-9}}$
0.01	$\mathbf{1.92 \times 10^{-9}}$
0.05	$\mathbf{1.86 \times 10^{-9}}$
0.1	$\mathbf{1.84 \times 10^{-9}}$
0.2	1.84×10^{-9}
0.3	1.84×10^{-9}
0.5	1.85×10^{-9}
0.7	1.87×10^{-9}
1	1.89×10^{-9}
1.5	1.94×10^{-9}
2	2.00×10^{-9}
2.5	2.06×10^{-9}
3	2.11×10^{-9}
3.5	2.16×10^{-9}
3.9	2.20×10^{-9}

Note: Data in bold was used for correlation shown in Figure D-2.1.

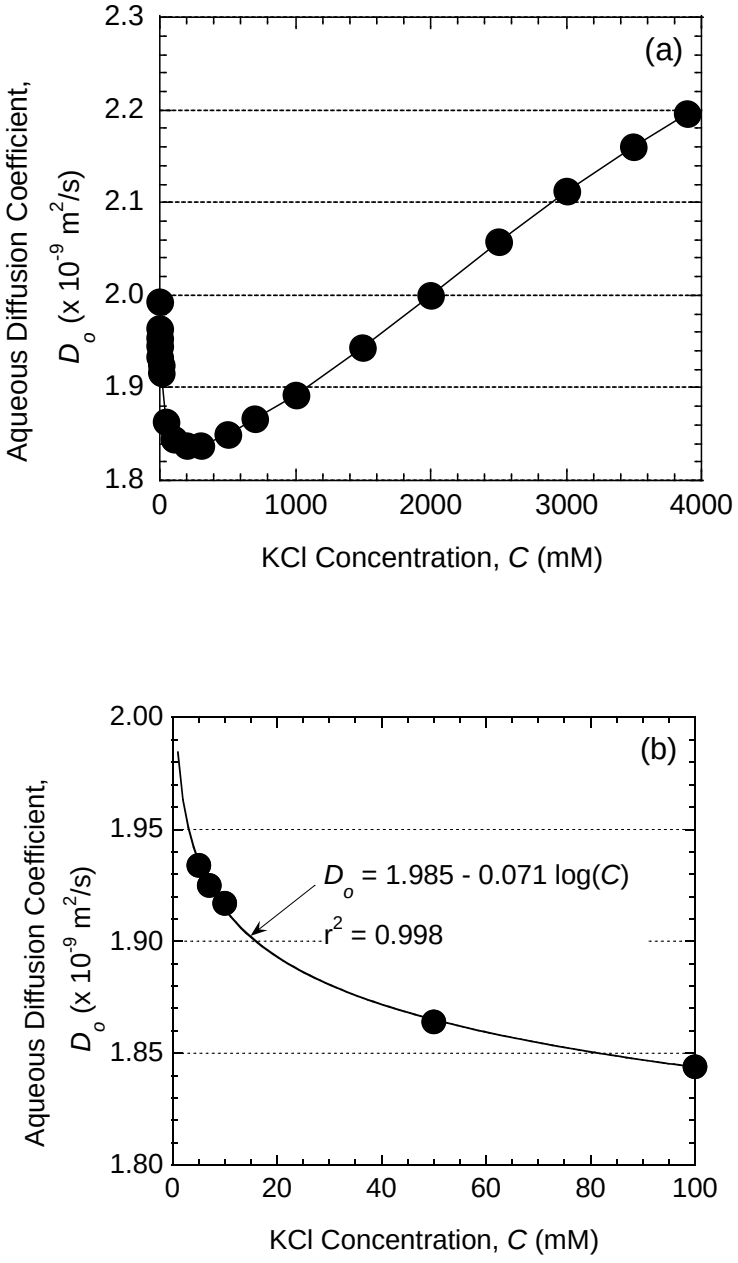

Figure D-2.1. Relationship between aqueous diffusion coefficient (D_o) of KCl solution at 25 °C and KCl concentration: (a) over a wide range of KCl concentrations; (b) over the concentration range relevant to this study (average concentration (C_{ave}) ranging from 9.0 mM to 25.6 mM) (data from Robinson and Stokes 1959).

APPENDIX E. SUPPLEMENTAL INFORMATION FOR MEMBRANE BEHAVIOR TESTS

Table E.1. Osmotic suctions for various salt solutions (Bulut et al. 2001).

Osmotic Suctions (kPa) at 25°C								
Concentration (M)	**KCl**	**NaCl**	**NaCl**	**NH_4Cl**	**Na_2SO_4**	**$CaCl_2$**	**$Na_2S_2O_3$**	**$MgCl_2$**
0.001	5	5	5	5	7	7	7	7
0.002	10	10	10	10	14	14	14	14
0.005	24	24	24	24	34	34	34	35
0.010	48	48	48	48	67	67	67	68
0.020	95	95	95	95	129	132	130	133
0.050	233	234	234	233	306	320	310	324
0.100	460	463	463	460	585	633	597	643
0.200	905	916	916	905	1115	1274	1148	1303
0.300	1348	1370	1370	1348	1620	1946	1682	2000
0.400	1789	1824	1824	1789	2108	2652	2206	2739
0.500	2231	2283	2283	2231	2582	3396	2722	3523
0.600	2674	2746	2746	2671	3045	4181	3234	4357
0.700	3116	3214	3214	3113	3498	5008	3744	5244
0.800	3562	3685	3685	3558	3944	5880	4254	6186
0.900	4007	4159	4159	4002	4384	6799	4767	7187
1.000	4452	4641	4641	4447	4820	7767	5285	8249
1.200	5354	5616	5616	5343	…	…	…	…
1.400	6261	6615	6615	6247	…	…	…	…
1.500	…	…	…	…	6998	13391	7994	14554
1.600	7179	7631	7631	7155	…	…	…	…
1.800	8104	8683	8683	8076	…	…	…	…
2.000	9043	9757	9757	9003	9306	20457	11021	22682
2.500	11440	12556	12556	11366	11901	29115	14489	32776

Notes:
Shaded = applicable range for this study.

Table E.2. Osmotic suctions for KCl solutions as a function of temperature (Campbell and Gardner 1971).

Osmotic Suctions (kPa) for KCl Solutions							
Concentration (M)	**0°C**	**10°C**	**15°C**	**20°C**	**25°C**	**30°C**	**35°C**
0.00	0	0	0	0	0	0	0
0.10	421	436	444	452	459	467	474
0.20	827	859	874	890	905	920	935
0.30	1229	1277	1300	1324	1347	1370	1392
0.40	1628	1693	1724	1757	1788	1819	1849
0.50	2025	2108	2148	2190	2230	2268	2306
0.60	2420	2523	2572	2623	2672	2719	2765
0.70	2814	2938	2996	3057	3116	3171	3226
0.80	3208	3353	3421	3492	3561	3625	3688
0.90	3601	3769	3846	3928	4007	4080	4153
1.00	3993	4185	4272	4366	4455	4538	4620

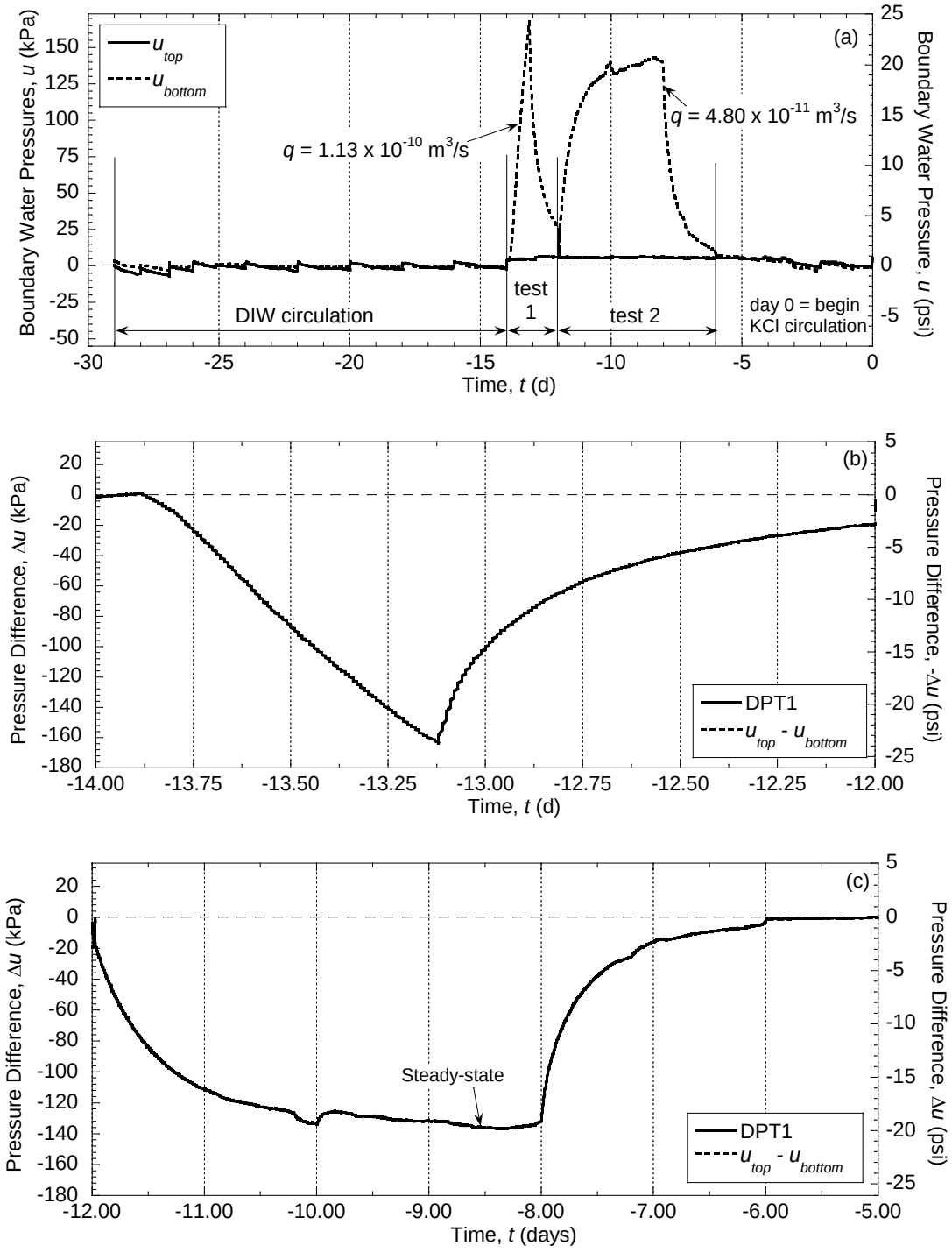

Figure E.1. Measured pressures during constant-flow hydraulic conductivity testing of saturated bentonite specimen: (a) pressures at the top and bottom boundaries during both tests; (b) pressure difference during test No. 1; (c) pressure difference during test No. 2.

Equations from Revil et al. (2011) Theoretical Model for Membrane Behavior

Model Description: Predicts membrane efficiency coefficient (ω) as a function of average concentration in the specimen (C_{ave}), for water-saturated specimens.

Required Input Parameters: Cation exchange capacity (CEC), porosity (n)

References:

Revil, A., Woodruff, W., and Lu, N. (2011). "Constitutive equations for coupled flows in clay materials." *Water Resources Research*, 47(5), W05548.

Model:

Equation for membrane behavior in unsaturated clay:

$$\omega = \frac{\sqrt{1+\Theta^2}-1}{\sqrt{1+\Theta}}$$

where:

- ω = osmotic coefficient or membrane efficiency coefficient
- Θ = dimensionless parameter at saturation, given by:

$$\Theta = \frac{10^{-3}(1-f)\rho_S}{2C_{ave}}\left(\frac{1-n}{n}\right)\mathrm{CEC}\,.$$

where:

- f = fraction of counterions in Stern layer = 0.90 (default value)
- ρ_s = density of solid phase = 2710 kg/m^3 for Na-bentonite specimens
- C_{ave} = average salinity in the specimen [Mol L^{-1}]
- CEC = soil CEC [meq g^{-1}] = 0.783 meq/gfor Na-bentonite specimens
- n = porosity [-] = 0.88 = average for Na-bentonite specimens

Figure E.2. Summary of theoretical model for membrane behavior in saturated clays (Revil et al. 2011).